

**DOCTORAL THESIS**

# Co-Metabolism of Mucins and Dietary Fibres by Gut Microbiota

Grete Raba

TALLINN UNIVERSITY OF TECHNOLOGY  
DOCTORAL THESIS  
11/2023

# **Co-Metabolism of Mucins and Dietary Fibres by Gut Microbiota**

GRETE RABA



TALLINN UNIVERSITY OF TECHNOLOGY

School of Science

Department of Chemistry and Biotechnology

This dissertation was accepted for the defence of the degree 30/03/2023

**Supervisor:**

Dr Kaarel Adamberg  
School of Science  
Tallinn University of Technology  
Tallinn, Estonia

**Co-supervisor:**

Assistant Professor Liisa Arike  
Department of Medical Biochemistry and Cell Biology  
University of Gothenburg  
Gothenburg, Sweden

**Opponents:**

Dr Elisabeth Lowe  
Medical School  
Newcastle University  
Newcastle upon Tyne, UK

Associate Professor Sabina Leanti La Rosa  
Faculty of Chemistry, Biotechnology and Food Science  
Norwegian University of Life Sciences  
Ås, Norway

**Defence of the thesis:** 05/05/2023, Tallinn

**Declaration:**

Hereby I declare that this doctoral thesis, my original investigation and achievement, submitted for the doctoral degree at Tallinn University of Technology has not been submitted for doctoral or equivalent academic degree.

Grete Raba

-----  
signature



European Union  
European Regional  
Development Fund



Investing  
in your future

Copyright: Grete Raba, 2023

ISSN 2585-6898 (publication)

ISBN 978-9949-83-962-9 (publication)

ISSN 2585-6901 (PDF)

ISBN 978-9949-83-963-6 (PDF)

Printed by Auratrükk

TALLINNA TEHNIKAÜLIKOO  
DOKTORITÖÖ  
11/2023

# Mutsiinide ja kiudainete kometabolism soolestiku mikrobiota poolt

GRETE RABA





# Contents

List of publications .....	7
Author's contribution to the publications .....	8
Introduction .....	9
Abbreviations .....	11
1 Literature review .....	12
1.1 Modulating the gut microbiota has immense health-beneficial potential .....	12
1.2 Gut transit rate and pH determine the physiological conditions for the gut bacteria .	13
1.3 Regular consumption of dietary fibres maintains the gut microbiota richness and functional balance.....	14
1.4 Gastrointestinal epithelium is protected by the mucus layer.....	15
1.5 The mucins and gut microbiota have a dynamic interplay .....	17
1.6 Downstream bacterial metabolism of glycans produces bio-active compounds which can be either beneficial or toxic to the host .....	19
2 Aims of the study .....	21
3 Materials and Methods.....	22
3.1 In vitro cultivation systems .....	22
3.2 DNA extraction, sequencing and bioinformatics .....	24
3.3 Analysis of microbial metabolites .....	24
3.4 Metaproteomics.....	25
3.5 Analysis of carbohydrate metabolism.....	25
3.6 Mucin analyses.....	26
3.7 Spheroid culture.....	26
3.8 Flow cytometry .....	26
3.9 Construction of metabolic networks and Flux Balance Analysis.....	26
3.10 Sequence-based metabolism mapping from metaproteomics.....	27
4 Results and discussion.....	28
4.1 The growth space of gut bacteria .....	28
4.1.1 Dilution rate selectively enhances slow- or fast-growing bacteria (Publication I) .	28
4.1.2 The pH and the dilution rate induce changes in the dynamics of mucus-degrading species (Publication II) .....	29
4.1.3 Complex dietary fibres support the development of highly diverse consortia (Manuscript).....	31
4.2 Microbiota co-metabolism of dietary fibres and mucins.....	34
4.2.1 The degradation of complex dietary fibres and mucin requires enzymes from several CAZyme families (Publication III and Manuscript).....	34
4.2.2 <i>Akkermansia muciniphila</i> degrades the mucin protein in co-culture (Manuscript)..	37
4.2.3 The metabolites from complex dietary fibre fermentation affect goblet cell mucin production (Manuscript).....	38
4.2.4 The downstream metabolism of complex dietary fibres (Manuscript) .....	39
5 Conclusions .....	42
References .....	44
Abstract.....	57
Lühikokkuvõte.....	59

Appendix 1 .....	61
Appendix 2 .....	75
Appendix 3 .....	85
Appendix 4 .....	97
Curriculum vitae.....	151
Elulookirjeldus.....	153

## List of publications

The thesis has been prepared based on the following three publications (I-III) and an additional manuscript that is currently in preparation. The full texts of the publications and the manuscript can be found in the Appendices 1-4.

- I Adamberg, K., **Raba, G.**, Adamberg, S. Use of changestat for growth rate studies of gut microbiota. *Frontiers in Bioengineering and Biotechnology*. 2020, 8, 24. doi: 10.3389/fbioe.2020.00024. PMID: 32117913.
- II **Raba, G.**, Adamberg, S., Adamberg, K. Acidic pH enhances butyrate production from pectin by faecal microbiota. *FEMS Microbiology Letters*. 2021, 368, 7. doi: 10.1093/femsle/fnab042. PMID: 33864456.
- III **Raba, G.**, Luis, A. S. Mucin utilization by gut microbiota - recent advances on characterization of key enzymes. *Essays in Biochemistry*. 2023 Jan 25:EBC20220121. doi: 10.1042/EBC20220121.
- Manuscript **Raba, G.**, Luis, A. S., Schneider, H., Morell, I., Jin, C., Adamberg, S., Hansson, G. C., Adamberg, K., Arike, L. Metabolic pathways of human microbiota co-utilization of fibres and colonic mucins. (Manuscript in preparation)



## **Author's contribution to the publications**

Contribution to the papers in this thesis are:

- I                    The author participated in the experimental work, analysed and interpreted the data and contributed to the manuscript preparation.
- II                   The author participated in the study design and performed all the experimental work. She collected, analysed and interpreted the data and wrote the manuscript draft.
- III                  The author contributed to collecting the studies included in the review. She wrote the first draft of the manuscript and participated in the editing of the manuscript.
- Manuscript       The author participated in the study design, wrote the manuscript draft and contributed to editing the draft and designing the figures. She performed the porcine colonic mucus extraction, cultivation and cell culture experiments and data analysis and interpretation. The author participated in the metaproteome and metabolome analyses.

## Introduction

The human gut microbiota has a crucial role in human health and disease. The bacteria survive in the gastrointestinal tract due to their ability to use a wide source of dietary and host-derived glycans as carbon source. The degradation and metabolism of these glycans produces energy and bioactive compounds that maintain the intestinal homeostasis of the host. However, imbalances in the microbiota composition and metabolism are linked to multiple diseases, such as inflammatory bowel disease, obesity and colorectal cancer. The onset of these diseases often begins with extensive degradation of the gut mucus layer, making it penetrable to bacteria who trigger an inflammatory response in the epithelium. Recent studies have shown that in addition to its passive protective function, the mucus also plays a key role in selecting the host microbiota composition. The main components of the mucus layer are large glycoproteins called mucins. In healthy individuals the mucin degradation is kept in balance by consumption of dietary fibres. These plant-derived polysaccharides are largely indigestible to humans and reach the colon where the bacteria utilise them as the preferred carbon source. However, in the absence of fermentable dietary fibres, some bacteria can switch to alternative energy sources, such as degradation of mucins, creating imbalances in the microbiota functions.

The microbiota-related diseases are increasingly common, especially in the technologically advanced parts of the world where humans have gone through rapid changes in their diet and lifestyle, altering their core microbiota composition. As a result, the microbiota diversity decreases with every generation, until some species become completely obsolete in said populations, lowering the functional potential of the host. Dietary fibres have been studied as promising modulators of gut microbiota as they keep a balance between fibre-degrading and mucin-degrading species. Moreover, these polysaccharides can potentially selectively enhance growth of commensal gut bacteria or increase the overall diversity of the consortium. Although some dietary fibres have already been marketed as prebiotic food supplements, their effect is poorly defined due to the large individual differences in consortia. Understanding the factors that influence microbiota growth under various physiological conditions could be a key to developing novel non-invasive and diet-based treatments to microbiota-related diseases.

This study aims to overcome some of these challenges by scanning the microbiota growth space in a systematic way so that the results could be translated to broader populations. The results are compiled into three scientific publications and a manuscript that is currently in preparation. Publications I and II explored the microbiota growth and metabolism under physiologically relevant transit times and pH values. The effect was elucidated in continuous cultures supplemented with porcine gastric mucin and two different dietary fibres. The growth space study was continued in the supporting manuscript (under preparation) where isothermal microcalorimetry was used for high-throughput screening of a panel of dietary fibres for their potential to increase microbiota diversity. Porcine colonic mucin was extracted in-house and used as an intrinsic co-substrate for polysaccharide fermentation. The degradation and downstream metabolism of selected dietary fibres and colonic mucin was elucidated combining taxonomic sequencing and metabolomics with metaproteomics and mathematical models. Potential prebiotic compounds were identified and their mechanisms of action elucidated. We determined key species and enzymes for the breakdown of the studied complex glycans. Additionally, a comprehensive review on the mucin utilization key

enzymes was compiled to support the findings of this study. The results of this dissertation have been presented at scientific seminars and conferences. The novelty and relevance of the findings for a broader audience has been recognised with a poster presentation award from an international conference. Together, the results contribute to a better understanding of the microbiota development and metabolism that can be manipulated to maximise beneficial microbiota-host interactions.

## Abbreviations

AGC	Automatic gain control
Acetyl-CoA	Acetyl coenzyme A
AgPAGE	Agarose-polyacrylamide gel electrophoresis
BCFA	Branched-chain fatty acid
BSS	Bristol stool scale
CAZymes	Carbohydrate-active enzymes
CE	Carbohydrate esterase
D	Dilution rate of continuous cultures
ESI	Electrospray ionization
FBA	Flux balance analysis
GABA	$\gamma$ -Aminobutyric acid
GC	Gas chromatography
GF	Germ-free
CFU	Colony-forming unit
GH	Glycoside hydrolase
HCD	Higher energy collision dissociation
HPLC	High-performance liquid chromatography
IBD	Inflammatory bowel disease
LC	Liquid chromatography
MS	Mass spectrometry
PCM	Porcine colonic mucin
PDA	Photodiode array
PEP	Phosphoenolpyruvate
PGM	Porcine gastric mucin
PL	Polysaccharide lyase
RI	Refractive index
RP	Reverse phase
SCFA	Short-chain fatty acid
TCA cycle	Tricarboxylic acid cycle
TCD	Thermal conductivity detector
TFA	Trifluoroacetic acid
UPLC	Ultra-performance liquid chromatography
UV	Ultraviolet

# 1 Literature review

## 1.1 Modulating the gut microbiota has immense health-beneficial potential

The human gut microbiota is defined as the sum of microbes colonizing the human gastrointestinal tract. About 99% of these microbes are bacteria, out of which 99% inhabit the colon. The microbial density increases from the proximal to the distal colon and from the epithelial cells towards the lumen (Sekirov et al. 2010). The latest estimations deem the number of bacteria in the colon to be approximately  $10^{13}$  (Sender, Fuchs, and Milo 2016). These bacteria are adapted to survive in the gut due to their ability to use a wide range of polysaccharides, especially dietary fibres and host glycans, as carbon source. The gut bacteria are a vital part of the human body as they help to ferment otherwise indigestible foods and produce energy and host-beneficial bioactive compounds. Moreover, they protect the host against invading species by competing for nutrients and space.

The species richness of the gut community has been shown to be a pivotal marker of the gut health. The richness and diversity reflect the stability and resilience of an ecosystem, whereas reduced microbiota diversity has been shown to correlate with gut diseases. It is estimated that the colon could house about 1000 different bacterial species (Xu and Gordon 2003). By the age of three, each of us has acquired our own unique set of bacteria that is similar to adult microbiota, although significant species-level changes occur throughout childhood (Arrieta et al. 2014). The composition of bacterial communities is affected by both internal and external factors (genetics, hormones, diet, lifestyle, environment, industry). The large variety of these factors makes it impossible to define a standard healthy gut microbiota composition. The average intestinal community of Estonians, however, is dominated by Bacteroidetes and Firmicutes (56 and 34%, respectively), followed by Proteobacteria (5%), Actinobacteria (1%) and others (Aasmets et al. 2022). This high prevalence of the Gram-negative Bacteroides and the Gram-positive Firmicutes is also common to microbiotas of individuals from other Western countries (Wexler and Goodman 2017; Huttenhower et al. 2012). Yet, immense individual differences in the gut communities give each person their own microbiota “fingerprint”.

The gut bacteria form an intertwined system where different species constantly interact with each other through supportive (mutual or commensal) or inhibitory (ammensal or competitive) relations. For example, this crosstalk between members of the microbiota is used for degradation of complex glycans (Ostrowski et al. 2022). Maintaining the bacterial diversity is crucial for the gut health and functional homeostasis. Overconsumption of processed foods, urbanization and decreased physical activity are considered primary reasons for the decrease in microbiota diversity in technologically developed countries. The loss of keystone species can lead to disruptions in the whole system. Indeed, lower microbiota diversity has been linked to diseases such as irritable bowel disease (IBD) (Alam et al. 2020; Clooney et al. 2021) and obesity (Boroni Moreira et al. 2012; Muscogiuri et al. 2019). Moreover, alterations in microbiota composition are connected to neurodegenerative diseases like Parkinson’s disease (Xie et al. 2022; Pereira et al. 2022). These diseases are an increasing problem, especially in the Western world where the diet and lifestyle of people has gone through rapid changes in a short amount of time. However, parameters like gut peristalsis and pH are largely determined by the diet. Moreover, the gut mucus layer which is the first line of defence

against inflammatory processes is also in a close dynamic relationship with the bacteria and the diet. A better understanding on these relations could be a key to developing non-invasive, diet-based treatments and preventions to diseases related to microbiota changes. Modulating the gut microbiota in a favourable direction has immense potential for the overall improvement of human health.

## 1.2 Gut transit rate and pH determine the physiological conditions for the gut bacteria

Among the physiological parameters that have a major impact on the gut microbiota composition and metabolism are the gut transit rate and the pH. The gut transit rate describes the gut peristalsis and is defined as the rate of which the stool passes through the gastrointestinal tract. It is often measured using Bristol Stool Scale (BSS) where a low score reflects firm stool and slow transit, while a high score reflects loose stool and fast transit (Lewis and Heaton 1997; Degen and Phillips 1996; Saad et al. 2010). The transit time affects bacterial growth through nutrient availability as prolonged transit decreases water activity and reduces nutrient mobility and enzymatic activity (Vandeputte et al. 2016). The transit also affects the epithelium-protecting mucus layer by disrupting it through mechanical shear forces, transporting the mucus towards the rectum (Gayer and Basson 2009). The gut transit rate is partially determined by the host diet as certain polysaccharides bind water and increase the volume and moving rate of the stool (Cummings 1984; Elia and Cummings 2007; de Vries, Miller, and Verbeke 2015).

The colonic transit rate is related to the bacterial growth rate which is described by the Monod equation:

$$\mu = \frac{\mu_{max} \cdot S}{(K_s + S)}$$

where  $\mu$  is the specific growth rate of the cell at a steady state,  $S$  is the limiting substrate and  $K_s$  is a constant describing the cell's affinity to the substrate (Monod 1978). Through this connection the transit rate selects for the gut bacteria. When the bacterial cell growth does not match the colonic transit rate, it needs to adhere to the host (for example, by getting trapped in the mucus layer) or it is washed out of the system (K. Adamberg and Adamberg 2018; K. Adamberg, Raba, and Adamberg 2020). However, the relationship between gut transit rate and cell growth rate is not linear because while the density of bacteria increases along the colon, the moving rate decreases.

In continuous cultivation, the transit time is reflected in the parameter called the dilution rate ( $D$ ). The steady state in *in vitro* continuous cultivation is achieved by a constant inflow of fresh medium and removal of the spent medium. This is done at a constant rate, the dilution rate. The dilution rate controls the concentration and availability of the substrate and is thereby directly related to the bacterial specific growth rate  $\mu$ . However, the relationship between gut transit rate and the human health remains to be understood. The slow transit rate positively correlates with both the species richness and proteolytic activity (Cummings and Englyst 1987; Vandeputte et al. 2016). While the first is considered as a marker for healthy gut, the latter is known to result in the production of potentially harmful metabolites. These examples demonstrate the need for a better understanding on how the transit rate determines the microbiota composition and metabolism.

The degradation of food components, release of organic acids, bile salts and water create a pH gradient along the gastrointestinal tract. The pH inside a healthy colon is

neutral or mildly acidic (pH 6.0-7.5) (Nugent et al. 2001). However, the pH can increase up to 8 in case of colorectal cancer (Kashtan et al. 1990; Ohigashi et al. 2013). Similarly, alkaline pH has been shown to accompany the constipation that is typical to colorectal cancer (Kojima et al. 2004). The colonic pH determines nutrient availability and enzymatic activity, thereby affecting microbiota growth and metabolism. It also influences bile solubility, ion availability and is an important factor determining the organization of the protective mucus layer (Duncan et al. 2009; Ambort et al. 2012).

The pH of the colon is highly impacted by the choice of diet. Degradation of dietary fibres in the proximal colon produces short-chain fatty acids (SCFAs) which lower the pH. However, the pH rises towards the distal parts of the colon. When the dietary fibres are utilised and the SCFAs absorbed, the bacteria begin to metabolize available proteins, releasing peptides, ammonia and urea which increase the pH (Russell et al. 2011; Aguirre et al. 2016). Moreover, the degradation of host mucin glycans releases amino sugars which raise the pH (Ottman et al. 2017). Both the pH and gut transit rate are powerful modulators of the gut microbiota composition and metabolism. Their manipulation through diet could be a key to developing novel pre- or synbiotics.

### **1.3 Regular consumption of dietary fibres maintains the gut microbiota richness and functional balance**

Dietary fibres are a class of complex polysaccharides found in the plant cell walls. They are the most structurally diverse compounds in the human diet. These polysaccharides can be made of a variety of different sugar residues, both hexoses and riboses. They can include either  $\alpha$ - or  $\beta$ -linkages and can be branched at several positions on a single monomer. Furthermore, they can form secondary structures or be linked to other common biological molecules to form conjugates such as glycoproteins and lipopolysaccharides. At the same time, they are largely undigestible by humans who lack the necessary enzymes. Thus, the polysaccharides reach the colon where gut bacteria can harness their vast repertoire of carbohydrate-active enzymes (CAZymes) to break down the fibres and use the sugar residues for energy metabolism. These properties make dietary fibres excellent for modulating the microbiota composition and metabolism. However, the use of dietary fibres as prebiotics requires that they elicit similar effects in broad populations – something that is complicated due to the interindividual variety of microbiota composition. Nevertheless, recent studies have shown that, despite the large differences in gut microbiota communities, more complex-structured dietary fibres can induce similar changes in consortia of different people (Deehan et al. 2020; T. M. Cantu-Jungles and Hamaker 2020; Thaisa M Cantu-Jungles et al. 2021).

The degradation of polysaccharides by gut microbiota is catalysed by different CAZymes such as glycoside hydrolases (GHs), polysaccharide lyases (PLs), carbohydrate esterases (CEs) and sulfatases (Drula et al. 2022; Barbeyron et al. 2016). The CAZymes are classified into families based on sequence-similarity. CAZymes of the same family share a conserved fold, catalytic mechanism and active site residues. The GHs and sulfatases can be either exo- or endo-active, depending on whether they hydrolyse glycans from one end or within the glycan chain (Wardman et al. 2022). The gut microbiota has been shown to encode for over 89 CAZyme families, whereas the human proteome is limited to only 17 CAZymes (Bhattacharya, Ghosh, and Mande 2015; Drula et al. 2022). The gut commensal genus *Bacteroides* is especially adapted to complex glycan degradation (Kaoutari et al. 2013). For example, *B. thetaiotaomicron* can express

at least 172 GHs (Xu et al. 2003). This rich repertoire of enzymes is needed to break down complex fibres such as pectin. It has been showed that a single bacterium can encode 54 different enzymes to degrade this plant polysaccharide (Luis et al. 2018). The degradation of polysaccharides by a bacterium can be carried out in a “selfish” mechanism where all the degradation products are imported into their periplasm for downstream metabolism. Alternatively, there can be crosstalk between members of the consortium in which case the products of one species are shared with the other. The latter mechanisms are still quite poorly understood as there is likely substantial overlap in the functional activities of various species. Interestingly, it has been shown that the degradation of some dietary fibres can have very specific geographical and/or cultural limitations. For example, some enzymes that are required for the degradation of algal polysaccharides are found only in populations whose diet regularly includes algae (Hehemann et al. 2010).

Consumption of dietary fibres in the diet helps to ensure the bacterial diversity in the colon and to suppress overgrowth of potential pathogens. Moreover, studies comparing single fibres and fibre mixtures show the latter to increase the microbiota diversity more effectively (Chung et al. 2018). The presence of dietary fibres in the colon is also needed to maintain the balance between fibre-degrading and mucolytic species. A study with mice demonstrated how the lack of dietary fibre induces overgrowth of mucus-degrading bacteria resulting in a weakened and penetrable mucus layer (Desai et al. 2016). Interestingly, even 1-day oscillations between fibre-free and fibre-rich diet induced fluctuations in bacterial abundances, demonstrating how dynamic this system is. Another study with mice showed how colonizing mice with a microbiota from normal-fed littermates protected the mucus layer from degradation even in mice on Western style diet (low in carbohydrates, high in saturated fats) (Schroeder et al. 2018). Similarly, in humans the so-called Western style diet and lifestyle is associated with decreased microbiota diversity and increased incidences of IBD (Martínez et al. 2015; Vangay et al. 2018; Clemente et al. 2015). Regular consumption of various dietary fibres is necessary to maintain the gut microbiota richness and to keep the fibre-degrading and mucus-degrading species in balance. This homeostasis ensures that the epithelium remains protected by the mucus layer.

#### **1.4 Gastrointestinal epithelium is protected by the mucus layer**

The gastrointestinal tract is lined with a mucus layer that protects and lubricates the gut and is simultaneously an interaction site between the host and the bacteria. The mucus is made of water (90-95%), electrolytes, lipids, proteins and other components (Paone and Cani 2020). In the colon, the mucus forms two layers: an almost sterile and structurally organized inner layer and a less defined outer layer that is mixed with bacteria and faecal content (Johansson et al. 2008). The mucus thickness is determined by the rate it is renewed by the epithelial cells and degraded by the microbiota and peristaltic forces. In humans the inner mucus layer thickness is around 300  $\mu\text{m}$  (Gustafsson et al. 2012). Measuring the outer layer thickness is complicated due to its unstructured nature, however it has been estimated to be double the thickness of the inner layer (Johansson, Holmén Larsson, and Hansson 2011).

Mucins are glycoproteins that are the main structural and functional components giving the mucus its gel-like properties. They bind water and protect the epithelium from mechanical stress as the peristaltic forces move the faecal matter along the gut. Fresh mucus is constantly secreted at a rate of ca 4  $\mu\text{m}/\text{min}$ , pushing the bacteria away from the epithelium (Gustafsson et al. 2012). Due to constant renewal and secretion, the mucus



performs as a surface cleaner, binding debris and bacteria and flushing them away from the epithelium. It acts as a first line of defence against potentially harmful microbes and compounds.

Mucins are continuously produced by goblet cells. The ratio of goblet cells to enterocytes increases along the gastrointestinal tract, positively correlating with the increase of bacterial numbers. In humans, this ratio begins at 4% in the duodenum and grows up to 16% in the distal colon (König et al. 2016; Paone and Cani 2020). The canonical goblet cells reside in the colonic crypts where they continuously secrete fresh mucin. In addition, there are so-called “sentinel goblet cells” which are at the crypt openings and secrete mucus in response to stress and bacterial invasion and are an additional line of defence (G. M. H. Birchenough et al. 2016). Recently, another sub-population of goblet cells was described: the intercrypt goblet cells (Nyström et al. 2021). These cells have a distinct expression profile and they secrete mucus which is more easily penetrable to smaller molecules and ions. It was shown that both the canonical and intercrypt goblet cell mucus are needed for maintaining the barrier function and protecting against colitis.

Mucins can be either transmembrane or secreted (Hansson 2020). The major mucin in the colon is a secreted gel-forming mucin 2 (MUC2). It is over 5000 amino acids long and weighs ca 2.7 MDa, with most of the molecular weight coming from the *O*-glycan sidechains (Allen, Hutton, and Pearson 1998; Axelsson, Asker, and Hansson 1998). The *O*-glycosylation gives the mucins their gel-forming properties. Moreover, these highly variable glycans cover the mucin protein backbone densely and protect it from host proteolytic and digestive enzymes as humans can cleave only a few glycan linkages (Van Der Post et al. 2013). The bulk of the mucin protein backbone is made of repeating Pro-Thr-Ser amino acids, called the PTS domain. The hydroxyl groups of Ser and Thr are the attachment site for the first *O*-glycan sugar, the *N*-acetylgalactosamine (GalNAc), while the structurally rigid Pro ensures that the mucin backbone remains unfolded in the Golgi apparatus so that the *O*-glycosylation process can take place (Bennett et al. 2012; Hansson 2020). The attachment of GalNAc residue to Ser or Thr initiates the *O*-glycosylation, after which galactose (Gal), *N*-acetylglucosamine (GlcNAc), GalNAc, *N*-acetylneuraminic acid (Neu5Ac) and sulphate groups can be added. The mucin *O*-glycosylation varies greatly between species and spatially along the gastrointestinal tract, being impacted by the host health, microbiota and enzymatic capabilities (Rodríguez-Piñeiro et al. 2013; Holmén Larsson et al. 2013).

After its synthesis, the MUC2 protein goes under dimerization via C-terminal disulphide bridges (in the ER) and subsequent trimerization via intermolecular disulphide bridges of N-terminal von Willebrand domains (in the Golgi apparatus) (Hansson 2020; Schroeder 2019). The resulting mucin oligomers are then packed into secretory vesicles where low pH and high Ca<sup>2+</sup> concentration help to maintain the structural organization (Ambort et al. 2012). Upon its secretion, the environmental changes and sudden hydration cause the mucin proteins to significantly expand (100 to 1000-fold increase in volume) and form 2D net-like sheets which interact with previously secreted mucins to form the 3D mucus layer. This scaffold acts as a diffusion barrier, letting through ions, nutrients, water, gases and other small molecules, while keeping the bacteria at bay. The other secreted mucins of the gastrointestinal tract are MUC6, MUC5AC and MUC5B (Hansson 2020). The latter are found in the stomach which is a common source for commercial mucin production. Compared to the mucins in the colon, the gastric mucins

contain less Neu5Ac and sulphate groups and are less uniform between individuals (Larsson et al. 2009; Karlsson et al. 1997).

The transmembrane mucins cover the apical surface of the enterocytes (Hansson 2020; Paone and Cani 2020). Transmembrane mucins have an intracellular cytoplasmic C-terminus, a transmembrane domain and one or multiple *O*-glycosylated PTS domains which are connected to the N-terminus (Paone and Cani 2020; Pelaseyed and Hansson 2020). The transmembrane mucins form an approximately 1  $\mu\text{m}$  thick densely glycosylated glycocalyx of enterocytes which protects the epithelium and is an important host-microbiota interaction site (Hansson 2020).

## 1.5 The mucins and gut microbiota have a dynamic interplay

It has become clear that mucus is not just a passive barrier, but in fact is in a dynamic relationship with the gut microbiota. The presence of bacteria is needed for the normal turnover of the mucus layer and, in turn, the mucin glycans select for the bacteria that can bind to mucins and utilise them as nutrient source (Johansson et al. 2015; Arike et al. 2020). Studies with germ-free (GF) and conventionally raised mice have demonstrated how the mucus of GF mice is abnormal: the glycosylation of mucins is different, the number of mucus-filled goblet cells is lower and the colonic inner mucus layer is penetrable to bacteria (Szentkuti et al. 1990; Kandori et al. 1996). However, the effect is reversed when the GF mice are colonised with a complex microbiota (Desai et al. 2016). The opposing phenomena of mucin glycans selecting the bacteria was demonstrated in a study with GF zebrafish and GF mice (Rawls et al. 2006). When the GF mice were given bacteria from conventionally raised zebrafish, the mice selected out the bacteria which were normal to mouse microbiota. The experiment was repeated in reverse with GF zebrafish and the same effect was seen, demonstrating how the host glycans play a role in selecting for the bacteria in microbiota.

The gut bacteria use their outer membrane proteins, lectins, adhesins, capsules, pili, flagella and fimbriae to interact with the mucins (Paone and Cani 2020). The adhesion to mucins is likely mediated through patches of specifically arranged glycans, not through single, poorly accessible glycans. The adhered bacteria can then degrade the mucins, utilising their wide repertoire of CAZymes. Different species use different strategies for mucin *O*-glycan degradation to secure a niche for colonization. A recent study on *Bacteroides thetaiotaomicron* sulfatases identified 11 sulfatases that were active on mucin *O*-glycans and had the potential to remove all possible mucin sulphate groups (Luis et al. 2021). Moreover, a single 3S-Gal sulfatase (BT1636) was found to be crucial for *B. thetaiotaomicron* growth on colonic *O*-glycans and in vivo colonization. In another study a single sulfatase (BF3134) was identified as essential for *Bacteroides fragilis* in vivo colonization (Donaldson et al. 2020). *Ruminococcus gnavus*, on the other hand, utilises trans-sialidases which convert the terminal Neu5Ac into 2,7-anhydro-Neu5Ac that cannot be metabolised by other gut bacteria (Tailford, Owen, et al. 2015; Bell et al. 2019). Interestingly, a trans-sialidase knock-out strain of *R. gnavus* lost the ability to colonise the mucus layer closer to the epithelium, showing a very specific niche that becomes available to the bacterium with this enzyme. *Bacteroides thetaiotaomicron* has been shown to modify mucus already before its secretion by specifically inducing fucosylation, securing itself a nutrient niche (Bry et al. 1996). In contrast, *B. thetaiotaomicron* can release Neu5Ac from mucin *O*-glycans, but cannot further metabolise this sugar, leaving it to be consumed by other gut bacteria like *Clostridium difficile* and *Salmonella typhimurium* who lack sialidase-activity (Ng et al. 2013). The bacterial metabolism of

sugars from *O*-glycans produces SCFAs like acetate, propionate and butyrate which are used by the epithelial cells for energy. Moreover, SCFAs can induce goblet cell differentiation and alternate mucin *O*-glycosylation (Wrzosek et al. 2013). Clearly there is a mutualistic relationship between the mucus and the bacteria.

However, imbalances in the microbiota composition and metabolism can lead to extensive degradation of the mucins, rendering the mucus layer damaged and penetrable. The pathogenic bacteria use their repertoire of mucin-degrading proteases, chemotaxis and flagella to penetrate the mucus, move against the flow and reach and adhere to the mucin glycans. The bacteria can also modify the mucus pH to destabilise the structures, further facilitating their adhesion to the glycans. Additionally, the bacteria might influence the expression and synthesis of mucins, allowing for an easier colonization. Finally, the spread of pathogenic bacteria can be aided by commensals who release sugar residues which the pathogens use for their proliferation in the mucus. These mechanisms render the mucus layer penetrable to the bacteria, letting them pass the first line of defence. Next, the sentinel goblet cells come into play by sensing the increased levels of bacterial products and releasing mucus plumes to wash away the pathogens. Finally, as the third defence mechanism, the goblet cells in the crypts would empty to increase the mucus volume. However, the regeneration of mucins is time-consuming and these defences cannot protect us against swarms of bacteria. If all these defences fail, the bacteria will have access to the epithelial cells, triggering an inflammatory response that can lead to the onset of disease.

It has been shown that alterations in the mucin *O*-glycosylation and mucus barrier function have a crucial role in the onset of diseases like IBD, obesity and colorectal cancer (Johansson et al. 2014; Schirmer et al. 2018; Schroeder et al. 2020; Coleman and Haller 2021). Patients with ulcerative colitis have a mucus layer that is penetrable to bacteria-sized particles (Johansson et al. 2014). The barrier function usually returns in patients who are in remission, although not always. Meanwhile, studies with MUC2 knock-out mice have shown that the resulting alterations in cell maturity and crypt morphology from the lack of MUC2 lead the mice to spontaneously develop IBD and colorectal cancer (Van der Sluis et al. 2006; Velcich et al. 2002).

The gut microbiota harbours members that are specialised to mucin degradation, such as *Akkermansia muciniphila*, and species such as *Bacteroides thetaiotaomicron* and *B. caccae* that are more flexible and can switch to host-derived mucin degradation in the absence of dietary glycans. As these generalists make up a significant proportion of the microbiota community, extensive degradation of mucin and the resulting inflammatory reactions can be ameliorated with a fibre-rich diet. In a study with mice colonised with a synthetic microbiota, including mucin specialists and generalists, the switch from fibre-rich to fibre-free diet resulted in an increased expression and activity of mucin-targeting CAZymes (Desai et al. 2016). At the same time, fibre targeting CAZymes activity and expression decreased. This led to a decreased thickness of the mucus layer which became susceptible to pathogenic *Citrobacter rodentium* invasion. Similar susceptibility to *C. rodentium* infection has been noted in MUC2 knock-out mice (Bergstrom et al. 2010). Together these results demonstrate how the balance between the bacteria and the diet have a crucial role in maintaining a healthy mucus layer. However, these dynamics are not always straightforward as exemplified by a study where administration of mucolytic *A. muciniphila* to mice fed a high-fat diet instead led to the thickening of the mucus layer (Everard et al. 2013). Understanding these complex relationships between the microbiota, mucus and diet are a key to developing novel prebiotics and therapeutics.

## 1.6 Downstream bacterial metabolism of glycans produces bio-active compounds which can be either beneficial or toxic to the host

The glycans from dietary fibre and mucin degradation are hydrolysed into five- or six-carbon monosaccharides which then undergo further catabolism by the gut microbiota. As a result, a variety of metabolites are produced which are used by both the bacteria and the host. The monosaccharides are first metabolised into phosphoenolpyruvate (PEP), either via the glycolysis pathway (six-carbon substrates) or the pentose phosphate pathway (five-carbon substrates). PEP is used for SCFA production, either directly or via the formation of pyruvate. The latter pathway provides the cell with extra ATP. Acetate can be produced either through decarboxylation of pyruvate, yielding acetyl-CoA which is then hydrolysed to acetate, or from CO<sub>2</sub> and formate over the Wood-Ljungdahl pathway (Ragsdale and Pierce 2008). Propionate is usually produced either from PEP through the TCA cycle utilising succinate and releasing CO<sub>2</sub>, or from lactate via the acrylate pathway (Koh et al. 2016; Hetzel et al. 2003). Alternatively, some bacteria have been shown to utilise a third pathway where propionate is produced via the hydrolysis of propane-1,2-diol (Reichardt et al. 2014). Butyrate production can go either via the classical pathway where two acetyl-CoA molecules form butyryl-CoA which is converted to butyrate, or an alternative pathway using exogenously derived acetate to form butyrate and acetyl-CoA (Duncan et al. 2002). All these pathways are driven by redox equivalents NADH and H<sub>2</sub> and the partial pressures of H<sub>2</sub> and CO<sub>2</sub>.

Fibre-rich diets increase the microbial diversity and SCFA production. Acetate, propionate and butyrate make up around 95% of the total SCFAs produced by the gut microbiota and are usually made at a molar ratio of ca 60:20:20 (John H Cummings and Englyst 1987; den Besten et al. 2013). The production is dependent of the host diet, microbiota composition and other host factors. The diet dictates how much fermentable substrate is available to the bacteria and different dietary fibres can result in different profiles of the produced SCFAs. Similarly, the metabolism of bacteria varies and thereby the community composition has a major impact on the profile of the SCFAs being produced. Especially sensitive to changes in the diet are members of the Firmicutes and Actinobacteria phyla who have specialised niche roles in the polysaccharide degradation (Makki et al. 2018). In contrast, *Bacteroides* genus are considered generalists who can easily switch to other glycan sources in the absence of fermentable polysaccharides. The secreted SCFAs are used by the host in several physiological functions such as maintaining the gut mucus layer, the epithelium (e.g., cell turnover and integrity of tight junctions), controlling the gut motility and forming the pH gradient inside the gastrointestinal tract (Kaiko et al. 2016; Dougherty et al. 2020; Bilotta et al. 2021; Schroeder et al. 2018; G. Birchenough et al. 2019). Imbalanced SCFA profiles have been associated with diseases like obesity, type 2 diabetes, metabolic syndrome and even neurological disorders (Samuel et al. 2008; Ridaura et al. 2013; Canfora et al. 2019; Dalile et al. 2019).

Polysaccharides like dietary fibres are the preferred substrate for gut bacteria. However, when the fibre becomes depleted or the colonic pH is raised, the bacteria can switch to fermentation of other substrates like dietary and host-derived proteins (Ratzke and Gore 2018; Krautkramer, Fan, and Bäckhed 2021). These proteins are first hydrolysed into peptides and amino acids using both the host and microbial enzymes (J. H. Cummings and Macfarlane 1991). Fermentation of the amino acids results in lower amounts of SCFAs and instead products like branched-chain fatty acids (BCFAs), amines, ammonia,

phenols, indoles, sulphides and N-nitroso compounds are formed, some of which are potentially toxic to the host (Smith and Macfarlane 1996; Krautkramer, Fan, and Bäckhed 2021; Fan and Pedersen 2021). A multitude of gut bacteria can catabolise basic amino acids into amines with various biological effects on the host. For example, arginine is catabolised into putrescine which enhances epithelial cell proliferation (Mouillé et al. 2003; Oliphant and Allen-Vercoe 2019). Putrescine can be further metabolised into spermidine or spermine. All three arginine fermentation products improve gut integrity by increasing tight junction protein expression and increasing mucus secretion (Chen et al. 2007; Rao et al. 2012). Arginine can also be used for  $\gamma$ -aminobutyric acid (GABA) production via the formation of glutamate. Alterations in GABA levels and the concomitant anxiety has been observed in mice with IBD (Bravo et al. 2011; Oliphant and Allen-Vercoe 2019). However, GABA can also be used for the production of succinate which can be further converted into propionate. The catabolism of another basic amino acid, lysine, produces cadaverine which has been shown to support cell proliferation and gut barrier function (Nakamura et al. 2021; Bekebrede et al. 2020). However, the host-beneficial effect needs further confirmation as elevated concentrations of cadaverine have also been associated with ulcerative colitis (Le Gall et al. 2011). The aromatic amino acid tyrosine can be converted into tyramine which has been shown to exert toxicity (del Rio et al. 2018).

The lower production of SCFAs during protein fermentation leads to a higher luminal pH, which in turn alters the structure and function of the microbiota (Raba, Adamberg, and Adamberg 2021; Ratzke and Gore 2018; Duncan et al. 2009). These changes in microbial metabolism and community structure can happen already after 24 hours of the diet shift (Desai et al. 2016). A study with mice showed that the microbiota changes induced by prolonged Western style diet, characterised by lowered amounts of dietary fibre, were mostly reversible within a single generation (Sonnenburg et al. 2016). However, continuation of this diet over multiple generations resulted in irreversible extinction of selected species – an effect that progressively worsened with every following generation. Similar effect has been shown in humans in a study comparing the microbiota of non-western population to that of their first- and second-generation immigrants in the USA (Vangay et al. 2018).

A similar microbial community can behave differently under various conditions. The combined effects of transit time, pH and diet largely determine the microbiota composition and their metabolism. Systematic studies of these parameters on a standardised microbial community give valuable insight into the functionality of gut microbiota. Understanding these dynamic relationships could be a key to maximising the beneficial potential of gut microbiota in a wider population.

## 2 Aims of the study

The main aim of this study was to investigate the growth space of faecal microbiota and the enzymatic degradation and co-metabolism of dietary fibres and mucins. The specific aims were as follows:

- Apply continuous culture approach to cultivate complex faecal microbiota on two dietary fibres (pectin and xylan) and porcine gastric mucin. Scan the microbiota growth space under physiologically relevant dilution rates and elucidate the co-metabolism of fibre and mucin.
- Use continuous cultivation to further investigate the combined effect of pH and dilution rate on the growth and metabolism of microbiota co-fermenting mucin and a chosen dietary fibre, pectin.
- Extract a unique substrate – porcine colonic mucin – and use it in the in vitro study of microbial metabolism of a panel of dietary fibres. Compare the results with widely used commercial porcine gastric mucins.
- Determine the microbiota modulating potential of different dietary fibres with various sugars and glycan linkages.
- Apply metaproteomic approach to study the specific dietary fibres and mucins co-degradation mechanisms and metabolic pathways. Combine the high-throughput omics methods with a novel cell culture spheroid model to study the potential effect of the microbial metabolites on goblet cells and mucin production.
- Support the experimental work with a review on the recent advances in characterization of mucin degrading enzymes in relation to human health.

### 3 Materials and Methods

Below is a summary of the methods used in this study. More details for every method are provided in Publications I-II and the supplementary Manuscript.

#### 3.1 In vitro cultivation systems

The continuous cultivations of bacterial growth space studies were carried out in an anaerobic bioreactor system (Biobundle™, Applikon) described in more detail in Publications I and II. In a chemostat culture the cells are kept in a quasi-steady state by controlling the medium inflow and outflow by an algorithm:

$$N = N_0 + a \cdot t$$

where  $N$  is the parameter being changed,  $N_0$  the initial value of the changed parameter,  $a$  the rate of changing the parameter  $N$ , and  $t$  the time.

The aim of Publication I was to elucidate the effect of dilution rate on the faecal microbiota composition and metabolism (Figure 1). The dilution rate was either gradually increased from 0.05 to 0.2 1/h or decreased from 0.2 to 0.05 1/h at a rate of 0.05 units per day (Figure 1). The range of the dilution rates correlated to bacterial specific growth rates, calculated from the colonic transit rate of digesta in people consuming Western diets, that ranges between 40-140 h, and the estimated number of bacteria which ranges from  $10^8$  to  $10^{11}$  cfu/g between the proximal colon and faeces. Samples were collected from the bioreactors after every 0.01 D-units (1/h) and centrifuged at 14,000 g and 4 °C for 5 min. The cell pellets and supernatants were stored at -80 °C or -20 °C, respectively, until further analyses.

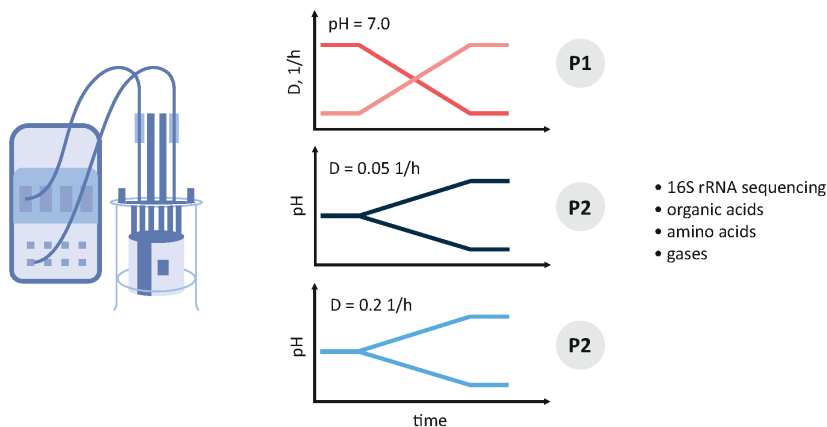


Figure 1. Schematic representation of the in vitro continuous cultivations from Publications I-II. The cultivations were carried out in bioreactor systems where the culture was first stabilised, followed by smooth change of either the dilution rate (P1) or the pH (P2), keeping the cells in a quasi-steady state. P1 – Publication I, P2 – Publication II, D – dilution rate.

The combined effect of pH and dilution rate on microbial composition and metabolism was studied in Publication II. The dilution rate was kept at constant  $D = 0.05$  or  $D = 0.2$  1/h and the pH either gradually increased from 7.0 to 8.0 or decreased from 7.0 to 6.0 (Figure 1). The pH was controlled by the addition of 1M NaOH. The dilution rates were chosen to represent slow and fast colonic transit rates. The tested pH range was chosen

to mimic both the healthy colonic pH (pH = 6.1-7.5) and an inflamed colon (pH up to 8). Samples were collected from the outflow after every 0.05 pH-units, separated into cell pellets and supernatants and stored at -80 or -20 °C, respectively, until further analyses. Details of culture conditions are provided in Publication II.

Co-metabolism of dietary fibres and mucins was studied in the supplementary Manuscript by batch cultivations in an isothermal microcalorimeter (TAM IV, TA Instruments). The cultures were grown in anaerobic conditions in sterile hermetically sealed glass vials (Figure 2). The samples were collected after 72h of incubation, separated into cell pellets and supernatants and stored at -80 and -20 °C, respectively, until further analyses.

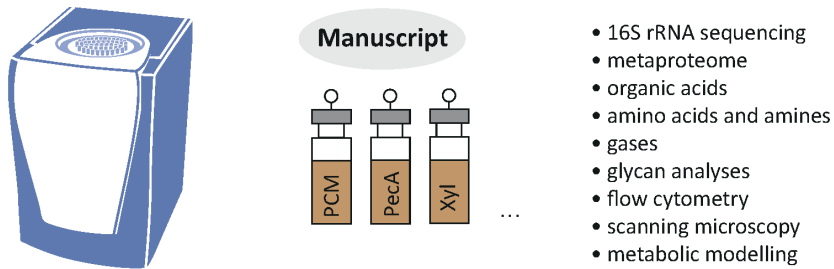


Figure 2. Scheme of batch cultivations, done in an isothermal microcalorimeter using hermetically sealed sterile glass vials. The medium in each vial was supplemented with the selected dietary fibre and/or mucin. PCM – porcine colonic mucin, PecA – apple pectin, Xyl – xylan.

An in-house prepared defined growth medium (pH = 7.2 ± 0.1) was used in all cultivations (see Publications I-II and Manuscript for the medium composition). The medium was supplemented with 2.5 g/L of the chosen dietary fibre and/or mucin, depending on the study (Table 1). The porcine colonic mucin (PCM), used in Manuscript was in-house extracted from flushed porcine colons, acquired from a local butcher (Saaremaa Meat Factory).

Table 1. List of substrates used in the Publications I-II and the Manuscript.

Publication	Cultivation method	Substrate	Supplier
P1	Chemostat, A-stat, De-stat	Beechwood xylan (Xyl)	Sigma-Aldrich (USA)
P1	Chemostat, A-stat, De-stat	Apple pectin (PecA)	Sigma-Aldrich (USA)
P2	D-stat	Apple pectin (PecA)	Sigma-Aldrich (USA)
Manuscript	Batch	Arabinogalactan (AG)	Sigma-Aldrich (USA)
Manuscript	Batch	Amylopectin (AP)	Sigma-Aldrich (USA)
Manuscript	Batch	β-glucan (B-gluc)	UNDERSUN BIOMEDTECH (China)
Manuscript	Batch	K-carrageenan (Car)	Sigma-Aldrich (USA)



Manuscript	Batch	Furcellaran (Fur)	Est-Agar AS (Estonia)
Manuscript	Batch	Galactooligosaccharides (GOS)	Friesland Campina (The Netherlands)
Manuscript	Batch	Dahlia inulin (InuD)	Sigma-Aldrich (USA)
Manuscript	Batch	High-performance inulin (InuHP)	Beneo Orafti (Belgium)
Manuscript	Batch	High-soluble inulin (InuHSI)	Beneo Orafti (Belgium)
Manuscript	Batch	Apple pectin (PecA)	Sigma-Aldrich (USA)
Manuscript	Batch	Citrus pectin (PecC)	Sigma-Aldrich (USA)
Manuscript	Batch	Psyllium (Psy)	Caremoli (Italy)
Manuscript	Batch	Xylooligosaccharides (XOS)	Anhui Elite Ind Co (China)
Manuscript	Batch	Beechwood xylan (Xyl)	Sigma-Aldrich (USA)
Manuscript	Batch	Porcine gastric mucin, Type II (PGM)	Sigma-Aldrich (USA)
Manuscript	Batch	Porcine colonic mucin (PCM)	In-house

All cultures in Publications I-II and Manuscript were inoculated with aliquots of the same microbial consortium prepared from pooled faecal samples from seven healthy adult donors. This strategy allowed us to overcome the interindividual differences in community while enabling to draw conclusions based on the studied parameter and compare the results of each study. The collection and handling of faecal samples was approved by the Tallinn Medical Research Ethics Committee, Estonia (protocol No. 554).

### 3.2 DNA extraction, sequencing and bioinformatics

DNA was extracted from the cell pellets using PureLink Microbiome DNA extraction kit (Thermo Fisher Scientific). The amplicons of Publication I were sequenced using Illumina MiSeq 2 x 150 v2 platform in Estonian Genome Centre, University of Tartu, Estonia. The sequencing libraries of Publication II and Manuscript were prepared in-house with Nextera XT Index Kit (Illumina) and the pooled libraries were sequenced using Illumina iSeq 100 platform and i1 reagent kit.

The DNA sequence data was analysed with BION-meta ([www.box.com/bion](http://www.box.com/bion)). The consensus reads were aligned to the SILVA reference 16S rDNA database v123 (Publications I and II) or v138 (Manuscript). The relative data of bacterial abundances from 16S rRNA sequencing was converted into quantitative values ( $X_i$ , g/L) using formula:

$$X_i = X_t \cdot A_i$$

where  $i$  is the bacterial taxon,  $X_t$  is the dry weight of the total biomass (g/l) and  $A_i$  is the relative abundance of taxon  $i$  in the sample.

### 3.3 Analysis of microbial metabolites

The culture supernatants were purified using 3 kDa cut-off filters (Amicon® Ultra 0.5 Filters, Merck). The concentrations of organic acids were measured by high-performance liquid chromatography (HPLC; Alliance 2795 system, Waters) equipped with Aminex HPX-87H column (1,300 x 7.8 mm, 9 µm particle size; BioRad). Refractive index (RI; model 2414, Waters) and UV (210 nm; model 2487, Waters) detectors were used for quantification. The chromatographic data were processed with Empower software (Waters).

Amines and free amino acids were determined with ultra-performance liquid chromatography (UPLC; Acquity, Waters). The standards and samples were derivatised using AccQ-Tag™ Ultra Derivatization Kit (Waters) and loaded onto AccQ-Tag Ultra RP column (2.1x100 mm, 1.7 µm particle size, 130 Å pore size; Waters). Photodiode array detector (PDA; 260 nm) was used for quantification. The data were processed with Empower 2 software (Waters).

The gas composition was analysed using gas chromatography (Agilent 490 MicroGC Biogas Analyzer, Agilent 269 Technologies Ltd.). CP-Molsieve 5A and CP-PoraPLOT U capillary columns and a thermal conductivity detector (TCD) were used for separation and quantification of gases. The gas volume of bioreactors in Publications I and II were recorded with MilliGascounter (Ritter).

### 3.4 Metaproteomics

The microbial cell pellets were dissolved in 60 µl of lysis buffer, heated at 95 °C for 5 minutes and ultrasonicated. Heating and sonication were repeated twice before centrifugation at 14,000 g for 5 min. The cell lysates (30 µl) were digested with LysC and trypsin using 30 kDa cut-off filters (NanoSep, Pall Life Sciences) according to Filter Aided Sample Preparation (FASP) protocol (Wiśniewski et al. 2009). The peptides were acidified with trifluoroacetic acid (TFA) to a final concentration of 0.5 % and 15 µg of peptides were cleaned and stored on C18-StageTip filters (Rappsilber, Mann, and Ishihama 2007) at -20 °C until analysis.

The peptides were analysed in triplicates with an EASY-nLC 1000 system (Thermo Fisher Scientific) connected to a Q-Exactive HF hybrid quadrupole-Orbitrap mass spectrometer (Thermo Fisher Scientific) through a nano electrospray ion source. The peptides were separated with an in-house packed column (150 x 0.075 mm; New Objective, Woburn; Reprosil-Pur C18-AQ 3 µm particles; Dr Maisch). Full mass spectra were acquired over a mass range 400-1600 m/z with a resolution of 60,000 (m/z 200) after accumulation of ions to a 3e6 target value based on predictive AGC from the previous full scan. Twelve most intense peaks with a charge state  $\geq 2$  were fragmented in the HCD collision cell with normalized collision energy of 27%, and tandem mass spectra were acquired in the Orbitrap mass analyzer with resolution of 15,000 and AGC target value of 1e5. The dynamic exclusion was 30 s and the maximum allowed ion accumulation times were 20 ms for full MS scans and 50 ms for tandem MS.

A custom database was constructed for the metaproteomic searches (see Manuscript). Protein sequences for each taxon in the custom database were downloaded from UniProt database (2021.01.14, uniprot.org), reference proteomes preferred where possible. The final custom database contained 291 bacterial as well as pig and human proteomes and was used for the final analysis of MS/MS spectra with MaxQuant (version 1.4) (Cox and Mann 2008).

### 3.5 Analysis of carbohydrate metabolism

All identified proteins were annotated for CAZymes using dbCAN (<http://bcb.unl.edu/dbCAN2/blast.php>). An automatic CAZyme annotation was carried out with three bioinformatic tools: HMMER, DIAMOND and Hotpep.

### 3.6 Mucin analyses

The protein composition of porcine gastric and colonic mucins (PGM and PCM, respectively) was analysed with MS system as described for metaproteomics. The raw MS/MS spectra were searched with MaxQuant (version 1.6.11.0) (Cox and Mann 2008) against pig database downloaded from UniProt (2020.09.12).

Porcine gastric and colonic mucins were separated on composite agarose-polyacrylamide (AgPAGE) gel, prepared according to the protocol of Schulz et al. (Schulz, Packer, and Karlsson 2002) and stained with Alcian blue.

The *O*-glycans of the porcine mucins were separated on an in-house packed column (10 cm x 250  $\mu$ m, 5  $\mu$ m porous graphite particles; Hypercarb, Thermo-Hypersil) and analysed by LC-ESI/MS (Thermo Electron).

### 3.7 Spheroid culture

The spheroid cultures were generated from distal colon crypts isolated from transgenic mice carrying mCherry-tagged human MUC2 (RedMUC2<sup>98trTg</sup>) (G. M. H. Birchenough et al. 2016; Miyoshi and Stappenbeck 2013) and used at passage numbers 11-16 for all assays. A wild-type (C57BL/6N; Taconic) mouse distal colon spheroid line was maintained simultaneously and used at passage numbers 15-20 as a negative control in all assays. The spheroid maintaining conditions and medium are described in more detail in Manuscript.

All animal work was approved by the Swedish Laboratory Animal Ethic Committee in Gothenburg, Sweden (ethical permits 2285-19, 3006-20) and conducted following the guidelines of Swedish animal welfare legislation.

### 3.8 Flow cytometry

The effect of microbial metabolites on the intestinal cells was studied by treating the colonic spheroids with culture supernatants and analysing the cells with the flow cytometer (Beckman Coulter Life Sciences). The assay setup and analysis are described in more detail in Manuscript.

### 3.9 Construction of metabolic networks and Flux Balance Analysis

The 100 most abundant taxa were divided into eight groups based on similar metabolism. Combined metabolic networks for each group were built based on information from public databases and combined to create a consortium type network. The relative abundances of different species in consortia were used to calculate stoichiometric coefficients. The final consortia metabolic network consisted of 2774 metabolites and 3752 reactions.

The Flux Balance Analysis (FBA) model was generated in Wolfram Mathematica (version 8.01) using in-house software built in MatLab (Orth, Thiele, and Palsson 2010). The FBA calculations were performed with an increasing automatic error step of  $\pm 1\%$  to input fluxes until a feasible solution was found.

### **3.10 Sequence-based metabolism mapping from metaproteomics**

The metabolism of faecal cultures in Manuscript was mapped using an in-house database of bacterial metabolism. The DNA sequences for enzymes for key metabolic reactions were selected from the database and BLASTed using a local NCBI blastx function. The resulting amino acid sequences were then mapped to the peptides from the metaproteomic analysis. The sum of matching peptides per taxon was considered as protein copy number. The taxa were divided into similar metabolic groups as in the metabolic networks of the Flux Balance Analysis.

## 4 Results and discussion

This dissertation is based on three publications and an additional manuscript (in preparation) studying the growth space of microbiota and the enzymatic degradation and co-metabolism of dietary fibres and mucin. The main results are presented as a summary and divided into sections. Detailed discussions are found in Publications I-III and the Manuscript.

### 4.1 The growth space of gut bacteria

#### 4.1.1 Dilution rate selectively enhances slow- or fast-growing bacteria (Publication I)

Continuous cultures are powerful tools for in vitro microbiota studies. They allow precise control over parameters such as substrate concentration, dilution rate and pH, making it possible to mimic various physiological conditions. Gut transit time is an important parameter that determines the specific growth rate of microbes in the gut and it has been shown that slow or fast transit time results in different microbiota. Hence, continuous culture approach was chosen to get more insight into the growth and metabolism of microbiota. The dilution rate of continuous culture imitates gut transit rate and is directly related to cell specific growth rate by controlling the availability of the substrate. The effect of dilution rate on the microbial community composition and metabolism was studied with a series of chemostat cultivations. The dilution rate was either gradually increased from 0.05 → 0.2 1/h (A-stat) or decreased from 0.2 → 0.05 1/h (De-stat) (Figure 1). The growth medium was supplemented with either apple pectin or beechwood xylan as the dietary fibre source and porcine gastric mucin as the *O*-glycan source (Table 1).

The dilution rate had a significant modulatory effect on the microbial composition. The growth of mucolytic *Akkermansia muciniphila* was significantly enhanced by lower dilution rate (Figure 3). In contrast, taxa such as *Bifidobacterium*, *Faecalibacterium* sp. and a group of Lachnospiraceae were significantly increased at  $D_{high}$ . These results agree with previous in vivo studies where the genera *Akkermansia* and *Ruminococcus* were found to be more prevalent in people with slow colonic transit, while Lachnospiraceae and *Bifidobacterium* correlate positively with high transit rate (Roager et al. 2016; Vandeputte et al. 2016; K. Adamberg and Adamberg 2018). The genus *Bacteroides* remained the prevailing taxon in all cultures at all dilution rates, demonstrating its key role in the dietary fibre degradation. Some taxa were selectively enriched by a specific substrate, especially Ruminococcaceae group UCG-013 which was one of the most abundant taxa on pectin but was never detected in the xylan-containing medium.

The production of acetate was highly substrate-specific, with almost twice as much acetate produced from pectin than from xylan (Figure 4). This is likely due to the methylated and acetylated backbone of pectin which is easily converted into acetate and carbon dioxide. As acetate made up nearly two thirds of all fermentation products at all dilution rates, it meant that the carbon balance ( $C_{substrates} - C_{products}$ ) was higher in xylan-containing medium. The formation of other metabolites, especially propionate and  $CO_2$ , was strongly dilution rate-dependent. The concentrations of propionate and  $CO_2$  were significantly higher at  $D_{low}$ , positively correlating with the increased abundance of propiogenic *A. muciniphila* at the same conditions. The anaerobic reductive TCA cycle decarboxylation of succinate into propionate and  $CO_2$  is beneficial as means to spend excess NADH. Notably more  $CO_2$  formed from pectin than from xylan. Interestingly,

although the abundances of butyrate producers (*Faecalibacterium sp.* and *Lachnospiraceae*) grew along with the increasing dilution rate, the concentrations of butyrate remained stable, indicating that other metabolites were produced instead (Figure 3 and Figure 4). These results establish the key role of dilution rate in the development of microbial community and its metabolism.

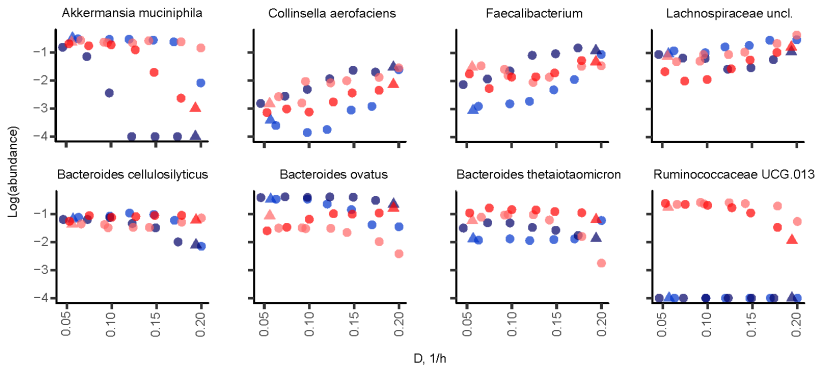


Figure 3. Bacterial taxa enriched on apple pectin (red) and xylan (blue) during A-stat (light colour) and De-stat (dark colour) cultivations. Samples were divided into groups ( $D < 0.07$  and  $D > 0.17$ ) for which mean values and standard deviations were calculated. Statistical significance was evaluated with a single parametric t-test with Benjamini-Hochberg correction and differences in groups were considered significant when  $p < 0.05$ . D - dilution rate (1/h).

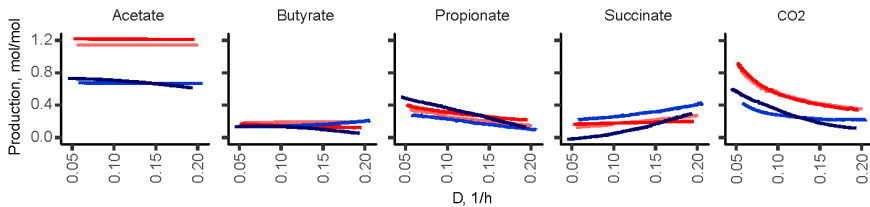


Figure 4. Fermentation product yields per carbohydrate consumed (mol/mol) on apple pectin (red) and xylan (blue) during A-stat (light colour) and De-stat (dark colour). Samples were divided into groups ( $D < 0.07$  and  $D > 0.17$ ) for which mean values and standard deviations were calculated. Statistical significance was evaluated with a single parametric t-test with Benjamini-Hochberg correction and differences in groups were considered significant when  $p < 0.05$ . D – dilution rate (1/h).

#### 4.1.2 The pH and the dilution rate induce changes in the dynamics of mucus-degrading species (Publication II)

The pH of the gastrointestinal tract varies spatially and is highly dependent on the individual's dietary habits and health. However, the data on the influence of pH on the development and metabolism of colonic microbiota are scarce. The combined effect of pH and dilution rate on the composition and metabolism of faecal microbiota was studied with changestat cultures. The pH was either smoothly increased from 7.0  $\rightarrow$  8.0 or decreased from 7.0  $\rightarrow$  6.0 (Figure 1). The cultivations were repeated at high and low dilution rates ( $D_{\text{high}} = 0.2$  1/h,  $D_{\text{low}} = 0.05$  1/h). Apple pectin was used as a source of dietary fibre and porcine gastric mucin as a source of mucin-type glycans (Table 1).

The most abundant taxon at both dilution rates and the whole pH range was *Bacteroides ovatus* (combining *B. ovatus*, *B. thetaiotaomicron* and *B. xylanisolvens* which could not be differentiated with the chosen sequencing method) (Figure 5). This is in line with the results from Publication I, showing central role of *Bacteroides* in dietary fibre degradation. Yet, some *Bacteroides* species were sensitive to pH, with *B. caccae* and *B. vulgatus* growing to higher abundance at lower pH, while *B. cellulosilyticus* and *B. uniformis* preferred higher pH (Figure 5). The concentrations of acetate, one of the main metabolites of *Bacteroides*, remained stable throughout the tested pH range (Figure 6). These results highlight that the colonic pH could be a crucial factor in determining the viability of various *Bacteroides* species in the gut, which in turn is important for maintaining colonic homeostasis and health due to their primary role in dietary fibre degradation.

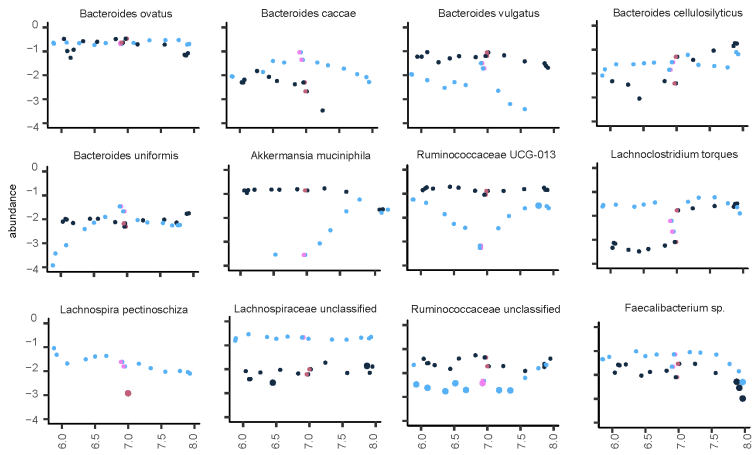


Figure 5. The dynamic changes in bacterial abundances (log scale) between pH 6.0 and 8.0 at dilution rates  $D_{low} = 0.05$  1/h (dark blue) and  $D_{high} = 0.2$  1/h (light blue). Dark and light pink dots indicate the steady state conditions at pH 7.0, at  $D_{low}$  and  $D_{high}$ , respectively. Samples were divided into groups (pH < 6.5 and pH > 0.7.5) for which mean values and standard deviations were calculated. Statistical significance was evaluated with a single parametric t-test with Benjamini-Hochberg correction and differences in groups were considered significant when  $p < 0.05$ . D – dilution rate.

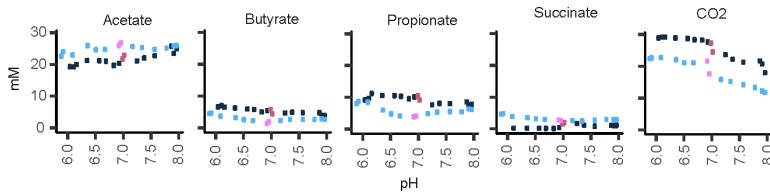


Figure 6. Fermentation product yields (mM) in pectin supplemented medium between pH 6.0 and 8.0 at dilution rates  $D_{low}=0.05$  1/h (dark blue) and  $D_{high} = 0.2$  1/h (light blue). Dark and light pink dots indicate the steady state conditions at pH 7.0, at  $D_{low}$  and  $D_{high}$ , respectively. Samples were divided into groups (pH < 6.5 and pH > 0.7.5) for which mean values and standard deviations were calculated. Statistical significance was evaluated with a single parametric t-test with Benjamini-Hochberg correction and differences in groups were considered significant when  $p < 0.05$ . D – dilution rate.

Extending the results from Publication I, *A. muciniphila* was among the most abundant taxa at  $D_{low}$  at the whole pH range (Figure 5). However, a surprising effect was seen at  $D_{high}$  where the growth was significantly pH-dependent. *A. muciniphila* was not able to compete and was washed out of the consortium at  $pH < 6.5$  ( $D_{high}$ ) but grew into elevated abundance at  $pH < 7.5$ . The other slow-growing mucolytic taxon, Ruminococcaceae UCG-013 group, was also more pH-sensitive at  $D_{high}$ , while remaining one of the most abundant species at  $D_{low}$ . In contrast, mucolytic *Lachnospiraceae* *Lachnospira pectinoschiza* and *Bacteroides caccae* had stable growths throughout the whole pH range at  $D_{high}$ , whereas their growth was significantly affected by the pH at  $D_{low}$ . *Lachnospira pectinoschiza* was among the most abundant species at  $D_{high}$ , whereas it remained undetected at  $D_{low}$ . Moreover, *Lachnospiraceae* unclassified preferred  $D_{high}$ , while Ruminococcaceae unclassified grew into higher abundance at  $D_{low}$ . Interestingly, both the abundance of commensal mucolytic *Faecalibacterium sp.* and the concentration of its main metabolite, butyrate, significantly decreased at  $pH < 7.5$  (Figure 5 and Figure 6). The decrease of butyrogenic species at higher pH agrees with previous studies showing a similar effect (Chung et al. 2016; Reichardt et al. 2018). Butyrate is used by the epithelial cells to create oxygen gradient in the intestinal crypts which is required for maintaining homeostasis (Allaire et al. 2018). The concentrations of propionate followed the abundances of propiogenic *A. muciniphila*, Ruminococcaceae UCG-013 and *Bacteroides ovatus* (Figure 5 and Figure 6). Propionate has been shown to promote epithelial turnover via enhancing cell speed (Bilotta et al. 2021). These pH- and dilution rate-sensitive shifts in the mucolytic species and their metabolites are likely to have an immense role on the epithelium and the mucus layer. Changes in the mucus composition and penetrability are heavily linked with diseases such as IBD and obesity (Johansson et al. 2014; Schirmer et al. 2018; Schroeder et al. 2020; Coleman and Haller 2021). Thereby the changes in mucin degradation and metabolism have important health concerns and warrant further studies.

#### **4.1.3 Complex dietary fibres support the development of highly diverse consortia (Manuscript)**

The dilution rate and pH were shown to be powerful modulators of the gut microbiota composition and metabolism. Both parameters are heavily influenced by the host diet, especially the consumption of dietary fibres. Fibres help to bind water to the chyme, thereby affecting the gut transit rate. Moreover, the degradation of fibres by microbiota produces metabolites such as short-chain fatty acids and amines which change the colonic pH. Different fibres have been shown to modulate the microbiota composition on species level. In addition, the more complex-structured fibres increase the gut microbiota diversity via crosstalk that is needed to break down complex glycans. A panel of 14 dietary fibres and oligosaccharides was used to study in vitro their potential to increase microbiota diversity (Table 1). The batch cultivations were carried out in a microcalorimeter system suitable for high-throughput screening (Figure 2).

The complexity of the fibre determined the growth of the consortia (Figure 7). Oligosaccharides and fibres with simple linear structure were fermented rapidly in single step, whereas the fibres with more complex bonds were degraded slowly in multiple phases (Figure 7a). The slow multiphasic degradation reflects the need for specialist taxa and/or crosstalk between the members of the microbiota. Indeed, the sequencing data revealed the communities grown on simple glycans to be less diverse, consisting mainly of fast-growing taxa such as *Bifidobacterium* (Figure 7b). As the complexity of fibre increased, so did the diversity of consortia, especially the amounts of various *Bacteroides*



species. The genus *Bacteroides* has been shown to be especially adapted to dietary fibre fermentation due to their large genomes that encode a variety of enzymes for polysaccharide degradation (Drula et al. 2022). With every fibre, the addition of porcine gastric mucin (PGM) prolonged the degradation and increased the microbiota diversity due to the need for additional enzymes for the breakdown of complex *O*-glycans (Figure 7). Interestingly, with poorly degradable viscous psyllium and the algal fibres furcellaran and  $\kappa$ -carrageenan, the addition of PGM resulted in a community similar to that of sole PGM (Figure 7b, Publication III Figures S1 and S2). This shows that in the absence of fermentable fibre, the community develops to specialize on host *O*-glycan utilization.

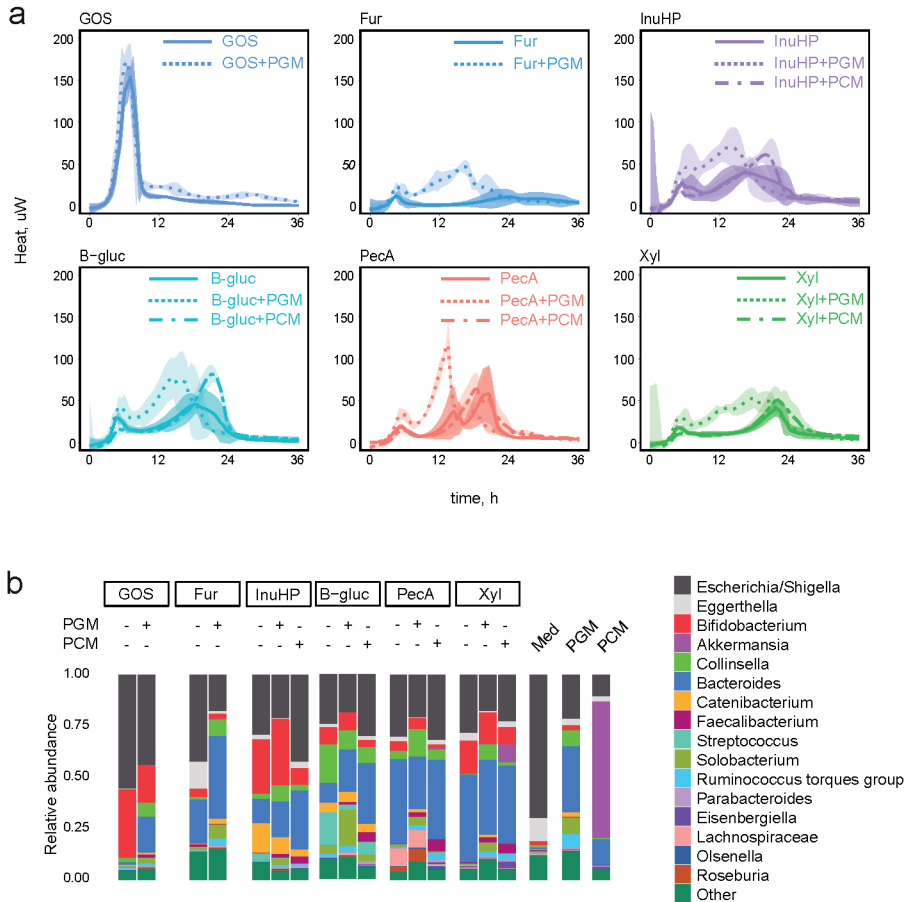


**Figure 7. Fermentation of dietary fibres and oligosaccharides by faecal microbiota. a, Heat evolution of selected substrate fermentation. Solid line represents average microbial growth curve on the selected poly- or oligosaccharide  $\pm$  95% CI, dotted line represents average microbial growth curve on the selected poly- or oligosaccharide + mucin  $\pm$  95% CI.  $n=2-7$ . b, Community composition on the selected substrates based on 16S rRNA sequencing. Average relative abundances of the top 17 genera.  $n=2-7$ . GOS – galactooligosaccharides, Fur – furcellaran, InuHP – high-performance inulin, B-gluc –  $\beta$ -glucan, PecA – apple pectin, Xyl – xylan, PGM – porcine gastric mucin, PCM – porcine colonic mucin, Med – growth medium control.**

The initial screening of the dietary fibre panel was done with a commercially available porcine gastric mucin as the *O*-glycan source. However, it is known that the mucin type varies along the gastrointestinal tract, with MUC5AC and MUC2 as the main mucins of the stomach and colon, respectively (Figure 8). On top of that, the two mucins share only 8% of their glycans, are differentially modified and our analysis suggests PGM to be severely hydrolysed (Figure 8, Publication III Figure S3). These differences are likely to significantly affect which bacteria can metabolise the glycans and thereby influence the consortia composition. PCM was in-house produced as a source of colonic *O*-glycans. The PCM was used in combination with three dietary fibres chosen for in-depth study of fibre and mucin co-fermentation: apple pectin, xylan and  $\beta$ -glucan (Figure 7). The fibres were chosen based on their distinctly different structures which require specific enzymes encoded in different bacteria for the degradation. A known prebiotic high-performance inulin was included as an easily degradable control.

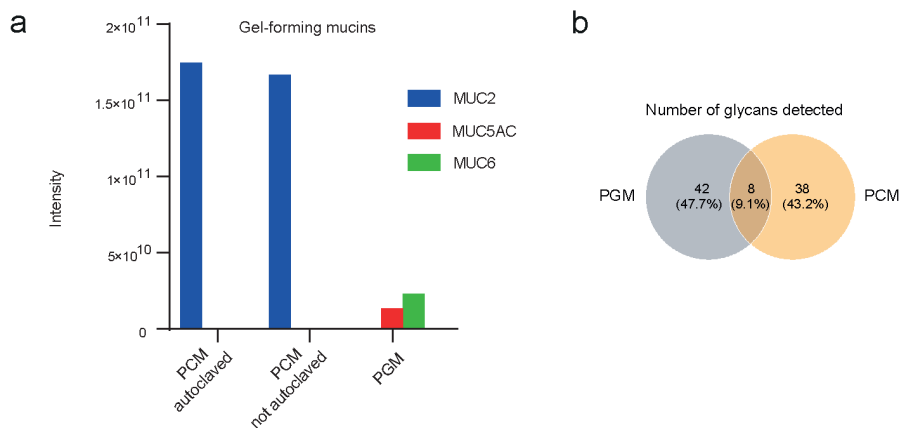


Figure 8. Analysis of PGM and PCM composition. **a**, Gel-forming mucins detected in different mucin samples by mass-spectrometry. **b**, The number of different glycans identified from PGM and PCM. MUC2 – Mucin-2, MUC5AC – Mucin-5AC, MUC6 – Mucin-6, PCM – porcine colonic mucin, PGM – porcine gastric mucin.

Compared to fibre+PGM, the PCM in combination with fibre enhanced the growth of gut commensals *Bacteroides* and *Faecalibacterium* and decreased the abundances of an opportunistic pathogen *Solobacterium* and a pathobiont *Collinsella* (Figure 7). Surprisingly, *A. muciniphila*, which did not grow on PGM or on any of its combinations with fibres, dominated the culture grown on PCM and was highly abundant on the combination of xylan+PCM (Figure 7). The most abundant taxa on inulin were *Catenibacterium* sp. and *Bifidobacterium* (Publication III Figure S5). The high abundances of *Collinsella*, *Streptococcus* and *Solobacterium* were characteristic to  $\beta$ -glucan fermentation. The fermentation of complex fibres pectin and xylan in combination with PCM boosted the growth of various *Bacteroides* species. Pectin selectively increased the abundance of *B. thetaiotaomicron* and *B. vulgatus*, while xylan enhanced the growth of *B. vulgatus* and unclassified *Bacteroides* (comprised of *B. acidifaciens*, *B. finegoldii*, *B. ovatus*, *B. xylanisolvens* and others which are inseparable with the used sequencing method) (Figure 9). Furthermore, known mucolytic *Bacteroides* species, such as *B. fragilis* and *B. caccae* abundances increased on fibre+PCM. These results further confirm *Bacteroides* central role in complex polysaccharide degradation. Interestingly, *Faecalibacterium*

*prausnitzii* and *Parabacteroides merdae* were able to grow only if both the fibre and mucin were available (Figure 9). For some species, such as *Ruminococcus torques* and *Eisenbergiella tayi*, the abundance was driven by PCM in combination with complex fibres pectin and xylan. *R. torques* is a known mucolytic species, while little is known of the butyrogenic *E. tayi* (Tailford, Crost, et al. 2015; Bernard et al. 2017). However, its concomitant growth with *A. muciniphila* is interesting and warrants a further investigation. Together, these results show how the more complex glycans induce the diversity of gut microbiota, especially by enhancing the growth of *Bacteroides*.

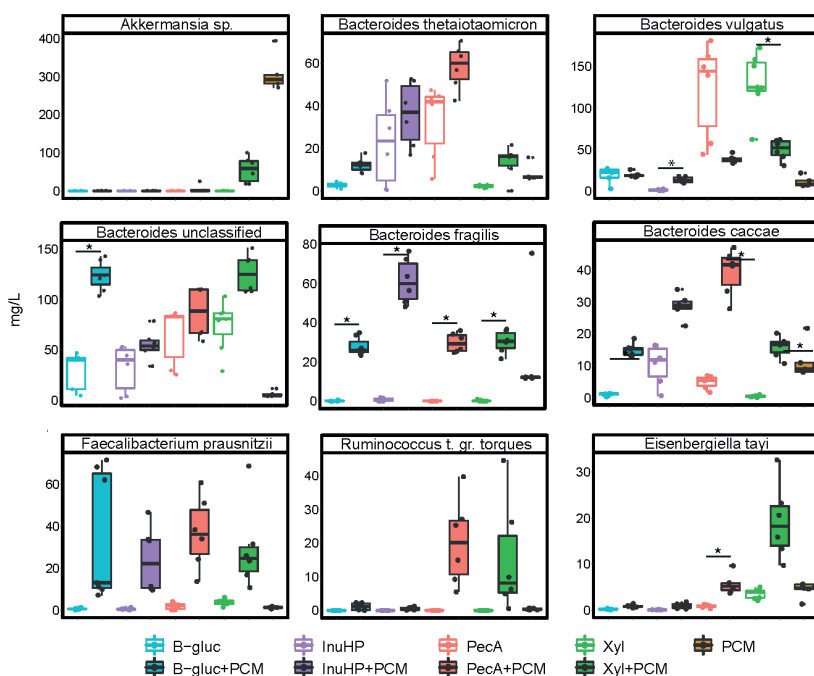


Figure 9. Boxplots showing changes in microbial numbers (mg/l) grown on the selected substrates. Colors indicate the choice of substrate, empty boxes represent samples from cultivation of fibre, filled boxes represent samples from cultivation of fibre+PCM or sole PCM. All replicates shown (two-tailed paired t-test, \* $p < 0.05$ ). B-gluc –  $\beta$ -glucan, InuHP – high-performance inulin, PecA – apple pectin, Xyl – xylan, PCM – porcine colonic mucin.

Systematic studies where a standardised microbial community is grown under various physiologically relevant conditions reveal the microbiota growth space. This information is crucial to make population-wide claims on how the microbiota could react to dietary interventions such as pre- and probiotics.

## 4.2 Microbiota co-metabolism of dietary fibres and mucins

### 4.2.1 The degradation of complex dietary fibres and mucin requires enzymes from several CAZyme families (Publication III and Manuscript)

The degradation of dietary fibres by gut bacteria has been studied previously and the information has been gathered into public databases which are continuously updated (Drula et al. 2022; Barbeyron et al. 2016). However, the gastrointestinal tract is covered

with another glycan source, the mucin. Some members of the microbiota can degrade mucin. Specific species and mucin degradation patterns are associated with diseases such as IBD and obesity. Yet, due to the unavailability of a suitable substrate the studies of colonic mucin degradation are scarce. It has remained unclear how the utilization of colonic mucin glycans affects the degradation of dietary fibres by the human microbiota. The co-metabolism of PCM in combination with inulin,  $\beta$ -glucan, pectin and xylan by faecal microbiota was studied by metaproteomics (Figure 10).

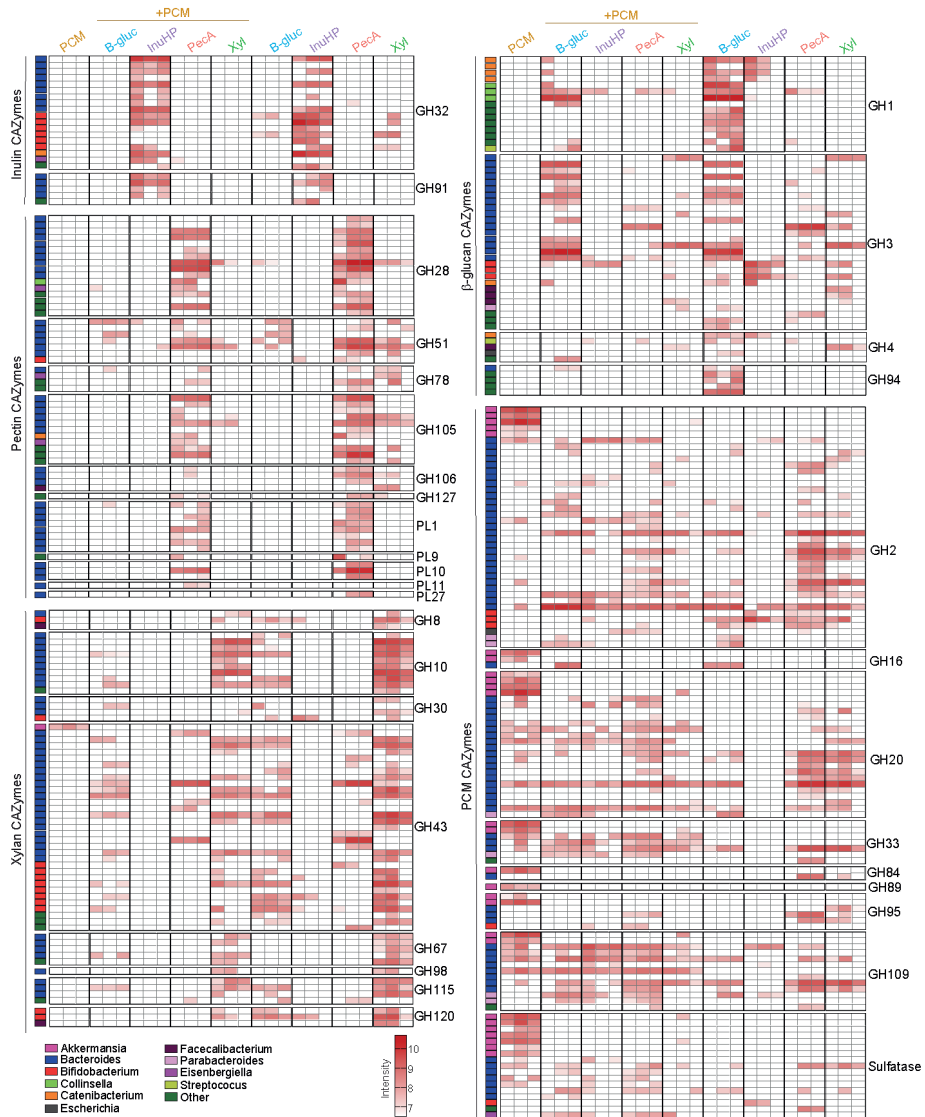


Figure 10. The CAZymes detected after community growth on selected substrates. Enzymes grouped by CAZyme families are shown as intensity of the protein level. For each protein the respective bacterial genus is displayed colour coded on the left side. Three independent replicates are shown. For accession numbers and full data see Publication III. PCM – porcine colonic mucin, B-gluc –  $\beta$ -glucan, InuHP – high-performance inulin, Peca – apple pectin, Xyl – xylan.

The metaproteomic analysis with custom database detected over 21,000 protein groups, out of which ca 3% were directly related to carbohydrate metabolism. Inulin was primarily degraded by *Bifidobacterium*, *Bacteroides* and *Catenibacterium* species, consistent with community composition analysis results (Publication III Figure S5). The glycoside hydrolases used for inulin degradation belonged to GH families 32 and 91 which have been previously reported as fructose-active enzymes (Drula et al. 2022) (Figure 10).

$\beta$ -glucan degradation was carried out by enzymes from GH families 1, 3 and 94, which cleave the  $\beta$ -glucose linkages (Figure 10). Although *Collinsella* and *Streptococcus* were among the most abundant taxa on  $\beta$ -glucan, only a few CAZymes were detected from them: four from *Collinsella* and one from *Streptococcus*. However, three of these enzymes were highly expressed on  $\beta$ -glucan, suggesting their central role in  $\beta$ -glucan degradation (Figure 10).

The degradation of pectin relied heavily on *Bacteroides* species (Figure 10). Pectin is a complex-structured dietary fibre consisting of three main polysaccharides: homogalacturonan and rhamnogalacturonan (RG) I and II. Several enzymes were detected which are known to be associated specifically with the degradation of RG I:  $\beta$ -galactosidases (GH2), polygalacturonases (GH28), arabinofuranosidases (GH51 and GH43), unsaturated rhamnogalacturonyl hydrolases (GH105), rhamnosidases (GH106) and lyases of families 1, 9, 10 and 11. RG II is one of the most complex polysaccharides in nature and thus required additional enzymes for its breakdown, such as sialidases (GH33), aceric acid hydrolases (GH127), rhamnosidases (GH78) and  $\alpha$ -galactosidases (GH95) (Figure 10). Some of the detected enzymes have been previously established as critical for the degradation of pectin, namely a PL1 enzyme (Ndeh et al. 2017) and an enzyme from PL27 enzyme (Munoz-Munoz et al. 2017).

Similar to pectin, the degradation of xylan was associated mainly with *Bacteroides* species (Figure 10). The degradation was mainly carried out by  $\beta$ -xylanases,  $\beta$ -glucuronidases, arabinofuranosidases and  $\beta$ -xylosidases from GH families 10, 30, 43, 51, 67, 98, 115 and 120, several of which are found in previously characterised *B. ovatus* xylan polysaccharide utilization loci (Rogowski et al. 2015). Interestingly, on both pectin and xylan, the number of CAZymes from *B. vulgatus* was higher in the absence of mucin.

The degradation of sole PCM was mainly carried out by *A. muciniphila*, positively correlating with its high abundance in the culture (Figure 7 and Figure 10). The addition of fibres to PCM increased the abundances and the number of CAZymes detected from mucolytic *Bacteroides* species, such as *B. caccae*, *B. fragilis* and *B. thetaiotaomicron*. Some of the detected enzymes [Amuc 1835 (GH33), Amuc 1120 (GH95), Amuc 0290 (GH2) and Amuc 1220 (GH89)] have been shown to be crucial for the growth of *A. muciniphila* on PGM (Davey et al. 2022). On the other hand, the endo-active *O*-glycanases from GH16 (Crouch et al. 2020) were only detected on sole PCM without fibre. Additionally, mucin *O*-glycan degradation increased the expression of  $\beta$ -galactosidases from GH2,  $\beta$ -N-acetylglucosaminidases from GH20 and GH84,  $\alpha$ -fucosidases from GH29 and GH95,  $\alpha$ -N-acetylglucosaminidases from GH89 and sialidases from GH33. Moreover, multiple sulfatases from *A. muciniphila*, *B. fragilis* and *B. ovatus* were detected, implying their important role in the removal of the protective sulphate groups from mucin *O*-glycans. The information about dietary fibre co-degradation with colonic mucin by complex faecal microbiota is crucial to elucidate the potential prebiotic effect of the fibre. The metaproteome-level analysis gives insight how various bacteria and their metabolism is affected by the dietary fibre supplement. Moreover, we identified several new, potentially substrate-specific CAZymes.

### 4.2.2 *Akkermansia muciniphila* degrades the mucin protein in co-culture (Manuscript)

The bacterial metabolism was evaluated by measuring the metabolites from spent medium and by mapping the metaproteome data to metabolic pathways. The culture grown on sole PCM had the highest concentration of propionate and the highest number of propionate synthesis enzymes, which is characteristic to *A. muciniphila* who dominated this community (Figure 7 and Figure 11).

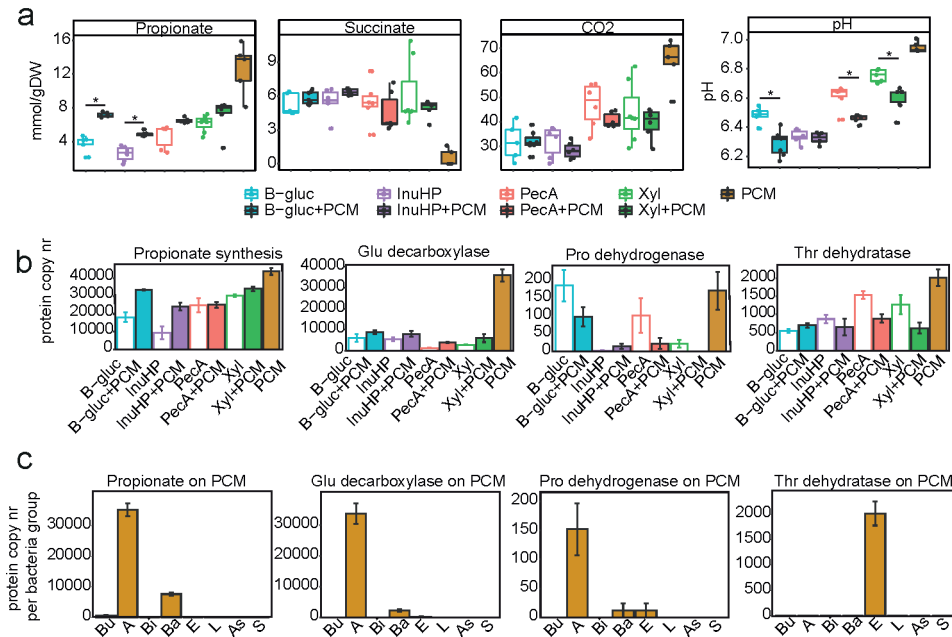


Figure 11. Metabolites from fermentation of selected substrates. **a**, Boxplots representing the concentrations of selected metabolites (mmol/gDW) and pH. All replicates shown (two-tailed paired t-test, \* $p < 0.05$ ). **b**, Average ( $\pm$ SEM) enzyme counts for reactions related to specific metabolite synthesis.  $n=3$ . **c**, Average ( $\pm$ SEM) enzyme counts per bacterial group for reactions related to specific metabolite synthesis.  $n=3$ . B-gluc –  $\beta$ -glucan, InuHP – high-performance inulin, PecA – apple pectin, Xyl – xylan, PCM – porcine colonic mucin.

The culture was also defined by the most effective conversion of succinate into CO<sub>2</sub> and propionate. *A. muciniphila* has been shown to produce succinate via the reductive TCA cycle (Ottman et al. 2017). However, succinate can also be produced from GABA. GABA is formed via the decarboxylation of glutamate (Glu), catalysed by Glu decarboxylase. GABA itself was not detected from the spent medium but significant amounts of Glu decarboxylase from *A. muciniphila* were detected from the culture of sole PCM, suggesting that GABA was fully converted into succinate, followed by conversion into propionate and CO<sub>2</sub> (Figure 11). Moreover, when acetyl-CoA – a necessary intermediate metabolite – is produced using pyruvate-formate lyase in combination with formate production, no NADH is released, which is needed for propionate synthesis. The metaproteomic analysis showed *A. muciniphila* to overcome this obstacle by primarily using pyruvate:ferredoxin oxidoreductase for the production of acetyl-CoA

(Publication III Figure S7). The latter pathway does not produce formate, agreeing with its negligible concentration on PCM (Publication III Figure 3).

Minor amounts of Glu were in the growth medium, but more could have been made from proline (Pro) from MUC2. Indeed, Pro dehydrogenase was detected from *A. muciniphila* on sole PCM (Figure 11). Likewise, increased amounts of threonine (Thr) dehydratase were detected from sole PCM fermentation, indicating that the culture used Thr for propionate production (Figure 11). As the backbone of MUC2 is made of repeating Pro-Thr-Ser units, these data suggest that the bacteria grown on sole PCM, especially *A. muciniphila*, were able to metabolise the protein backbone of MUC2. This was further indicated by the neutral pH of the culture (Figure 11a). The metabolism of glycans results in the formation of short chain fatty acids which lower the pH of the growth environment. However, if *A. muciniphila* was able to utilise the MUC2 protein, free peptides were released in addition to ammonia from amino sugar metabolism (Ottman et al. 2017) which would act as a buffer and explain the neutral pH of the culture. Together, these results support the hypothesis of MUC2 backbone being degraded by *A. muciniphila*. This agrees with some of the previous studies with *A. muciniphila* pure cultures that suggest this bacterium to be able to cleave mucin proteins (Davey et al. 2022; Meng et al. 2021; Trastoy et al. 2020). However, it is surprisingly in contrast to a study which demonstrated *A. muciniphila*'s inability to grow on colonic mucin in pure culture (Luis et al. 2021). This highlights the need to study microbiota as a bacterial community where each bacterium's behaviour is impacted by its crosstalk with the other members.

#### **4.2.3 The metabolites from complex dietary fibre fermentation affect goblet cell mucin production (Manuscript)**

The SCFAs and amines formed during glycan catabolism are bioactive compounds which affect the host in a multitude of ways. Their effect on the mucus production, however, is poorly understood. Amines like cadaverine and putrescine can improve cell proliferation and gut barrier function, whereas tyramine has been shown to be potentially toxic to the cells (Nakamura et al. 2021; del Rio et al. 2018; Bekebrede et al. 2020). Butyrate with its anti-inflammatory properties has been long considered as a host-beneficial compound, but a study with mouse spheroids demonstrated butyrate's inhibitory effect on colonic stem cell proliferation (Kaiko et al. 2016). It seems that the most effective enhancement of gut barrier function derives from a mixture of metabolites from a diverse microbiota (Park et al. 2016; Dougherty et al. 2020; Bilotta et al. 2021). To see if the resulting metabolites from complex dietary fibre and PCM fermentation exert any effect on colonic goblet cells or mucus production, a spheroid model was used. Primary cells from transgenic mice, carrying mCherry-tagged human MUC2 were grown into spheroids and treated with the supernatants from fermentation of complex glycans. The fluorescent cell count and intensity was compared to the control cells to evaluate the increase of goblet cells and MUC2, respectively (Figure 12). The metabolites from fermentation of pectin and xylan had a positive effect on both the number of goblet cells and their intensity, suggesting an enhanced production of MUC2. This result is in line with the previous studies, as both pectin and xylan induced the most diverse consortia with mixed-acids fermentation. However, these are preliminary results from a very complex system and further studies are needed to elucidate the molecular mechanisms behind this potentially beneficial effect.

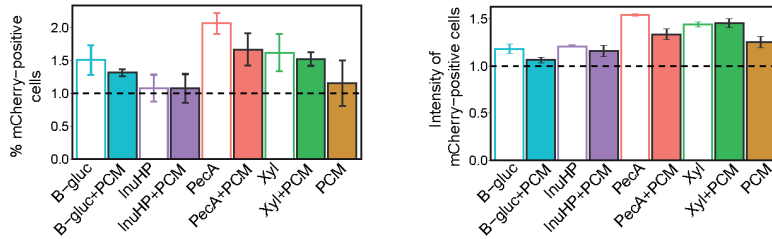


Figure 12. The effect of microbial metabolites on murine colonic spheroids and mCherry-tagged MUC2 production. Counts and signal intensity of mCherry-positive goblet cells as a result of treating the spheroids with metabolites from fermentation of the selected substrates, measured by flow cytometry and normalized against medium control. Average  $\pm$  SEM,  $n=3-4$ . B-gluc –  $\beta$ -glucan, InuHP – high-performance inulin, PecA – apple pectin, Xyl – xylan, PCM – porcine colonic mucin.

#### 4.2.4 The downstream metabolism of complex dietary fibres (Manuscript)

The fermentation of complex dietary fibres pectin and xylan resulted in the most diverse microbial consortia. We saw that the breakdown of these glycans required enzymes from several different CAZyme families and the downstream metabolism resulted in mixed acids production. Furthermore, these metabolites exerted a potentially beneficial effect on the colonic goblet cells and MUC2 production. These properties make pectin and xylan potential prebiotic compounds to improve gut health. However, to elucidate their beneficial effects it is important to understand their metabolism by complex faecal microbiota. The downstream metabolism of sugars from complex glycans was investigated by metaproteomics. The bacteria from cultures of pectin, xylan and PCM were divided into groups of similar metabolism (see Materials and Methods). The enzymes for carbohydrate metabolism reactions were mapped to the bacterial groups and the metabolic pathways for substrate degradation were constructed (Figure 13). In parallel, an FBA model was constructed and used to validate the results.

Both methods confirmed *A. muciniphila* to be the most active taxon on PCM (Figure 13 and Figure 14). *A. muciniphila* consumed mostly GlcNAc, GalNAc and fucose to produce propionate, CO<sub>2</sub> and acetate. The addition of pectin to the medium caused a change in the consortium. *A. muciniphila* was not able to compete with the bacteroides and butyric (especially *F. prausnitzii*) groups who were the most active taxa on pectin+PCM. The bacteroides group was also the main active taxa on xylan+PCM. The *Bacteroides* can produce propionate and acetate, while butyrogenic species synthesise butyrate. The high abundance and activity of these species on complex glycans agrees with the metabolites analysis showing mixed acids fermentation. Interestingly, on xylan+PCM *A. muciniphila* was able to grow into high abundance (Figure 7b). This reflects in the xylan+PCM metabolism, where *A. muciniphila* participates in several of the pathways and more propionate is produced compared to pectin+PCM (Figure 11a and Figure 13). The metaproteome analysis together with FBA calculations suggest pectin and xylan to be potential prebiotics which enhance the activities of commensal *Bacteroides* species, *F. prausnitzii*, *A. muciniphila* in addition to increasing the overall microbiota diversity.



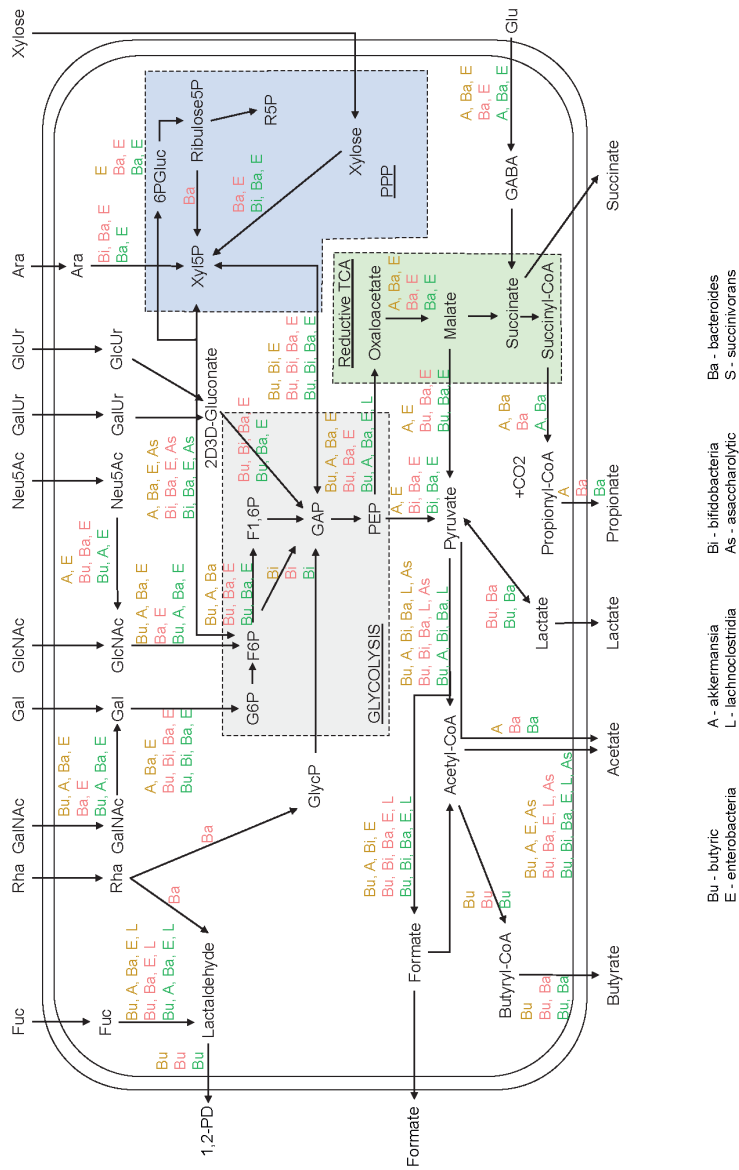


Figure 13. The degradation of glycans from dietary fibres and mucin based on the metaproteomic analysis. n=3. Fuc – fucose, Rha – rhamnose, GalNAC – N-acetylgalactosamine, GlcNAC – N-acetylglucosamine, Neu5Ac – N-acetylneuraminic acid, GalUr – galacturonic acid, GlcUr – glucuronic acid, 1,2-PED – propane-1,2-diol, GlycP – glycerone phosphate, G6P –  $\alpha$ -D-glucose-6-phosphate, F6P –  $\beta$ -D-glucose-6-phosphate, F1,6P –  $\beta$ -D-fructose-1,6-bisphosphate, GAP – D-glyceraldehyde-3-phosphate, 2D3D-Gluconate- 2-dehydro-3-deoxy-D-gluconate, Ribulose5P – D-ribulose-5-phosphate, Xyl5P – D-xylulose-5-phosphate, PEP – phosphoenolpyruvate, R5P – D-ribose-5-phosphate, Glu – glutamate, GABA –  $\gamma$ -aminobutyric acid, SuccinylCoA – succinyl-coenzyme A, AcetylCoA – acetyl-coenzyme A, PriopionylCoA – propionyl-coenzyme A.

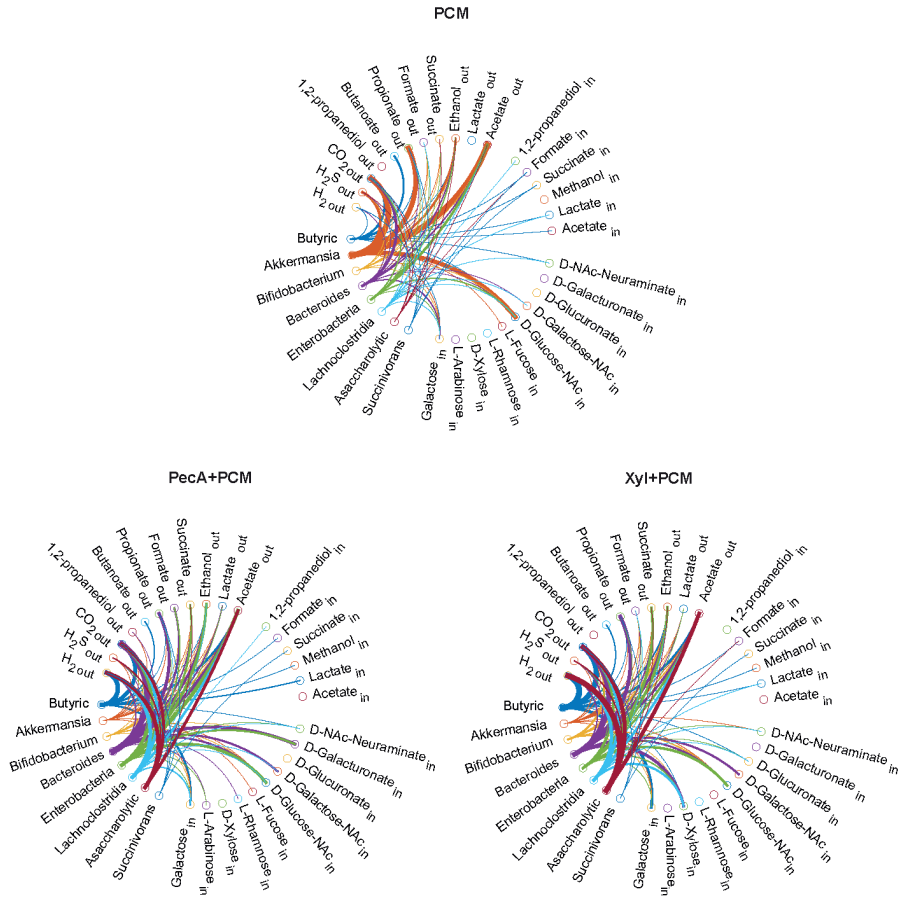


Figure 14. The degradation of glycans from dietary fibres and mucin and cross-feeding between bacterial groups based on Flux Balance Analysis. The bacteria were divided into 8 groups based on their similar metabolism (see text).  $n=3$ . PecA – apple pectin, Xyl – xylan, PCM – porcine colonic mucin.

## 5 Conclusions

The gut microbiota plays an integral role in maintaining the human health. Modulating the gut microbiota composition and metabolism through dietary intervention could be a key to preventing or treating diseases such as IBD, obesity and colorectal cancer. Dietary supplements in the form of pre- and probiotics have been on the market for years. However, their health claims are poorly defined due to the complexity of host-microbiota interactions and the high individual differences in microbiota composition. The study presented in this dissertation aimed to systematically elucidate the microbiota growth space under a range of physiologically relevant conditions. Furthermore, the study explored the mechanisms of dietary fibre and mucin co-metabolism. All experiments were done with the same standardised microbial community to bypass the individual variations of faecal sample donors and to allow comparison of results between experiments. The resulting datasets offer valuable insight into the growth and metabolism of complex gut microbiota under various conditions.

The first aim of the study was to scan the gut microbiota growth space at dilution rates and pH range that mimic the physiological conditions of the colon in health and disease. The mucus-degrading bacteria were especially susceptible to changes in the dilution rate and the pH. The in vitro dilution rate correlates with gut transit rate. Together with pH these parameters are directly related to and manipulated by the host diet. Modifying either of the parameters significantly altered the ratios of the known mucolytic bacteria in the consortium. Moreover, these fluctuations in the species abundances were also reflected in the metabolite profiles. Imbalances in the mucus degradation and renewal are directly related to several diseases. Mucolytic bacteria have a crucial role in preserving colonic homeostasis and the varying growth rates and metabolism of different species affects their mucin degradation efficiency. Therefore, it is important to maintain a balance in the species abundances. The confirming of this highly dynamic nature of mucin degraders makes them an interesting target for future therapies aimed at improving the mucus barrier function.

The next aims were to extract porcine colonic mucin, a unique substrate, and to use it in the in vitro fermentations to determine the modulating potential of various dietary fibres in the absence or presence of intestinal mucins. One strategy to avoid mucus penetrability is to keep the mucus- and fibre-degrading species in balance. The most straightforward way to do this is to maintain a diverse gut microbiota. We saw the bacterial diversity to be extremely dependent on the choice of substrate. The simple-structured fibres and oligosaccharides did not need specialist taxa for degradation. This benefitted the fast-growing saccharolytic species who outgrew other bacteria and dominated the consortia. However, the breakdown of more complex fibres required taxa with specific enzymatic capabilities. This increased the microbial diversity and inter-species crosstalk. The growths of various *Bacteroides* species were especially enhanced on complex glycans. This is likely due to the large genomes of the *Bacteroides*, which encode many different CAZymes. Some very specific substrate preferences were demonstrated, such as when Ruminococcaceae group UCG-013 became one of the most abundant taxa on apple pectin, while it was not able to grow in the consortium in xylan-supplemented medium. Specific modulatory effect was also demonstrated for porcine gastric and colonic mucins. The differences in the structures and glycan composition of these two mucins had a significant effect on selecting the composition of

consortia grown on these substrates. Out of the tested substrates, the complex fibres pectin and xylan induced the growth of the most diverse consortia.

The final experimental aim of the study was to apply metaproteomic analysis in combination with targeted metabolomics to elucidate the degradation and co-metabolism of dietary fibres and intestinal mucins. Additionally, a novel intestinal stem cell spheroid model was used to study the potential effect of the microbial metabolites on goblet cells and mucin production. The more diverse the microbial community, the more possibilities for interactions between the bacteria there are, increasing the microbiota's functional capacity. We detected many of the glycan degradation enzymes which have been previously described from pure cultures grown on the same dietary fibres as included in this study. Furthermore, we identified some novel substrate-specific enzymes, hinting at possible consortium-specific behaviour and/or crosstalk. For example, we showed how *Akkermansia muciniphila* in the consortium was able to cleave the MUC2 protein. This was a surprising result, as previous studies have shown *A. muciniphila* pure cultures to be unable to grow on colonic mucins. The metaproteome-level analysis together with mathematical modelling confirmed the *Bacteroides* to be the most active genus in degradation of complex fibres pectin and xylan. Interestingly, while pectin simultaneously enhanced the growth of various butyrate producers such as *Faecalibacterium prausnitzii*, xylan increased the abundances of *A. muciniphila*. Both species are considered as probiotics. These results demonstrate that the complex polysaccharides could be used to selectively modulate the microbiota in a host-beneficial way. The diverse consortia grown on pectin and xylan produced mixed acids and amines which had a positive effect on the growth of colonic goblet cells and on MUC2 production. These aspects make pectin and xylan promising candidates for prebiotics.

Lastly, the experimental work on mucin degradation was supported with a review on the recent advances on characterization of mucin utilization enzymes of the bacteria.

The results of this dissertation provide valuable information on microbiota's growth and metabolism under a range of physiologically relevant conditions. We identified apple pectin and xylan as potential candidates for prebiotics. Both dietary fibres have a complex structure that requires specialist taxa and crosstalk for their breakdown. Similarly important is the demonstration of the highly dynamic nature of the mucus degrading species. As these bacteria have a major role in maintaining the gut mucus barrier function, this information could be used for designing future therapies. The systematic approach with standardised microbial community allows to interpret the results from this study to a wider community.

## References

- Aasmets, Oliver, Kertu Liis Krigul, Kreete Lüll, Andres Metspalu, and Elin Org. 2022. "Gut Metagenome Associations with Extensive Digital Health Data in a Volunteer-Based Estonian Microbiome Cohort." *Nature Communications* 13 (1). Springer US: 1–11. doi:10.1038/s41467-022-28464-9.
- Adamberg, K., and S. Adamberg. 2018. "Selection of Fast and Slow Growing Bacteria from Fecal Microbiota Using Continuous Culture with Changing Dilution Rate." *Microbial Ecology in Health and Disease* 29 (1). Taylor & Francis: 1549922. doi:10.1080/16512235.2018.1549922.
- Adamberg, Kaarel, Grete Raba, and Signe Adamberg. 2020. "Use of Changestat for Growth Rate Studies of Gut Microbiota." *Frontiers in Bioengineering and Biotechnology* 8 (February): 1–12. doi:10.3389/fbioe.2020.00024.
- Aguirre, Marisol, Anat Eck, Marjorie E. Koenen, Paul H.M. Savelkoul, Andries E. Budding, and Koen Venema. 2016. "Diet Drives Quick Changes in the Metabolic Activity and Composition of Human Gut Microbiota in a Validated in Vitro Gut Model." *Research in Microbiology* 167 (2). Elsevier Masson SAS: 114–25. doi:10.1016/j.resmic.2015.09.006.
- Alam, Mohammad Tauqueer, Gregory C.A. Amos, Andrew R.J. Murphy, Simon Murch, Elizabeth M.H. Wellington, and Ramesh P. Arasaradnam. 2020. "Microbial Imbalance in Inflammatory Bowel Disease Patients at Different Taxonomic Levels." *Gut Pathogens* 12 (1). BioMed Central: 1–8. doi:10.1186/s13099-019-0341-6.
- Allaire, Joannie M., Shauna M. Crowley, Hong T. Law, Sun Young Chang, Hyun Jeong Ko, and Bruce A. Vallance. 2018. "The Intestinal Epithelium: Central Coordinator of Mucosal Immunity." *Trends in Immunology* 39 (9). Elsevier Ltd: 677–96. doi:10.1016/j.it.2018.04.002.
- Allen, Adrian, David A. Hutton, and Jeffrey P. Pearson. 1998. "The MUC2 Gene Product: A Human Intestinal Mucin." *International Journal of Biochemistry and Cell Biology* 30 (7): 797–801. doi:10.1016/S1357-2725(98)00028-4.
- Ambort, Daniel, Malin E.V. Johansson, Jenny K. Gustafsson, Harriet E. Nilsson, Anna Ermund, Bengt R. Johansson, Philip J.B. Koeck, Hans Hebert, and Gunnar C. Hansson. 2012. "Calcium and PH-Dependent Packing and Release of the Gel-Forming MUC2 Mucin." *Proceedings of the National Academy of Sciences of the United States of America* 109 (15): 5645–50. doi:10.1073/pnas.1120269109.
- Arike, Liisa, Andrus Seiman, Sjoerd van der Post, Ana M. Rodriguez Piñeiro, Anna Ermund, André Schütte, Fredrik Bäckhed, Malin E.V. Johansson, and Gunnar C. Hansson. 2020. "Protein Turnover in Epithelial Cells and Mucus along the Gastrointestinal Tract Is Coordinated by the Spatial Location and Microbiota." *Cell Reports* 30 (4): 1077-1087.e3. doi:10.1016/j.celrep.2019.12.068.
- Arrieta, Marie Claire, Leah T. Stiemsma, Nelly Amenyogbe, Eric Brown, and Brett Finlay. 2014. "The Intestinal Microbiome in Early Life: Health and Disease." *Frontiers in Immunology* 5 (AUG): 1–18. doi:10.3389/fimmu.2014.00427.
- Axelsson, Magnus A.B., Noomi Asker, and Gunnar C. Hansson. 1998. "O-Glycosylated MUC2 Monomer and Dimer from LS 174T Cells Are Water-Soluble, Whereas Larger MUC2 Species Formed Early during Biosynthesis Are Insoluble and Contain Nonreducible Intermolecular Bonds." *Journal of Biological Chemistry* 273 (30). © 1998 ASBMB. Currently published by Elsevier Inc; originally published by American Society for Biochemistry and Molecular Biology.: 18864–70. doi:10.1074/jbc.273.30.18864.

- Barbeyron, Tristan, Loraine Brillet-Guéguen, Wilfrid Carré, Cathelène Carrière, Christophe Caron, Mirjam Czjzek, Mark Hoebeke, and Gurvan Michel. 2016. "Matching the Diversity of Sulfated Biomolecules: Creation of a Classification Database for Sulfatases Reflecting Their Substrate Specificity." *PLoS ONE* 11 (10): 1–33. doi:10.1371/journal.pone.0164846.
- Bekebrede, Anna F., Jaap Keijer, Walter J.J. Gerrits, and Vincent C.J. de Boer. 2020. "The Molecular and Physiological Effects of Protein-Derived Polyamines in the Intestine." *Nutrients* 12 (1): 1–18. doi:10.3390/nu12010197.
- Bell, Andrew, Jason Brunt, Emmanuelle Crost, Laura Vaux, Ridvan Nepravishta, C. David Owen, Dimitrios Latousakis, et al. 2019. "Elucidation of a Sialic Acid Metabolism Pathway in Mucus-Foraging Ruminococcus Gnavus Unravels Mechanisms of Bacterial Adaptation to the Gut." *Nature Microbiology* 4 (12). Springer US: 2393–2404. doi:10.1038/s41564-019-0590-7.
- Bennett, Eric P., Ulla Mandel, Henrik Clausen, Thomas A. Gerken, Timothy A. Fritz, and Lawrence A. Tabak. 2012. "Control of Mucin-Type O-Glycosylation: A Classification of the Polypeptide GalNAc-Transferase Gene Family." *Glycobiology* 22 (6): 736–56. doi:10.1093/glycob/cwr182.
- Bergstrom, Kirk S.B., Vanessa Kissoon-Singh, Deanna L. Gibson, Caixia Ma, Marinieve Montero, Ho Pan Sham, Natasha Ryz, et al. 2010. "Muc2 Protects against Lethal Infectious Colitis by Disassociating Pathogenic and Commensal Bacteria from the Colonic Mucosa." *PLoS Pathogens* 6 (5). doi:10.1371/journal.ppat.1000902.
- Bernard, Kathryn, Tamara Burdz, Deborah Wiebe, Brittany M. Balcewich, Tina Zimmerman, Philippe Lagacé-Wiens, Linda M.N. Hoang, and Anne Marie Bernier. 2017. "Characterization of Isolates of Eisenbergiella Tayi, a Strictly Anaerobic Gram-Stain Variable Bacillus Recovered from Human Clinical Materials in Canada." *Anaerobe* 44: 128–32. doi:10.1016/j.anaerobe.2017.03.005.
- Besten, Gijs den, Katja Lange, Rick Havinga, Theo H. van Dijk, Albert Gerding, Karen van Eunen, Michael Müller, et al. 2013. "Gut-Derived Short-Chain Fatty Acids Are Vividly Assimilated into Host Carbohydrates and Lipids." *American Journal of Physiology - Gastrointestinal and Liver Physiology* 305 (12): 900–910. doi:10.1152/ajpgi.00265.2013.
- Bhattacharya, Tanudeep, Tarini Shankar Ghosh, and Sharmila S. Mande. 2015. "Global Profiling of Carbohydrate Active Enzymes in Human Gut Microbiome." *PLoS ONE* 10 (11): 1–20. doi:10.1371/journal.pone.0142038.
- Bilotta, Anthony J., Chunyan Ma, Wenjing Yang, Yanbo Yu, Yu Yu, Xiaojing Zhao, Zheng Zhou, Suxia Yao, Sara M. Dann, and Yingzi Cong. 2021. "Propionate Enhances Cell Speed and Persistence to Promote Intestinal Epithelial Turnover and Repair." *Cmgh* 11 (4): 1023–44. doi:10.1016/j.jcmgh.2020.11.011.
- Birchenough, George M.H., Elisabeth E.L. Nystrom, Malin E.V. Johansson, and Gunnar C. Hansson. 2016. "A Sentinel Goblet Cell Guards the Colonic Crypt by Triggering Nlrp6-Dependent Muc2 Secretion." *Science* 352 (6293): 1535–42. doi:10.1126/science.aaf7419.
- Birchenough, George, Bjoern O. Schroeder, Fredrik Bäckhed, and Gunnar C. Hansson. 2019. "Dietary Destabilisation of the Balance between the Microbiota and the Colonic Mucus Barrier." *Gut Microbes* 10 (2). Taylor & Francis: 246–50. doi:10.1080/19490976.2018.1513765.

- Boroni Moreira, A. P., T. Fiche Salles Teixeira, C. do Gouveia Peluzio, and R. de Cássia Gonçalves Alfenas. 2012. "Gut Microbiota and the Development of Obesity." *Nutricion Hospitalaria* 27 (5): 1408–14. doi:10.3305/nh.2012.27.5.5887.
- Bravo, Javier A., Paul Forsythe, Marianne V. Chew, Emily Escaravage, Hélène M. Savaignac, Timothy G. Dinan, John Bienenstock, and John F. Cryan. 2011. "Ingestion of Lactobacillus Strain Regulates Emotional Behavior and Central GABA Receptor Expression in a Mouse via the Vagus Nerve." *Proceedings of the National Academy of Sciences of the United States of America* 108 (38): 16050–55. doi:10.1073/pnas.1102999108.
- Bry, Lynn, Per G Falk, Tore Midtvedt, and Jeffrey Gordon. 1996. "A Model of Host-Microbial Interactions in an Open Mammalian Ecosystem." *Science*. doi:10.1126/science.273.5280.1380.
- Canfora, Emanuel E., Ruth C.R. Meex, Koen Venema, and Ellen E. Blaak. 2019. "Gut Microbial Metabolites in Obesity, NAFLD and T2DM." *Nature Reviews Endocrinology* 15 (5). Springer US: 261–73. doi:10.1038/s41574-019-0156-z.
- Cantu-Jungles, T. M., and B. R. Hamaker. 2020. "New View on Dietary Fiber Selection for Predictable Shifts in Gut Microbiota." *MBio* 11 (1): 1–8. doi:10.1128/mBio.02179-19.
- Cantu-Jungles, Thaisa M, Nuseybe Bulut, Eponine Chambry, Andrea Ruthes, Marcello Iacomini, and Ali Keshavarzian. 2021. "Dietary Fiber Hierarchical Specificity: The Missing Link for Predictable and Strong Shifts in Gut Bacterial Communities." doi:https://doi.org/10.1128/mBio.01028-21.
- Chen, Jie, Jaladanki N. Rao, Tongtong Zou, Lan Liu, Bernard S. Marasa, Lan Xiao, Xing Zeng, Douglas J. Turner, and Jian Ying Wang. 2007. "Polyamines Are Required for Expression of Toll-like Receptor 2 Modulating Intestinal Epithelial Barrier Integrity." *American Journal of Physiology - Gastrointestinal and Liver Physiology* 293 (3): 568–76. doi:10.1152/ajpgi.00201.2007.
- Chung, Wing Sun Faith, Alan W. Walker, Petra Louis, Julian Parkhill, Joan Vermeiren, Douwina Bosscher, Sylvia H. Duncan, and Harry J. Flint. 2016. "Modulation of the Human Gut Microbiota by Dietary Fibres Occurs at the Species Level." *BMC Biology* 14 (1). BMC Biology: 1–13. doi:10.1186/s12915-015-0224-3.
- Chung, Wing Sun Faith, Alan W. Walker, Joan Vermeiren, Paul O. Sheridan, Douwina Bosscher, Vicenta Garcia-Campayo, Julian Parkhill, Harry J. Flint, and Sylvia H. Duncan. 2018. "Impact of Carbohydrate Substrate Complexity on the Diversity of the Human Colonic Microbiota." *FEMS Microbiology Ecology* 95 (1). Oxford University Press: 1–13. doi:10.1093/femsec/fiy201.
- Clemente, Jose C., Erica C. Pehrsson, Martin J. Blaser, Kuldip Sandhu, Zhan Gao, Bin Wang, Magda Magris, et al. 2015. "The Microbiome of Uncontacted Amerindians." *Science Advances* 1 (3). doi:10.1126/sciadv.1500183.
- Clooney, Adam G., Julia Eckenberger, Emilio Laserna-Mendieta, Kathryn A. Sexton, Matthew T. Bernstein, Kathy Vagianos, Michael Sargent, et al. 2021. "Ranking Microbiome Variance in Inflammatory Bowel Disease: A Large Longitudinal Intercontinental Study." *Gut* 70 (3): 499–510. doi:10.1136/gutjnl-2020-321106.
- Coleman, Olivia I., and Dirk Haller. 2021. "Microbe–Mucus Interface in the Pathogenesis of Colorectal Cancer." *Cancers* 13 (4): 1–18. doi:10.3390/cancers13040616.
- Cox, Jürgen, and Matthias Mann. 2008. "MaxQuant Enables High Peptide Identification Rates, Individualized p.p.b.-Range Mass Accuracies and Proteome-Wide Protein Quantification." *Nature Biotechnology* 26 (12): 1367–72. doi:10.1038/nbt.1511.

- Crouch, Lucy I., Marcelo V. Liberato, Paulina A. Urbanowicz, Arnaud Baslé, Christopher A. Lamb, Christopher J. Stewart, Katie Cooke, et al. 2020. "Prominent Members of the Human Gut Microbiota Express Endo-Acting O-Glycanases to Initiate Mucin Breakdown." *Nature Communications* 11 (1). Springer US. doi:10.1038/s41467-020-17847-5.
- Cummings, J. H., and G. T. Macfarlane. 1991. "The Control and Consequences of Bacterial Fermentation in the Human Colon." *Journal of Applied Bacteriology* 70 (6): 443–59. doi:10.1111/j.1365-2672.1991.tb02739.x.
- Cummings, John H. 1984. "Constipation, Dietary Fibre and the Control of Large Bowel Function." *Postgraduate Medical Journal* 60 (709): 811–19. doi:10.1136/pgmj.60.709.811.
- Cummings, John H, and Hans N Englyst. 1987. "Fermentation in the Human Large Intestine and the Available Substrates." *American Journal of Clinical Nutrition*, no. March.
- Dalile, Boushra, Lukas Van Oudenhove, Bram Vervliet, and Kristin Verbeke. 2019. "The Role of Short-Chain Fatty Acids in Microbiota–Gut–Brain Communication." *Nature Reviews Gastroenterology and Hepatology* 16 (8). Springer US: 461–78. doi:10.1038/s41575-019-0157-3.
- Davey, Lauren, Lee Dolat, Zachary Holmes, Eduard Ansaldo, and U C Berkeley. 2022. "Mucin Foraging Enables Akkermansia Muciniphila to Compete against Other Microbes in the Gut and to Modulate Host Sterol Biosynthesis." *Under Review at Nature Portfolio*.
- Deehan, Edward C., Chen Yang, Maria Elisa Perez-Muñoz, Nguyen K. Nguyen, Christopher C. Cheng, Lucila Triador, Zhengxiao Zhang, Jeffrey A. Bakal, and Jens Walter. 2020. "Precision Microbiome Modulation with Discrete Dietary Fiber Structures Directs Short-Chain Fatty Acid Production." *Cell Host and Microbe* 27 (3): 389-404.e6. doi:10.1016/j.chom.2020.01.006.
- Degen, L. P., and S. F. Phillips. 1996. "How Well Does Stool Form Reflect Colonic Transit?" *Gut* 39 (1): 109–13. doi:10.1136/gut.39.1.109.
- Desai, Mahesh S., Anna M. Seekatz, Nicole M. Koropatkin, Nobuhiko Kamada, Christina A. Hickey, Mathis Wolter, Nicholas A. Pudlo, et al. 2016. "A Dietary Fiber-Deprived Gut Microbiota Degrades the Colonic Mucus Barrier and Enhances Pathogen Susceptibility." *Cell* 167 (5): 1339-1353.e21. doi:10.1016/j.cell.2016.10.043.
- Donaldson, Gregory P., Wen Chi Chou, Abigail L. Manson, Peter Rogov, Thomas Abeel, James Bochicchio, Dawn Ciulla, et al. 2020. "Spatially Distinct Physiology of Bacteroides Fragilis within the Proximal Colon of Gnotobiotic Mice." *Nature Microbiology* 5 (5). Springer US: 746–56. doi:10.1038/s41564-020-0683-3.
- Dougherty, Michael W., Oleksandr Kudin, Marcus Mühlbauer, Josef Neu, Raad Z. Gharaibeh, and Christian Jobin. 2020. "Gut Microbiota Maturation during Early Human Life Induces Enterocyte Proliferation via Microbial Metabolites." *BMC Microbiology* 20 (1). BMC Microbiology: 1–14. doi:10.1186/s12866-020-01892-7.
- Drula, Elodie, Marie Line Garron, Suzan Dogan, Vincent Lombard, Bernard Henrissat, and Nicolas Terrapon. 2022. "The Carbohydrate-Active Enzyme Database: Functions and Literature." *Nucleic Acids Research* 50 (D1). Oxford University Press: D571–77. doi:10.1093/nar/gkab1045.



- Duncan, Sylvia H., Adela Barcenilla, Colin S. Stewart, Susan E. Pryde, and Harry J. Flint. 2002. "Acetate Utilization and Butyryl Coenzyme A (CoA): Acetate-CoA Transferase in Butyrate-Producing Bacteria from the Human Large Intestine." *Applied and Environmental Microbiology* 68 (10): 5186–90. doi:10.1128/AEM.68.10.5186-5190.2002.
- Duncan, Sylvia H., Petra Louis, John M. Thomson, and Harry J. Flint. 2009. "The Role of PH in Determining the Species Composition of the Human Colonic Microbiota." *Environmental Microbiology* 11 (8): 2112–22. doi:10.1111/j.1462-2920.2009.01931.x.
- Elia, M., and J. H. Cummings. 2007. "Physiological Aspects of Energy Metabolism and Gastrointestinal Effects of Carbohydrates." *European Journal of Clinical Nutrition* 61: S40–74. doi:10.1038/sj.ejcn.1602938.
- Everard, Amandine, Clara Belzer, Lucie Geurts, Janneke P. Ouwerkerk, Céline Druart, Laure B. Bindels, Yves Guiot, et al. 2013. "Cross-Talk between Akkermansia Muciniphila and Intestinal Epithelium Controls Diet-Induced Obesity." *Proceedings of the National Academy of Sciences of the United States of America* 110 (22): 9066–71. doi:10.1073/pnas.1219451110.
- Fan, Yong, and Oluf Pedersen. 2021. "Gut Microbiota in Human Metabolic Health and Disease." *Nature Reviews Microbiology* 19 (1). Springer US: 55–71. doi:10.1038/s41579-020-0433-9.
- Gall, Gwénaëlle Le, Samah O. Noor, Karyn Ridgway, Louise Scovell, Crawford Jamieson, Ian T. Johnson, Ian J. Colquhoun, E. Kate Kemsley, and Arjan Narbad. 2011. "Metabonomics of Fecal Extracts Detects Altered Metabolic Activity of Gut Microbiota in Ulcerative Colitis and Irritable Bowel Syndrome." *Journal of Proteome Research* 10 (9): 4208–18. doi:10.1021/pr2003598.
- Gayer, Christopher P., and Marc D. Basson. 2009. "The Effects of Mechanical Forces on Intestinal Physiology and Pathology." *Cellular Signalling* 21 (8). Elsevier B.V.: 1237–44. doi:10.1016/j.cellsig.2009.02.011.
- Gustafsson, Jenny K., Anna Ermund, Malin E.V. Johansson, André Schütte, Gunnar C. Hansson, and Henrik Sjövall. 2012. "An Ex Vivo Method for Studying Mucus Formation, Properties, and Thickness in Human Colonic Biopsies and Mouse Small and Large Intestinal Explants." *American Journal of Physiology - Gastrointestinal and Liver Physiology* 302 (4): 430–38. doi:10.1152/ajpgi.00405.2011.
- Hansson, Gunnar C. 2020. "Mucins and the Microbiome." *Annual Review of Biochemistry* 89: 769–93. doi:10.1146/annurev-biochem-011520-105053.
- Hehemann, Jan Hendrik, Gaëlle Correc, Tristan Barbeyron, William Helbert, Mirjam Czjzek, and Gurvan Michel. 2010. "Transfer of Carbohydrate-Active Enzymes from Marine Bacteria to Japanese Gut Microbiota." *Nature* 464 (7290): 908–12. doi:10.1038/nature08937.
- Hetzel, Marc, Matthias Brock, Thorsten Selmer, Antonio J. Pierik, Bernard T. Golding, and Wolfgang Buckel. 2003. "Acryloyl-CoA Reductase from Clostridium Propionicum: An Enzyme Complex of Propionyl-CoA Dehydrogenase and Electron-Transferring Flavoprotein." *European Journal of Biochemistry* 270 (5): 902–10. doi:10.1046/j.1432-1033.2003.03450.x.
- Holmén Larsson, Jessica M, Kristina A Thomsson, Ana M Rodríguez-Piñeiro, Hasse Karlsson, and Gunnar C Hansson. 2013. "Studies of Mucus in Mouse Stomach, Small Intestine, and Colon. III. Gastrointestinal Muc5ac and Muc2 Mucin O-Glycan Patterns Reveal a Regiospecific Distribution." *American Journal of Physiology. Gastrointestinal and Liver Physiology* 305 (5): G357-363. doi:10.1152/ajpgi.00048.2013.

- Huttenhower, Curtis, Dirk Gevers, Rob Knight, Sahar Abubucker, Jonathan H. Badger, Asif T. Chinwalla, Heather H. Creasy, et al. 2012. "Structure, Function and Diversity of the Healthy Human Microbiome." *Nature* 486 (7402). Nature Publishing Group: 207–14. doi:10.1038/nature11234.
- Johansson, Malin E.V., Jenny K. Gustafsson, Jessica Holmen-Larsson, Karolina S. Jabbar, Lijun Xia, Hua Xu, Fayez K. Ghishan, et al. 2014. "Bacteria Penetrate the Normally Impenetrable Inner Colon Mucus Layer in Both Murine Colitis Models and Patients with Ulcerative Colitis." *Gut* 63 (2): 281–91. doi:10.1136/gutjnl-2012-303207.
- Johansson, Malin E.V., Jessica M. Holmén Larsson, and Gunnar C. Hansson. 2011. "The Two Mucus Layers of Colon Are Organized by the MUC2 Mucin, Whereas the Outer Layer Is a Legislator of Host-Microbial Interactions." *Proceedings of the National Academy of Sciences of the United States of America* 108 (SUPPL. 1): 4659–65. doi:10.1073/pnas.1006451107.
- Johansson, Malin E.V., Hedvig E. Jakobsson, Jessica Holmén-Larsson, André Schütte, Anna Ermund, Ana M. Rodríguez-Piñeiro, Liisa Arike, et al. 2015. "Normalization of Host Intestinal Mucus Layers Requires Long-Term Microbial Colonization." *Cell Host and Microbe* 18 (5): 582–92. doi:10.1016/j.chom.2015.10.007.
- Johansson, Malin E.V., Mia Phillipson, Joel Petersson, Anna Velcich, Lena Holm, and Gunnar C. Hansson. 2008. "The Inner of the Two Muc2 Mucin-Dependent Mucus Layers in Colon Is Devoid of Bacteria." *Proceedings of the National Academy of Sciences of the United States of America* 105 (39): 15064–69. doi:10.1073/pnas.0803124105.
- Kaiko, Gerard E., Stacy H. Ryu, Olivia I. Koues, Patrick L. Collins, Lilianna Solnica-Krezel, Edward J. Pearce, Erika L. Pearce, Eugene M. Oltz, and Thaddeus S. Stappenbeck. 2016. "The Colonic Crypt Protects Stem Cells from Microbiota-Derived Metabolites." *Cell* 165 (7). Elsevier Inc.: 1708–20. doi:10.1016/j.cell.2016.05.018.
- Kandori, Hitoshi, Kazuhiro Hirayama, Makio Takeda, and Kunio Doi. 1996. "Histochemical, Lectin-Histochemical and Morphometrical Characteristics of Intestinal Goblet Cells of Germfree and Conventional Mice." *Experimental Animals*. doi:10.1538/expanim.45.155.
- Kaoutari, Abdessamad El, Fabrice Armougom, Jeffrey I. Gordon, Didier Raoult, and Bernard Henrissat. 2013. "The Abundance and Variety of Carbohydrate-Active Enzymes in the Human Gut Microbiota." *Nature Reviews Microbiology* 11 (7). Nature Publishing Group: 497–504. doi:10.1038/nrmicro3050.
- Karlsson, Niclas G., Henrik Nordman, Hasse Karlsson, Ingemar Carlstedt, and Gunnar C. Hansson. 1997. "Glycosylation Differences between Pig Gastric Mucin Populations: A Comparative Study of the Neutral Oligosaccharides Using Mass Spectrometry." *Biochemical Journal* 326 (3): 911–17. doi:10.1042/bj3260911.
- Kashtan, Hanoach, Hartley S. Stern, David J.A. Jenkins, Gregoire Roger, Kazy Hay, Alexandra L. Jenkins, Solomon Minkin, and W. Robert Bruce. 1990. "Manipulation of Fecal PH by Dietary Means." *Preventive Medicine* 19 (6): 607–13. doi:10.1016/0091-7435(90)90057-Q.
- Koh, Ara, Filipe De Vadder, Petia Kovatcheva-Datchary, and Fredrik Bäckhed. 2016. "From Dietary Fiber to Host Physiology: Short-Chain Fatty Acids as Key Bacterial Metabolites." *Cell* 165 (6): 1332–45. doi:10.1016/j.cell.2016.05.041.
- Kojima, M., K. Wakai, S. Tokudome, K. Tamakoshi, H. Toyoshima, Y. Watanabe, N. Hayakawa, et al. 2004. "Bowel Movement Frequency and Risk of Colorectal Cancer in a Large Cohort Study of Japanese Men and Women." *British Journal of Cancer* 90 (7): 1397–1401. doi:10.1038/sj.bjc.6601735.

- König, Julia, Jerry Wells, Patrice D. Cani, Clara L. García-Ródenas, Tom MacDonald, Annick Mercenier, Jacqueline Whyte, Freddy Troost, and Robert Jan Brummer. 2016. "Human Intestinal Barrier Function in Health and Disease." *Clinical and Translational Gastroenterology* 7 (10). doi:10.1038/ctg.2016.54.
- Krautkramer, Kimberly A., Jing Fan, and Fredrik Bäckhed. 2021. "Gut Microbial Metabolites as Multi-Kingdom Intermediates." *Nature Reviews Microbiology* 19 (2): 77–94. doi:10.1038/s41579-020-0438-4.
- Larsson, Jessica M. Holmén, Hasse Karlsson, Henrik Sjövall, and Gunnar C. Hansson. 2009. "A Complex, but Uniform O-Glycosylation of the Human MUC2 Mucin from Colonic Biopsies Analyzed by NanoLC/MSn." *Glycobiology* 19 (7): 756–66. doi:10.1093/glycob/cwp048.
- Lewis, S. J., and K. W. Heaton. 1997. "Increasing Butyrate Concentration in the Distal Colon by Accelerating Intestinal Transit." *Gut* 41 (2): 245–51. doi:10.1136/gut.41.2.245.
- Luis, Ana S., Jonathon Briggs, Xiaoyang Zhang, Benjamin Farnell, Didier Ndeh, Aurore Labourel, Arnaud Baslé, et al. 2018. "Dietary Pectic Glycans Are Degraded by Coordinated Enzyme Pathways in Human Colonic Bacteroides." *Nature Microbiology* 3 (2). Springer US: 210–19. doi:10.1038/s41564-017-0079-1.
- Luis, Ana S., Chunsheng Jin, Gabriel Vasconcelos Pereira, Robert W.P. Glowacki, Sadie R. Gugel, Shaleni Singh, Dominic P. Byrne, et al. 2021. "A Single Sulfatase Is Required to Access Colonic Mucin by a Gut Bacterium." *Nature* 598 (7880). Springer US: 332–37. doi:10.1038/s41586-021-03967-5.
- Makki, Kassem, Edward C. Deehan, Jens Walter, and Fredrik Bäckhed. 2018. "The Impact of Dietary Fiber on Gut Microbiota in Host Health and Disease." *Cell Host and Microbe* 23 (6): 705–15. doi:10.1016/j.chom.2018.05.012.
- Martínez, Inés, James C. Stegen, Maria X. Maldonado-Gómez, Murat A. Eren, Peter M. Siba, Andrew R. Greenhill, and Jens Walter. 2015. "The Gut Microbiota of Rural Papua New Guineans: Composition, Diversity Patterns, and Ecological Processes." *Cell Reports* 11 (4): 527–38. doi:10.1016/j.celrep.2015.03.049.
- Meng, Xin, Wencheng Wang, Tianqi Lan, Wanxin Yang, Dahai Yu, Xuexun Fang, and Hao Wu. 2021. "A Purified Aspartic Protease from Akkermansia muciniphila Plays an Important Role in Degrading Muc2." *International Journal of Molecular Sciences* 22 (6): 1–2. doi:10.3390/ijms22063122.
- Miyoshi, Hiroyuki, and Thaddeus S. Stappenbeck. 2013. "In Vitro Expansion and Genetic Modification of Gastrointestinal Stem Cells in Spheroid Culture." *Nature Protocols* 8 (12): 2471–82. doi:10.1038/nprot.2013.153.
- Monod, Jacques. 1978. "La Technique De Culture Continue Théorie Et Applications." *Selected Papers in Molecular Biology by Jacques Monod*, no. 18: 184–204. doi:10.1016/b978-0-12-460482-7.50023-3.
- Mouillé, Béatrice, Serge Delpal, Camille Mayeur, and François Blachier. 2003. "Inhibition of Human Colon Carcinoma Cell Growth by Ammonia: A Non-Cytotoxic Process Associated with Polyamine Synthesis Reduction." *Biochimica et Biophysica Acta - General Subjects* 1624 (1–3): 88–97. doi:10.1016/j.bbagen.2003.09.014.
- Munoz-Munoz, José, Alan Cartmell, Nicolas Terrapon, Arnaud Baslé, Bernard Henrissat, and Harry J. Gilbert. 2017. "An Evolutionarily Distinct Family of Polysaccharide Lyases Removes Rhamnose Capping of Complex Arabinogalactan Proteins." *Journal of Biological Chemistry* 292 (32): 13271–83. doi:10.1074/jbc.M117.794578.

- Muscogiuri, Giovanna, Elena Cantone, Sara Cassarano, Dario Tuccinardi, Luigi Barrea, Silvia Savastano, and Annamaria Colao. 2019. "Gut Microbiota: A New Path to Treat Obesity." *International Journal of Obesity Supplements* 9 (1). Springer US: 10–19. doi:10.1038/s41367-019-0011-7.
- Nakamura, Atsuo, Shin Kurihara, Daisuke Takahashi, Wakana Ohashi, Yutaka Nakamura, Shunsuke Kimura, Masayoshi Onuki, et al. 2021. "Symbiotic Polyamine Metabolism Regulates Epithelial Proliferation and Macrophage Differentiation in the Colon." *Nature Communications* 12 (1). Springer US: 1–14. doi:10.1038/s41467-021-22212-1.
- Ndeh, Didier, Artur Rogowski, Alan Cartmell, Ana S. Luis, Arnaud Baslé, Joseph Gray, Immacolata Venditto, et al. 2017. "Complex Pectin Metabolism by Gut Bacteria Reveals Novel Catalytic Functions." *Nature* 544 (7648). Nature Publishing Group: 65–70. doi:10.1038/nature21725.
- Ng, Katharine M., Jessica A. Ferreyra, Steven K. Higginbottom, Jonathan B. Lynch, Purna C. Kashyap, Smita Gopinath, Natasha Naidu, et al. 2013. "Microbiota-Liberated Host Sugars Facilitate Post-Antibiotic Expansion of Enteric Pathogens." *Nature* 502 (7469). Nature Publishing Group: 96–99. doi:10.1038/nature12503.
- Nugent, S. G., D. Kumar, D. S. Rampton, and D. F. Evans. 2001. "Intestinal Luminal PH in Inflammatory Bowel Disease: Possible Determinants and Implications for Therapy with Aminosalicylates and Other Drugs." *Gut* 48 (4): 571–77. doi:10.1136/gut.48.4.571.
- Nyström, Elisabeth E.L., Beatriz Martinez-Abad, Liisa Arike, George M.H. Birchenough, Eric B. Nonnecke, Patricia A. Castillo, Frida Svensson, Charles L. Bevins, Gunnar C. Hansson, and Malin E.V. Johansson. 2021. "An Intercrypt Subpopulation of Goblet Cells Is Essential for Colonic Mucus Barrier Function." *Science* 372 (6539). doi:10.1126/science.abb1590.
- Ohgashi, Seiji, Kazuki Sudo, Daiki Kobayashi, Osamu Takahashi, Takuya Takahashi, Takashi Asahara, Koji Nomoto, and Hisashi Onodera. 2013. "Changes of the Intestinal Microbiota, Short Chain Fatty Acids, and Fecal PH in Patients with Colorectal Cancer." *Digestive Diseases and Sciences* 58 (6): 1717–26. doi:10.1007/s10620-012-2526-4.
- Oliphant, Kaitlyn, and Emma Allen-Vercoe. 2019. "Macronutrient Metabolism by the Human Gut Microbiome: Major Fermentation by-Products and Their Impact on Host Health." *Microbiome* 7 (1). Microbiome: 1–15. doi:10.1186/s40168-019-0704-8.
- Orth, Jeffrey D., Ines Thiele, and Bernhard O. Palsson. 2010. "What Is Flux Balance Analysis?" *Nature Biotechnology* 28 (3). Nature Publishing Group: 245–48. doi:10.1038/nbt.1614.
- Ostrowski, Matthew P., Sabina Leanti La Rosa, Benoit J. Kunath, Andrew Robertson, Gabriel Pereira, Live H. Hagen, Neha J. Varghese, et al. 2022. "Mechanistic Insights into Consumption of the Food Additive Xanthan Gum by the Human Gut Microbiota." *Nature Microbiology* 7 (4). Springer US: 556–69. doi:10.1038/s41564-022-01093-0.
- Ottman, Noora, Mark Davids, Maria Suarez-Diez, Sjef Boeren, Peter J. Schaap, Vitor A. P. Martins dos Santos, Hauke Smidt, Clara Belzer, and Willem M. de Vos. 2017. "Genome-Scale Model and Omics Analysis of Metabolic Capacities of *Akkermansia muciniphila* Reveal a Preferential Mucin-Degrading Lifestyle." Edited by Robert M. Kelly. *Applied and Environmental Microbiology* 83 (18): 1–15. doi:10.1128/AEM.01014-17.

- Paone, Paola, and Patrice D. Cani. 2020. "Mucus Barrier, Mucins and Gut Microbiota: The Expected Slimy Partners?" *Gut* 69 (12): 2232–43. doi:10.1136/gutjnl-2020-322260.
- Park, Jung Ha, Takenori Kotani, Tasuku Konno, Jajar Setiawan, Yasuaki Kitamura, Shinya Imada, Yutaro Usui, et al. 2016. "Promotion of Intestinal Epithelial Cell Turnover by Commensal Bacteria: Role of Short-Chain Fatty Acids." *PLoS ONE* 11 (5): 1–22. doi:10.1371/journal.pone.0156334.
- Pelaseyed, Thaher, and Gunnar C. Hansson. 2020. "Membrane Mucins of the Intestine at a Glance." *Journal of Cell Science* 133 (5). doi:10.1242/JCS.240929.
- Pereira, Pedro A.B., Drupad K. Trivedi, Justin Silverman, Ilhan Cem Duru, Lars Paulin, Petri Auvinen, and Filip Scheperjans. 2022. "Multiomics Implicate Gut Microbiota in Altered Lipid and Energy Metabolism in Parkinson's Disease." *Npj Parkinson's Disease* 8 (1). Springer US: 1–17. doi:10.1038/s41531-022-00300-3.
- Post, Sjoerd Van Der, Durai B. Subramani, Malin Bäckström, Malin E.V. Johansson, Malene B. Vester-Christensen, Ulla Mandel, Eric P. Bennett, et al. 2013. "Site-Specific O-Glycosylation on the MUC2 Mucin Protein Inhibits Cleavage by the Porphyromonas Gingivalis Secreted Cysteine Protease (RgpB)." *Journal of Biological Chemistry* 288 (20): 14636–46. doi:10.1074/jbc.M113.459479.
- Raba, Grete, Signe Adamberg, and Kaarel Adamberg. 2021. "Acidic PH Enhances Butyrate Production from Pectin by Faecal Microbiota." *FEMS Microbiology Letters* 368 (7). Oxford University Press: 1–8. doi:10.1093/femsle/fnab042.
- Ragsdale, Stephen W., and Elizabeth Pierce. 2008. "Acetogenesis and the Wood-Ljungdahl Pathway of CO<sub>2</sub> Fixation." *Biochimica et Biophysica Acta - Proteins and Proteomics* 1784 (12): 1873–98. doi:10.1016/j.bbapap.2008.08.012.
- Rao, Jaladanki N., Navneeta Rathor, Ran Zhuang, Tongtong Zou, Lan Liu, Lan Xiao, Douglas J. Turner, and Jian Ying Wang. 2012. "Polyamines Regulate Intestinal Epithelial Restitution through TRPC1-Mediated Ca<sup>2+</sup> Signaling by Differentially Modulating STIM1 and STIM2." *American Journal of Physiology - Cell Physiology* 303 (3): 308–17. doi:10.1152/ajpcell.00120.2012.
- Rappsilber, Juri, Matthias Mann, and Yasushi Ishihama. 2007. "Protocol for Micro-Purification, Enrichment, Pre-Fractionation and Storage of Peptides for Proteomics Using StageTips." *Nature Protocols* 2 (8): 1896–1906. doi:10.1038/nprot.2007.261.
- Ratzke, Christoph, and Jeff Gore. 2018. "Modifying and Reacting to the Environmental PH Can Drive Bacterial Interactions." *PLOS Biology* 16 (3): e2004248. <https://dx.plos.org/10.1371/journal.pbio.2004248>.
- Rawls, John F., Michael A. Mahowald, Ruth E. Ley, and Jeffrey I. Gordon. 2006. "Reciprocal Gut Microbiota Transplants from Zebrafish and Mice to Germ-Free Recipients Reveal Host Habitat Selection." *Cell* 127 (2): 423–33. doi:10.1016/j.cell.2006.08.043.
- Reichardt, Nicole, Sylvia H. Duncan, Pauline Young, Alvaro Belenguer, Carol McWilliam Leitch, Karen P. Scott, Harry J. Flint, and Petra Louis. 2014. "Phylogenetic Distribution of Three Pathways for Propionate Production within the Human Gut Microbiota." *ISME Journal* 8 (6). Nature Publishing Group: 1323–35. doi:10.1038/ismej.2014.14.
- Reichardt, Nicole, Maren Vollmer, Grietje Holtrop, Freda M. Farquharson, Daniel Wefers, Mirko Bunzel, Sylvia H. Duncan, et al. 2018. "Specific Substrate-Driven Changes in Human Faecal Microbiota Composition Contrast with Functional Redundancy in Short-Chain Fatty Acid Production." *ISME Journal* 12 (2). Nature Publishing Group: 610–22. doi:10.1038/ismej.2017.196.

- Ridaura, Vanessa K., Jeremiah J. Faith, Federico E. Rey, Jiye Cheng, Alexis E. Duncan, Andrew L. Kau, Nicholas W. Griffin, et al. 2013. "Gut Microbiota from Twins Discordant for Obesity Modulate Metabolism in Mice." *Science* 341 (6150). doi:10.1126/science.1241214.
- Rio, Beatriz del, Begoña Redruello, Victor Ladero, Santiago Cal, Alvaro J. Obaya, and Miguel A. Alvarez. 2018. "An Altered Gene Expression Profile in Tyramine-Exposed Intestinal Cell Cultures Supports the Genotoxicity of This Biogenic Amine at Dietary Concentrations." *Scientific Reports* 8 (1): 1–8. doi:10.1038/s41598-018-35125-9.
- Roager, Henrik M., Lea B.S. Hansen, Martin I. Bahl, Henrik L. Frandsen, Vera Carvalho, Rikke J. Gøbel, Marlene D. Dalgaard, et al. 2016. "Colonic Transit Time Is Related to Bacterial Metabolism and Mucosal Turnover in the Gut." *Nature Microbiology* 1 (9). Nature Publishing Group: 1–9. doi:10.1038/nmicrobiol.2016.93.
- Rodríguez-Piñeiro, Ana M., Joakim H. Bergström, Anna Ermund, Jenny K. Gustafsson, André Schütte, Malin E.V. Johansson, and Gunnar C. Hansson. 2013. "Studies of Mucus in Mouse Stomach, Small Intestine, and Colon. II. Gastrointestinal Mucus Proteome Reveals Muc2 and Muc5ac Accompanied by a Set of Core Proteins." *American Journal of Physiology - Gastrointestinal and Liver Physiology* 305 (5). doi:10.1152/ajpgi.00047.2013.
- Rogowski, Artur, Jonathon A. Briggs, Jennifer C. Mortimer, Theodora Tryfona, Nicolas Terrapon, Elisabeth C. Lowe, Arnaud Baslé, et al. 2015. "Glycan Complexity Dictates Microbial Resource Allocation in the Large Intestine." *Nature Communications* 6 (May). doi:10.1038/ncomms8481.
- Russell, Wendy R., Silvia W. Gratz, Sylvia H. Duncan, Grietje Holtrop, Jennifer Ince, Lorraine Scobbie, Garry Duncan, et al. 2011. "High-Protein, Reduced-Carbohydrate Weight-Loss Diets Promote Metabolite Profiles Likely to Be Detrimental to Colonic Health." *American Journal of Clinical Nutrition* 93 (5): 1062–72. doi:10.3945/ajcn.110.002188.
- Saad, Richard J., Satish S.C. Rao, Kenneth L. Koch, Braden Kuo, Henry P. Parkman, Richard W. McCallum, Michael D. Sitrin, Gregory E. Wilding, Jack R. Semler, and William D. Chey. 2010. "Do Stool Form and Frequency Correlate with Whole-Gut and Colonic Transit Results from a Multicenter Study in Constipated Individuals and Healthy Controls." *American Journal of Gastroenterology* 105 (2). Nature Publishing Group: 403–11. doi:10.1038/ajg.2009.612.
- Samuel, Buck S., Abdullah Shaito, Toshiyuki Motoike, Federico E. Rey, Fredrik Backhed, Jill K. Manchester, Robert E. Hammer, et al. 2008. "Effects of the Gut Microbiota on Host Adiposity Are Modulated by the Short-Chain Fatty-Acid Binding G Protein-Coupled Receptor, Gpr41." *Proceedings of the National Academy of Sciences of the United States of America* 105 (43): 16767–72. doi:10.1073/pnas.0808567105.
- Schirmer, Melanie, Eric A. Franzosa, Jason Lloyd-Price, Lauren J. McIver, Randall Schwager, Tiffany W. Poon, Ashwin N. Ananthakrishnan, et al. 2018. "Dynamics of Metatranscription in the Inflammatory Bowel Disease Gut Microbiome." *Nature Microbiology* 3 (3). Springer US: 337–46. doi:10.1038/s41564-017-0089-z.
- Schroeder, Bjoern O. 2019. "Fight Them or Feed Them: How the Intestinal Mucus Layer Manages the Gut Microbiota." *Gastroenterology Report* 7 (1): 3–12. doi:10.1093/gastro/goy052.

- Schroeder, Bjoern O., George M.H. Birchenough, Meenakshi Pradhan, Elisabeth E.L. Nyström, Marcus Henricsson, Gunnar C. Hansson, and Fredrik Bäckhed. 2020. "Obesity-Associated Microbiota Contributes to Mucus Layer Defects in Genetically Obese Mice." *Journal of Biological Chemistry* 295 (46): 15712–26. doi:10.1074/jbc.RA120.015771.
- Schroeder, Bjoern O, George M H Birchenough, Marcus Ståhlman, Liisa Arike, Malin E V Johansson, Gunnar C Hansson, and Fredrik Bäckhed. 2018. "Bifidobacteria or Fiber Protect against Diet-Induced Microbiota-Mediated Colonic Mucus Deterioration." *Cell Host Microbe* 23 (1): 27–40. doi:10.1016/j.chom.2017.11.004.
- Schulz, Benjamin L., Nicolle H. Packer, and Niclas G. Karlsson. 2002. "Small-Scale Analysis of O-Linked Oligosaccharides from Glycoproteins and Mucins Separated by Gel Electrophoresis." *Analytical Chemistry* 74 (23): 6088–97. doi:10.1021/ac025890a.
- Sekirov, Inna, Shannon L. Russell, L. Caetano M Antunes, and Brett B. Finlay. 2010. "Gut Microbiota in Health and Disease." *Physiological Reviews* 90 (3): 859–904. doi:10.1152/physrev.00045.2009.
- Sender, Ron, Shai Fuchs, and Ron Milo. 2016. "Are We Really Vastly Outnumbered? Revisiting the Ratio of Bacterial to Host Cells in Humans." *Cell* 164 (3). Elsevier Inc.: 337–40. doi:10.1016/j.cell.2016.01.013.
- Sluis, Maria Van der, Barbara A.E. De Koning, Adrianus C.J.M. De Bruijn, Anna Velcich, Jules P.P. Meijerink, Johannes B. Van Goudoever, Hans A. Büller, et al. 2006. "Muc2-Deficient Mice Spontaneously Develop Colitis, Indicating That MUC2 Is Critical for Colonic Protection." *Gastroenterology* 131 (1): 117–29. doi:10.1053/j.gastro.2006.04.020.
- Smith, E. A., and G. T. Macfarlane. 1996. "Enumeration of Human Colonie Bacteria Producing Phenolic and Indolic Compounds: Effects of PH, Carbohydrate Availability and Retention Time on Dissimilatory Aromatic Amino Acid Metabolism." *Journal of Applied Bacteriology* 81 (3): 288–302. doi:10.1111/j.1365-2672.1996.tb04331.x.
- Sonnenburg, Erica D., Samuel A. Smits, Mikhail Tikhonov, Steven K. Higginbottom, Ned S. Wingreen, and Justin L. Sonnenburg. 2016. "Diet-Induced Extinctions in the Gut Microbiota Compound over Generations." *Nature* 529 (7585). Nature Publishing Group: 212–15. doi:10.1038/nature16504.
- Szentkuti, L., H. Riedesel, M. L. Enss, K. Gaertner, and W. von Engelhardt. 1990. "Pre-Epithelial Mucus Layer in the Colon of Conventional and Germ-Free Rats." *The Histochemical Journal* 22 (9): 491–97. doi:10.1007/BF01007234.
- Tailford, Louise E., Emmanuelle H. Crost, Devon Kavanaugh, and Nathalie Juge. 2015. "Mucin Glycan Foraging in the Human Gut Microbiome." *Frontiers in Genetics* 5 (FEB). doi:10.3389/fgene.2015.00081.
- Tailford, Louise E., C. David Owen, John Walshaw, Emmanuelle H. Crost, Jemma Hardy-Goddard, Gwenaelle Le Gall, Willem M. De Vos, Garry L. Taylor, and Nathalie Juge. 2015. "Discovery of Intramolecular Trans-Sialidases in Human Gut Microbiota Suggests Novel Mechanisms of Mucosal Adaptation." *Nature Communications* 6 (May). Nature Publishing Group: 1–12. doi:10.1038/ncomms8624.
- Trastoy, Beatriz, Andreas Naegeli, Itxaso Anso, Jonathan Sjögren, and Marcelo E. Guerin. 2020. "Structural Basis of Mammalian Mucin Processing by the Human Gut O-Glycopeptidase OgpA from *Akkermansia muciniphila*." *Nature Communications* 11 (1). Springer US: 1–14. doi:10.1038/s41467-020-18696-y.

- Vandeputte, Doris, Gwen Falony, Sara Vieira-Silva, Raul Y. Tito, Marie Joossens, and Jeroen Raes. 2016. "Stool Consistency Is Strongly Associated with Gut Microbiota Richness and Composition, Enterotypes and Bacterial Growth Rates." *Gut* 65 (1): 57–62. doi:10.1136/gutjnl-2015-309618.
- Vangay, Pajau, Abigail J. Johnson, Tonya L. Ward, Gabriel A. Al-Ghalith, Robin R. Shields-Cutler, Benjamin M. Hillmann, Sarah K. Lucas, et al. 2018. "US Immigration Westernizes the Human Gut Microbiome." *Cell* 175 (4). Elsevier Inc.: 962-972.e10. doi:10.1016/j.cell.2018.10.029.
- Velcich, Anna, Wan Cai Yang, Joerg Heyer, Alessandra Fragale, Courtney Nicholas, Stephanie Viani, Raju Kucherlapati, Martin Lipkin, Kan Yang, and Leonard Augenlicht. 2002. "Colorectal Cancer in Mice Genetically Deficient in the Mucin Muc2." *Science* 295 (5560): 1726–29. doi:10.1126/science.1069094.
- Vries, Jan de, Paige E. Miller, and Kristin Verbeke. 2015. "Effects of Cereal Fiber on Bowel Function: A Systematic Review of Intervention Trials." *World Journal of Gastroenterology* 21 (29): 8952–63. doi:10.3748/wjg.v21.i29.8952.
- Wardman, Jacob F., Rajneesh K. Bains, Peter Rahfeld, and Stephen G. Withers. 2022. "Carbohydrate-Active Enzymes (CAZymes) in the Gut Microbiome." *Nature Reviews Microbiology* 20 (9). Springer US: 542–56. doi:10.1038/s41579-022-00712-1.
- Wexler, Aaron G., and Andrew L. Goodman. 2017. "An Insider's Perspective: Bacteroides as a Window into the Microbiome." *Nature Microbiology* 2 (April). Macmillan Publishers Limited. doi:10.1038/nmicrobiol.2017.26.
- Wiśniewski, Jacek R., Alexandre Zougman, Nagarjuna Nagaraj, and Matthias Mann. 2009. "Universal Sample Preparation Method for Proteome Analysis." *Nature Methods* 6 (5): 359–62. doi:10.1038/nmeth.1322.
- Wrzosek, Laura, Sylvie Miquel, Marie-Louise Noordine, Stephan Bouet, Marie Joncquel Chevalier-Curt, Veronique Robert, Catherine Philippe, et al. 2013. "Bacteroides Thetaiotaomicron and Faecalibacterium Prausnitzii Influence the Production of Mucus Glycans and the Development of Goblet Cells in the Colonic Epithelium of a Gnotobiotic Model Rodent." *BMC Biology* 144 (5): S-59. doi:10.1016/s0016-5085(13)60210-3.
- Xie, Aoji, Elizabeth Ensink, Peipei Li, Juozas Gordevičius, Lee L. Marshall, Sonia George, John Andrew Pospisilik, et al. 2022. "Bacterial Butyrate in Parkinson's Disease Is Linked to Epigenetic Changes and Depressive Symptoms." *Movement Disorders* 37 (8): 1644–53. doi:10.1002/mds.29128.
- Xu, Jian, Magnus K. Bjursell, Jason Himrod, Su Deng, Lynn K. Carmichael, Herbert C. Chiang, Lora V. Hooper, and Jeffrey I. Gordon. 2003. "A Genomic View of the Human-Bacteroides Thetaiotaomicron Symbiosis." *Science* 299 (5615): 2074–76. doi:10.1126/science.1080029.
- Xu, Jian, and Jeffrey I. Gordon. 2003. "Honor Thy Symbionts." *Proceedings of the National Academy of Sciences of the United States of America* 100 (18): 10452–59. doi:10.1073/pnas.1734063100.



## Acknowledgements

First and foremost, my sincere gratitude goes to my supervisors Kaarel Adamberg and Liisa Arike for accepting me as your student and guiding me through this all. You have introduced me to the slimy world of microbiota and mucins which I have found immensely interesting and hope to continue exploring together. You have been my mentors, always ready to discuss any questions I have. I would like to thank professor Raivo Vilu for sparking my interest in the microscopic bubble reactors we call bacteria. I am thankful to all my colleagues from the Institute of Chemistry and Biotechnology and from the Centre of Food and Fermentation Technologies with whom we have worked together over the years. I appreciate the labmates from Mucin Biology Groups for their warm welcome of me to their group and I look forward to continue working with them in the future.

I am forever grateful to my family who has always supported and believed in me. You have provided me with warmth, love and everything I could ask for. I am also lucky to be surrounded by wonderful friends who have offered some much-needed fun diversions. You have helped me keep my sanity.

This work has been funded by Estonian Ministry of Science and Education Institutional Funding (IUT1927) and the European Regional Development Fund (EU48667). The works of Publication III and Manuscript were additionally supported by the National Institute of Health grant (R01 DK125445), The Knut and Alice Wallenberg Foundation grant (2017.0028), Bill and Melinda Gates Foundation grant (OPP1202459), Wilhelm and Martina Lundgren's Foundation, the Swedish Research council grants (2017-00958 and 2021-01409, Swedish Society for Medical Research (S21-0026) and Sahlgrenska Academy International Starting Grant (GU2021/1070). Travel grants by European Regional Development Fund Education and Youth Board (5.10-6.1/20/20-2) and Archimedes Foundation (16-3.5/2011) enabled the visits to my co-supervisor's lab in Gothenburg University. Financial support from Doctoral School of Biomedicine and Biotechnology and from the Archimedes foundation was used to attend international scientific conferences.

## Abstract

### Co-metabolism of mucins and dietary fibres by gut microbiota

The gut microbiota is a crucial part of the host gastrointestinal system. It carries out vital functions, such as degradation of indigestible complex dietary fibres from the diet. The gut bacteria are adapted to utilising these substrates because of their large genomes which encode various carbohydrate-active enzymes. Diet-derived fermentable polysaccharides are the preferred carbon source for most gut bacteria. However, in the absence or depletion of dietary fibres some bacteria can switch to other energy sources, such as host-derived glycans like mucins. Mucins are large glycoproteins that are the primary structural components of the epithelium-covering mucus layer. The mucus lubricates the gastrointestinal tract and protects the epithelial cells from contact with the bacteria. The mucus layer is constantly renewed by secretion of gel-like mucins by goblet cells in the intestinal crypts. The degradation of mucins by select members of the microbiota is part of the intestinal homeostasis and provides the host with energy and bioactive compounds. Yet, when the gut microbial community becomes imbalanced, the mucolytic taxa can overgrow the fibre-degrading species, leading to excess mucin degradation. In this case the mucus barrier function gets impaired and the mucus becomes penetrable to bacteria. When bacteria come into contact with the epithelium, it can lead to inflammation and disease. Therefore, it is of utmost importance to maintain a diverse gut microbiota where different taxa are in balance.

A way to support gut diversity is through dietary interventions such as consumption of dietary fibres, either from food or as supplements. Several such prebiotics are already on the market. However, their health claims are poorly defined due to the complexity and large individual variances of the host-microbiota systems. Moreover, the studies on dietary fibres utilisation by gut microbiota often neglect the presence of host glycans such as mucins. The study presented in this dissertation aims to overcome these obstacles by studying the mucin and dietary fibre co-metabolism systematically under various physiologically relevant conditions. The microbial community was standardised by pooling several faecal samples from healthy donors and using aliquots of the same consortium as inoculums for every cultivation experiment in this study. This strategy allows comparing the results between different experiments.

The microbiota growth space was studied in continuous and batch cultures. A range of transit rates, pH values and substrates were scanned to elucidate their effect on microbiota growth and metabolism. 16S rRNA sequencing, chromatography and mass spectrometry were used to analyse the consortia composition and metabolism. A spheroid model was used to assess substrates' potential prebiotic effect to the host. Finally, mathematical models were applied to validate the analytics.

All three studied parameters had significant microbiota modulating effects. Especially susceptible to changes were the mucin degraders whose abundances varied greatly under the range of tested conditions. This finding offers an interesting candidate for future follow-up studies to find potential targets to improve the gut barrier function. By manipulating the growth of different mucolytic species through diet, a desired consortium could be achieved to either increase or decrease mucus degradation. On a similar note, a surprising effect was demonstrated for mucin degrading *Akkermansia muciniphila*. Previously it was shown that in pure cultures this bacterium is unable to grow on porcine colonic mucins. However, this study showed it becoming the dominant

species of coculture on porcine colonic mucin, utilising both the *O*-glycans and the mucin protein. Additionally, the study demonstrates how the more complex-structured polysaccharides increase the microbial diversity, especially the growth of various *Bacteroides* species. The breakdown of these dietary fibres requires enzymes from several different families and the downstream metabolism is carried out by multiple bacterial groups. Finally, the work highlighted the suitability of a novel substrate, colonic mucin, as co-substrate for microbiota growth studies.

Altogether, these results elucidate the growth and metabolism of complex microbiota under conditions that mimic host physiological state in health and disease.

## Lühikokkuvõte

### Mutsiinide ja kiudainete kometabolism soolestiku mikrobioota poolt

Soolestiku mikrobioota on oluline osa peremeesorganismi seedetraktist. Mikrobioota täidab eluks vajalikke funktsioone nagu toidus olevate seedumatute kiudainete lagundamine. Soolestiku bakterid on selliste substraatide kasutamiseks adapteerinud tänu nende suurtele genoomidele, mis kodeerivad erinevaid süsivesikute lagundamise ensüüme. Enamik soolestiku baktereid kasutavad süsiniku allikana eelistatult toidust pärit fermenteeritavaid polüsahhariide. Kuid kiudainete puudumisel või otsa saamisel suudavad mõned bakterid lülituda ümber ning kasutada teisi energiaallikaid, näiteks peremehe poolt toodetud glükaane nagu mutsiinid. Mutsiinid on suured glükoproteiinid, mis annavad epiteeliumi katvale limakihile tema struktuuri. See limakiht libestab seedetrakti ja kaitseb epiteelrakke kokkupuute eest bakteritega. Soolestiku krüptides asuvad karikarakud sekreteerivad jooksvalt geelitaolisi mutsiine, hoides niimoodi limakihti pidevas uuendamises. Mutsiinide lagundamine valitud mikrobioota liikmete poolt on osa soolestiku homöostaasist, varustades peremeest energia ja bioaktiivsete ühenditega. Siiski, kui soole mikroobne kooslus läheb tasakaalust välja, võivad mukolüütilised taksonid võtta võimu kiudaineid lagundavate liikide üle, millega kaasneb üleliigne mutsiini lagundamine. Sellisel juhul kannatab limakihi kaitsefunktsioon ja lima võib muutuda bakteritele läbitavaks. Bakterite kontakt epiteeliumiga võib viia põletiku ja haiguste tekkeni. Seetõttu on ülimalt oluline säilitada mitmekülgne soolestiku mikrobioota, kus erinevad taksonid on omavahel tasakaalus.

Soolestiku mitmekesisust on võimalik toetada läbi toitumise, näiteks tarbides kiudaineid kas toidust või toidulisanditena. Mitmed sellised prebiootikumid on juba turul, kuid peremehe-mikrobioota süsteemid on keerulised ning suure individuaalse erinevusega, mistõttu on selliste toidulisandite tervisealaseid väiteid keeruline defineerida. Lisaks sellele ei arvesta mikrobioota kiudainete tarbimise uuringud sageli peremehe toodetud glükaanide nagu mutsiinide olemasoluga. Selles väitekirjas esitatud uurimuse eesmärgiks oli lahendada neid probleeme, uurides mutsiinide ja kiudainete kometabolismi süstemaatiliselt, imiteerides erinevaid füsioloogilisi tingimusi. Mikroobikooslus standardiseeriti, segades kokku fekaaliproovid mitmelt doonorilt ning kasutades sama koosluse alikvoote igas kultiveerimiskatses. Selline strateegia võimaldab võrrelda eksperimentide vahelisi tulemusi.

Mikrobioota kasvuruumi määramiseks kasutati nii läbivoolu kui annuskultuure. Skaneeriti läbikäigu kiiruste ja pH vahemikke ning erinevaid substraate et mõista nende mõju mikrobioota kasvule ja metabolismile. 16S rRNA sekveneerimise, kromatograafia ja massispektromeetria abil analüüsiti koosluse koostist ja metabolismi. Sferoidmudeli abil hinnati substraatide potentsiaalset prebiootilist efekti peremehele. Lõpetuseks rakendati matemaatilisi mudeleid, et valideerida analüütilised tulemused.

Kõik kolm uuritud parameetrit avaldasid mikrobiootale olulist moduleerivat mõju. Mutsiini lagundajad olid muutustele eriti vastuvõtlikud ning nende osakaalud erinevates tingimustes varieerusid oluliselt. See avastus pakub huvitava kandidaadi tulevastele uuringutele, leidmaks potentsiaalseid sihtmärke, mille kaudu parandada soolestiku kaitsefunktsiooni. Manipuleerides dieedi kaudu erinevate mukolüütiliste liikide kasvu võiks olla võimalik saavutada soovitud kooslus, mis kas suurendaks või vähendaks limakihi lagundamist. Lisaks õnnestus demonstreerida üllatavat efekti mutsiinilagundaja *Akkermansia muciniphila* puhul. Varasemad uuringud on näidanud, et selle bakteri

puhaskultuurid ei ole võimelised kasvama sea jämesoole mutsiini peal. Seevastu käesolevas uuringus demonstreeriti, kuidas *A. muciniphila* domineerib sea jämesoole peal kasvatatud segakooslust ning tarvitab nii mutsiini *O*-glükaane kui ka valgulist osa. Lisaks näidati siin töös, kuidas keerulise struktuuriga kiudained suurendavad mikroobset mitmekesisust, eriti erinevate *Bacteroides* liikide kasvu. Selliste polüsahhariidide lagundamiseks oli vaja erinevatest perekondadest pärit ensüüme ning vabanenud suhkruid kasutasid edasi mitmed bakterite rühmad. Lõpetuseks näitasid uuringu tulemused uudse substraadi, jämesoole mutsiini, sobivust kosubstraadina mikrobiota kasvu uuringutel.

Kokkuvõtvalt selgitavad need tulemused mikrobiota kasvu ja metabolismi tingimustes, mis imiteerivad peremehe füsioloogiat nii terves kui haiguslikus seisundis.

## Appendix 1

### Publication I

Adamberg, K., **Raba, G.**, Adamberg, S. Use of changestat for growth rate studies of gut microbiota. *Frontiers in Bioengineering and Biotechnology*. 2020, 8, 24. doi: 10.3389/fbioe.2020.00024. PMID: 32117913.





# Use of Changestat for Growth Rate Studies of Gut Microbiota

Kaarel Adamberg<sup>1,2\*</sup>, Grete Raba<sup>1</sup> and Signe Adamberg<sup>1</sup>

<sup>1</sup> Department of Chemistry and Biotechnology, Tallinn University of Technology, Tallinn, Estonia, <sup>2</sup> Center of Food and Fermentation Technologies, Tallinn, Estonia

Human colon microbiota, composed of hundreds of different species, is closely associated with several health conditions. Controlled *in vitro* cultivation and up-to-date analytical methods make possible the systematic evaluation of the underlying mechanisms of complex interactions between the members of microbial consortia. Information on reproducing fecal microbial consortia can be used for various clinical and biotechnological applications. In this study, chemostat and changestat cultures were used to elucidate the effects of the physiologically relevant range of dilution rates on the growth and metabolism of adult fecal microbiota. The dilution rate was kept either at  $D = 0.05$  or  $D = 0.2$  1/h in chemostat cultures, while gradually changing from 0.05 to 0.2 1/h in the A-stat and from 0.2 to 0.05 1/h in the De-stat. Apple pectin as a substrate was used in the chemostat experiments and apple pectin or birch xylan in the changestat experiments, in the presence of porcine mucin in all cases. The analyses were comprised of HPLC for organic acids, UPLC for amino acids, GC for gas composition, 16S-rDNA sequencing for microbial composition, and growth parameter calculations. It was shown that the abundance of most bacterial taxa was determined by the dilution rate on both substrates. *Bacteroides ovatus*, *Bacteroides vulgatus*, and *Faecalibacterium* were prevalent within the whole range of dilution rates. *Akkermansia muciniphila* and Ruminococcaceae UCG-013 were significantly enriched at  $D = 0.05$  1/h, while *Bacteroides caccae*, Lachnospiraceae unclassified and *Escherichia coli* clearly preferred  $D = 0.2$  1/h. In the chemostat cultures, the production of organic acids and gases from pectin was related to the dilution rate. The ratio of acetate, propionate and butyrate was 5:2:1 ( $D = 0.05$  1/h) and 14:2:1 ( $D = 0.2$  1/h). It was shown that the growth rate-related characteristics of the fecal microbiota were concise in both directions between  $D = 0.05$  and 0.2 1/h. Reproducible adaptation of the fecal microbiota was shown in the continuous culture with a changing dilution rate: changestat. Consortia cultivation is a promising approach for research purposes and several biotechnological applications, including the production of multi-strain probiotics and fecal transplantation mixtures.

**Keywords:** continuous cultivation, changestat, fecal microbiota, apple pectin, birch xylan

## INTRODUCTION

The cultivation of fecal consortia is essential for understanding the mechanisms behind the coexistence of gut microbial species under changing environmental conditions. This information is required in biotechnological and clinical applications, although better defined methods are required for safer procedures. As the desired consortia can be composed of tens or even hundreds of strains,

## OPEN ACCESS

### Edited by:

Thomas Egli,  
ETH Zürich, Switzerland

### Reviewed by:

Lars Regestein,  
Leibniz Institute for Natural Product  
Research and Infection Biology,  
Germany

Sergio Revah,  
Autonomous Metropolitan University,  
Mexico

### \*Correspondence:

Kaarel Adamberg  
kaarel.adamberg@taltech.ee

### Specialty section:

This article was submitted to  
Bioprocess Engineering,  
a section of the journal  
Frontiers in Bioengineering and  
Biotechnology

**Received:** 30 August 2019

**Accepted:** 13 January 2020

**Published:** 07 February 2020

### Citation:

Adamberg K, Raba G and  
Adamberg S (2020) Use  
of Changestat for Growth Rate  
Studies of Gut Microbiota.  
*Front. Bioeng. Biotechnol.* 8:24.  
doi: 10.3389/fbioe.2020.00024



e.g., next generation probiotics, the cultivation of a balanced consortium saves time and labor compared to the production of single cultures. Moreover, the biomass yields of pure cultures can remain below those of natural bacterial communities, because of a deficiency of several growth factors produced by other consortia members. In this field, the culturomics approach has been developed, where a set of different media are used to cultivate each isolate in a multi-parallel approach (Lagier et al., 2012). This approach has expanded the range of microorganisms that can be cultivated in the lab. The reintroduction of fecal microbiota is a promising method to cure certain gastrointestinal conditions (Petrof et al., 2013). Previously, the most diverse stool substitute containing 33 single fecal isolates was developed by Petrof et al. (2013) to cure antibiotic-resistant *Clostridium difficile*-induced colitis. Also, batch cultures have been used for the production of fecal biomass to treat diarrhea caused by *C. difficile* infection (Jorup-Rönström et al., 2012). Batch cultures are most commonly used for high-throughput small-scale parallel experiments. However, such conditions as substrate concentrations and the accumulation of metabolites are continuously changing. Furthermore, the overgrowth of fast-growing bacteria in mixed cultures is common for batch cultures; for instance, an over 10% increase in *Escherichia coli* from the total population has been reported (Brahma et al., 2017; Adamberg et al., 2018). Thus, it is difficult to analyze the actual selectivity of a tested substrate. Consequently, batch technologies are well suited for high throughput screening or for the industrial production of biomass, but have limited value for studies of specific growth mechanisms and the metabolism of complex microbial consortia.

In a microbial consortium, the steady state composition is defined by complex microbial interactions. These interactions can be supportive (mutual or commensal) or inhibitory (ammensal or competitive), and are driven by residual concentrations of substrates, bacterial metabolites and cross-feeding between different bacteria (Gottschal, 1990). By cultivating 37 mouse gut bacteria in continuous mode, Freter et al. (1983) demonstrated that the population dynamics of indigenous intestinal bacteria are controlled by one or a few substrates. Chung et al. (2019) studied the degradation of five different fibers or fiber mixtures by fecal microbiota in a chemostat and showed that mixed fiber substrates led to the growth of more diverse microbiota than inulin alone. In the cultures of gut microbes, cross-feeding has been supposed to be one of the most important factors for gut microbiota richness. To explain the interactions between different microorganisms in a consortium, in addition to cell modeling, simple culture systems, such as defined mixed cultures and single substrates, should be studied first. This makes it possible to elucidate the primary degraders and substrates (hetero- or autotrophies), auxotrophies and compounds derived from cross-feeding. The dynamic data for predicting bacterial behavior in communities can be best obtained from continuous cultures at low substrate concentrations (Russell and Baldwin, 1979; Tannock, 2017). For example, ecological studies have shown that growth under multiple substrate limitations at very low dilution rates supports species having high growth efficiency (higher yield) but low maximal specific growth rate (Gottschal, 1990). Auxotrophy to a

specific compound can be used to promote a species in a mixed culture by supplementing the culture medium with this substrate. Two species containing batch experiments revealed that acetate or lactate produced by *Bacteroides* or *Bifidobacterium* stimulated the growth of butyric acid producing bacteria, while formate and hydrogen enhanced methanogens (Rowland et al., 2018). The dynamics and stability of freshly collected fecal cultures have been studied by several groups, although the use of fresh samples does not allow for direct comparison of the results from different studies (Miller and Wolin, 1981; Macfarlane et al., 1998; Sghir et al., 1998; McDonald et al., 2013; Yen et al., 2015; Chung et al., 2016; von Martels et al., 2017).

The determination of community composition is essential in microbiota research. Next-generation sequencing methods, such as 16S rDNA analysis and whole genome sequencing (WGS), are high throughput approaches that make it possible to identify all of the taxa in whole consortia, but only semi-quantitatively as proportions of the bacteria in a consortium. To obtain quantitative data, bacterial counting through flow cytometry, dry weight analysis or plate counting should be carried out in parallel. Moreover, to determine the taxa of low abundance, the coverage of sequences has to be proportionally higher. Also, species level analysis might require more detailed sequence analysis (WGS) than is available by 16S rDNA sequencing. For the quantitative analysis of bacteria in fecal consortia, species are usually assessed by fluorescent *in situ* hybridization with 16S rRNA probes (Langendijk et al., 1995), although as each species requires a specific probe, this approach is limited by the number of species analyzed or is expensive in an array setup, such as HITChip (Rajilić-Stojanović et al., 2009).

With all cultivation models it should be kept in mind that the specific growth rate of bacteria is not linearly related to the colonic transit rate, since the density of bacteria gradually increases, while the moving rate decreases along the colon. An alternative continuous cultivation technology, changestat, in which all cultivation parameters are computer-controlled, has been developed in our lab. In changestat, the effect of a selected parameter is studied by the gradual change in this parameter within a certain range, while keeping all other conditions constant (Paalme et al., 1995; Kasemets et al., 2003; Adamberg et al., 2015). Our recent study highlighted the importance of dilution rate in determining the composition and diversity of fecal microbiota (Adamberg and Adamberg, 2018). It was also shown that by using de-celerostat (De-stat), the fast- and slow-growing consortia were differentiated from the fecal microbiota during the same experiment (Adamberg and Adamberg, 2018). To analyze whether these results were too biased depending on the starting point, we carried out experiments in both directions: gradually moving dilution rates from slow to fast (accelerostat: A-stat) and from fast to slow (De-stat), between 0.05 and 0.2 1/h.

The main aims of the current study were: (1) to elucidate the reproducibility of the chemostat cultures by using the same adult fecal pool, (2) to study the effects of dilution rate on the dynamics and metabolism of fecal microbiota by using A-stat and De-stat cultures, and (3) to elucidate the metabolism of two common dietary fibers, pectin and xylan, by fecal microbiota. Food is an important factor in modulating colonic microbiota and through

bacterial metabolism promoting health-supporting or disease-activating mechanisms. Pectins are a part of the daily diet, consumed in the form of fruits and vegetables and used as food additives. Xylans are abundant in nature as major constituents of hemicellulose in plant cells.

## MATERIALS AND METHODS

### Fecal Inoculum

Fecal samples were collected from seven healthy adult volunteers (19–37 years old, Caucasian, both male and female) and homogenized in four volumes of 5% DMSO-containing buffer, as described in Adamberg et al. (2015). The exclusion criteria included the use of supplements of prebiotics and probiotics, laxatives and antibiotics for 4 weeks prior to donation. Equal volumes of the seven fecal slurries were pooled together and aliquots were kept at  $-80^{\circ}\text{C}$  for repetitive cultivation experiments. Similar sample preparation (standardization by pooling) has also been used and approved by others for *in vitro* testing in the TIM-2 proximal colon model (Aguirre et al., 2015; Bussolo de Souza et al., 2019).

### Defined Base Medium

The defined growth medium was prepared in a 0.05 M potassium phosphate buffer made from 1 M stock solutions (mL/L):  $\text{K}_2\text{HPO}_4$  (28.9) and  $\text{KH}_2\text{PO}_4$  (21.1); mineral salts (mg/L):  $\text{MgSO}_4 \cdot 7\text{H}_2\text{O}$  (36),  $\text{FeSO}_4 \cdot 7\text{H}_2\text{O}$  (0.1),  $\text{CaCl}_2$  (9),  $\text{MnSO}_4 \cdot \text{H}_2\text{O}$  (3),  $\text{ZnSO}_4 \cdot 7\text{H}_2\text{O}$  (1),  $\text{CoSO}_4 \cdot 7\text{H}_2\text{O}$  (1),  $\text{CuSO}_4 \cdot 5\text{H}_2\text{O}$  (1),  $(\text{NH}_4)_6\text{Mo}_7\text{O}_{24} \cdot 4\text{H}_2\text{O}$  (1),  $\text{NaCl}$  (527); hemin (5 mg/L); vitamin K1 (0.5 mg/L); L-amino acids (g/L): Ala (0.044), Arg (0.023), Asn (0.038), Asp (0.038), Glu (0.036), Gln (0.018), Gly (0.032), His (0.027), Ile (0.060), Leu (0.120), Lys-HCl (0.080), Met (0.023), Phe (0.050), Pro (0.041), Ser (0.095), Thr (0.041), Trp (0.009), Val (0.060), Tyr (0.015); vitamins (mg/L): biotin (0.25), Ca-pantothenate (0.25), folic acid (0.25), nicotinamide (0.25), pyridoxine-HCl (0.50), riboflavin (0.25), thiamine-HCl (0.25) and other components (g/L): bile salts (0.5),  $\text{NaHCO}_3$  (2.0), Tween-80 (0.5), Na-thioglycolate (0.5), and Cys-HCl (0.5, freshly made). The carbohydrate substrates were sterilized separately and mixed with the medium before cultivation. Two substrate combinations, either birch xylan (Sigma-Aldrich, United States) or apple pectin (Sigma-Aldrich, United States) with porcine mucin (Type II, Sigma Aldrich, United States), were added to the base medium in equal amounts (2.5 g/L each). The pH of the growth medium was  $7.2 \pm 0.1$ .

### Fermentation System

The Biobundle cultivation system consisted of the ADI 1030 bio-controller and cultivation control program “BioXpert” (Applikon, Netherlands). The fermenter was equipped with sensors for pH,  $\text{pO}_2$ , and temperature. Variable speed pumps for feeding and outflow were controlled by a De-stat or A-stat algorithm:  $D = D_0 - d \cdot t$  or  $D = D_0 + a \cdot t$ , respectively, where  $D$  is the dilution rate (1/h),  $D_0$  is the initial dilution rate,  $d$  and  $a$  are the deceleration and acceleration rate ( $1/\text{h}^2$ ), respectively, and  $t$  is the time (h). In accelerostat (A-stat), the dilution rate

was gradually increased from 0.05 to 0.2 1/h and in decelerostat (De-stat) the dilution rate was gradually decreased from 0.2 to 0.05 1/h in accordance with the typical transit rate of the human colon (Adamberg and Adamberg, 2018). pH was controlled by a 1M NaOH addition according to the pH set-point. The culture volume was kept constant (300 mL) by monitoring the weight of the fermenter with the PC-linked balance and outflow pump. The pH of the culture was kept at 7.0 and the temperature was kept constant at  $36.6^{\circ}\text{C}$ . The medium in the feeding bottle and the fermenter was flushed with sterile-filtered nitrogen gas (99.9%, AGA) overnight before inoculation and throughout the cultivation to maintain anaerobiosis. Nitrogen flushing was on during the whole experiment. Two mL of the pooled fecal culture was inoculated to start the experiment.

The cultivation algorithm was started 15–17 h after inoculation in the midst of the exponential growth of bacteria. The dilution rate was stabilized at either 0.05 or 0.2 1/h, at pH 7.0, and run for stabilization at these conditions by 6–7 residence times. After achieving a stable titration rate and gas production, the dilution rate was decreased to 0.05 1/h or increased to 0.2 1/h at a rate of 0.05 units per day (the experimental timeline is presented in **Figure 1**). The dilution rate interval was chosen to cover the realistic growth rates of luminal bacteria in the colon. The range of the specific growth rate of the bacteria was calculated based on the colonic transit time of digesta in people consuming Western diets, which varies from 40 to 140 h (median 60–70 h) (Burkitt et al., 1972; Cummings et al., 1976; Fallingborg et al., 1989), and the estimated amount of bacteria, which increases from  $10^8$  in the proximal colon to  $10^{11}$  cfu/g in feces (Sender et al., 2016). Considering both the period the bacteria have for degradation of dietary fibers and the coinciding increase in the bacterial biomass in the colon, the specific growth rate of the bacteria decreased from 0.3 to 0.02 1/h. Thus, the range of the dilution rates tested in the cultivation experiments, 0.05–0.2 1/h, was chosen.

### Analytical Methods

Samples from the outflow were collected on ice, centrifuged (14,000 g, 5 min,  $4^{\circ}\text{C}$ ) and stored separately as pellets and supernatants at  $-20^{\circ}\text{C}$  until HPLC analyses (sugars and organic acids), UPLC analyses (amino acids), and microbial 16S rDNA sequencing were carried out.

For chromatographic analyses, culture supernatants were filtered using AmiconR Ultra-10K Centrifugal Filter Devices, cut-off 3 kDa according to the manufacturer's instructions (Millipore, United States). The concentrations of organic acids (succinate, lactate, formate, acetate, propionate, isobutyrate, butyrate, isovalerate, and valerate), ethanol and free sugars (mono-, di-, and trisaccharides) were determined by high-performance liquid chromatography (HPLC, Alliance 2795 system, Waters, Milford, MA, United States), using BioRad HPX-87H column (Hercules, CA, United States) with isocratic elution of 0.005 M  $\text{H}_2\text{SO}_4$  at a flow rate of 0.5 mL/min and at  $35^{\circ}\text{C}$ . Refractive index (RI) (model 2414; Waters, United States) and UV (210 nm; model 2487; Waters, United States) detectors were used for quantification of the substances. The detection limit for the HPLC method was 0.1 mM. Concentrations of

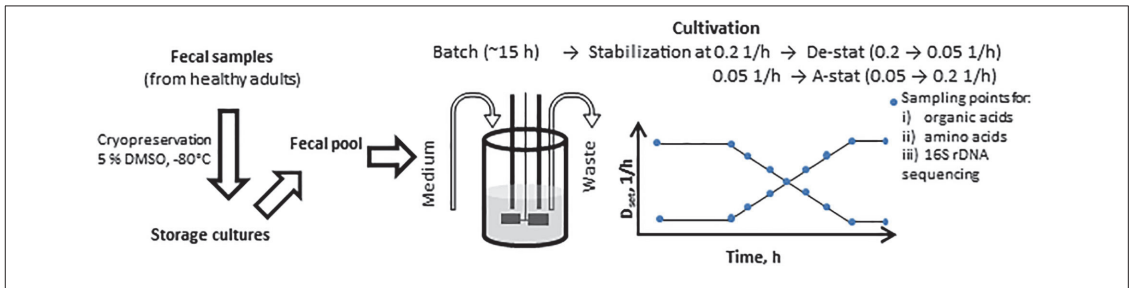


**FIGURE 1 |** Scheme of the A-stat (accelerostat) and De-stat (decelerostat) experimental set-up. The pooled fecal inoculum was added into 300 ml growth medium at time 0 h followed by batch phase (ca 15 h) until mid- exponential growth phase. Then continuous mode was started and after the stabilization of the fecal culture at  $D = 0.2$  1/h (De-stat) or  $D = 0.05$  1/h (A-stat, 6-7 residential times in total), the dilution rate was gradually decreased down to 0.05 1/h or increased up to 0.2 1/h (deceleration or acceleration rate 0.05 1/h per day), respectively, followed by re-stabilization for approximately 2 residential times. The same procedure was applied for two substrate combinations (birch xylan + mucin and, apple pectin + mucin).  $D_{set}$  indicates the controlled change of the dynamics of the pre-set dilution rate.

amino acids and amines were determined with an amino acid analyzer (UPLC; Waters, Milford, United States) according to the manufacturer’s instructions. The detection limit of the method was 0.01 mM. All standard substrates were of analytical grade. Empower software (Waters, United States) was used for the processing of HPLC and UPLC data.

The composition of the gas outflow ( $H_2$ ,  $CO_2$ ,  $H_2S$ ,  $CH_4$ , and  $N_2$ ) was analyzed using an Agilent 490 Micro GC Biogas Analyzer (Agilent 269 Technologies Ltd., United States) connected to a thermal conductivity detector. The volume of the gas flow was regularly recorded.

The Redox potential of the growth medium and culture supernatant was measured by a pH/Redox meter using an InLab® Redox electrode (Mettler Toledo).

The biomass dry weight was measured gravimetrically by centrifuging the biomass from a 10 mL culture, washing twice with distilled water and drying in an oven at 105°C for 24 h.

### DNA Extraction and Amplification

DNA was extracted from the pellets using a PureLink Microbiome DNA extraction kit (Thermo Fisher Scientific, United Kingdom) according to the manufacturer’s instructions. Universal primers:

S-D-Bact-0341-b-S-17 Forward (5’TCGTCGGCAGCGTCAG ATGTGTATAAGAGACAGCCTACGGGNGGCWGCAG) and S-D-Bact-0785-a-A-21 Reverse (5’GTCTCGTGGGCTCGGA GATGTGTATAAGAGACAGGACTACHVGGGTATCTAATCC) were used for PCR amplification of the V3-V4 hypervariable regions of the 16S rRNA genes (Klindworth et al., 2013). The amplified region was 390–410 bp long and an average of 67,000 reads per sample were obtained. The mixture of amplicons was sequenced using an Illumina MiSeq 2 × 250 v2 platform (Estonian Genome Centre, University of Tartu, Estonia).

### Taxonomic Profiling of Microbiota Samples

The DNA sequence data was analyzed using a BION-meta<sup>1</sup>, currently unpublished open source program, according to the

<sup>1</sup>www.box.com/bion

author’s instructions. Sequences were first cleaned at both ends using a 99.5% minimum quality threshold for at least 18 of 20 bases for 5’-end and 28 of 30 bases for 3’-end, then joined, followed by the removal of contigs shorter than 350 bp. Then sequences were cleaned of chimeras and clustered by 95% oligonucleotide similarity (k-mer length of 8 bp, step size 2 bp). Lastly, consensus reads were aligned to the SILVA reference 16S rDNA database (v123) using a word length of 8 and similarity cut-off of 90%. The bacterial designation was analyzed at different taxonomic levels, down to species if applicable.

### Calculations

For quantitative data analysis, the relative data of bacterial abundances from 16S rDNA sequencing analysis were first converted to quantitative values  $[X_i$  (g/L), where  $i$  illustrates bacterial taxa  $i$ ] by the formula:  $X_i = X_t \cdot A_i$ , where  $X_t$  is the dry weight of the total biomass of bacteria (g/L) and  $A_i$  is the relative abundance of bacterial taxa  $i$  in the sample.

The growth characteristics of the bacteria in A-stat and De-stat experiments were calculated based on bacterial mass, total volume of medium pumped out from the fermenter ( $V_{OUT}$ , L) and product concentrations in the culture medium (mol/L) as follows:

$$\mu = \frac{d(V_{OUT})}{V \times dt} + \frac{d(X_t)}{dt \times X_t} \tag{1}$$

$$Q_{Si} = \frac{S_i \times d(V_{OUT})}{V \times X_t \times dt} - \frac{d(S_i)}{dt \times X_t} \tag{2}$$

$$Q_{Pi} = \frac{P_i \times d(V_{OUT})}{V \times X_t \times dt} + \frac{d(P_i)}{dt \times X_t} \tag{3}$$

where  $\mu$  is the specific growth rate (1/h),  $Q_S$  is the specific consumption rate of carbohydrate (in carbon equivalents, mol-C/g- $X_t$ /h),  $S_i$  is the concentration of consumed carbohydrate  $i$  (C-mol/L),  $Q_{Pi}$  is the specific production rate of product  $i$  (mol-prod/g- $X_t$ /h),  $P_i$  is the concentration of product  $i$  (mol/L),  $V$  is the current fermenter volume (L),  $V_{OUT}$  is the outflow volume and  $t$  is the cultivation time (h).

## Statistical Analysis

Concentrations of metabolites or abundances of bacteria from three independent experiments were compared by average values and by unpaired and t-test (unadjusted  $P$ -values  $< 0.05$  were considered significant) for chemostat point comparison. To compare differences in bacterial abundances and metabolite productions during A-stat and De-stat experiments, samples were divided into two groups: (1) samples taken at  $D < 0.07$  1/h (slow growth) and (2) samples taken at  $D > 0.17$  1/h (fast growth). Average and standard deviation of bacterial abundances and metabolite productions were calculated in both groups and a single parametric t-test was used to estimate statistical significance.

## Ethics Statement

This study was approved by the Tallinn Medical Research Ethics Committee, Estonia (protocol no. 554).

## RESULTS

### Reproducibility of Chemostat Cultures of Fecal Microbiota

Until now, continuous fecal cultures have mostly been inoculated with fresh fecal inocula and information on reproducibility of this type of experiment is scarce. Hence, the aim of this work was to elucidate the reproducibility of the continuous fecal cultures. To elucidate the reproducibility of the growth of biological replicates of adult pooled fecal microbiota, six chemostat cultures (three at  $D_{low} = 0.05$  1/h and three at  $D_{high} = 0.2$  1/h) in a defined base medium with apple pectin and mucin were carried out.

### Formation of Organic Acids and Gases

The production of organic acids and gases from pectin and mucin was related to the specific growth rate (Figure 2). The most abundant organic acid in all chemostat cultures was acetate [ $23.2 \pm 3.1$  and  $25.2 \pm 2.0$  mM at  $D_{low}$  (0.05 1/h) and  $D_{high}$  (0.2 1/h), respectively]. Compared to  $D_{high}$ , the production of propionate, butyrate and carbon dioxide was more enhanced at  $D_{low}$ . At  $D_{low}$ ,  $9.4 \pm 0.3$  mM propionate and less than 4 mM succinate were produced, while at  $D_{high}$ , concentrations of propionate and succinate were practically equal ( $4.2 \pm 0.3$  and  $3.9 \pm 0.8$  mM, respectively). The ratio of acetate, propionate and butyrate was 5:2:1 at  $D_{low}$  and 14:2:1 at  $D_{high}$ . Similar to the product profile at  $D_{low}$ , a ratio of 4:2:1 for acetate:propionate:butyrate was reported by Larsen et al. (2019) in TIM-2 experiments. In accordance with the organic acid profiles, about twice as much carbon dioxide was produced at  $D_{low}$  than at  $D_{high}$  ( $20.3 \pm 2.4$  and  $10.5 \pm 2.8$  mmol per L medium, respectively). On average, the relative difference between parallels of the concentrations of propionate, butyrate and lactate in stabilized fecal cultures (after six residential times) remained below 10% and that of acetate below 25% at both dilution rates ( $D_{low}$  and  $D_{high}$ ).

In addition to organic acids and gases, the consumption of amino acids was analyzed. It was determined that amino

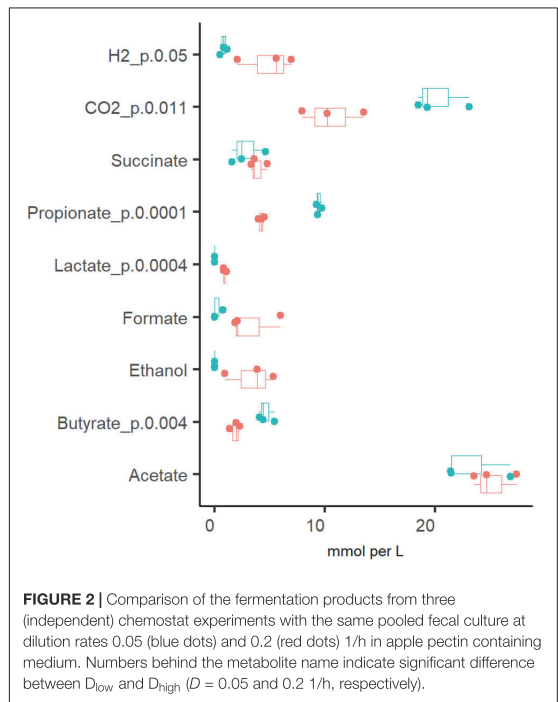


**FIGURE 2** | Comparison of the fermentation products from three (independent) chemostat experiments with the same pooled fecal culture at dilution rates 0.05 (blue dots) and 0.2 (red dots) 1/h in apple pectin containing medium. Numbers behind the metabolite name indicate significant difference between  $D_{low}$  and  $D_{high}$  ( $D = 0.05$  and  $0.2$  1/h, respectively).

acids were fully depleted from the culture medium at both dilution rates, except for alanine and branched-chain amino acids (BCAA), which were practically not consumed at  $D_{high}$  (Figure 3). The increased production of propionate, butyrate and CO<sub>2</sub> at  $D_{low}$  was accompanied by the conversion of BCAA to isobutyric ( $0.27 \pm 0.29$  mM) and isovaleric acids ( $0.87 \pm 0.82$  mM). Another amino acid degradation product significantly higher at  $D_{low}$  was H<sub>2</sub>S ( $0.76 \pm 0.12$  vs.  $0.36 \pm 0.09$  mmol per L medium at  $D_{low}$  vs.  $D_{high}$ , respectively) derived from the sulfur-containing amino acids Cys and Met. At  $D_{high}$ , isoleucine and leucine were consumed in the range required for biomass formation (0.18–0.24 and 0.45–0.58 mmol/gDW, respectively). **Supplementary Table S2** Chemostat, based on the amino acid contents in the biomass of *E. coli* (0.22 and 0.37 mmol/gDW for Ile and Leu, respectively; Valgepea et al., 2011) and *Lactococcus lactis* (0.25 and 0.37 mmol/gDW for Ile and Leu, respectively; Adamberg et al., 2012). As the total amount of biomass produced was 0.5–0.7 g/L (**Supplementary Table S2** Chemostat), the consumption of other amino acids exceeded 1.6–5.5 times the amount required for biomass synthesis, except for serine, which was consumed about 10 times as much. Serine is the major amino acid in mucins and may be converted to acetate. However, serine degradation ( $2.1$  and  $2.6$  mmol/gDW at  $D_{low}$  and  $D_{high}$ , respectively) could not have contributed to more than 5% of the total acetate production ( $39$  and  $51$  mmol/gDW at  $D_{low}$  vs.  $D_{high}$ , respectively) as 80–86% of the carbon was derived

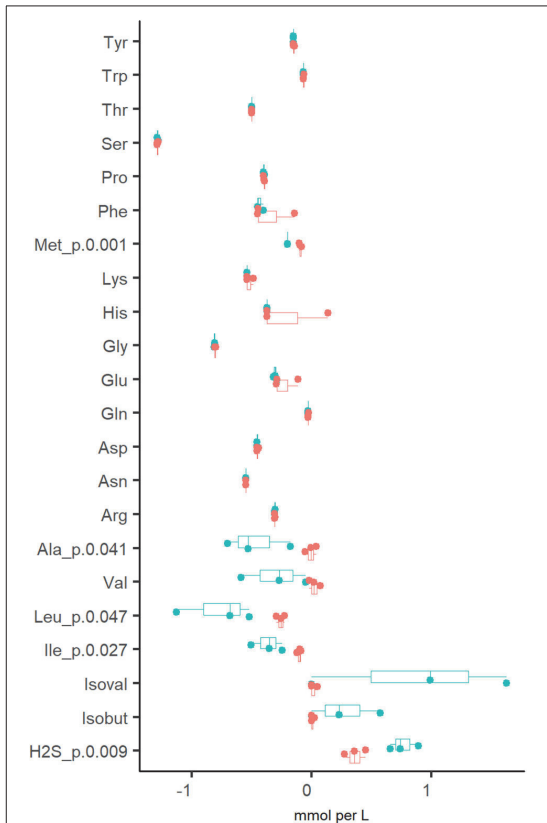


**FIGURE 3 |** Comparison of amino acid consumptions and related metabolites (branched chain fatty acids and H<sub>2</sub>S) from three independent chemostat experiments of fecal culture at dilution rate 0.05 (blue dots) and 0.2 (red dots) 1/h in apple pectin medium. Positive values indicate the production and negative values indicate the consumption of the amino acid. Numbers behind the metabolite name indicate significant difference between D<sub>low</sub> and D<sub>high</sub> (D = 0.05 and 0.2 1/h, respectively). isoval, isovalerate; isobut, isobutyrate.

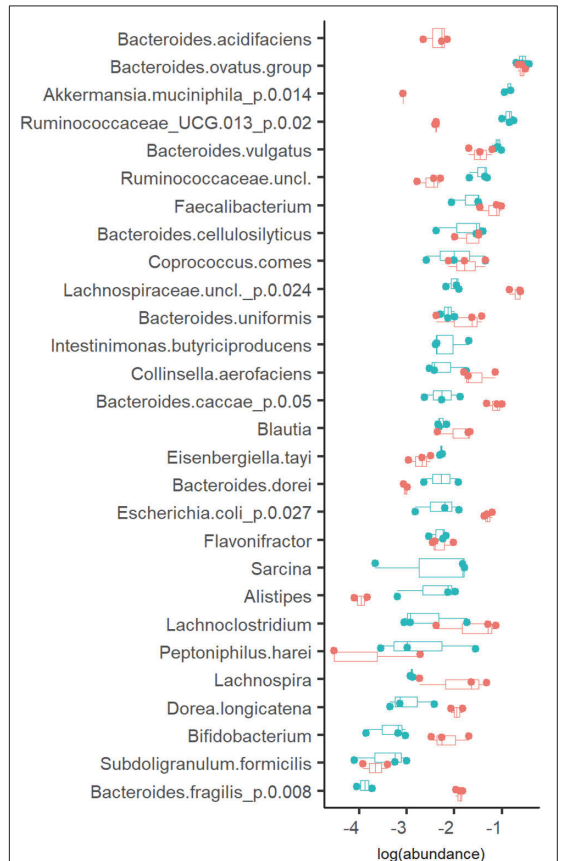


**FIGURE 4 |** Abundance of bacteria (in log scale) at dilution rate 0.05 (blue dots) and 0.2 (red dots) 1/h in apple pectin medium. Each dot represents an independent chemostat experiment. Numbers behind the metabolite name indicate significant difference between D<sub>low</sub> and D<sub>high</sub> (D = 0.05 and 0.2 1/h, respectively).

from carbohydrate fermentation. The overall carbon recovery was 79% and 67% at D<sub>low</sub> and D<sub>high</sub>, respectively, showing that some products were under-determined or missing, especially at high dilution rate.

**Growth Rate Specific Differences of Fecal Microbiota**

The profiles of the metabolic products were in accordance with the bacterial compositions detected (Figures 2–4). Three taxa clearly prevalent at both dilution rates were the acetate- and propionate- or succinate-producing species *Bacteroides ovatus* (17 and 14%, at D<sub>low</sub> and D<sub>high</sub>, respectively), *Bacteroides vulgatus* (7.9 and 3.6%, at D<sub>low</sub> and D<sub>high</sub>, respectively) and butyrate-producing bacterium *Faecalibacterium* (2.4 and 7.2%, at D<sub>low</sub> and D<sub>high</sub>, respectively). Also several other bacteria were abundant (1–4% of the total population) at both dilution rates, such as mixed acid (acetate, propionate and butyrate) fermenting

bacteria, and the acetate- and propionate-producing *Bacteroides uniformis* and *Bacteroides cellulosilyticus* (Figure 4). At D<sub>low</sub> the mucin degrading species *Akkermansia muciniphila* and a group of Ruminococcaceae UCG-013 (from 0.1 to 16% and from 0.5 to 14%, respectively) were significantly enriched. In different, at D<sub>high</sub>, *Bacteroides caccae*, Lachnospiraceae unclassified and mainly acetate-producing *E. coli* (7.7%, 21% and 6.3% of total reads, respectively) became dominant. The butyrate-producing bacterium *Intestinimonas butyriciproducens* and *Sarcina* were detected only at D<sub>low</sub>, whereas *Bacteroides acidifaciens* was found only at D<sub>high</sub>. The increased production of ethanol and formate at D<sub>high</sub> can be linked to higher abundances of *Dorea* and *Blautia*.

A remarkable enrichment of Enterobacteriaceae (up to 60% of total population) was observed in batch phase before starting the

continuous flow. The amount of *E. coli* formed nearly 50% of the microbial population but decreased to about 10% in a chemostat stabilized at  $D_{high}$ , and to 1.2% at  $D_{low}$ . These data confirm the competitiveness of the fast-growing *E. coli* at high dilution rates.

### Comparison of A-Stat and De-Stat Cultures

Changes in the dilution rate in both directions between 0.05 to 0.2 1/h, starting from the stabilized cultures of pooled fecal microbiota in apple pectin and birch xylan media, were analyzed. In A-stat, the dilution rate was gradually increased from 0.05 to 0.2 1/h, and in De-stat the dilution rate was gradually decreased from 0.2 to 0.05 1/h. The stabilization of the chemostat culture was controlled by the titration rate of sodium hydroxide, indicating the rate of acid production rate, and the gas production rate (Supplementary Figure S1). Average fluctuations of these parameters below 5% within the last three residential times were considered to be stable cultures to start the changestat algorithm (on average, six or seven residential volumes were needed to achieve the stable cultures).

### Formation of Organic Acids and Gases

In total, of one mole of carbohydrates, 1.2–1.3 and 1.7–1.9 mol of acids were produced in xylan and pectin supplemented media, respectively. Acetate formed in nearly two thirds of all fermentation products and its production did not depend on the dilution rate (Figure 5). Except for acetate and carbon dioxide, the formation of other metabolites from pectin and xylan was comparable in both directions of the dilution rate change (from 0.05 to 0.2 and from 0.2 to 0.05 1/h). Almost twice as much acetate was produced from xylan than from pectin (0.6–0.7 and 1.1–1.2 mol per mole of carbohydrates consumed, respectively). As

xylose is a five-carbon sugar and galacturonic acid is a six-carbon compound, the lower amount of acids produced in the xylan medium can partly be explained by these differences. However, at all dilution rates, the carbon balance ( $C_{substrates} - C_{products}$ ) was still lower in the xylan- than in the pectin-containing medium (average values  $74 \pm 5\%$  and  $82 \pm 2\%$ , respectively). The formation of other metabolites, especially carbon dioxide and propionate, was strongly dilution rate-dependent. The synthesis of carbon dioxide was 0.9 and 0.4 mmol per L medium at  $D_{low}$  and at  $D_{high}$  in the pectin medium in both experimental directions (A-stat and De-stat). A similar trend was observed for xylan, suggesting that the production of carbon dioxide is linked to the growth rate rather than the substrate. To compensate for the change in the carbon flux caused by the decreased production of  $CO_2$ , the succinate production increased, especially in the xylan medium. For example, in the A-stat experiment of the xylan medium, the reduction of  $CO_2$  production from 0.42 to 0.22 mol per mole of carbohydrates was compensated for by enhanced formation of succinate (0.26 to 0.42 at  $D = 0.05$  1/h and  $D = 0.2$  1/h, respectively) and formate (0.02 to 0.2 mol per mol carbohydrates at  $D = 0.05$  1/h and  $D = 0.2$  1/h, respectively). Similarly, propionate synthesis was decreased as a response to increasing formate production, keeping the carbon flux consistent (0.27 to 0.09 mol per mol carbohydrates at  $D = 0.05$  1/h and  $D = 0.2$  1/h, respectively). A reverse correlation between concentrations of propionic and succinic acids was observed. In comparing the gas production, notably less carbon dioxide (0.3–0.4 mol per mole of carbohydrates consumed) was formed from xylan, built of xylose, a five-carbon molecule, at all dilution rates. Carbon dioxide may originate from succinate to propionate conversion or butyrate production or demethoxylation of methoxylated galacturonic acid (Figure 5).

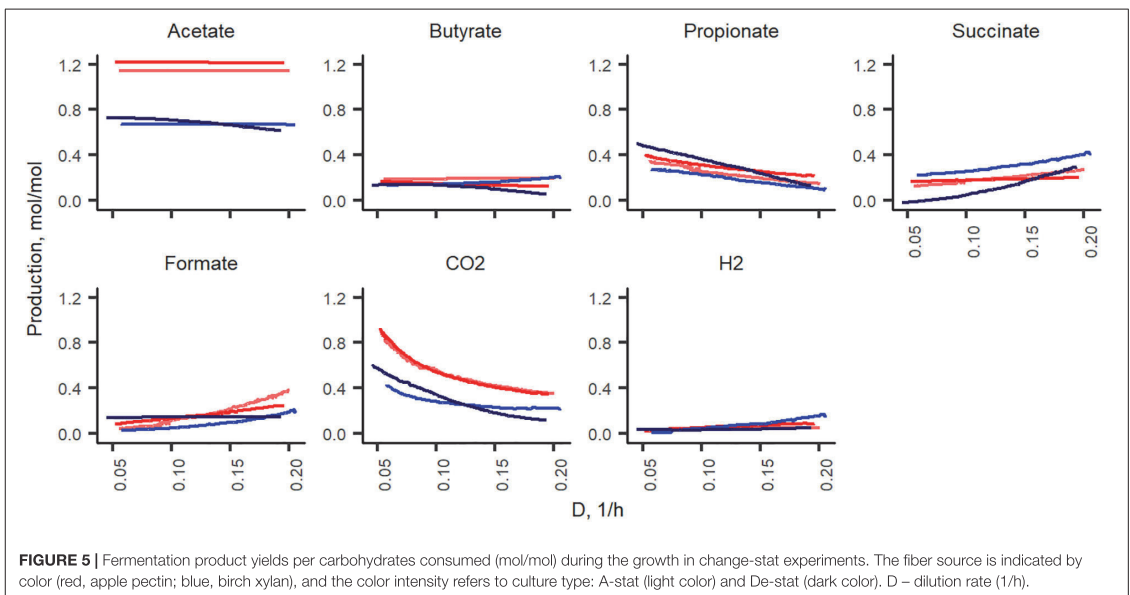


**FIGURE 5 |** Fermentation product yields per carbohydrates consumed (mol/mol) during the growth in change-stat experiments. The fiber source is indicated by color (red, apple pectin; blue, birch xylan), and the color intensity refers to culture type: A-stat (light color) and De-stat (dark color). D – dilution rate (1/h).

The described changes were characteristic under both directions of the dilution rate (A-stat and De-stat). These data suggest that the acceleration rate applied allowed the culture to adapt to the changing conditions.

### Consumption and Formation of Amino Acids

Similarly to the chemostat cultures, most of the amino acids were completely depleted from the medium, except for alanine and BCAA (Table 1). The consumption of valine and leucine increased at lower dilution rates. The formation of isobutyrate and isovalerate was practically missing at high dilution rates, but they were produced in concentrations of 2.2–11 and 13–44 mmol/mol-carbohydrates, respectively, at low dilution rates ( $D < 1/h$ ) (Table 1). In both media, the alanine metabolism was more intensive at low dilution rates (up to 14 mmol/mol-carbohydrates). The degradation of the reducing agent cysteine to  $H_2S$  up to 41 mmol/mol-carbohydrates was observed at low dilution rates in all experiments (Table 1), which corresponds to the degradation of 22% of the total cysteine.

### Growth Rate Specific Changes in Fecal Microbiota

The initial fecal slurry contained 88 bacterial species with abundance above 0.1% and, of these, 25 species had abundance higher than 1% (Supplementary Table S1). During the chemostat and the following A-stat and De-stat cultivations, the species richness decreased to 27–32 and 10–18 species with abundance of 0.1 and 1% with apple pectin and xylan, respectively. A significant decrease in species richness has been shown by other authors (McDonald et al., 2013; Chung et al., 2016). The abundance of the majority of bacterial taxa was determined by the dilution rate on both substrates. The prevailing genus in the consortia – *Bacteroides* (up to 58% of the total population) – adapted well within the whole range of specific growth rates tested. However, the abundances of some species, such as *B. ovatus* and *Bacteroides cellulosilyticus*, tended to decrease at higher dilution rates (A-stat) in the xylan-supplemented medium ( $p = 0.02$ ) (Figure 6). Pectin selectively enriched the Ruminococcaceae group UCG013, which was never detected in the xylan-containing medium. The abundance of the Ruminococcaceae group UCG-013 was also related to the dilution rate being 17% at lower dilution rates and down

to 5% at dilution rates below  $D < 0.15$  in both change directions (Figure 6). These data are in accordance with the chemostat results.

Significant increases in abundances of *Collinsella aerofaciens* ( $p = 0.002$ ), *E. coli* ( $p = 0.001$ ), *Faecalibacterium prausnitzii* ( $p = 0.009$ ) and a group of Lachnospiraceae (closest similarity to *Coprococcus*,  $p = 0.008$ ) (median abundances 1.6, 12, 5.1, and 19%, respectively) were observed at dilution rates above 0.17 1/h on both substrates. Although the abundances of butyrate-producing bacteria (*Faecalibacterium*, *Coprococcus*, and Lachnospiraceae) increased along with the increasing dilution rate, the tested substrates and conditions did not enhance the production of butyrate, resulting in other fermentation products instead.

At higher dilution rates, the increased formate production was accompanied by higher amounts of species from the genus *Lachnoclostridium* that are known to be involved in formate production. The abundance of the prevailing species at dilution rates below 0.07 1/h, *A. muciniphila* (median abundance 22%) decreased significantly at dilution rates above 0.17 1/h (abundance > 1%) in all changestat experiments. This is in accordance with the production of propionic acid, the characteristic metabolite of *Akkermansia* (Figure 5). Another taxa inhibited at higher dilution rates was *Intestinimonas* (Figure 6).

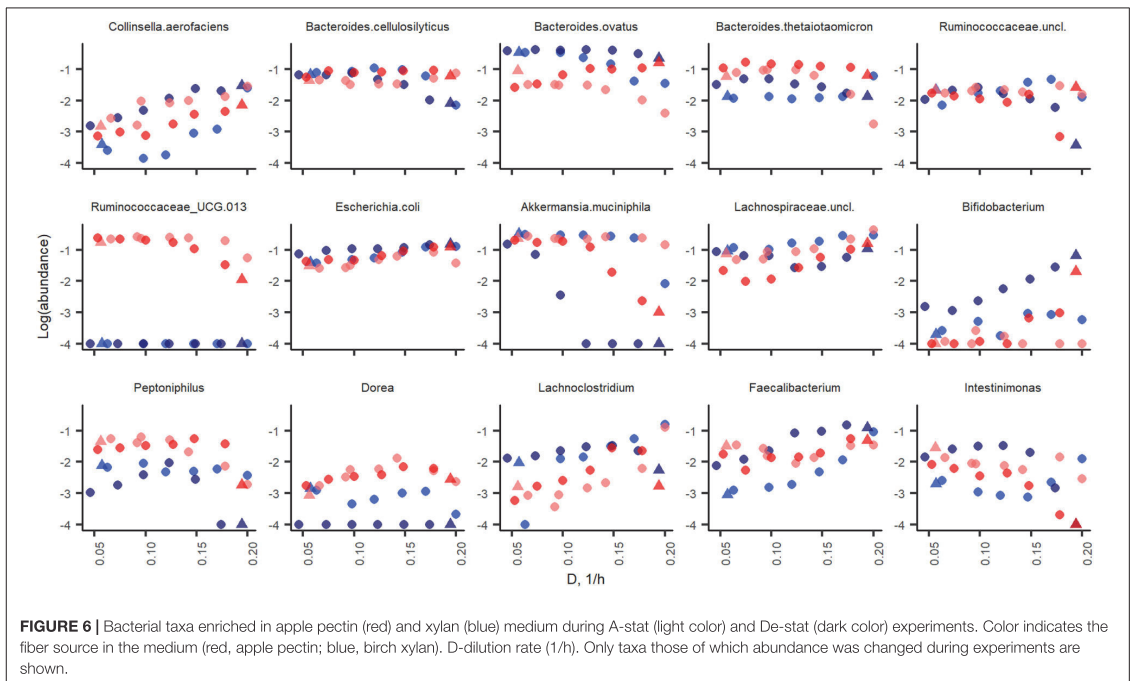
## DISCUSSION

In continuous cultures, the environmental parameters, including substrate concentrations, pH, and flow rate, can be precisely controlled. The *in vivo* situation in the colon probably remains somewhere between chemostat and batch states, i.e., the availability of fermentable substrates decreases, the amounts of metabolites change dynamically and pH moves toward the alkaline region slowly. Our results demonstrate that the changestat techniques, the A-stat and De-stat, can be applied to study the effects of growth rate on the composition and metabolism of fecal microbiota. Using the same fecal inoculum, we showed that continuous cultures are reproducible at dilution rates of  $D = 0.2$  and 0.05 1/h. The dilution rate during the stabilization phase impacts the results of

**TABLE 1** | Consumption of amino acids and formation of degradation products from amino acids (mmol per mol carbohydrates consumed) during A-stat and De-stat experiments and significantly different at fast or slow dilution rate.

Experiment*	State**	D, 1/h	Isobutyrate	Isovalerate	H <sub>2</sub> S	Ala	Ile	Leu
Xyl_A	SS	0.058	2.2	13.6	22.1	11.0	6.4	12.7
Xyl_D	Q	0.058	ND	ND	29.7	2.3	4.8	12.6
Xyl_D	SS	0.193	ND	23.9	7.4	ND	2.8	6.8
Xyl_A	Q	0.193	ND	1.0	12.4	3.4	4.1	5.5
Pec_A	SS	0.055	11.3	44.1	29.1	6.9	10.6	16.3
Pec_D	Q	0.054	2.7	17.1	41.3	14.3	8.8	15.2
Pec_D	SS	0.196	0.2	1.8	12.2	ND	5.7	8.5
Pec_A	Q	0.197	4.1	12.2	16.0	ND	5.4	2.2

\*A and D indicate A-stat and De-stat, respectively. \*\*SS and Q indicate steady state and quasi steady state, respectively. ND, not detected.



the following culture characteristics. Therefore, the microbiota and metabolite patterns were comparatively analyzed in A-stat and De-stat cultures in a defined base medium containing mucin and either apple pectin or xylan. Similar microbiota and metabolite structures were observed within the scanned range of dilution rates in both directions, from  $D = 0.05$  to  $0.2$  1/h or vice versa. The data of the steady state point of the chemostat at  $D = 0.2$  1/h and the end point of the A-stat ( $D = 0.2$  1/h) coincided well. Thus, the fecal culture was able to adapt to the change rate applied. This shows that by using suitable acceleration or deceleration rates it is possible to achieve a state of culture comparable to those of classical chemostat cultures. This is new information for consortia cultivation, although it has long been known for pure cultures.

In a previous De-stat study with fecal samples from children (5–15 years old), similar structural changes in the fecal microbiota were seen (Adamberg and Adamberg, 2018). This suggests that for this age group adult-like microbiota are mostly established. Moreover, these data indicate the crucial role of the growth rate in metabolism and the structure of colon microbiota. For example, in both studies, the taxa clearly preferring high dilution rates were *C. aerofaciens*, *Bifidobacterium*, *B. vulgatus*, *E. coli*, *Lachnospira* and *Lachnospiraceae*, whereas *A. muciniphila* and the Ruminococcaceae group UCG-013 were enriched at low dilution rates. Accordingly, *in vivo* studies have shown that *Akkermansia* and ruminococci are more prevalent in people with slow colonic transit,

while *Bifidobacterium* and *Lachnospiraceae* correlate with high transit rates (Kim et al., 2015; Roager et al., 2016; Vandeputte et al., 2016). The impact of pectin structure on the dynamics metabolism and fecal microbiota has been shown by Larsen et al. (2019). Highly methoxylated pectins were shown to stimulate *F. prausnitzii*, commonly referred to as a health-promoting species. In both of our studies with apple pectin, the abundance of *Faecalibacterium* was 1–7% of the total population within the whole range of dilution rates, indicating the importance of pectin for the growth of colonic *Faecalibacterium* (the current study, and Adamberg and Adamberg, 2018).

Similarities between child and adult fecal pools were also observed at the metabolic level, but with some minor differences. Although the abundances of *Faecalibacterium* in adult and child cultures were similar (1.9–5.2% and 4.5–7.5%, respectively), about twice as much butyrate and  $\text{CO}_2$  were produced by adults' than by children's consortia at slow dilution rates, suggesting higher activity of the butyrate producers in adult microbiota. The dynamics of other metabolites, including BCFA and  $\text{H}_2\text{S}$ , from the degradation of amino acids was comparable in both fecal consortia. The enhanced production of propionate, as well as the extensive use of amino acids and BCFA formation at low specific growth rates, may be related to a shortage of energy, ammonia, or  $\text{NAD}^+$  regeneration. These properties are known for pure cultures (Tempest, 1984) but seem to also be common for fecal microbial consortia (Adamberg and Adamberg, 2018).  $K_s$  values of carbohydrates and amino acids



for different species should be measured to determine the carbon or nitrogen limitation, but these data are very scarce for gut bacteria.

The application of changestat makes it possible to elucidate the mechanisms of the co-existence of different bacteria by adapting mixed cultures under different environmental conditions. The cultivation of microbial consortia instead of single cultures is a promising approach for several biotechnological applications, including the development of multi-strain probiotics or material for fecal transplantation. As mentioned above, this and previous studies reveal that various consortia can be generated using continuous cultivation strategies. Still, the question remains of how to produce safe consortia with desired properties and/or therapeutic effects. Thus, detailed information is needed about selective pressure on the development of bacterial consortia under various environmental conditions: pH, the availability and concentration of substrate, dilution rate, selective additives, defining the inocula, etc. The changestat approach makes it possible to scan selected environmental conditions in an adaptive manner; providing an opportunity to predict appropriate conditions for the development of a consortium with a desired bacterial pattern.

## CONCLUSION

The changestat experiments presented in this paper showed that continuous cultures of complex fecal consortia are reproducible in chemostat. Similar microbiota and metabolite changes were observed within the scanned range of dilution rates in changestat cultures in both directions, from  $D = 0.05$  to  $0.2$  1/h or vice versa. This is new information for consortia cultivation, although it has long been known for pure cultures.

Our work confirmed that dilution rate is a crucial trigger in consortia development. Some species, such as propionate-producing *B. ovatus* and *B. vulgatus* and butyrate-producing *Faecalibacterium*, were prevalent within the whole range of dilution rates, while the mucin-degrading bacterium *A. muciniphila* and some ruminococci were enriched at low dilution rates only.

The production of organic acids and gases from pectin in the presence of mucin was related to the dilution rate in chemostat cultures. The ratio of acetate, propionate and butyrate was 5:2:1 at  $D = 0.5$  1/h and 14:2:1 at  $D = 0.2$  1/h. Most amino acids were completely depleted from the medium except for alanine and BCAA, which were metabolized to isobutyric and isovaleric acids in chemostat as well as changestat cultures.

For further analysis of the interactions in complex consortia, other gut-relevant environmental conditions and substrates available in the colon will be studied. It should be stressed that, in addition to high-throughput sequencing analysis, it is necessary to concentrate on the growth and metabolism of fecal consortia to work out novel methods for bacterial therapies. Changestat cultures make it possible to screen the combined effects of important environmental and feed parameters, such as acidity,

temperature, medium composition, dilution rate, and the effects of inocula and multiple substrates.

## DATA AVAILABILITY STATEMENT

The datasets analyzed for this study can be found in the European Nucleotide Archive on the site PRJEB33931 (ERP116764, dataset name "Run26\_cult2").

## ETHICS STATEMENT

The studies involving human participants were reviewed and approved by the Tallinn Medical Research Ethics Committee, Estonia (protocol No. 554). The patients/participants provided their written informed consent to participate in this study.

## AUTHOR CONTRIBUTIONS

KA and SA designed the study. KA, GR, and SA carried out the experiments and data analyses. KA drafted the first manuscript. GR and SA contributed by writing and editing the final manuscript. All authors approved the submitted version.

## FUNDING

This work was supported by the Estonian Ministry of Science and Education, Project number IUT1927.

## ACKNOWLEDGMENTS

We would like to thank the Estonian Ministry of Science and Education for their funding. We are grateful to Betti Nigul for help in performing the growth experiments and Madis Jaagura for carrying out the bioinformatic analyses.

## SUPPLEMENTARY MATERIAL

The Supplementary Material for this article can be found online at: <https://www.frontiersin.org/articles/10.3389/fbioe.2020.00024/full#supplementary-material>

**FIGURE S1** | On-line measured data that are used for stability analyses during chemostat before A-stat (left side figures) or De-stat (right side figures) experiments. Upper figures show data in xylan + mucin medium and lower figures in apple pectin medium. Base rate, titration rate of 1M NaOH (ml/min); rGas, gas production rate (ml/min); D, dilution rate (1/h).

**TABLE S1** | Abundances of bacteria in the inocula and samples from A-stat and De-stat experiments.

**TABLE S2** | Production of metabolites per carbohydrate consumed (mol/mol-carbohydrates and mmol/gDW), carbon recovery, and biomass yield (gDW/g-carbohydrates) during A-stat and De-stat experiments.

## REFERENCES

- Adamberg, K., and Adamberg, S. (2018). Selection of fast and slow growing bacteria from fecal microbiota using continuous culture with changing dilution rate. *Microb. Ecol. Health Dis.* 29:1549922. doi: 10.1080/16512235.2018.1549922
- Adamberg, K., Kolk, K., Jaagura, M., Vilu, R., and Adamberg, S. (2018). The composition and metabolism of faecal microbiota is specifically modulated by different dietary polysaccharides and mucin: an isothermal microcalorimetry study. *Benef. Microbes* 9, 21–34. doi: 10.3920/BM2016.0198
- Adamberg, K., Seiman, A., and Vilu, R. (2012). Increased biomass yield of *Lactococcus lactis* by reduced overconsumption of amino acids and increased catalytic activities of enzymes. *PLoS One*. 7:e48223. doi: 10.1371/journal.pone.0048223
- Adamberg, K., Valgepea, K., and Vilu, R. (2015). Advanced continuous cultivation methods for systems microbiology. *Microbiology* 161, 1707–1719. doi: 10.1099/mic.0.000146
- Aguirre, M., Eck, A., Koenen, M. E., Savelkoul, P. H. M., Budding, A. E., and Venema, K. (2015). Evaluation of an optimal preparation of human standardized fecal inocula for in vitro fermentation studies. *J. Microbiol. Methods* 117, 78–84. doi: 10.1016/j.mimet.2015.07.019
- Brahma, S., Martinez, L., Walter, J., Clarke, J., Gonzalez, T., Menon, R., et al. (2017). Impact of dietary pattern of the fecal donor on in vitro fermentation properties of whole grains and brans. *J. Funct. Foods* 29, 281–289. doi: 10.1016/j.jff.2016.12.042
- Burkitt, D. P., Walker, A. R. P., and Painter, N. S. (1972). Effect of dietary fibre on stools and transit-times, and its role in the causation of disease. *Lancet* 30, 1408–1411. doi: 10.1016/s0140-6736(72)92974-1
- Bussolo de Souza, C., Jonathan, M., Saad, S. M. I., Schols, H. A., and Venema, K. (2019). Degradation of fibres from fruit by-products allows selective modulation of the gut bacteria in an in vitro model of the proximal colon. *J. Funct. Foods* 57, 275–285. doi: 10.1016/j.jff.2019.04.026
- Chung, W. S. F., Walker, A. W., Louis, P., Parkhill, J., Vermeiren, J., Bosscher, D., et al. (2016). Modulation of the human gut microbiota by dietary fibres occurs at the species level. *BMC Biol.* 14:3. doi: 10.1186/s12915-015-0224-3
- Chung, W. S. F., Walker, A. W., Vermeiren, J., Sheridan, P. O., Bosscher, D., Garcia-Campayo, V., et al. (2019). Impact of carbohydrate substrate complexity on the diversity of the human colonic microbiota. *FEMS Microbiol. Ecol.* 95:fy201. doi: 10.1093/femsec/fy201
- Cummings, J. H., Jenkins, D. J. A., and Wiggins, H. S. (1976). Measurement of the mean transit time of dietary residue through human gut. *Gut* 17, 210–218. doi: 10.1136/gut.17.3.210
- Fallingborg, J., Christensen, L. A., Ingeman-Nielsen, M., Jacobsen, B. A., Abildgaard, K., and Rasmussen, H. H. (1989). PH-profile and regional transit times of the normal gut measured by a radiotelemetry device. *Aliment. Pharmacol. Ther.* 3, 605–613.
- Freter, R., Stauffer, E., Cleven, D., Holdeman, L., and Moore, W. E. C. (1983). Continuous-flow cultures as in vitro models of the ecology of large intestinal flora. *Infect. Immun.* 39, 666–675. doi: 10.1128/iai.39.2.666-675.1983
- Gottschal, J. C. (1990). Different types of continuous culture in -ecological studies. *Methods Microbiol.* 22, 87–124. doi: 10.1016/s0580-9517(08)70240-x
- Jorup-Rönström, C., Håkanson, A., Sandell, S., Edvinsson, O., Midtvedt, T., Persson, A. K., et al. (2012). Fecal transplant against relapsing *Clostridium difficile*-associated diarrhea in 32 patients. *Scand. J. Gastroenterol.* 47, 548–552. doi: 10.3109/00365521.2012.672587
- Kasemets, K., Drews, M., Nisamedtinov, I., Adamberg, K., and Paalme, T. (2003). Modification of a-stat for the characterization of microorganisms. *J. Microbiol. Methods* 55, 187–200. doi: 10.1016/S0167-7012(03)00143-X
- Kim, S. E., Choi, S. C., Park, K. S., Park, M. I., Shin, J. E., Lee, T. H., et al. (2015). Change of fecal flora and effectiveness of the short-term VSL#3 probiotic treatment in patients with functional constipation. *J. Neurogastroenterol. Motil.* 21, 111–120. doi: 10.5056/jnm14048
- Klindworth, A., Pruesse, E., Schweer, T., Peplies, J., Quast, C., Horn, M., et al. (2013). Evaluation of general 16S ribosomal RNA gene PCR primers for classical and next-generation sequencing-based diversity studies. *Nucleic Acids Res.* 41, 1–11. doi: 10.1093/nar/gks808
- Lagier, J.-C., Armougom, F., Million, M., Hugon, P., Pagnier, I., Robert, C., et al. (2012). Microbial culturomics: paradigm shift in the human gut microbiome study. *Clin. Microbiol. Infect.* 18, 1185–1193. doi: 10.1111/1469-0691.12023
- Langendijk, P., Schut, F., Jansen, G., Raangs, G., Kamphuis, G., Wilkinson, M., et al. (1995). Quantitative fluorescence in situ hybridization of *Bifidobacterium* spp. with genus-specific 16S rRNA-targeted probes and its application in fecal samples. *Appl. Environ. Microbiol.* 61, 3069–3075.
- Larsen, N., Bussolo de Souza, C., Krych, L., Cahú, T. B., Wiese, M., Kot, W., et al. (2019). Potential of pectins to beneficially modulate the gut microbiota depends on their structural properties. *Front. Microbiol.* 10:223. doi: 10.3389/fmicb.2019.00223
- Macfarlane, S., Quigley, M. E., Hopkins, M. J., Newton, D. F., and Macfarlane, G. T. (1998). Polysaccharide degradation by human intestinal bacteria during growth under multi-substrate limiting conditions in a three-stage continuous culture system. *FEMS Microbiol. Ecol.* 26, 231–243. doi: 10.1016/S0168-6496(98)00039-7
- McDonald, J. A. K., Schroeter, K., Fuentes, S., Heikamp-deJong, I., Khursigara, C. M., de Vos, W. M., et al. (2013). Evaluation of microbial community reproducibility, stability and composition in a human distal gut chemostat model. *J. Microbiol. Methods* 95, 167–174. doi: 10.1016/j.mimet.2013.08.008
- Miller, T. L., and Wolin, M. J. (1981). Fermentation by the human large intestine microbial community in an in vitro semicontinuous culture system. *Appl. Environ. Microbiol.* 42, 400–407. doi: 10.1128/aem.42.3.400-407.1981
- Paalme, T., Kahru, A., Elken, R., Vanatalu, K., Tiisma, K., and Vilu, R. (1995). The computer-controlled continuous culture of *Escherichia Coli* with smooth change of dilution rate (A-Stat). *J. Microbiol. Methods* 24, 145–153. doi: 10.1016/0167-7012(95)00064-x
- Petrof, E. O., Gloor, G. B., Vanner, S. J., Weese, S. J., Carter, D., Daigneault, M. C., et al. (2013). Stool substitute transplant therapy for the eradication of clostridium difficile infection: 'RePOOPulating' the gut. *Microbiome* 1:3. doi: 10.1186/2049-2618-1-3
- Rajilić-Stojanović, M., Heilig, H. G. H. J., Molenaar, D., Kajander, K., Surakka, A., Smidt, H., et al. (2009). Development and application of the human intestinal tract chip, a phylogenetic microarray: analysis of universally conserved phylotypes in the abundant microbiota of young and elderly adults. *Environ. Microbiol.* 11, 1736–1751. doi: 10.1111/j.1462-2920.2009.01900.x
- Roager, H. M., Hansen, L. B. S., Bahl, M. I., Frandsen, H. L., Carvalho, V., Göbel, R. J., et al. (2016). Colonic transit time is related to bacterial metabolism and mucosal turnover in the gut. *Nat. Microbiol.* 1:16093. doi: 10.1038/nmicrobiol.2016.93
- Rowland, I., Gibson, G., Heinken, A., Scott, K., Swann, J., Thiele, I., et al. (2018). Gut microbiota functions: metabolism of nutrients and other food components. *Eur. J. Nutr.* 57, 1–24. doi: 10.1007/s00394-017-1445-8
- Russell, J. B., and Baldwin, R. L. (1979). Comparison of substrate affinities among several rumen bacteria: a possible determinant of rumen bacterial competition. *Appl. Environ. Microbiol.* 37, 531–536. doi: 10.1128/aem.37.3.531-536.1979
- Sender, R., Fuchs, S., and Milo, R. (2016). Are we really vastly outnumbered? Revisiting the ratio of bacterial to host cells in humans. *Cell* 164, 337–340. doi: 10.1016/j.cell.2016.01.013
- Sghir, A., Chow, J. M., and Mackie, R. I. (1998). Continuous culture selection of bifidobacteria and lactobacilli from human faecal samples using fructooligosaccharide as selective substrate. *J. Appl. Microbiol.* 85, 769–777. doi: 10.1111/j.1365-2672.1998.00590.x
- Tannock, G. W. (2017). *Understanding Bowel Bacteria*. Hoboken, NJ: John Wiley & Sons, Inc.
- Tempest, D. (1984). The status of YATP and maintenance energy as biologically interpretable phenomena. *Annu. Rev. Microbiol.* 38, 459–486. doi: 10.1146/annurev.micro.38.1.459
- Valgepea, K., Adamberg, K., and Vilu, R. (2011). Decrease of energy spilling in *Escherichia coli* continuous cultures with rising specific growth rate and carbon wasting. *BMC Syst. Biol.* 5, 106.
- Vandeputte, D., Falony, G., Vieira-Silva, S., Tito, R. Y., Joossens, M., and Raes, J. (2016). Stool consistency is strongly associated with gut microbiota richness and composition. Enterotypes and bacterial growth rates. *Gut* 65, 57–62. doi: 10.1136/gutjnl-2015-309618

- von Martels, J. Z. H., Sadabad, M. S., Bourgonje, A. R., Blokzijl, T., Dijkstra, G., Faber, K. N., et al. (2017). The role of gut microbiota in health and disease: *in vitro* modeling of host-microbe interactions at the aerobe-anaerobe interphase of the human gut. *Anaerobe* 44, 3–12. doi: 10.1016/j.anaerobe.2017.01.001
- Yen, S., McDonald, J. A. K., Schroeter, K., Oliphant, K., Sokolenko, S., Blondeel, E. J. M., et al. (2015). Metabolomic analysis of human fecal microbiota: a comparison of feces-derived communities and defined mixed communities. *J. Proteome Res.* 14, 1472–1482. doi: 10.1021/pr5011247

**Conflict of Interest:** The authors declare that the research was conducted in the absence of any commercial or financial relationships that could be construed as a potential conflict of interest.

Copyright © 2020 Adamberg, Raba and Adamberg. This is an open-access article distributed under the terms of the Creative Commons Attribution License (CC BY). The use, distribution or reproduction in other forums is permitted, provided the original author(s) and the copyright owner(s) are credited and that the original publication in this journal is cited, in accordance with accepted academic practice. No use, distribution or reproduction is permitted which does not comply with these terms.

## Appendix 2

### Publication II

**Raba, G.**, Adamberg, S., Adamberg, K. Acidic pH enhances butyrate production from pectin by faecal microbiota. *FEMS Microbiology Letters*. 2021, 368, 7. doi: 10.1093/femsle/fnab042. PMID: 33864456.



RESEARCH LETTER – Food Microbiology

# Acidic pH enhances butyrate production from pectin by faecal microbiota

Grete Raba<sup>1,†</sup>, Signe Adamberg<sup>1</sup> and Kaarel Adamberg<sup>1,2,\*</sup><sup>1</sup>Department of Chemistry and Biotechnology, Tallinn University of Technology, Akadeemia tee 15, Tallinn, Estonia and <sup>2</sup>Center of Food and Fermentation Technologies, Akadeemia tee 15A, Tallinn, Estonia

\*Corresponding author: Department of Chemistry and Biotechnology, Tallinn University of Technology, Akadeemia tee 15, 12618, Tallinn, Estonia. Tel: +372 620 2955; E-mail: kaarel.adamberg@taltech.ee

One sentence summary: pH is a crucial trigger in the development and metabolic activity of faecal microbial consortia.

Editor: Gisele LaPointe

†Grete Raba, <http://orcid.org/0000-0002-7764-3878>

## ABSTRACT

Environmental pH and gut transit rate are the key factors determining the dynamics of colonic microbiota. In this study, the effect of changing pH on the composition and metabolism of pooled faecal microbiota was elucidated at physiologically relevant dilution rates  $D_{\text{high}} = 0.2$  and  $D_{\text{low}} = 0.05$  1/h. The results showed the best adaptability of *Bacteroides ovatus* within the pH range 6.0–8.0 at both dilution rates. The butyrate producing *Faecalibacterium* and *Coprococcus comes* were extremely sensitive to  $\text{pH} > 7.5$ , while the abundance of *Akkermansia muciniphila* increased significantly at  $\text{pH} > 7$  at  $D_{\text{high}}$ , causing a pH-dependant shift in the dynamics of mucin degrading species. Increased gas formation was observed at  $\text{pH} < 6.5$ . Substantially more  $\text{CO}_2$  was produced at  $D_{\text{low}}$  than at  $D_{\text{high}}$  (18–29 vs 12–23 mmol per L medium, respectively). Methane was produced only at  $D_{\text{low}}$  and  $\text{pH} > 7$ , consistent with the simultaneous increased abundance of *Methanobrevibacter smithii*. Our study confirmed the importance of pH in the development of faecal microbiota in pectin-supplemented medium. Fermentation of other dietary fibres can be studied using the same approach. The significance of pH should be more emphasized in gut research and diagnostics.

**Keywords:** continuous culture; changestat; faecal microbiota; pH; growth rate; apple pectin

## INTRODUCTION

Human gastrointestinal tract contains trillions of bacteria which are in a dynamic relationship with the host. These bacteria can break down complex polysaccharides such as plant-derived dietary fibres, which are indigestible by host digestive enzymes (Martens et al. 2011; Kaoutari et al. 2013). Consumption of dietary fibre as a part of normal diet ensures the diversity of the colon microbial consortium and helps to suppress overgrowth of potential pathogens (O’Keefe 2016; Chung et al. 2018; Schroeder et al. 2018). Bacterial metabolites provide energy and substrates for mucin-producing epithelial cells and protect from gastrointestinal diseases (Martens, Neumann and Desai 2018; Schroeder et al. 2018; Birchenough et al. 2019; Schroeder 2019). Recent advances

in cultivation and analytical methods provide tools to study these interactions and to elucidate the relationships between gut microbiome and human health.

Nutrient and energy metabolism in human colon depends on colonic transit rate as it influences the specific growth rates of gut bacteria. The density of bacteria increases along the colon while the transit rate decreases, causing a non-linear relationship. Parameters such as environmental pH, peristalsis, redox potential and others affect the composition and physiology of gut microbiota and vice versa (Duncan et al. 2009; Vandeputte et al. 2015; Chung et al. 2016; Roager et al. 2016). The effect of pH on the growth of faecal microbiota has been studied by Chung et al. (2016) and on the growth of individual strains by Duncan

Received: 31 July 2020; Accepted: 15 April 2021

© The Author(s) 2021. Published by Oxford University Press on behalf of FEMS. All rights reserved. For permissions, please e-mail: [journals.permissions@oup.com](mailto:journals.permissions@oup.com)

et al. (2009). Moreover, the gastrointestinal acidity depends on an individual's dietary habits. Certain polysaccharides bind substantial amounts of water and increase the volume and moving rate of the chyme (Cummings 1984; Elia and Cummings 2007; de Vries, Miller and Verbeke 2015). Degradation of polysaccharides, release of organic acids, absorption of bile salts and water create a pH gradient inside the large intestine (Cummings and Macfarlane 1991).

Mucins, the main components of intestinal mucus, provide substrate for mucin-degrading bacteria such as *Akkermansia muciniphila* and *Bacteroides thetaiotaomicron* (Van Bueren et al. 2017; Van Herreweghen et al. 2017). Pectins are a group of carbohydrates found in the cell walls and middle lamellae of fruits and vegetables and are common in human diet. Pectins are structurally complex and contain arabinan, arabinogalactan and galactan side chains connected to a galacturonan backbone (Muzzarelli et al. 2012). Such dietary fibres are important in modulating the composition of the gut microbial consortium and in controlling the colonic transit rate (Parker et al. 2010; Larsen et al. 2019). The effect of pectins from citrus and apple as substrates for faecal microbiota was recently studied by us (Adamberg and Adamberg 2018; Adamberg, Raba and Adamberg 2020).

Composition and metabolic responses to various changes of environmental parameters can be studied by using a pooled faecal inoculum (Aguirre et al. 2014, 2015; de Souza et al. 2019; Adamberg, Raba and Adamberg 2020). Microbiota standardisation by pooling is useful for studying the growth trends in a complex faecal consortium, unaffected by variations from individual donors. Although resulting in slightly higher biodiversity, the majority of OTUs are shared in pooled and individual samples (Aguirre et al. 2014). Advanced cultivation methods enable to mimic specific conditions of human gut with precise computer-controlled algorithms and frequent sampling (Chung et al. 2016, 2018; Adamberg, Raba and Adamberg 2020). In a chemostat (D-stat), a chosen environmental parameter is gradually changed while all the other parameters are kept constant, allowing to scan a steady state growth space within a single experiment (Kasemets et al. 2003; Adamberg, Valgepea and Vilu 2015). An essential advantage of continuous cultures over *in vivo* experiments is the precise control of the environmental and nutritional parameters to elucidate specific effects of, for example, a single substrate or dilution rate on the microbial diversity and metabolic potential (Adamberg, Raba and Adamberg 2020).

The aim of the present study was to elucidate the effect of smooth change of pH on the composition and metabolism of pooled faecal microbiota. A range of pH between 6.0 and 8.0 was scanned at dilution rates  $D_{\text{low}} = 0.05$  1/h and  $D_{\text{high}} = 0.2$  1/h, corresponding to slow and fast colonic transit rates, respectively.

## MATERIALS AND METHODS

### Faecal inoculum

Faecal samples were donated by seven healthy volunteers (19–37 years old, Caucasian). Exclusion criteria comprised the use of prebiotics and probiotics, laxatives and antibiotics four weeks prior to sample collection. Faecal samples were homogenized in 4 volumes of 5% DMSO-containing PBS buffer as described previously (Adamberg et al. 2015). Equal volumes of seven faecal slurries were pooled and 2 mL aliquots were kept at  $-80^{\circ}\text{C}$  for use in repeated cultivation experiments.

### Defined base medium and substrates

The defined growth medium (pH  $7.2 \pm 0.1$ ) was prepared in 0.05 M potassium phosphate buffer made from 1 M stock solutions (ml/L):  $\text{K}_2\text{HPO}_4$  (28.9) and  $\text{KH}_2\text{PO}_4$  (21.1). The medium contained mineral salts (mg/L):  $\text{MgSO}_4 \cdot 7\text{H}_2\text{O}$  (36),  $\text{FeSO}_4 \cdot 7\text{H}_2\text{O}$  (0.1),  $\text{CaCl}_2$  (9),  $\text{MnSO}_4 \cdot \text{H}_2\text{O}$  (3),  $\text{ZnSO}_4 \cdot 7\text{H}_2\text{O}$  (1),  $\text{CoSO}_4 \cdot 7\text{H}_2\text{O}$  (1),  $\text{CuSO}_4 \cdot 5\text{H}_2\text{O}$  (1),  $(\text{NH}_4)_6\text{Mo}_7\text{O}_{24} \cdot 4\text{H}_2\text{O}$  (1), NaCl (527); hemin (5 mg/L); vitamin K1 (0.5 mg/L); L-amino acids (g/L): Ala (0.044), Arg (0.023), Asn (0.038), Asp (0.038), Glu (0.036), Gln (0.018), Gly (0.032), His (0.027), Ile (0.060), Leu (0.120), Lys-HCl (0.080), Met (0.023), Phe (0.050), Pro (0.041), Ser (0.095), Thr (0.041), Trp (0.009), Val (0.060), Tyr (0.015); vitamins (mg/L): biotin (0.25), Ca-pantothenate (0.25), folic acid (0.25), nicotinamide (0.25), pyridoxine-HCl (0.50), riboflavin (0.25), thiamine-HCl (0.25) and (g/L): bile salts (0.5),  $\text{NaHCO}_3$  (2.0), Tween-80 (0.5), N-thioglycolate (0.5), Cys-HCl (0.5). The medium was supplemented with porcine gastric mucin (2.5 g/L; Type II, Sigma-Aldrich, USA). Apple pectin (2.5 g/L; Sigma-Aldrich, USA) was used as a widely consumed dietary fibre in Estonian.

### Cultivation system and culture conditions

Four continuous cultivation experiments were carried out to study the combined effect of dilution rate and pH on faecal microbiota: (i) gradual pH decrease from 7.0 to 6.0 ( $D = 0.05$  1/h), (ii) pH increase from 7.0 to 8.0 ( $D = 0.05$  1/h), (iii) pH decrease from 7.0 to 6.0 ( $D = 0.2$  1/h) and (iv) pH increase from 7.0 to 8.0 ( $D = 0.2$  1/h), all at  $36.6^{\circ}\text{C}$ .

D-stat cultivation experiments were carried out in a 1 litre fermenter using Biobundle cultivation system controlled by 'BioXpert' software (Applikon, The Netherlands) as described in Adamberg and Adamberg (2018). Culture volume was kept constant 300 mL by monitoring the weight of the fermenter with PC-linked balance and outflow pump. Feeding and outflow were controlled with variable speed pumps controlled by D-stat algorithm:  $N = N_0 + a \cdot t$ , where "N" is the parameter that is being changed (in this case pH), " $N_0$ " is the initial value of the parameter, "a" is the rate of change of parameter N (unit per hour), and "t" is the time (h).

Cell growth in steady state is described by Monod equation:  $\mu = \mu_{\text{max}} \cdot S / (K_s + S)$ , where  $\mu$  is the specific growth rate of the cell, S is the limiting substrate and  $K_s$  is a constant describing the cell's affinity to the substrate (Monod 1950). In a chemostat culture, the dilution rate D is directly related to  $\mu$ , as the dilution rate controls the inflow of the limiting substrate. Thus, bacteria with a low specific growth rate may be washed out at a high dilution rate and vice versa (Adamberg and Adamberg 2018; Adamberg, Raba and Adamberg 2020). Two different dilution rates,  $D_{\text{low}} = 0.05$  1/h and  $D_{\text{high}} = 0.2$  1/h were tested to represent slow and fast transit rates of the human colon (Cummings, Jenkins and Wiggins 1976; Fallingborg et al. 1989; Koziolk et al. 2015; Maurer et al. 2015; Roager et al. 2016). The dilution rates were chosen to promote the growth of physiologically relevant consortium whose specific growth rate was calculated based on the estimation of the colonic transit time on a Western diet between 10–120 h and the increase of bacterial counts from  $10^8$  in proximal colon to  $10^{11}$  cfu/g in the faeces (Sender et al. 2016).

The healthy colonic pH is neutral or mildly acidic (pH = 6.1–7.5; Nugent et al. 2001) but may increase up to pH 8 in the case of colorectal cancer (Kashtan et al. 1990; Ohigashi et al. 2013). Moreover, protein-rich diets can increase the colonic pH as a result of ammonia release from protein fermentation (Russell et al. 2011;

Aguirre et al. 2016). pH of the *in vitro* culture was controlled by the addition of 1M NaOH. The D-stat algorithm was started during the exponential growth phase of the bacteria, 15–17 h after inoculation. Culture stability was evaluated by a stabilization of the titration (indicating the acid production rate) and gas production rates. Average fluctuations of these parameters below 5% within the last three residential times were considered as indicator of a stable culture to start the changestat algorithm. In average, 6–7 residential volumes were needed to achieve stable cultures. When stabilized at pH 7, the pH was either gradually changed from 7.0 to 6.0 or from 7.0 to 8.0 with acceleration rates  $a = 0.005$  and  $0.02$  U/h, corresponding to  $D_{low}$  and  $D_{high}$ , respectively (Fig. S1, Supporting Information). This strategy allowed to start all experiments from a comparable steady state.

The feeding medium and the culture were flushed with sterile-filtered nitrogen gas (99.9%, AGA) overnight before inoculation and throughout the experiments to maintain anaerobiosis in the fermenter. The redox potential of the outflow culture was monitored regularly using InLab®Redox electrode (Mettler Toledo, USA). Samples were taken from the fermenter after every 0.05pH-units.

## Analytical methods

Samples from the fermenter outflow were collected on ice, centrifuged (14 000 g, 5 min, +4°C) and stored separately as supernatants and cell pellets at –20°C until analysis. The supernatants were filtered using Amicon Ultra-10K Centrifugal Filter Devices, cut-off 3 kDa (Millipore, USA). Concentrations of succinate, lactate, formate, acetate, propionate, isobutyrate, butyrate, isovalerate and valerate were determined by HPLC (Alliance 2795 system; Waters, USA) equipped with BioRad HPX 87H column (Hercules, USA) with isocratic elution of 0.005 M H<sub>2</sub>SO<sub>4</sub>, flow rate 0.5 mL/min, 35°C. The RI (model 2414; Waters, USA) and UV (210 nm; model 2487; Waters, USA) detectors were used for quantification. Amino acid concentrations were determined with UPLC (Acquity; Waters, USA). The chromatographic data were processed in Empower software (Waters, USA).

Gas volume was recorded using MilliGascounter (Ritter, Germany). Composition of the gas outflow was analysed with gas analyser (Agilent 490 MicroGC Biogas Analyser; Agilent 269 Technologies Ltd., USA). Soluble gas concentration (c) in the culture liquid was calculated using Henry law:  $c = H^{CP} \cdot p$ , where p is the partial pressure of the given gas in the gas phase and  $H^{CP}$  (M/atm) is the effective Henry constant of the given gas dependent on pH (Sander 2015).

## DNA extraction, sequencing and taxonomic profiling

DNA was extracted from the cell pellets using PureLink Microbiome DNA extraction kit (Thermo Fisher Scientific, UK). Universal primers: F515 5'-GTGCCAGCMGCCGCGTAA-3' and R806 5'-GGACTACHVGGGTWTCTAAT-3' were used for PCR amplification of the V4 hypervariable regions of the 16S rRNA genes. Sequencing libraries were prepared with Nextera XT Index Kit (Illumina). Prepared libraries were quantified using Qubit™ dsDNA HS Assay Kit (quantitation range 0.2–100 ng; Thermo Fisher Scientific) or Qubit™ dsDNA BR Assay Kit (quantitation range 2–1000 ng; Thermo Fisher Scientific). All reagent kits were handled in accordance with manufacturer's instructions. Pooled libraries were sequenced using Illumina iSeq 100 platform and i1 reagent kit. The amplified region was 250–280 bp long and in average 75 474 reads per sample were obtained.

The DNA sequence data was analysed using BION-meta ([www.box.com/bion](http://www.box.com/bion)). The sequences were first cleaned at both ends using a 99.5% minimum quality threshold for at least 18 of 20 bases for 5'-end and 28 of 30 bases for 3'-end, then joined, followed by the removal of contigs shorter than 250 bp. The sequences were then cleaned of chimeras and clustered by 95% oligonucleotide similarity (k-mer length of 8 bp, step size 2 bp). Lastly, consensus reads were aligned to the SILVA reference 16S rDNA database (v123) using a word length of 8 and similarity cut-off of 90%.

## Statistical analysis

Differences in bacterial abundances and metabolite productions during D-stat experiments were calculated by dividing samples into two groups: (i) samples taken at pH < 6.5 (low pH) and (ii) samples taken at pH > 7.5 (high pH). Mean values and standard deviations of bacterial abundances and metabolite productions were calculated in both groups and single parametric t-test Benjamini-Hochberg correction of P-values was used to estimate statistical significance.

## Ethics statement

The study was approved by the Tallinn Medical Research Ethics Committee, Estonia (protocol No. 554).

## RESULTS

### The effect of pH on the metabolism of apple pectin by faecal microbiota at low dilution rate ( $D_{low} = 0.05$ 1/h)

The most abundant taxa at  $D_{low}$  within the whole pH range tested were *Bacteroides ovatus* (that combines *B. ovatus*, *B. thetaio-taomicron* and *B. xylanisolvens* which could not be differentiated by SILVA 16S rDNA reference database v123), Ruminococcaceae UCG-013 and *Akkermansia muciniphila* (Fig. 1). *B. ovatus* is a common species in the human colon and its active growth has been shown at pH 6.0–6.9 (Chung et al. 2016). As opposed to Ruminococcaceae UCG-013 and *A. muciniphila*, *B. ovatus* was highly abundant also at  $D_{high}$ . The other taxa with distinctly higher abundance at  $D_{low}$  were *Bacteroides dorei/vulgatus*, *Alistipes* sp. and Ruminococcaceae UCG-002 (Fig. 1).

The growth of *B. cellulolyticus*, *Clostridium subterminale*, *Clostridium tertium* and *Sutterella wadsworthensis* was significantly favored at pH > 7 (Fig. 2). In contrast, growth of *Dorea longicatena*, *Faecalibacterium* sp. and *Escherichia coli*, were supported by pH < 7.

The metabolite patterns followed the microbiota along with the pH change. The molar ratio of acetate:propionate:butyrate was 1:0.47:0.34 at pH 6 and 1:0.31:0.16 at pH 8. Acetate, the main metabolite of many gut bacteria, was produced within the whole pH range and at both dilution rates (Fig. 3). Slightly less acetate was detected at low pH (19 vs 25 mM at pH 6.0 vs pH 8.0, respectively). Significant correlations between the consortial changes and acetate production could not be elucidated from these data.

In accordance with the prevalence of *B. ovatus*, Ruminococcaceae and *A. muciniphila*, production of propionate and butyrate was seen throughout the whole tested pH range with slightly lower values at higher pH-s (Fig. 3). The family Ruminococcaceae includes several butyrate producing genera such as *Faecalibacterium*. In agreement with the decreasing abundance of *Faecalibacterium*, significantly less butyrate was formed at pH > 7.5, compared to that at pH < 6.5. However, similar trend was not observed for other Ruminococcaceae.



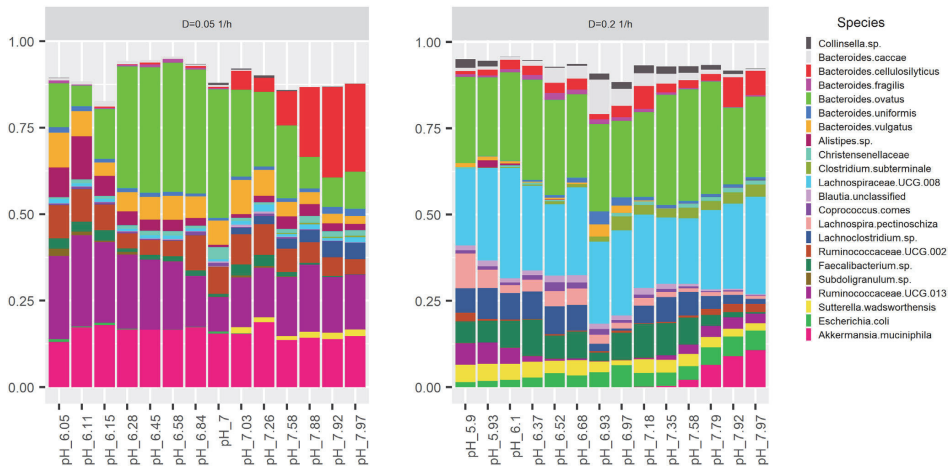


Figure 1. Dynamic changes of the dominant species of faecal microbiota in pectin supplemented medium during changing the pH from 6.0 to 8.0, at dilution rates  $D_{low} = 0.05$  1/h (left) and  $D_{high} = 0.2$  1/h (right).

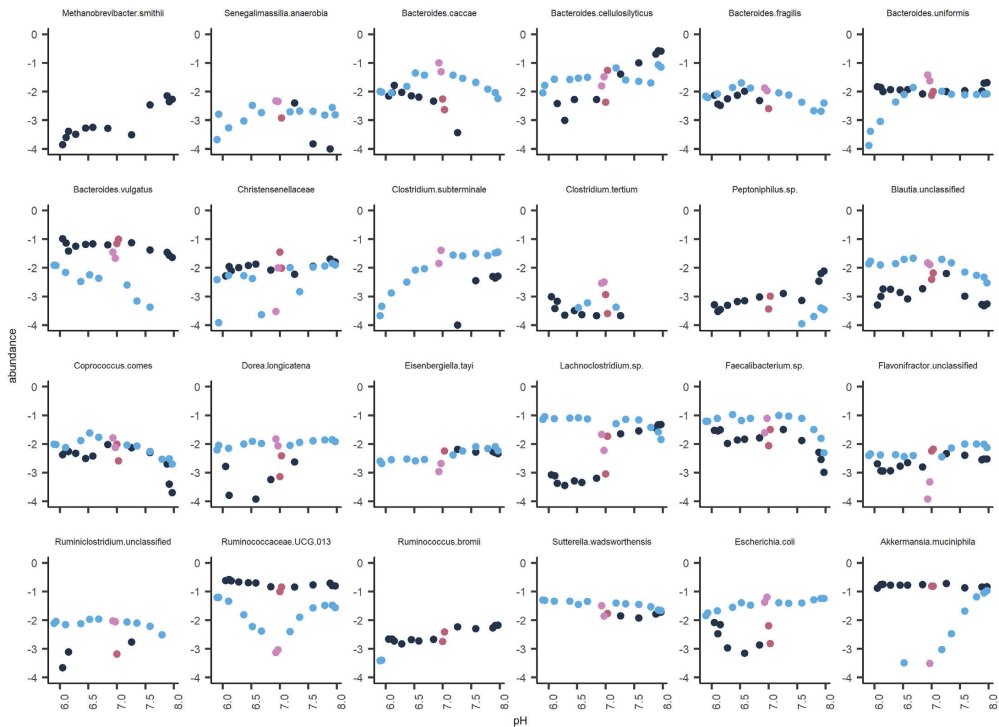
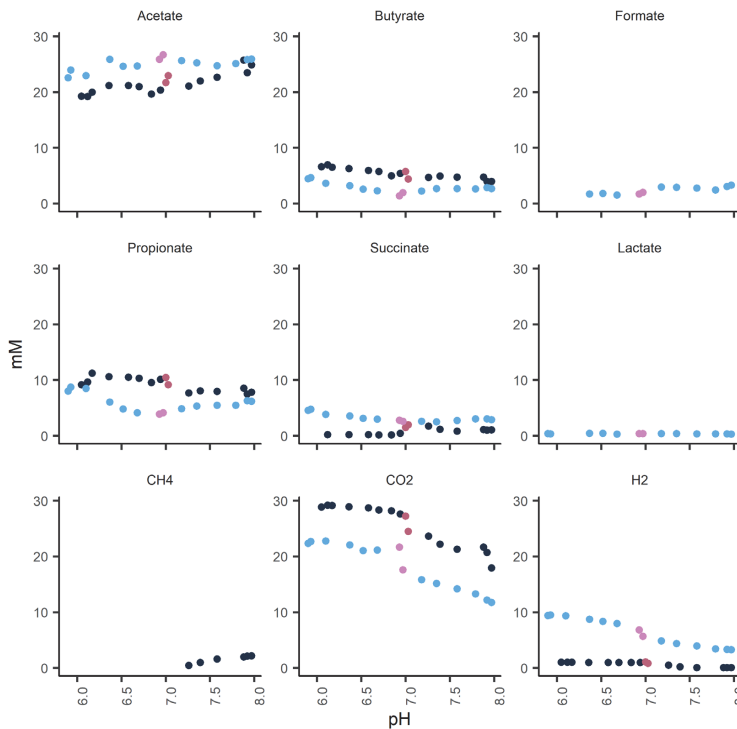


Figure 2. Dynamic changes of the abundances (log scale) of the species of significant difference ( $P$ -value < 0.05) between pH 6.0 and 8.0 at dilution rates  $D_{low} = 0.05$  1/h (dark blue dots) and  $D_{high} = 0.2$  1/h (light blue dots). Dark and light pink dots indicate the steady state conditions at pH = 7.0, before increase or decrease of the pH at  $D_{low}$  and  $D_{high}$ , respectively. The species detected at least 0.5% in at least one sample are shown. Data on abundances of all bacteria and  $P$ -values can be found in the Table S1, Supporting Information.



**Figure 3.** Dynamic changes of the metabolites (acids in mM, gases in mmol per L medium) produced by faecal microbiota in pectin supplemented medium at pH between 6.0 and 8.0 at two dilution rates:  $D_{low} = 0.05$  1/h (dark blue dots) and  $D_{high} = 0.2$  1/h (light blue dots). Dark and light pink dots indicate the steady state conditions at pH = 7.0, before increase or decrease of the pH at  $D_{low}$  and  $D_{high}$ , respectively. Data on metabolite concentrations and P-values can be found in the Supplementary Table S1, Supporting Information.

Notable changes in gas formation profiles were seen depending on the dilution rate and changing pH. The amount of carbon dioxide, the main gaseous product, was 27 mmol per L medium at pH 6.0 but only 18 mmol per L medium at pH 8.0 at  $D_{low}$ . Methanogenesis is a process carried out by slow-growing archaea who convert acetate, carbon dioxide and hydrogen gas into methane. Production of methane at  $D_{low}$  was observed at pH >7, in accordance with the increase of *Methanobrevibacter smithii* from < 0.05 (pH 7.5) to 0.5% (pH 7.9) (Fig. 2). Methanogenic species in general are sensitive to the accumulation of organic acids, especially propionate, and typically have neutral or slightly alkaline pH optima (Angelidaki et al. 2011). However, occurrence of *M. smithii* in our experiments at  $D_{low}$ , with elevated concentrations of propionate, suggests its tolerance to propionate. Similarly, Barredo and Evison (1991) have reported increased methane production by *M. smithii* at pH 8.0 despite the presence of propionate. Conversion of  $CO_2$  (and  $H_2$ ) into  $CH_4$  could partially explain the drop of  $CO_2$  (and a small drop in hydrogen concentrations) at increasing pH. In addition,  $CO_2$  is fixed during production of succinate, amount of which was rising at pH > 7.

Most of the amino acids from the growth medium were depleted at  $D_{low}$  (Table S1, Supporting Information). Distinctly higher concentrations of isobutyrate, isovalerate and valerate — the metabolites derived from the breakdown of the branched chain amino acids (BCAA) were found, compared to those at  $D_{high}$  (Fig. 4). Production of hydrogen sulphide was more preva-

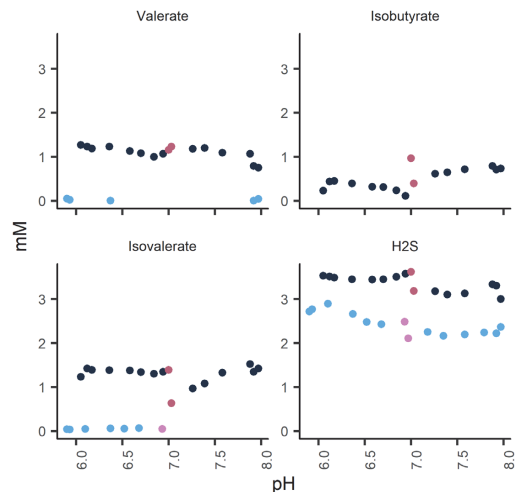


**Figure 4.** Dynamic changes in concentrations of valerate, isovalerate, isobutyrate (mM) and hydrogen sulphide (mmol per L medium) during the growth of faecal microbiota on apple pectin at pH between 6.0 AND 8.0 at two dilution rates:  $D_{low} = 0.05$  1/h (dark blue dots), and  $D_{high} = 0.2$  1/h (light blue dots). Dark and light pink dots indicate the steady state conditions at pH = 7.0 before increase or decrease of the pH at  $D_{low}$  and  $D_{high}$ , respectively. Data on metabolite concentrations and P-values can be found in the Table S1, Supporting Information.

lent at  $D_{low}$ . This agrees with our previous findings about conversion of the reducing agent cysteine into  $H_2S$  by faecal microbiota at low dilution rate (Adamberg and Adamberg 2018; Adamberg, Raba and Adamberg 2020).

### The effect of pH on the metabolism of apple pectin by faecal microbiota at high dilution rate ( $D_{high} = 0.2$ 1/h)

The most abundant taxa at  $D_{high}$  throughout the tested pH range were *B. ovatus* and *Lachnospiraceae* UCG-008 (Fig. 1). The growth of some other species, namely *Bifidobacterium bifidum*, *Clostridium subterminale*, *Dorea longicatena*, *Lachnospiridium torques*, *Sutterella wadsworthensis* and *Escherichia coli*, was also favored by  $D_{high}$  (Fig. 1). The most distinct difference in microbial composition between the two dilution rates was the prevalence of various *Ruminococcaceae* at  $D_{low}$ , and that of *Lachnospiraceae* at  $D_{high}$ . Two species from the family *Lachnospiraceae*, *Lachnospira pectinoschiza* and *Lachnospiridium lactaris*, were highly abundant (1–5%) at  $D_{high}$ , whilst not detected at  $D_{low}$ .

Growth of *B. dorei/vulgatus*, *Blautia* unclassified and *Faecalibacterium* was significantly stimulated at  $pH < 7$  (Fig. 2). In contrast, the abundances of *Bacteroides uniformis*, *C. subterminale* and *A. muciniphila*, increased significantly at  $pH > 7$ . Competitiveness of *A. muciniphila* at alkaline pH at  $D_{high}$  was especially interesting, considering that this species is known to have a low specific growth rate. Although being below the detection limit in a steady state at pH 7, its population achieved levels comparable to those at  $D_{low}$  at pH 8. *Bifidobacterium bifidum* and *Bacteroides caccae* had the highest abundances around neutral pH (6.5–7.5), a feature that was not seen for other taxa, neither at  $D_{high}$  or  $D_{low}$  (Fig. 2). Significant reorganisation within the genus *Bacteroides* was observed regarding to the dilution rate (Fig. 2). While *Bacteroides caccae* was more prevalent at  $D_{high}$ , the opposite was observed for *B. dorei/vulgatus*.

Acetate was the main metabolite produced at all pH values (23–27 mM, Fig. 3). Molar ratio of acetate:propionate:butyrate was 1:0.35:0.20 at pH 6 and 1:0.24:0.10 at pH 8. At  $D_{high}$ , trace amounts of lactate were seen, which were not detected at  $D_{low}$ . This is most likely linked to the higher abundance of *Bifidobacterium bifidum* at  $D_{high}$ .

Substantially less  $CO_2$  was produced at  $D_{high}$  than at  $D_{low}$  (12–23 vs 18–29 mmol per L medium). Similar to  $D_{low}$ , decrease in production of  $CO_2$  and  $H_2$  was observed with the change of pH towards alkaline (Fig. 3). No methane was detected at  $D_{high}$ .

The majority of amino acids were depleted from the culture medium within the whole pH range at  $D_{high}$  (Table S1, Supporting Information). Notable amounts of alanine, leucine, isoleucine and valine were detected at  $D_{high}$ . Between pH 6.3–7.9, only 15%–30% of BCAA were metabolized. Below pH 6.3, the consumption of BCAA decreased even more and was minuscule at pH 6 (Table S1, Supporting Information). This was supported by the negligible amounts of metabolites of BCAA fermentation.

## DISCUSSION

The species *Bacteroides caccae*, *B. cellulosilyticus*, *B. ovatus* and *B. thetaiotaomicron*, *Faecalibacterium* and *Lachnospira pectinoschiza* comprised 30%–50% of the total population in the faecal cultures grown in apple pectin supplemented medium. The prevalence of these pectin-degrading bacteria (Sirotek et al. 2004; Bidle et al. 2013; Magnúsdóttir et al. 2017) emphasizes the importance of primary fibre degraders in faecal microbiota. Interestingly, along with the increasing pH, the composition of the

pectin-degrading taxa changed from butyrate-producing *Faecalibacterium* and *Lachnospira* to propionate-producing *B. cellulosilyticus*. This indicates the dynamics of microbiota and metabolite patterns in the colonic environment in regard to the acid formation and pH. Pure cultures of *B. caccae* were shown to convert apple pectin into acetate and propionate (Sirotek et al. 2004). Depending on the species, *Bacteroides* may produce either succinate, propionate, or both in parallel with acetate. The production of propionate via succinate requires  $CO_2$  which is used for regeneration of  $NAD^+$ . On the other hand, when propionate is produced via catabolism of pyruvate,  $CO_2$  is released. Our data suggest that  $D_{low}$  favours the development of consortia that produce propionate through succinate and  $CO_2$ , while  $D_{high}$  supports the fast growing microbes that produce succinate without its further conversion into propionate.

A surprising dilution rate specific effect was seen for mucin degrading bacteria *Akkermansia* and *Lachnospiridium* (*L. torques* and *L. gnavus*). These bacteria can degrade mucins but have different pH optima. At  $D_{high}$ , the abundance of *lachnospiridia* decreased while that of *A. muciniphila* increased along with the rise of pH from 7 to 8. This trend was not seen at  $D_{low}$ . Although *A. muciniphila* is generally regarded as a beneficial gut bacterium, its abundance may increase in the case of colorectal cancer (CRC) progression along with elevated pH ( $pH > 7.5$ ) (Weir et al. 2013; Zackular et al. 2013; Borges-Canha et al. 2015). Moreover, we saw the decline of butyrate producing taxa as well as lower concentrations of butyrate at  $pH > 7.5$ , that often occur together with CRC. Moreover, the alkaline pH usually accompanies slow gastrointestinal transit (Lewis and Heaton 1997) and constipation, that is typical for CRC (Kojima et al. 2004). This suggests that alkaline environments enable this bacterium to acquire benefits over *lachnospiridia* or other mucin degrading bacteria such as *Bifidobacterium bifidum*, *B. caccae* and *B. fragilis* which abundances decreased at higher pH. *A. muciniphila* was a dominant bacterium also at  $D_{low}$ , independent of the pH.

High pH in colonic lumen is one of the key parameters related to CRC (Kashtan et al. 1990; Walker and Walker 1992; Ohigashi et al. 2013), however, the data on the influence of alkaline environment on the development of colon microbiota are missing. It might be explained by the relevance of alkaline pH to protein fermentation resulting in formation of ammonia from amino acids. Branched short chain fatty acids (BCFA) isobutyrate and isovalerate, which are produced during protein degradation have been considered to be biomarkers for gut health as protein fermentation by genera such as *Bacteroides* and *Clostridium* can yield phenols, p-cresol and biogenic amines—potentially harmful compounds for the intestinal epithelium (Aguirre et al. 2016; Rios-Covian et al. 2020). Our results revealed the increase of proteolytic bacteria (*Clostridium*, *Escherichia*) along with the decrease of butyrate producers (*Faecalibacterium*, *Blautia*, *Lachnospira*) at  $pH > 7.5$ , even in the presence of fermentable carbohydrate pectin. A decrease in abundances of *Faecalibacterium* and *Blautia* as a result of changing pH from 5.5 to 6.9 in chemostat experiments with apple pectin as substrate ( $D = 0.04$  1/h) was reported by Chung et al. (2016). Similarly, Reichardt et al. (2018) showed an enhanced growth of butyrate producers in faecal microbiota at pH 5.5, compared to that at pH 6.5. In parallel with the decreasing abundances of butyrate producers, we saw an increase in production of BCFA at  $D_{low}$ . In addition, at pH close to 8, the increased solubility of  $H_2S$  would lead to formation of  $HS^-$  ions, that might inhibit the butyrate producing bacteria.

Methane production was detected only at  $D_{low}$ . Increased methane formation is also related to higher proportion of colonic methanogenic microbes in CRC patients. We observed

gradual increase of *Methanobrevibacter* together with that of methane production while changing the pH > 7.5 at D<sub>low</sub>. *Methanobrevibacter* is commonly associated with slow transit microbiomes (Vandeputte et al. 2015), however, the effect of pH on its growth has not been described earlier. The increased abundance of *Methanobrevibacter* may be related to its lower sensitivity to H<sub>2</sub>S, while the abundances of butyrate-producing H<sub>2</sub>S-sensitive bacteria such as *Faecalibacterium* decreased along with the increase of H<sub>2</sub>S concentrations. The main source of H<sub>2</sub>S was cysteine, added to the culture medium. According to MetaCyc.org database, *Alistipes*, *B. cellulosityticus*, *B. ovatus*, *Escherichia coli*, and *Klebsiella* (all detected in this study) can convert cysteine to H<sub>2</sub>S. Reaction of H<sub>2</sub>S with metal (for example iron) ions results in formation of insoluble sulphides that are not available for bacterial cells. For anaerobic bacteria, however, iron in the form of ferredoxins is extremely important for regeneration of the whole redox system.

In conclusion, we showed that pH is a crucial trigger in the development of continuously growing faecal consortia. The longest experiments demonstrated the pH-specific changes in the faecal microbiota, for example in relation to alkaline pH environment, often associated with pathologies. The species such as *B. ovatus* were prevalent within the whole range of pH, while butyrate producing *Faecalibacterium* or *Coprococcus comes* were severely inhibited at pH > 7.5. Further variations in the composition and metabolism were caused by the dilution rate, representing either fast or slow colonic transit rate. Consequently, the concomitant bacterial metabolites have specific health effects. The effect of pH on the fermentation of other dietary fibres, and their combinations, by faecal microbiota can be studied by applying a similar cultivation approach. As the pH of the colonic environment is directly related to diet, science-driven diet modifications could be an easy solution to support gut health.

## SUPPLEMENTARY DATA

Supplementary data are available at [FEMSLE](https://femsle.onlinelibrary.wiley.com/doi/10.1111/femsle.12156) online.

## ACKNOWLEDGEMENTS

The authors would like to thank Madis Jaagura for carrying out the bioinformatic analyses.

## FUNDING

The project has received funding from the Institutional Research Funding (IUT 1927) of the Estonian Ministry of Education and Research and the European Regional Development Fund project EU48667.

**Conflicts of Interest.** None declared.

## REFERENCES

- Adamberg K, Adamberg S. Selection of fast and slow growing bacteria from fecal microbiota using continuous culture with changing dilution rate. *Microb Ecol Health Dis* 2018;**29**:1549922.
- Adamberg K, Raba G, Adamberg S. Use of Changestat for Growth Rate Studies of Gut Microbiota. *Front Bioeng Biotech* 2020;**8**:1–12.
- Adamberg K, Tomson K, Talve T et al. Levan enhances associated growth of *Bacteroides*, *Escherichia*, *Streptococcus* and *Faecalibacterium* in fecal microbiota. *PLoS One* 2015;**10**:1–18.
- Adamberg K, Valgepea K, Vilu R. Advanced continuous cultivation methods for systems microbiology. *Microbiology* 2015;**161**:1707–19.
- Aguirre M, Eck A, Koenen ME et al. Diet drives quick changes in the metabolic activity and composition of human gut microbiota in a validated in vitro gut model. *Res Microbiol* 2016;**167**:114–25.
- Aguirre M, Eck A, Koenen ME et al. Evaluation of an optimal preparation of human standardized fecal inocula for in vitro fermentation studies. *J Microbiol Methods* 2015;**117**:78–84.
- Aguirre M, Ramiro-Garcia J, Koenen ME et al. To pool or not to pool? Impact of the use of individual and pooled fecal samples for in vitro fermentation studies. *J Microbiol Methods* 2014;**107**:1–7.
- Angelidaki I, Karakashev D, Batstone DJ et al. *Biomethanation and Its Potential*. 1st ed. Elsevier Inc., 2011.
- Barredo MS, Evison LM. Effect of propionate toxicity on methanogen-enriched sludge, *Methanobrevibacter smithii*, and *Methanospirillum hungatii* at different pH values. *Appl Environ Microbiol* 1991;**57**:1764–9.
- Biddle A, Stewart L, Blanchard J et al. Untangling the genetic basis of fibrolytic specialization by lachnospiraceae and ruminococcaceae in diverse gut communities. *Diversity* 2013;**5**:627–40.
- Birchough G, Schroeder BO, Bäckhed F et al. Dietary destabilization of the balance between the microbiota and the colonic mucus barrier. *Gut Microbes* 2019;**10**:246–50.
- Borges-Canha M, Portela-Cidade JP, Dinis-Ribeiro M et al. Role of colonic microbiota in colorectal carcinogenesis: a systematic review. *Rev Española Enfermedades Dig* 2015;**107**:659–71.
- Chung WSF, Walker AW, Louis P et al. Modulation of the human gut microbiota by dietary fibres occurs at the species level. *BMC Biol* 2016;**14**:1–13.
- Chung WSF, Walker AW, Vermeiren J et al. Impact of carbohydrate substrate complexity on the diversity of the human colonic microbiota. *FEMS Microbiol Ecol* 2018;**95**:1–13.
- Cummings JH, Jenkins DJA, Wiggins HS. Measurement of the mean transit time of dietary residue through human gut. *Gut* 1976;**17**:210–8.
- Cummings JH, Macfarlane GT. The control and consequences of bacterial fermentation in the human colon. *J Appl Bacteriol* 1991;**70**:443–59.
- Cummings JH. Constipation, dietary fibre and the control of large bowel function. *Postgrad Med J* 1984;**60**:811–9.
- de Souza CB, Jonathan M, Saad SMI et al. Degradation of fibres from fruit by-products allows selective modulation of the gut bacteria in an in vitro model of the proximal colon. *J Funct Foods* 2019;**57**:275–85.
- de Vries J, Miller PE, Verbeke K. Effects of cereal fiber on bowel function: a systematic review of intervention trials. *World J Gastroenterol* 2015;**21**:8952–63.
- Duncan SH, Louis P, Thomson JM et al. The role of pH in determining the species composition of the human colonic microbiota. *Environ Microbiol* 2009;**11**:2112–22.
- Elia M, Cummings JH. Physiological aspects of energy metabolism and gastrointestinal effects of carbohydrates. *Eur J Clin Nutr* 2007;**61**:S40–74.
- Fallingborg J, Christensen LA, Ingeman-Nielsen M et al. pH-profile and regional transit times of the normal gut measured by a radiotelemetry device. *Aliment Pharmacol Ther* 1989;**3**:605–14.
- Kaoutari AE, Armougoum F, Gordon JJ et al. The abundance and variety of carbohydrate-active enzymes in the human gut microbiota. *Nat Rev Microbiol* 2013;**11**:497–504.

- Kasemets K, Drews M, Nisamedtinov I et al. Modification of A-stat for the characterization of microorganisms. *J Microbiol Methods* 2003;**55**:187–200.
- Kashtan H, Stern HS, Jenkins DJA et al. Manipulation of fecal pH by dietary means. *Prev Med* 1990;**19**:607–13.
- Kojima M, Wakai K, Tokudome S et al. Bowel movement frequency and risk of colorectal cancer in a large cohort study of Japanese men and women. *Br J Cancer* 2004;**90**:1397–401.
- Koziolek M, Grimm M, Becker D et al. Investigation of pH and temperature profiles in the GI tract of fasted human subjects using the IntelliCap system. *J Pharm Sci* 2015;**104**:2855–63.
- Larsen N, De Souza CB, Krych L et al. Potential of pectins to beneficially modulate the gut microbiota depends on their structural properties. *Frontiers in Microbiology* 2019;**10**:1–13.
- Lewis SJ, Heaton KW. Increasing butyrate concentration in the distal colon by accelerating intestinal transit. *Gut* 1997;**41**:245–51.
- Magnúsdóttir S, Heinken A, Kutt L et al. Generation of genome-scale metabolic reconstructions for 773 members of the human gut microbiota. *Nat Biotechnol* 2017;**35**:81–9.
- Martens EC, Lowe EC, Chiang H et al. Recognition and degradation of plant cell wall polysaccharides by two human gut symbionts. *PLoS Biol* 2011;**9**:e1001221. DOI: 10.1371/journal.pbio.1001221.
- Martens EC, Neumann M, Desai MS. Interactions of commensal and pathogenic microorganisms with the intestinal mucosal barrier. *Nat Rev Microbiol* 2018;**16**:457–70.
- Maurer JM, Schellekens RCA, van Rieke HM et al. Gastrointestinal pH and transit time profiling in healthy volunteers using the IntelliCap system confirms ileo-colonic release of ColoPulse tablets. *PLoS One* 2015;**10**:1–17.
- Monod J. [The technique of continuous culture, theory and applications]. *Ann Inst Pasteur* 1950;**79**:390–410, (in French).
- Muzzarelli RAA, Boudrant J, Meyer D et al. Current views on fungal chitin /chitosan, human chitinases, food preservation, glucans, pectins and inulin : a tribute to Henri Braconnot, precursor of the carbohydrate polymers science, on the chitin bicentennial. *Carbohydr Polym* 2012;**87**:995–1012.
- Nugent SG, Kumar D, Rampton DS et al. Intestinal luminal pH in inflammatory bowel disease: possible determinants and implications for therapy with aminosaliculates and other drugs. *Gut* 2001;**48**:571–7.
- O’Keefe SJD. Diet, microorganisms and their metabolites, and colon cancer. *Nat Rev Gastroenterol Hepatol* 2016;**13**:691–706.
- Ohigashi S, Sudo K, Kobayashi D et al. Changes of the intestinal microbiota, short chain fatty acids, and fecal pH in patients with colorectal cancer. *Dig Dis Sci* 2013;**58**:1717–26.
- Parkar SG, Redgate EL, Wibisono R et al. Gut health benefits of kiwifruit pectins: comparison with commercial functional polysaccharides. *J Funct Foods* 2010;**2**:210–8.
- Reichardt N, Vollmer M, Holtrop G et al. Specific substrate-driven changes in human faecal microbiota composition contrast with functional redundancy in short-chain fatty acid production. *ISME J* 2018;**12**:610–22.
- Rios-Covian D, González S, Nogaacka AM et al. An overview on fecal short-chain fatty acids along human life and as related with body mass index: associated dietary and anthropometric factors. *Front Microbiol* 2020;**11**:1–9.
- Roager HM, Hansen LBS, Bahl MI et al. Colonic transit time is related to bacterial metabolism and mucosal turnover in the gut. *Nature Microbiol* 2016;**1**:1–9.
- Russell WR, Gratz SW, Duncan SH et al. High-protein, reduced-carbohydrate weight-loss diets promote metabolite profiles likely to be detrimental to colonic health. *Am J Clin Nutr* 2011;**93**:1062–72.
- Sander R. Compilation of Henry’s law constants (version 4.0) for water as solvent. *Atmos Chem Phys* 2015;**15**:4399–981.
- Schroeder BO, Birchenough GMH, Ståhlman M et al. Bifidobacteria or fiber protect against diet-induced microbiota-mediated colonic mucus deterioration. *Cell Host & Microbe* 2018;**23**:27–40.e7.
- Schroeder BO. Fight them or feed them: how the intestinal mucus layer manages the gut microbiota. *Gastroenterology Report* 2019;**7**:3–12.
- Sender R, Fuchs S, Milo R. Are we really vastly outnumbered? Revisiting the ratio of bacterial to host cells in humans. *Cell* 2016;**164**:337–40.
- Sirotek K, Slováková L, Kopečný J et al. Fermentation of pectin and glucose, and activity of pectin-degrading enzymes in the rabbit caecal bacterium *Bacteroides caccae*. *Lett Appl Microbiol* 2004;**38**:327–32.
- Van Bueren AL, Mulder M, Van Leeuwen S et al. Prebiotic galactooligosaccharides activate mucin and pectic galactan utilization pathways in the human gut symbiont *Bacteroides thetaiotaomicron*. *Sci Rep* 2017;**7**:1–13.
- Vandeputte D, Falony G, Vieira-Silva S et al. Stool consistency is strongly associated with gut microbiota richness and composition, enterotypes and bacterial growth rates. *Gut* 2016;**65**:57–62.
- Van Herreweghen F, Van den Abbeele P, De Mulder T et al. In vitro colonisation of the distal colon by *Akkermansia muciniphila* is largely mucin and pH dependent. *Beneficial Microbes* 2017;**8**:81–96.
- Walker ARP, Walker BF. Faecal pH and colon cancer. *Letters* 1992:572.
- Weir TL, Manter DK, Sheflin AM et al. Stool Microbiome and Metabolome Differences between Colorectal Cancer Patients and Healthy Adults. *PLoS One* 2013;**8**:e70803. DOI: 10.1371/journal.pone.0070803.
- Zackular JP, Baxter NT, Iverson KD et al. The gut microbiome modulates colon tumorigenesis. *MBio* 2013;**4**:1–9.

## Appendix 3

### Publication III

**Raba, G.,** Luis, A. S. Mucin utilization by gut microbiota - recent advances on characterization of key enzymes. *Essays in Biochemistry*. 2023 Jan 25:EBC20220121. doi: 10.1042/EBC20220121.



## Review Article

# Mucin utilization by gut microbiota: recent advances on characterization of key enzymes

Grete Raba<sup>1</sup> and  Ana S. Luis<sup>2</sup><sup>1</sup>Department of Chemistry and Biotechnology, Tallinn University of Technology, Akadeemia tee 15 12618, Tallinn, Estonia; <sup>2</sup>Department of Medical Biochemistry and Cell Biology, University of Gothenburg, Box 440, 405 30 Gothenburg, Sweden

Correspondence: Ana S. Luis (ana.luis@medkem.gu.se)



The gut microbiota interacts with the host through the mucus that covers and protects the gastrointestinal epithelium. The main component of the mucus are mucins, glycoproteins decorated with hundreds of different *O*-glycans. Some microbiota members can utilize mucin *O*-glycans as carbons source. To degrade these host glycans the bacteria express multiple carbohydrate-active enzymes (CAZymes) such as glycoside hydrolases, sulfatases and esterases which are active on specific linkages. The studies of these enzymes in an *in vivo* context have started to reveal their importance in mucin utilization and gut colonization. It is now clear that bacteria evolved multiple specific CAZymes to overcome the diversity of linkages found in *O*-glycans. Additionally, changes in mucin degradation by gut microbiota have been associated with diseases like obesity, diabetes, irritable bowel disease and colorectal cancer. Thereby understanding how CAZymes from different bacteria work to degrade mucins is of critical importance to develop new treatments and diagnostics for these increasingly prevalent health problems. This mini-review covers the recent advances in biochemical characterization of mucin *O*-glycan-degrading CAZymes and how they are connected to human health.

## Introduction

The human gut harbours a complex and diverse microbial community, the gut microbiota, that has an essential role on human health. The gut microbiota colonizes the mucus layer that covers the intestinal epithelium [1]. The properties of this mucus layer are variable along the gastrointestinal (GI) tract. In the small intestine the mucus forms a single loose layer. However, in the colon the mucus is organized into two layers: the inner layer, attached to the epithelium, is tightly arranged and it is almost devoid of bacteria, whereas the outer mucus layer is loosely arranged and is heavily colonized by the microbiota (Figure 1A) [1]. This double-layer organization of the colonic mucus is essential to the host health. The outer layer provides the ideal habitat for the bacteria to thrive in the gut environment, while the impenetrable inner mucus layer acts as a barrier keeping the bacteria away from the intestinal epithelium preventing close contact and inflammation [2]. The major components of the mucus are mucins, heavily *O*-glycosylated glycoproteins (Figure 1B). These host glycans have a major role in determining which bacteria can successfully colonise the host [1,3,4]. At the same time, some members of the human microbiota have been shown to be able to forage on mucins and if excessive, the bacterial degradation of mucins can lead to alterations on microbiota composition and a thinner and penetrable mucus barrier (Figure 1A) [5–7]. It is now clear that alterations on both the microbiota and the mucus barrier function, can lead to multiple diseases such as obesity, diabetes, colorectal cancer and inflammatory bowel disease (IBD) [6–9]. Therefore, understanding the mechanisms of degradation and utilization of mucins by the gut microbiota could have a key role on finding treatments to prevent or control diseases characterized by the excessive bacterial erosion of the mucus layer.

Received: 14 December 2022

Revised: 04 January 2023

Accepted: 09 January 2023

Version of Record published:  
25 January 2023



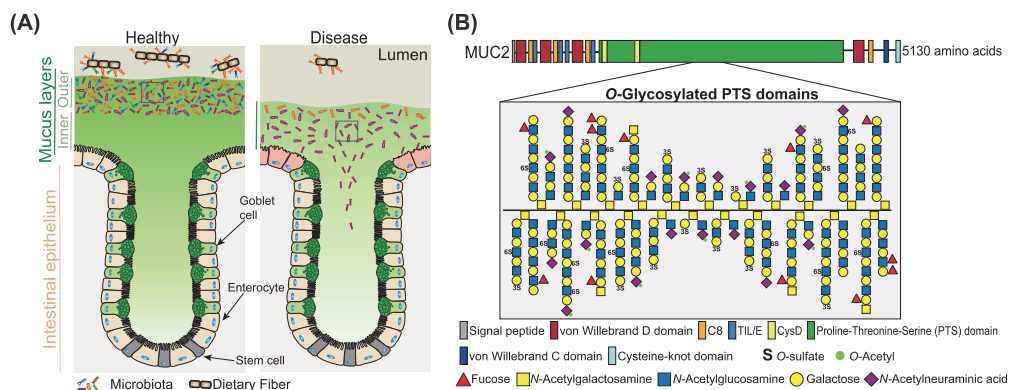


**Figure 1. Overview of colonic mucus layers**

(A) In the healthy colon the mucus is organized as the inner and outer mucus layer, which have low and high bacterial colonization, respectively. The major components of the mucus layer are mucins that are synthesized and secreted by goblet cells. In diseases, such as ulcerative colitis, there is an increase in the mucus layer penetrability and bacteria can be found close to the inflamed intestinal epithelium. (B) Schematic representation of the MUCIN 2 (MUC2). In the mucus layer, MUC2 is organized in a complex network due to N- and C-terminal disulfide bounds. This glycoprotein is heavily O-glycosylated in proline, threonine and serine (PTS) domains. The MUC2 monomer backbone has a molecular weight of around 500 kDa which goes up to 2.5 MDa after glycosylation.

## Select members of the microbiota can degrade mucin O-glycans

Mucins can be membrane-bound or secreted. Membrane mucins are a part of the glycocalyx of mucosal surfaces where they are involved in cell signalling and act as a last defence line to keep bacteria away from the epithelium [10]. Secreted mucins are the main components of the mucus and give it its viscous gel-like properties. The mucus composition along the GI tract is variable with Mucin5AC (MUC5AC) and Mucin2 (MUC2) being the most common mucins in the stomach and intestine, respectively (Figure 1B) [1]. The mucin protein backbone is characterized by having multiple repeating units of proline-threonine-serine (PTS) domains that are extensively decorated with complex O-glycans made of N-acetylgalactosamine (GalNAc), galactose (Gal) and N-acetylglucosamine (GlcNAc) chains capped with sialic acid, sulfate and fucose (Fuc) in multiple positions and blood groups generating multiple terminal epitopes (Figure 2). A single mucin can contain more than a hundred different O-glycan structures with these sugars making up to 80% of the total mucin molecular weight [1,11]. Importantly, the O-glycosylation varies spatially along the GI tract and between different species. In humans and pigs, there is an increasing gradient of sialylation and sulfation along the GI tract, whereas the opposite is observed for fucosylation [12–16]. Such variations in glycosylation will have a significant impact on the microbiota utilization of these complex glycans. Indeed, a recent study showed that *Akkermansia muciniphila*, a bacterium known to grow on O-glycans of porcine gastric mucins (PGM), failed to grow on colonic O-glycans [17]. Therefore, to address the mechanisms of degradation of mucins, it is critical to understand the structural variability of mucin O-glycosylation.

To degrade O-glycans, the gut bacteria encode multiple carbohydrate active enzymes (CAZymes) such as glycoside hydrolases (GHs), carbohydrate esterases (CE) and sulfatases. CAZymes are classified into families based of sequence similarity in the databases CAZy (GHs and CEs) and SulfAtlas (only sulfatases) [18,19]. Inside a family the proteins share a conserved fold, catalytic mechanism and active site residues. Additionally, depending on the cleavage site, the GHs and sulfatases are also classified as either exo- or endo-active with the former hydrolysing glycans from one end and the latter within the glycan chain [20].

## CAZymes active on terminal mucin capping structures

The substitution of mucins with sialic acid, sulfate, fucose and blood groups creates a barrier against degradation by the microbiota (Figure 2). To utilize mucin glycans the bacteria need to encode specific enzymes that remove the various capping structures. The different enzymes active on the mucin substitutions are described below.

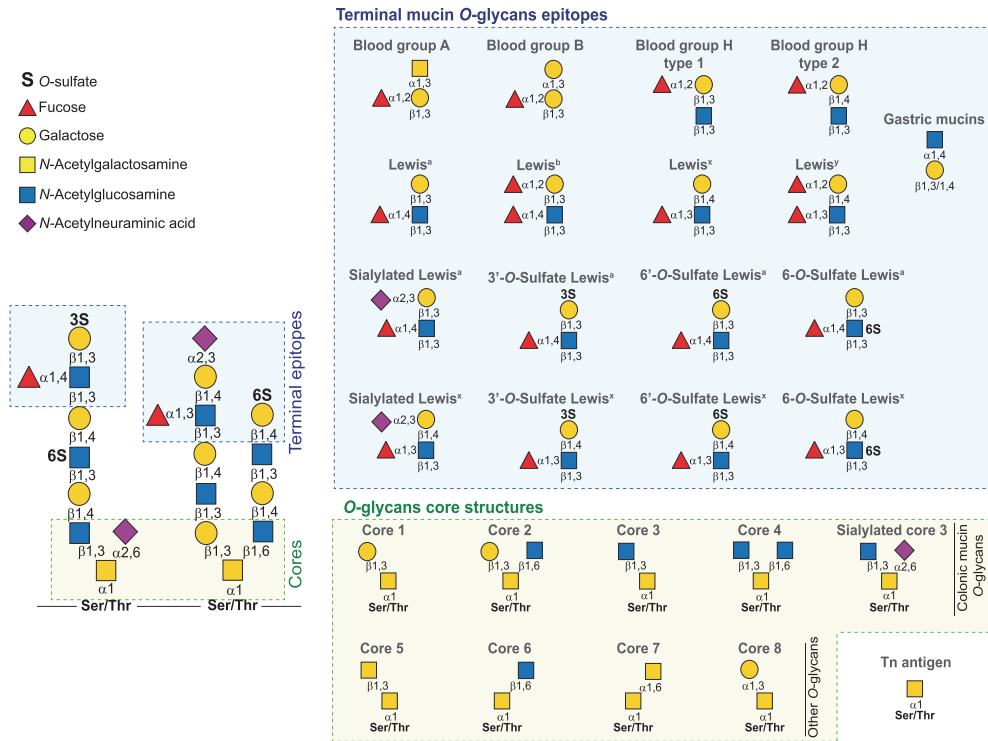


**Figure 2. Schematic representation of mucin O-glycan structures**  
 Different terminal epitopes and cores structures highlighted inside the blue and yellow boxes, respectively. Sugars are shown according to the Symbol Nomenclature for Glycan system [60].

## Sulfatases

In mucins, sulfation occurs O-linked to Gal at positions 3, 4 and 6 (3S-, 4S- and 6S-Gal, respectively) and to GlcNAc in position 6 (6S-GlcNAc). Sulfation on Gal is always terminal whereas 6S-GlcNAc can be terminal or internal (Figure 2) [17]. Sulfation is variable between species with 3S-Gal and 6S-GlcNAc being common in porcine colonic mucins while human colonic mucins also show a high level of 6S-Gal [13,15,21]. The sulfation on 4S-Gal is present on saliva mucins that transit through the GI tract where they become an available carbon source for the gut microbiota [22]. Several members of the human microbiota encode sulfatases that remove the sulfate capping group allowing access to O-glycan (Figure 3) [17]. The microbial sulfatase activity has been previously associated with colitis, a type of IBD [23]. Additionally, it has been shown that *Bacteroides thetaiotaomicron*, a prominent member of the human microbiota, can lead to colitis in a susceptible animal model and the development of this disease is dependent of active sulfatases [24]. Despite the link between sulfatases and disease, these enzymes remain poorly characterized. Recently, a study identified the activity of 12 of the 28 sulfatases encoded by *B. thetaiotaomicron* [17]. Surprisingly, 11 on these enzymes are active on sulfated linkages found on mucin O-glycans. Together these enzymes can potentially remove all the sulfate groups found in mucin. However, only 4 sulfatases were found active on colonic mucin O-glycans, cleaving specifically sulfation of 3S-Gal or 6S-GlcNAc. The present study also identified the first sulfatase active on 3S-linked to GalNAc (3S-GalNAc), a linkage not yet identified in mucin or other host glycans [17]. The structural characterization of *B. thetaiotaomicron* sulfatases showed for the first time that these enzymes evolved different specificity determinants to specifically recognize the target linkage within different glycan contexts [17,25]. Importantly, the present study identified a single 3S-Gal sulfatase (BT1636) as essential to *B. thetaiotaomicron* growth on colonic O-glycans and *in vivo* fitness during a competitive gut colonization [25]. A similar key role of sulfatases in gut colonization was also shown in *Bacteroides fragilis*. BF3134, a homolog of the 6S-GlcNAc enzymes characterized in

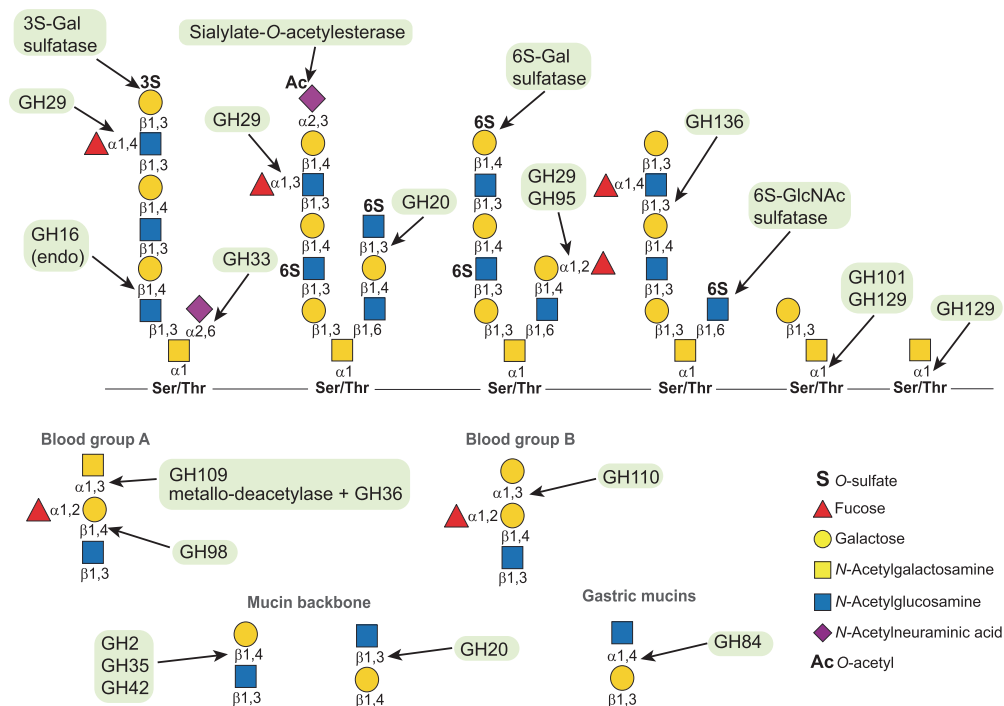


**Figure 3. Specificity of mucin O-glycans CAZymes**

The arrows point to the linkage cleaved by the different enzymes shown inside green boxes. Sugars are shown according to the Symbol Nomenclature for Glycan system [60]; GHXXX, glycoside hydrolase family XXX.

*B. thetaiotaomicron*, has been shown to have a key role in *B. fragilis* *in vivo* fitness in presence of an invading strain suggesting that sulfatases are also important in securing colonization within the gut [26].

Sulfation in 6S-GlcNAc is a major substitution found in colonic mucins of human, pigs and mice. To remove this sulfation some gut bacteria, such as *Prevotella* and *Bifidobacterium bifidum*, developed an alternative mechanism of overcoming the 6S-GlcNAc blockage. These bacteria do not use sulfatases but instead their genomes encode a GH20 that cleaves terminal 6S-GlcNAc (Figure 3) [27,28]. In *B. bifidum*, this 6-sulfo- $\beta$ -N-acetylglucosaminidase is expressed at the bacteria cell surface and it has been shown to be active on PGM [28]. However, the specificity of these GH20 enzymes against colonic mucins remains unclear. Overall, all the mucin active enzymes that cleave sulfation have evolved to recognize sulfate groups at the terminal positions suggesting that these enzymes act in the initial stages of mucin degradation by microbiota members.

## Sialidases

On O-glycans, terminal sialic acid residues are found  $\alpha$ 2,3/2,6-linked to Gal and GalNAc (Figure 2) [13]. Humans only have N-acetylneuraminic acid (Neu5Ac) while pigs also have N-glycolylneuraminic acid [17]. Colonic mucins are highly sialylated and the ability to cleave and/or utilize sialic acid has a key role in gut colonization. To cleave sialic acid most bacteria encode one or several GH33 sialidases (Figure 3) [29]. These enzymes can be classified either as trans-sialidases that cleave  $\alpha$ 2,3 linkages, or hydrolytic sialidases that cleave all sialic acid linkages. Trans-sialidases were identified on *Ruminococcus gnavus* where the activity of these enzymes converts Neu5Ac into 2,7-anhydro-Neu5Ac that is specifically metabolized by this bacterium [30,31]. This modification of the sialic acid confers an advantage within the gut environment where *R. gnavus* does not need to compete with other bacteria to utilize this O-glycan monosaccharide. Recently, it was shown that the deletion of the trans-sialidase impaired the *R. gnavus* growth on mucin and, *in vivo*, the mutant had a fitness defect when competing with the WT strain [31].

Interestingly, in monocolonized mice the mutant strain lost the ability to colonize the colonic mucus layer closer to the intestinal epithelium indicating that the trans-sialidase is required to colonize the niches within the mucus barrier [31]. The bacteria relying on hydrolytic sialidases that utilize sialic acid have all the required enzymes for Neu5Ac metabolism grouped together into Nan clusters [29]. For bacteria with incomplete Nan clusters, Neu5Ac can be used in interspecies crosstalk. For example, *B. thetaiotaomicron* can release Neu5Ac from mucin glycans, but lacks the enzymes for its further metabolism, thereby leaving the Neu5Ac residues to be consumed by other bacteria in the environment such as *Salmonella typhimurium* and *Clostridium difficile* who lack sialidase-activity [32]. More recently, founding member of the GH156 family displayed activity against  $\alpha$ 2,3/2,6-Neu5Ac on short oligosaccharides [33]. This new enzyme was initially isolated from hot spring metagenomes but the taxonomic display shows that the genome of gut microbiota members, such as, *Parabacteroides merdae* and *Parabacteroides johnsonii*, also encode GH156 enzymes [18]. Although the characterized enzyme failed to show activity in glycans presented on the surface of cancer cells, the activity of these enzymes was not yet addressed on complex O-glycans [34].

## Fucosidases

On mucin O-glycans, fucose can be  $\alpha$ 1,2-linked to Gal or  $\alpha$ 1,3/1,4-linked to GlcNAc which determines the different H type or Lewis antigen epitopes (Figure 2) [11]. To cleave fucose the gut bacteria rely on fucosidases from families GH29 and GH95 (Figure 3). While the GH95 are known to be  $\alpha$ 1,2-fucosidases, members of GH29 family can act on all fucose linkages found in mucins [18]. The GH29 enzymes can be divided into two subfamilies (A or B) according to their specificity. GH29-A have a broad specificity and act on *p*-nitrophenyl(*p*NP)- $\alpha$ -fucoside, while GH29-B specifically cleave  $\alpha$ 1,3/1,4-fucose [35]. In presence of mucin, bacteria up-regulate the expression of multiple fucosidases indicating that the removal of fucose is critical to growth and/or to access other sugars in O-glycans [3,6,36]. Additionally, fucose released by gut commensals, like *B. thetaiotaomicron*, can also be scavenged by pathogens, such as enterohaemorrhagic *Escherichia coli*, leading to the increased expression of virulence factors and gut colonization [37]. Despite the importance of fucosidases, the characterization of the substrate specificity of these enzymes remains limited to few members and such activities have only been shown against synthetic oligosaccharides and not complex O-glycans. *B. thetaiotaomicron* encodes nine GH29 and four GH95 genes that can be associated in mucin degradation. So far, only 4 of the GH29s enzymes have been characterized. BT2970 and BT4136 are active on *p*NP- $\alpha$ -fucoside [35,38]. BT1625 and BT2192 are 1,3/1,4-fucosidases. BT2192 specifically acts on trisaccharide substrates (Lewis<sup>a</sup> and Lewis<sup>x</sup>) while BT1625 is active against all Lewis antigens [35,39]. For *B. fragilis* only four GH29s out of the 12 predicted fucosidases have been previously characterized [40]. BF0810 was only active on *p*NP- $\alpha$ -fucoside while BF0028 also showed weak activity against  $\alpha$ 1,2 and  $\alpha$ 1,3 linkages. BF3242 and BF3591 were able to cleave  $\alpha$ 1,2/1,3/1,4-fucose. However, BF3591 displays a preference to  $\alpha$ 1,3-Fuc found in Lewis<sup>x/y</sup>, common epitopes found in mucins [40]. Recently a study aiming the characterization of fucosidase activity in different *Ruminococcus gnavus* strains showed that two GH29s encoded by the E1 and ATCC 29149 strains preferably cleave  $\alpha$ 1,3/1,4-Fuc and  $\alpha$ 1,2-Fuc, respectively. Interestingly, only one enzyme from E1 strain (E1\_10125) was able to accommodate terminal sialic acid modifications, a common feature in O-glycans [36].

An alternative mechanism to remove fucose can be cleaving the terminal oligosaccharides containing this substitution. Recently, a member of GH136, a family populated with lacto-*N*-biosidases, was shown to specifically release Lewis<sup>a</sup> and Lewis<sup>x</sup> from human milk oligosaccharides, a substrate that is similar to O-glycans [41]. This enzyme identified in *Roseburia inulinivorans* evolved to recognize Fuc- $\alpha$ 1,4-GlcNAc at the subsite-1 (Figure 3). Interestingly, it was shown that this bacterium also encodes a GH29 specific towards  $\alpha$ 1,4-fucose [41]. Although these enzymes were not shown to be active on mucin O-glycans it would be interesting to determine if mucin degrading bacteria encode GH136 or/and  $\alpha$ 1,4-specific GH29s that are able to cleave terminal fucosylated oligosaccharides.

## Enzymes cleaving A/B blood groups and other additional capping structures

To access mucins gut bacteria have also evolved to encode enzymes that remove blood groups. To remove blood group A and B bacteria can deploy  $\alpha$ -*N*-acetylgalactosaminidases (GH109) and  $\alpha$ -galactosidases (GH110), respectively (Figure 3) [42]. Very few members of these families have been characterized so far. In GH110 it has been shown that *B. thetaiotaomicron* and *B. fragilis* encode enzymes that specifically recognize the trisaccharide B group [Gal- $\alpha$ 1,3(Fuc $\alpha$ 1,2)-Gal] and enzymes that are active on both linear and branched Gal- $\alpha$ 1,3-Gal oligosaccharides [43]. Recently a GH109 enzyme of *A. muciniphila* was shown to display both  $\alpha$ -retaining and  $\beta$ -inverting mechanisms releasing the same product ( $\alpha$ -GalNAc) from  $\alpha$ -GalNAc and  $\beta$ -GalNAc substrates, respectively [44]. This

dual mechanism can allow the bacterium to access different glycans such as mucins or glycolipids that cover epithelium cells. To remove A/B blood groups, bacteria can also encode endo- $\beta$ 1,4-galactosidases (GH98 enzymes) (Figure 3) [45]. Of relevance, a GH98 enzyme from *Ruminococcus gnavus* ATCC29149 was shown to release GalNAc- $\alpha$ 1,3(Fuc $\alpha$ 1,2-)Gal from PGM [46]. Interestingly, this enzyme enables *R. gnavus* E1 (a strain lacking GH98s) to grow on the released trisaccharide and also the underlying *O*-glycans exposed after enzyme treatment. It was suggested that in *Ruminococcus* species the GH98s can be critical to the utilization of mucin glycans [46]. Recently a study aiming to identify novel blood group cleaving enzymes encoded by the microbiota revealed an alternative mechanism to remove these epitopes. *Flavonifractor plautii* deploys two enzymes to specifically remove blood group A [47]. First, a metallo-GalNAc-deacetylase converts the terminal GalNAc to *N*-galactosamine (GalN) that acts as a substrate for a novel GH36  $\alpha$ -galactosaminidase (Figure 3) [47]. The sequential action of these enzymes allows the quick conversion of blood group A to group H demonstrating that the gut microbiota evolved different mechanisms to remove terminal epitopes found on mucins.

Additional terminal capping structures, such as  $\alpha$ 1,4-GlcNAc, can be found in gastric mucins [48]. Although this epitope is not found on colonic mucin, several gut bacteria encode  $\alpha$ -*N*-acetylglucosaminidases (GH89) that can remove this linkage from mucins passing through the gut lumen (Figure 3) [6,11]. At last, *O*-acetylation in sialic acid is a common modification on colonic mucins that blocks the access of bacterial sialidases [13]. To overcome this barrier, some microbiota members express sialate-*O*-acetylsterases (Figure 3). Although not much is known about these enzymes, EstA, an acetylsterase expressed by *B. thetaiotaomicron* and *B. fragilis*, enables *E. coli* to access sialic acid and grow on mucin [49]. Interestingly, EstA is a specific 9-*O*-acetylsterase that requires the spontaneous migration of the *O*-acetyl group from carbon 7 to 9 to be active [49]. Since *O*-acetylation is a common feature of human colonic mucins, further studies are required to characterize novel *O*-glycan specific *O*-acetylsterases and understand the role of such enzymes in gut colonization.

## CAZymes active on mucin *O*-glycans backbone and cores

Upon the cleavage of the terminal capping sugars bacteria can access the protected *O*-glycans backbone. The cleavage of these can happen through the sequential action of  $\beta$ -galactosidases and  $\beta$ -*N*-acetylglucosaminidases that cleave  $\beta$ -Gal and  $\beta$ -GlcNAc. Several bacteria known as able to grow on *O*-glycans express several enzymes with such specificities; however, almost none of these enzymes have ever been tested on colonic mucins. Internal Gal is  $\beta$ 1,4-linked to GlcNAc whereas terminal Gal can be linked  $\beta$ 1,3 or  $\beta$ 1,4 generating type 1 or type 2 epitopes, respectively. Additionally, core 1 and 2 also contain Gal- $\beta$ 1,3-GalNAc. (Figure 2) [11]. These linkages can be cleaved by  $\beta$ -galactosidases from families GH2, GH35 and GH42 (Figure 3) [18]. *A. muciniphila* genome encodes 6 GH2 enzymes. Only 3 of these proteins were characterized showing that this bacterium has evolved to target all the different linkages found in mucin [50]. Amuc.0771, Amuc.1666 and Amuc.0924 specifically cleave Gal- $\beta$ 1,3-GlcNAc, Gal- $\beta$ 1,4-GlcNAc and Gal- $\beta$ 1,3-GalNAc, respectively. Only Amuc.0771 and Amuc.0924 display activity on PGM which is consistent with the high abundance of type 1 linkages on this substrate [50]. A GH35 from *A. muciniphila* was also shown to be active on core 1 and core 2 structures. However, the activity of mucins was never shown for this enzyme [51]. After Gal has been cleaved, the  $\beta$ -*N*-acetylglucosaminidases (GH20 and GH84) will then cleave the exposed GlcNAc (Figure 3). These enzymes have been mostly characterized on short glycans or against *p*NP substrates [52–55]. Additionally, families GH101 and GH129 are populated with enzymes that share structural similarities and target mucin cores with different specificities (Figure 3) [56]. GH129 enzymes are highly abundant in *Bifidobacterium* and specifically cleave Tn antigen (GalNAc- $\alpha$ 1-Ser) but can also act on core 1 (Gal- $\beta$ 1,3-GalNAc- $\alpha$ 1-Ser) [57]. The family GH101 is encoded in genomes of Actinobacteria and several Firmicutes and these endo-enzymes specifically target core 1 [58].

Endo-active enzymes that cleave within *O*-glycans offer an additional mechanism to access these sugars without the need to remove capping groups. Such endo-acting *O*-glycanases were recently identified in GH16 family (Figure 3) [59]. Interestingly, these endo- $\beta$ 1,4-galactosidases require the removal of sialic acid prior to the activity [59]. Since these enzymes are encoded by commensals such as *B. thetaiotaomicron*, *B. fragilis* and *A. muciniphila*, the blockage of this enzymatic activity by sialic acid can represent an adaptation to limit the access of these bacteria to mucin glycans within the colonic mucus layer.

### Summary

- Some gut microbiota members are able to break down and utilize complex mucin *O*-glycans that are found in the colonic mucus layer.

- Gut bacteria express specific enzymes to target all the different linkages found on O-glycans. However, most of the enzymes lack a characterization on complex colonic mucin O-glycans.
- Enzymes cleaving terminal epitopes, such as sulfatases and sialidases, have a key role in bacterial gut colonization.
- Understanding the mechanisms of mucin O-glycans degradation and utilization by microbiota members can reveal key enzymes that are potential drug targets in diseases associated with the increase of bacterial foraging on mucins and the disruption of the protective colonic mucus layers, such as IBD, obesity and colorectal cancer.

## Competing Interests

The authors declare that there are no competing interests associated with the manuscript.

## Funding

A.S.L is supported by grants from the Swedish Research Council [grant number VR 2021-01409]; the Swedish Society for Medical Research (Svenska Sällskapet för Medicinsk Forskning, grant number S21-0026); Sahlgrenska Academy International Starting Grant [grant number 2021/1070]; Wilhelm och Martina Lundgrens Vetenskapsfond [grant number 2022-4021]; G.R. is supported by European Regional Development Fund Education and Youth Board [grant number 5.10-6.1/20/20-2]; Archimedes Foundation [grant number 16-3.5/2011]; and Ministry of Education and Research base funding for Tallinn University of Technology.

## Open Access

Open access for this article was enabled by the participation of University of Gothenburg in an all-inclusive *Read & Publish* agreement with Portland Press and the Biochemical Society.

## Author Contribution

G.R. and A.S.L. wrote the manuscript. A.S.L. prepared the figures.

## Abbreviations

CAZyme, carbohydrate-active enzyme; CE, carbohydrate esterase; Fuc, fucose; Gal, galactose; GalNAc, *N*-acetylgalactosamine; GH, glycoside hydrolase; GI, gastrointestinal; GlcNAc, *N*-acetylglucosamine; IBD, inflammatory bowel disease; Muc2, Mucin2; Neu5Ac, *N*-acetylneuraminic acid; PGM, porcine gastric mucin; *p*NP, *p*-nitrophenyl; PTS, proline-threonine-serine.

## References

- 1 Hansson, G.C. (2020) Mucins and the microbiome. *Annu. Rev. Biochem.* **89**, 769–793, <https://doi.org/10.1146/annurev-biochem-011520-105053>
- 2 Johansson, M.E., Phillipson, M., Petersson, J., Velcich, A., Holm, L. and Hansson, G.C. (2008) The inner of the two Muc2 mucin-dependent mucus layers in colon is devoid of bacteria. *Proc. Natl. Acad. Sci. U.S.A.* **105**, 15064–15069, <https://doi.org/10.1073/pnas.0803124105>
- 3 Martens, E.C., Chiang, H.C. and Gordon, J.I. (2008) Mucosal glycan foraging enhances fitness and transmission of a saccharolytic human gut bacterial symbiont. *Cell Host Microbe*. **4**, 447–457, <https://doi.org/10.1016/j.chom.2008.09.007>
- 4 Sommer, F., Adam, N., Johansson, M.E., Xia, L., Hansson, G.C. and Backhed, F. (2014) Altered mucus glycosylation in core 1 O-glycan-deficient mice affects microbiota composition and intestinal architecture. *PLoS ONE* **9**, e85254, <https://doi.org/10.1371/journal.pone.0085254>
- 5 Johansson, M.E., Gustafsson, J.K., Holmen-Larsson, J., Jabbar, K.S., Xia, L., Xu, H. et al. (2014) Bacteria penetrate the normally impenetrable inner colon mucus layer in both murine colitis models and patients with ulcerative colitis. *Gut* **63**, 281–291, <https://doi.org/10.1136/gutjnl-2012-303207>
- 6 Desai, M.S., Seekatz, A.M., Koropatkin, N.M., Kamada, N., Hickey, C.A., Wolter, M. et al. (2016) A dietary fiber-deprived gut microbiota degrades the colonic mucus barrier and enhances pathogen susceptibility. *Cell* **167**, 1339e1321–1353e1321, <https://doi.org/10.1016/j.cell.2016.10.043>
- 7 Schroeder, B.O., Birchenough, G.M.H., Stahlman, M., Arike, L., Johansson, M.E.V., Hansson, G.C. et al. (2018) Bifidobacteria or Fiber Protects against Diet-Induced Microbiota-Mediated Colonic Mucus Deterioration. *Cell Host Microbe* **23**, 27e27–40e27, <https://doi.org/10.1016/j.chom.2017.11.004>
- 8 Everard, A., Belzer, C., Geurts, L., Ouwerkerk, J.P., Druart, C., Bindels, L.B. et al. (2013) Cross-talk between *Akkermansia muciniphila* and intestinal epithelium controls diet-induced obesity. *Proc. Natl. Acad. Sci. U.S.A.* **110**, 9066–9071, <https://doi.org/10.1073/pnas.1219451110>
- 9 Png, C.W., Linden, S.K., Gilshenan, K.S., Zoetendal, E.G., McSweeney, C.S., Sly, L.I. et al. (2010) Mucolytic bacteria with increased prevalence in IBD mucosa augment in vitro utilization of mucin by other bacteria. *Am. J. Gastroenterol.* **105**, 2420–2428, <https://doi.org/10.1038/ajg.2010.281>
- 10 Layunta, E., Javerfelt, S., Dolan, B., Arike, L. and Pelaseyed, T. (2021) IL-22 promotes the formation of a MUC17 glycocalyx barrier in the postnatal small intestine during weaning. *Cell Rep.* **34**, 108757, <https://doi.org/10.1016/j.celrep.2021.108757>

- 11 Tailford, L.E., Crost, E.H., Kavanaugh, D. and Juge, N. (2015) Mucin glycan foraging in the human gut microbiome. *Front. Genet.* **6**, 81, <https://doi.org/10.3389/fgene.2015.00081>
- 12 Robbe, C., Capon, C., Coddeville, B. and Michalski, J.C. (2004) Structural diversity and specific distribution of O-glycans in normal human mucins along the intestinal tract. *Biochem. J.* **384**, 307–316, <https://doi.org/10.1042/BJ20040605>
- 13 Robbe, C., Capon, C., Maes, E., Rousset, M., Zweibaum, A., Zanetta, J.P. et al. (2003) Evidence of regio-specific glycosylation in human intestinal mucins: presence of an acidic gradient along the intestinal tract. *J. Biol. Chem.* **278**, 46337–46348, <https://doi.org/10.1074/jbc.M302529200>
- 14 Larsson, J.M., Karlsson, H., Sjövall, H. and Hansson, G.C. (2009) A complex, but uniform O-glycosylation of the human MUC2 mucin from colonic biopsies analyzed by nanoLC/MSn. *Glycobiology* **19**, 756–766, <https://doi.org/10.1093/glycob/cwp048>
- 15 Thomsson, K.A., Bäckström, M., Holmén Larsson, J.M., Hansson, G.C. and Karlsson, H. (2010) Enhanced detection of sialylated and sulfated glycans with negative ion mode nanoliquid chromatography/mass spectrometry at high pH. *Anal. Chem.* **82**, 1470–1477, <https://doi.org/10.1021/ac902602e>
- 16 Holmen Larsson, J.M., Thomsson, K.A., Rodriguez-Pineiro, A.M., Karlsson, H. and Hansson, G.C. (2013) Studies of mucus in mouse stomach, small intestine, and colon. III. Gastrointestinal Muc5ac and Muc2 mucin O-glycan patterns reveal a regiospecific distribution. *Am. J. Physiol. Gastrointest. Liver Physiol.* **305**, G357–G363, <https://doi.org/10.1152/ajpgi.00048.2013>
- 17 Luis, A.S., Jin, C., Pereira, G.V., Glowacki, R.W.P., Gugel, S.R., Singh, S. et al. (2021) A single sulfatase is required to access colonic mucin by a gut bacterium. *Nature* **598**, 332–337, <https://doi.org/10.1038/s41586-021-03967-5>
- 18 Drula, E., Garron, M.L., Dogan, S., Lombard, V., Henrissat, B. and Terrapon, N. (2022) The carbohydrate-active enzyme database: functions and literature. *Nucleic Acids Res.* **50**, D571–D577, <https://doi.org/10.1093/nar/gkab1045>
- 19 Barbeyron, T., Brillet-Gueguen, L., Carre, W., Carriere, C., Caron, C., Czjzek, M. et al. (2016) Matching the diversity of sulfated biomolecules: creation of a classification database for sulfatases reflecting their substrate specificity. *PLoS ONE* **11**, e0164846, <https://doi.org/10.1371/journal.pone.0164846>
- 20 Wardman, J.F., Bains, R.K., Rahfeld, P. and Withers, S.G. (2022) Carbohydrate-active enzymes (CAZymes) in the gut microbiome. *Nat. Rev. Microbiol.* **20**, 542–556, <https://doi.org/10.1038/s41579-022-00712-1>
- 21 Thomsson, K.A., Karlsson, H. and Hansson, G.C. (2000) Sequencing of sulfated oligosaccharides from mucins by liquid chromatography and electrospray ionization tandem mass spectrometry. *Anal. Chem.* **72**, 4543–4549, <https://doi.org/10.1021/ac000631b>
- 22 Everest-Dass, A.V., Jin, D., Thaysen-Andersen, M., Nevalainen, H., Kolarich, D. and Packer, N.H. (2012) Comparative structural analysis of the glycosylation of salivary and buccal cell proteins: innate protection against infection by *Candida albicans*. *Glycobiology* **22**, 1465–1479, <https://doi.org/10.1093/glycob/cws112>
- 23 Larsson, J.M., Karlsson, H., Crespo, J.G., Johansson, M.E., Eklund, L., Sjövall, H. et al. (2011) Altered O-glycosylation profile of MUC2 mucin occurs in active ulcerative colitis and is associated with increased inflammation. *Inflamm. Bowel Dis.* **17**, 2299–2307, <https://doi.org/10.1002/ibd.21625>
- 24 Hickey, C.A., Kuhn, K.A., Donermeyer, D.L., Porter, N.T., Jin, C., Cameron, E.A. et al. (2015) Colitogenic bacteroides thetaiotaomicron antigens access host immune cells in a sulfatase-dependent manner via outer membrane vesicles. *Cell Host Microbe*. **17**, 672–680, <https://doi.org/10.1016/j.chom.2015.04.002>
- 25 Luis, A.S., Basle, A., Byrne, D.P., Wright, G.S.A., London, J.A., Jin, C. et al. (2022) Sulfated glycan recognition by carbohydrate sulfatases of the human gut microbiota. *Nat. Chem. Biol.* **18**, 841–849, <https://doi.org/10.1038/s41589-022-01039-x>
- 26 Donaldson, G.P., Chou, W.C., Manson, A.L., Rogov, P., Abeel, T., Bochicchio, J. et al. (2020) Spatially distinct physiology of *Bacteroides fragilis* within the proximal colon of gnotobiotic mice. *Nat. Microbiol.* **5**, 746–756, <https://doi.org/10.1038/s41564-020-0683-3>
- 27 Rho, J.H., Wright, D.P., Christie, D.L., Clinch, K., Furneaux, R.H. and Robertson, A.M. (2005) A novel mechanism for desulfation of mucin: identification and cloning of a mucin-desulfating glycosidase (sulfoglycosidase) from *Prevotella* strain RS2. *J. Bacteriol.* **187**, 1543–1551, <https://doi.org/10.1128/JB.187.5.1543-1551.2005>
- 28 Katoh, T., Maeshibu, T., Kikkawa, K.I., Gotoh, A., Tomabechi, Y., Nakamura, M. et al. (2017) Identification and characterization of a sulfoglycosidase from *Bifidobacterium bifidum* implicated in mucin glycan utilization. *Biosci. Biotechnol. Biochem.* **81**, 2018–2027, <https://doi.org/10.1080/09168451.2017.1361810>
- 29 Juge, N., Tailford, L. and Owen, C.D. (2016) Sialidases from gut bacteria: a mini-review. *Biochem. Soc. Trans.* **44**, 166–175, <https://doi.org/10.1042/BST20150226>
- 30 Tailford, L.E., Owen, C.D., Walshaw, J., Crost, E.H., Hardy-Goddard, J., Le Gall, G. et al. (2015) Discovery of intramolecular trans-sialidases in human gut microbiota suggests novel mechanisms of mucosal adaptation. *Nat. Commun.* **6**, 7624, <https://doi.org/10.1038/ncomms8624>
- 31 Bell, A., Brunt, J., Crost, E., Vaux, L., Nepravishta, R., Owen, C.D. et al. (2019) Elucidation of a sialic acid metabolism pathway in mucus-foraging *Ruminococcus gnavus* unravels mechanisms of bacterial adaptation to the gut. *Nat. Microbiol.* **4**, 2393–2404, <https://doi.org/10.1038/s41564-019-0590-7>
- 32 Ng, K.M., Ferreyra, J.A., Higginbottom, S.K., Lynch, J.B., Kashyap, P.C., Gopinath, S. et al. (2013) Microbiota-liberated host sugars facilitate post-antibiotic expansion of enteric pathogens. *Nature* **502**, 96–99, <https://doi.org/10.1038/nature12503>
- 33 Chuzel, L., Ganatra, M.B., Rapp, E., Henrissat, B. and Taron, C.H. (2018) Functional metagenomics identifies an exosialidase with an inverting catalytic mechanism that defines a new glycoside hydrolase family (GH156). *J. Biol. Chem.* **293**, 18138–18150, <https://doi.org/10.1074/jbc.RA118.003302>
- 34 Bule, P., Chuzel, L., Blagova, E., Wu, L., Gray, M.A., Henrissat, B. et al. (2019) Inverting family GH156 sialidases define an unusual catalytic motif for glycosidase action. *Nat. Commun.* **10**, 4816, <https://doi.org/10.1038/s41467-019-12684-7>
- 35 Sakurama, H., Tsutsumi, E., Ashida, H., Katayama, T., Yamamoto, K. and Kumagai, H. (2012) Differences in the substrate specificities and active-site structures of two alpha-L-fucosidases (glycoside hydrolase family 29) from *Bacteroides thetaiotaomicron*. *Biosci. Biotechnol. Biochem.* **76**, 1022–1024, <https://doi.org/10.1271/bbb.111004>
- 36 Wu, H., Rebello, O., Crost, E.H., Owen, C.D., Walpole, S., Bennati-Granier, C. et al. (2020) Fucosidases from the human gut symbiont *Ruminococcus gnavus*. *Cell. Mol. Life Sci.* **78**, 675–693, <https://doi.org/10.1007/s00018-020-03514-x>

- 37 Pacheco, A.R., Curtis, M.M., Ritchie, J.M., Munera, D., Waldor, M.K., Moreira, C.G. et al. (2012) Fucose sensing regulates bacterial intestinal colonization. *Nature* **492**, 113–117, <https://doi.org/10.1038/nature11623>
- 38 Shaikh, F.A., Lammerts van Bueren, A., Davies, G.J. and Withers, S.G. (2013) Identifying the catalytic acid/base in GH29 alpha-L-fucosidase subfamilies. *Biochemistry* **52**, 5857–5864, <https://doi.org/10.1021/bi400183q>
- 39 Briiliute, J., Urbanowicz, P.A., Luis, A.S., Basle, A., Paterson, N., Rebello, O. et al. (2019) Complex N-glycan breakdown by gut *Bacteroides* involves an extensive enzymatic apparatus encoded by multiple co-regulated genetic loci. *Nat. Microbiol.* **4**, 1571–1581, <https://doi.org/10.1038/s41564-019-0466-x>
- 40 Liu, P., Zhang, H., Wang, Y., Chen, X., Jin, L., Xu, L. et al. (2020) Screening and characterization of an  $\alpha$ -L-fucosidase from *Bacteroides fragilis* NCTC9343 for synthesis of fucosyl-N-acetylglucosamine disaccharides. *Appl. Microbiol. Biotechnol.* **104**, 7827–7840, <https://doi.org/10.1007/s00253-020-10759-w>
- 41 Pichler, M.J., Yamada, C., Shuoker, B., Alvarez-Silva, C., Gotoh, A., Leth, M.L. et al. (2020) Butyrate producing colonic Clostridiales metabolise human milk oligosaccharides and cross feed on mucin via conserved pathways. *Nat. Commun.* **11**, 3285, <https://doi.org/10.1038/s41467-020-17075-x>
- 42 Rahfeld, P. and Withers, S.G. (2019) Towards universal donor blood: enzymatic conversion of A and B to O type. *J. Biol. Chem.* **295**, 325–334, <https://doi.org/10.1074/jbc.REV119.008164>
- 43 Liu, Q.P., Yuan, H., Bennett, E.P., Levery, S.B., Nudelman, E., Spence, J. et al. (2008) Identification of a GH110 subfamily of alpha 1,3-galactosidases: novel enzymes for removal of the alpha 3Gal xenotransplantation antigen. *J. Biol. Chem.* **283**, 8545–8554, <https://doi.org/10.1074/jbc.M709020200>
- 44 Teze, D., Shuoker, B., Chaberski, E.K., Kunstmann, S., Fredslund, F., Nielsen, T.S. et al. (2020) The catalytic acid–base in GH109 resides in a conserved GGHHG loop and allows for comparable  $\alpha$ -retaining and  $\beta$ -inverting activity in an N-acetylgalactosaminidase from *Akkermansia muciniphila*. *ACS Catalysis* **10**, 3809–3819, <https://doi.org/10.1021/acscatal.9b04474>
- 45 Anderson, K.M., Ashida, H., Maskos, K., Dell, A., Li, S.C. and Li, Y.T. (2005) A clostridial endo-beta-galactosidase that cleaves both blood group A and B glycotopes: the first member of a new glycoside hydrolase family, GH98. *J. Biol. Chem.* **280**, 7720–7728, <https://doi.org/10.1074/jbc.M414099200>
- 46 Wu, H., Crost, E.H., Owen, C.D., van Bakel, W., Martinez Gascuena, A., Latoussakis, D. et al. (2021) The human gut symbiont *Ruminococcus gnavus* shows specificity to blood group A antigen during mucin glycan foraging: Implication for niche colonisation in the gastrointestinal tract. *PLoS Biol.* **19**, e3001498, <https://doi.org/10.1371/journal.pbio.3001498>
- 47 Rahfeld, P., Sim, L., Moon, H., Constantinescu, I., Morgan-Lang, C., Hallam, S. et al. (2019) An enzymatic pathway in the human gut microbiome that converts A to universal O type blood. *Nat. Microbiol.* **4**, 1475–1485, <https://doi.org/10.1038/s41564-019-0469-7>
- 48 Karlsson, N.G., Nordman, H., Karlsson, H., Carlstedt, I. and Hansson, G.C. (1997) Glycosylation differences between pig gastric mucin populations: a comparative study of the neutral oligosaccharides using mass spectrometry. *Biochem. J.* **326**, 911–917, <https://doi.org/10.1042/bj3260911>
- 49 Robinson, L.S., Lewis, W.G. and Lewis, A.L. (2017) The sialate O-acetyltransferase EstA from gut *Bacteroidetes* species enables sialidase-mediated cross-species foraging of 9-O-acetylated sialoglycans. *J. Biol. Chem.* **292**, 11861–11872, <https://doi.org/10.1074/jbc.M116.769232>
- 50 Kosciow, K. and Deppenmeier, U. (2020) Characterization of three novel beta-galactosidases from *Akkermansia muciniphila* involved in mucin degradation. *Int. J. Biol. Macromol.* **149**, 331–340, <https://doi.org/10.1016/j.ijbiomac.2020.01.246>
- 51 Guo, B.S., Zheng, F., Crouch, L., Cai, Z.P., Wang, M., Bolam, D.N. et al. (2018) Cloning, purification and biochemical characterisation of a GH35 beta-1,3/beta-1,6-galactosidase from the mucin-degrading gut bacterium *Akkermansia muciniphila*. *Glycoconj. J.* **35**, 255–263, <https://doi.org/10.1007/s10719-018-9824-9>
- 52 Robb, M., Robb, C.S., Higgins, M.A., Hobbs, J.K., Paton, J.C. and Boraston, A.B. (2015) A Second beta-Hexosaminidase Encoded in the *Streptococcus pneumoniae* Genome Provides an Expanded Biochemical Ability to Degrade Host Glycans. *J. Biol. Chem.* **290**, 30888–30900, <https://doi.org/10.1074/jbc.M115.688630>
- 53 Xu, W., Yang, W., Wang, Y., Wang, M. and Zhang, M. (2020) Structural and biochemical analyses of beta-N-acetylhexosaminidase Am0868 from *Akkermansia muciniphila* involved in mucin degradation. *Biochem. Biophys. Res. Commun.* **529**, 876–881, <https://doi.org/10.1016/j.bbrc.2020.06.116>
- 54 Chen, X., Wang, J., Liu, M., Yang, W., Wang, Y., Tang, R. et al. (2019) Crystallographic evidence for substrate-assisted catalysis of beta-N-acetylhexosaminidase from *Akkermansia muciniphila*. *Biochem. Biophys. Res. Commun.* **511**, 833–839, <https://doi.org/10.1016/j.bbrc.2019.02.074>
- 55 Chen, X., Li, M., Wang, Y., Tang, R. and Zhang, M. (2019) Biochemical characteristics and crystallographic evidence for substrate-assisted catalysis of a beta-N-acetylhexosaminidase in *Akkermansia muciniphila*. *Biochem. Biophys. Res. Commun.* **517**, 29–35, <https://doi.org/10.1016/j.bbrc.2019.06.150>
- 56 Sato, M., Liebschner, D., Yamada, Y., Matsugaki, N., Arakawa, T., Wills, S.S. et al. (2017) The first crystal structure of a family 129 glycoside hydrolase from a probiotic bacterium reveals critical residues and metal cofactors. *J. Biol. Chem.* **292**, 12126–12138, <https://doi.org/10.1074/jbc.M117.777391>
- 57 Kiyohara, M., Nakatomi, T., Kurihara, S., Fushinobu, S., Suzuki, H., Tanaka, T. et al. (2012) Ashida, alpha-N-acetylglactosaminidase from infant-associated bifidobacteria belonging to novel glycoside hydrolase family 129 is implicated in alternative mucin degradation pathway. *J. Biol. Chem.* **287**, 693–700, <https://doi.org/10.1074/jbc.M111.277384>
- 58 Koutsoulis, D., Landry, D. and Guthrie, E.P. (2008) Novel endo-alpha-N-acetylglactosaminidases with broader substrate specificity. *Glycobiology* **18**, 799–805, <https://doi.org/10.1093/glycob/cwn069>
- 59 Crouch, L.L., Liberato, M.V., Urbanowicz, P.A., Basle, A., Lamb, C.A., Stewart, C.J. et al. (2020) Prominent members of the human gut microbiota express endo-acting O-glycanases to initiate mucin breakdown. *Nat. Commun.* **11**, 4017, <https://doi.org/10.1038/s41467-020-17847-5>
- 60 Neelamegham, S., Aoki-Kinoshita, K., Bolton, E., Frank, M., Lisacek, F., Lutteke, T. et al. (2019) Updates to the Symbol Nomenclature for Glycans guidelines. *Glycobiology* **29**, 620–624, <https://doi.org/10.1093/glycob/cwz045>





## Appendix 4

### **Manuscript**

**Raba, G.**, Luis, A. S., Schneider, H., Morell, I., Jin, C., Adamberg, S., Hansson, G. C., Adamberg, K., Arike, L. Metabolic pathways of human microbiota co-utilization of fibres and colonic mucins. (In preparation).



1 **METABOLIC PATHWAYS OF HUMAN MICROBIOTA CO-UTILIZATION OF FIBRES**  
2 **AND COLONIC MUCINS**

3 Grete Raba<sup>1</sup>, Ana S. Luis<sup>2</sup>, Hannah Schneider<sup>2</sup>, Indrek Morell<sup>3</sup>, Chunsheng Jin<sup>2</sup>,  
4 Signe Adamberg<sup>1</sup>, Gunnar C. Hansson<sup>2</sup>, Kaarel Adamberg<sup>1,3\*</sup>, Liisa Arike<sup>2\*</sup>

5 <sup>1</sup> Department of Chemistry and Biotechnology, Tallinn University of Technology, Tallinn, Estonia

6 <sup>2</sup> Department of Medical Biochemistry and Cell Biology, University of Gothenburg, Gothenburg,  
7 Sweden

8 <sup>3</sup> Center of Food and Fermentation Technologies, Tallinn, Estonia

9 \* e-mail: kaarel.adamberg@taltech.ee, liisa.arike@gu.se

10  
11 **ABSTRACT**

12 The human gut microbiota is crucial for degrading dietary fibres from the diet. However, some of  
13 these bacteria can also degrade host glycans, such as mucins, the main component of the protective  
14 gut mucus layer. Specific microbiota species and mucin degradation patterns are associated with  
15 inflammatory processes in the colon. Yet, it remains unclear how the utilization of mucin glycans  
16 affects the degradation of dietary fibres by the human microbiota. Here, we used 14 dietary fibres  
17 and oligosaccharides to study in vitro the dynamics of mucin and dietary fibre degradation by the  
18 human faecal microbiota. Three dietary fibres (apple pectin,  $\beta$ -glucan and xylan) showed clearly  
19 distinguishing modulatory effects on faecal microbiota composition. The utilization of mucin in  
20 cultures led to alterations in microbiota composition and metabolites. Co-metabolism of mucin and  
21 complex dietary fibres promoted formation of mixed acids and biogenic amines which have been  
22 shown to be beneficial to the host. Interestingly, the metaproteome analysis showed the central role  
23 of the *Bacteroides* in degradation of complex fibres while *Akkermansia muciniphila* was the main  
24 degrader of porcine colonic mucin but not gastric mucin. This work demonstrates the intricacy of  
25 complex glycan metabolism by the gut microbiota and how the utilization of host glycans leads to  
26 alterations in the metabolism of dietary fibres.

## 30 INTRODUCTION

31 The human gut microbiota has an immense impact on human health and disease. These bacteria are  
32 well adapted to survive in the gastrointestinal tract due to their ability to utilise a wide range of  
33 polysaccharides, especially dietary fibres and host glycans, as carbon source. The degradation of  
34 polysaccharides into monosaccharides by microbiota is catalysed by different carbohydrate-active  
35 enzymes (CAZymes) such as glycoside hydrolases (GH), polysaccharide lyases (PL), carbohydrate  
36 esterases (CE) and sulfatases. CAZymes are classified into families according to their sequence  
37 similarity<sup>1,2</sup>. The metabolism of the resulting monosaccharides by the bacteria provides the host  
38 with an amplitude of beneficial metabolites such as short-chain fatty acids and biogenic amines<sup>3-5</sup>.

39 The microbiota in the gut colonises the mucus layer that acts simultaneously as a protective barrier  
40 and an interaction site between the intestinal epithelium and the bacteria<sup>6</sup>. The major component  
41 of the colonic mucus layer is Mucin-2, a heavily *O*-glycosylated glycoprotein produced by goblet cells  
42 in the colonic crypts. The presence of gut microbes is required for normal epithelial development,  
43 mucin turnover and the development of an impenetrable mucus barrier<sup>7-9</sup>. However, some  
44 microbiota species can degrade and utilise mucins as carbon source. Indeed, imbalances in the  
45 microbiota composition and metabolism have been shown to promote the expansion of mucin-  
46 degrading bacteria and impaired mucus barrier function. It has been proposed that mucin  
47 degradation and/or the respective shifts in the microbiota metabolism have a crucial role in the  
48 development of diseases such as inflammatory bowel disease (IBD) and obesity<sup>10,11</sup>. Yet, it remains  
49 unclear how the gut microbiota metabolises mucins and how this process is affected by the presence  
50 of dietary fibres.

51 Previous studies have disclosed how microbiota members have evolved to degrade plant cell wall  
52 polysaccharides. However, the study of the mechanisms behind colonic mucin degradation and  
53 utilization has been significantly limited due to the lack of an available substrate. Recent studies  
54 have been focused on characterising specific enzymes from known species able to grow on porcine  
55 gastric mucin (PGM), such as *Akkermansia muciniphila*, *Bacteroides thetaiotaomicron*, *Bacteroides*  
56 *fragilis* and *Bacteroides caccae*<sup>12-15</sup>. However, the human gut microbiota is a complex consortium of  
57 hundreds of interacting species. It is likely that within the microbiota dynamic environment some  
58 bacteria will rely on specific systems evolved for selfish utilization of glycans, whereas other  
59 members of the microbiota will share oligosaccharides and metabolites, allowing the growth of  
60 additional bacteria unable to access the complex glycans. To address these dynamic interactions,  
61 human faecal microbiota has been used in in vitro studies of the co-metabolism of polysaccharides  
62 and porcine gastric mucin<sup>16-19</sup>. However, it should be emphasized that the glycosylation of mucins

63 varies along the gastrointestinal tract<sup>20,21</sup>. Recently, it was shown that some bacterial species able to  
64 grow on PGM do not grow on porcine colonic *O*-glycans<sup>15</sup>. Therefore, it is likely that differences in  
65 mucin *O*-glycosylation have a major impact on the microbiota community. As the fermentation of  
66 dietary fibres happens mainly in the colon, the use of colonic mucins as co-substrate is required to  
67 mimic the physiological conditions. To understand the impact of colonic mucin on the fermentation  
68 of complex dietary glycans, we cultivated human faecal microbiota on a panel of 14 dietary fibres  
69 and oligosaccharides. We studied the co-metabolism of diet- and host-derived glycans on a  
70 metaproteome level. Our data shows the specific modulatory effect of different glycans and how the  
71 presence of mucins alters dietary fibre metabolism.

72

73 **RESULTS**

74

75 *The substrate determines the microbiota composition of faecal consortium*

76 Faecal samples from seven healthy donors were pooled to generate a complex inoculum that  
77 overcomes interindividual differences in microbiota. We used isothermal microcalorimetry to  
78 cultivate the resulting microbial community on a panel of 14 dietary fibres and oligosaccharides  
79 (Supplementary Table S1) to study the ability of these bacteria to utilise different complex glycans.  
80 We supplemented the growth medium with porcine gastric mucin (PGM) to study the impact of host  
81 gastrointestinal glycans on dietary fibre fermentation. The community growth heat flows were  
82 recorded, where tall and narrow peaks indicate fast degradation of the substrate, while lower  
83 amounts of released heat suggest poor degradation. The bacterial growth correlated with the  
84 structure and complexity of the substrate (Fig. 1a, S1). Oligosaccharides and simple fibres, such as  
85 galactooligosaccharides, were rapidly fermented while complex and/or poorly soluble fibres, such as  
86  $\kappa$ -carrageenan, high-performance inulin,  $\beta$ -glucan, apple pectin and xylan led to a slower and  
87 multiphasic release of heat, suggesting cross-feeding between specific members of the microbiota  
88 (Fig. 1a, S1). The co-fermentation of fibres with PGM resulted in prolonged growth, suggesting that  
89 the presence of mucins leads to alterations in the community composition (Fig. 1a, S1).

90 **Figure 1** Fermentation of 14 dietary fibres and oligosaccharides by faecal microbiota using  
91 isothermal microcalorimetry. **a**, Heat evolution of substrate fermentation. Solid line represents  
92 average microbial growth curve on the selected poly- or oligosaccharide  $\pm$  95% CI, dotted line  
93 represents average microbial growth curve on the selected poly- or oligosaccharide + mucin  $\pm$  95%  
94 CI. n=2-7. **b**, Community composition on the selected substrates based on 16S rRNA sequencing.  
95 Average relative abundances of the top 17 genera. n=2-7. **c**, The number of different glycans  
96 identified from porcine gastric mucin (PGM) and porcine colonic mucin (PCM). **d**, Ordination plot of  
97 Bray-Curtis distances between microbial communities from cultivations on the selected substrates.  
98 Colours indicate the choice of dietary fibre, empty round dots represent samples from cultivation of  
99 fibre, filled round dots represent samples from cultivation of fibre+PCM or sole PCM. **e**, Boxplots  
100 showing changes in microbial numbers (mg/l) grown on the selected substrates. Colours indicate the  
101 choice of substrate, empty boxes represent samples from cultivation of fibre, filled boxes represent  
102 samples from cultivation of fibre+PCM or sole PCM. All replicates shown (two-tailed paired t-test, \*p  
103 < 0.05). GOS – galactooligosaccharides, Fur – furcellaran, InuHP – high-performance inulin, B-gluc –  
104  $\beta$ -glucan, PecA – apple pectin, Xyl – xylan, PGM – porcine gastric mucin, PCM – porcine colonic  
105 mucin, Med – growth medium control.

106 **Supplementary Figure 1** Heat evolution of substrate fermentation. Solid line represents average  
107 microbial growth curve on the selected poly- or oligosaccharide  $\pm$  95% CI, dotted line represents  
108 average microbial growth curve on the selected poly- or oligosaccharide + mucin  $\pm$  95% CI. n=2-7. AP  
109 – amylopectin, InuHSI – high-soluble inulin, XOS – xylooligosaccharides, Car –  $\kappa$ -carrageenan, InuD –

110 dahlia inulin, AG – arabinogalactan, PecC – citrus pectin, Psy – psyllium, PGM – porcine gastric  
111 mucin, PCM – porcine colonic mucin, Med – growth medium control.

112

113 Next, we used 16S rRNA sequencing to determine the microbial composition after growth on  
114 different substrates. The medium without any glycans promoted the growth of a simple community  
115 dominated by *Escherichia/Shigella* and *Eggerthella* species (>80% of the consortium) (Fig. 1b).  
116 Supplementing the medium with dietary or mucin-type glycans led to an increase in the diversity of  
117 the community, indicating that the metabolism of such sugars has a key role in the community  
118 development (Fig. S2a). None of the single-fibre fermentations reached the microbial complexity of  
119 the inoculum (Fig. S2b). However, the complex fibres supported the development of more diverse  
120 consortia compared to the fast-fermented glycans (Fig. S2a). Simple glycans and fructose polymers  
121 enhanced the abundances of *Bifidobacteria*, whereas the complex fibres promoted the abundances  
122 of *Bacteroides* (Fig. 1b, S2c). This is consistent with studies showing that *Bacteroides* are adapted to  
123 break down complex glycans<sup>22</sup>. Supplementing the cultures with PGM increased the overall  
124 microbial diversity when compared to the respective fibre only (Fig. S2a). Moreover, with the fibres  
125 on which we observed a limited growth ( $\kappa$ -carrageenan, furcellaran, psyllium) (Fig. 1a, S1), the  
126 addition of PGM led to a microbial composition similar to that of sole PGM, indicating that such  
127 alterations in diversity were due to the presence of mucin and not to the utilization of the insoluble  
128 polysaccharides (Fig. 1b, S2c). The presence of PGM promoted the growth of *Ruminococcus torques*  
129 and *Bacteroides*, two known mucin degraders<sup>23,24</sup>, and *Faecalibacterium* who has been shown to be  
130 in a syntrophic relationship with mucin degraders<sup>25</sup> (Fig. 1b). This indicates that in the absence of  
131 dietary fibres, host glycans promote the growth of a different microbial community well adapted to  
132 degrade this complex substrate.

133 **Supplementary Figure 2** Consortia composition assessed by 16S rRNA sequencing. **a**, Simpson alpha  
134 diversity indices for the panel of tested substrates. All replicates shown. **b**, The microbial  
135 composition of the inoculum. Pooled faecal samples from seven healthy donors. Average relative  
136 abundances of the top 21 genera. n=2 (separate aliquots of the pooled inoculum). **c**, Community  
137 composition on the selected substrates. Average relative abundances of the top 17 genera. n=2-7.  
138 Med – growth medium control, Inoc – inoculum control, AP – amylopectin, GOS –  
139 galactooligosaccharides, InuHSI – high-soluble inulin, XOS - xylooligosaccharides, Car –  $\kappa$ -  
140 carrageenan, Fur – furcellaran, InuD – dahlia inulin, InuHP – high-performance inulin, AG –  
141 arabinogalactan, B-gluc –  $\beta$ -glucan, PecA – apple pectin, PecC – citrus pectin, Psy – psyllium, Xyl –  
142 xylan, PGM – porcine gastric mucin, PCM – porcine colonic mucin.

143

144 To further understand how the metabolism of complex fibres and mucin affects the microbiota,  $\beta$ -  
145 glucan, apple pectin and xylan were selected for an in-depth study based on their distinctly different



146 molecular structures that require specific enzymes encoded in different bacteria for degradation  
147 (Fig. S3). A known prebiotic, high-performance inulin was included as an easily fermentable control.  
148 Additionally, as the dietary fibres are metabolised mainly in the colon, the co-cultures were  
149 performed, using porcine colonic mucin (PCM), instead of PGM. Gastric and colonic mucins are  
150 distinct, with MUC5AC and MUC2 being prevalent in the stomach and colon, respectively (Fig. S4a).  
151 Indeed, the glycome analysis of PGM and PCM showed that these mucins share only 9% of the *O*-  
152 glycans, with PGM being mainly fucosylated, while PCM was highly sulfated (Fig. 1c, S4b). Moreover,  
153 our analysis suggested PGM to be severely hydrolysed which is likely to lead to a faster fermentation  
154 of this substrate (Fig. S4c, S1). Together, these results indicate that PCM is a more physiologically  
155 relevant mucin source to address the impact of these host glycans on microbiota communities.

156 **Supplementary Figure 3** Schematic representation of the polysaccharides and different putative  
157 CAZyme families targeting the respective linkages for **a**,  $\beta$ -glucan. **b**, inulin. **c**, pectin. **d**, xylan. **e**,  
158 mucin *O*- and *N*-glycans. Monosaccharide symbols are shown according to the Symbol Nomenclature  
159 for Glycan system <sup>75</sup>. GH – glycoside hydrolase, PL – polysaccharide lyase, CE – carbohydrate  
160 esterase.

161 **Supplementary Figure 4** Analysis of porcine gastric mucin (PGM) and colonic mucin (PCM)  
162 composition. **a**, Gel-forming mucins detected in different mucin samples by mass-spectrometry.  
163 Most abundant uncharacterised proteins in each sample were annotated with BLAST as: MUC2 –  
164 UniProt A0A4X1UH57; MUC5AC – UniProt A0A4X1UGK3; MUC6 – UniProt A0A4X1VZC0. **b**, Different  
165 glycan modifications detected in PGM and PCM. **c**, Mucin samples separated on a composite gel.  
166 MUC2 – Mucin-2, MUC5AC – Mucin-5AC, MUC6 – Mucin-6, PCM – porcine colonic mucin, PGM –  
167 porcine gastric mucin.

168

169 As expected, the cultivations showed that both the fibre and the mucin affect the growth dynamics  
170 and the diversity of the microbial community (Fig. 1a, Fig. S2a). The addition of PCM increased the  
171 consortia homogeneity between replicates, but distinct separate clusters were still formed based on  
172 the dietary fibre (Fig. 1d). Compared to fibre+PGM, the fibre+PCM combinations increased the  
173 abundances of gut commensals *Bacteroides* and *Faecalibacterium* and decreased the abundances of  
174 an opportunistic pathogen *Solobacterium* and a pathobiont *Collinsella* (Fig. 1b). PCM also increased  
175 the abundances of some non-mucin degraders, such as *Ruminococcus bromii* and *Olsenella*  
176 *scatoligenes* (Fig. 1e, S5a). Interestingly, although *Akkermansia sp.* could not compete in the  
177 community grown on sole PGM or any of the fibre combinations with PGM, it dominated the  
178 consortium on sole PCM as well as being highly abundant on the combination of xylan+PCM (Fig. 1b,  
179 e). For some species, such as *Ruminococcus torques* and *Eisenbergiella tayi*, the abundance was  
180 driven by PCM in combination with complex fibres pectin and xylan (Fig. 1e). Inulin fermentation was  
181 characterised by high abundances of *Catenibacterium sp.*, and *Bifidobacteria* (Fig. 1b, Fig. S5b). B-

182 glucan specifically increased the abundances of *Collinsella*, *Streptococcus* and *Solobacterium* (Fig. 1b,  
183 Fig. 5c). The complex fibres pectin and xylan led to an overall expansion of *Bacteroides* (Fig. 1b).  
184 Pectin promoted the growth of *B. thetaiotaomicron* and *B. vulgatus*, species known to be able to  
185 degrade this complex polysaccharide<sup>26</sup>, while xylan notably promoted the growth of *B. vulgatus* and  
186 unclassified *Bacteroides* (including *B. acidifaciens*, *B. finegoldii*, *B. ovatus*, *B. xylanisolvens* and others  
187 which are inseparable with the used sequencing method) (Fig. 1e). In both cases the abundance of *B.*  
188 *vulgatus* was higher without colonic mucin. Interestingly, *Faecalibacterium prausnitzii* and  
189 *Parabacteroides merdae* were able to grow only if both the fibre and mucin were available (Fig. 1e,  
190 S5a). Together, these results suggest that the co-metabolism of dietary fibres and gastric or colonic  
191 mucins promote the growth of different microbiota communities.

192 **Supplementary Figure 5** Boxplots showing changes in microbial numbers (mg/l) grown on the  
193 selected substrates. Colours indicate the choice of substrate, empty boxes represent samples from  
194 cultivation of fibre, filled boxes represent samples from cultivation of fibre+PCM or sole PCM. All  
195 replicates shown (two-tailed paired t-test, \*p < 0.05). **a**, Taxa affected by mucin addition. **b**, The  
196 most abundant taxa growing on InuHP. **c**, The most abundant taxa growing on B-gluc. B-gluc –  $\beta$ -  
197 glucan, InuHP – high-performance inulin, PecA – apple pectin, Xyl – xylan, PCM – porcine colonic  
198 mucin.

199

#### 200 *Degradation mechanisms of different polysaccharides by human gut microbiota*

201 The putative community enzymes implicated in the degradation of the different glycans were  
202 determined by metaproteomics. More than 21 000 protein groups were identified, out of which ca  
203 3% were CAZymes and binding proteins, such as carbohydrate-binding modules involved in  
204 polysaccharide recognition, uptake and degradation, by the gut microbiota (Supplementary Table S2,  
205 S3). The degradation of inulin was associated with GHs from families 32 and 91, known to be  
206 populated only with fructose-active enzymes<sup>1</sup> (Fig. 2). These GHs were expressed by  
207 *Bifidobacterium*, *Catenibacterium* and *Bacteroides* species, consistent with the high abundance of  
208 these bacteria by 16S rRNA sequencing (Fig. 2, 1b, 1e, S5b). B-glucan degradation relied on enzymes  
209 from families GH1, GH3 and GH94 that cleave  $\beta$ -glucose linkages (Fig. 2). The 16S rRNA sequencing  
210 showed an increase in *Collinsella* and *Streptococcus* abundances (Fig. 1b, S5c). Although only four  
211 *Collinsella* and one *Streptococcus* CAZymes were detected, three of these enzymes were among the  
212 most expressed proteins on  $\beta$ -glucan, suggesting that these bacteria have a key role in  $\beta$ -glucan  
213 degradation within the community. Despite the increased abundance of *Solobacterium* on  $\beta$ -glucan,  
214 no CAZymes of this species were detected, suggesting that this bacterium relies on cross-feeding.  
215 Additionally, we identified multiple CAZymes from *Bacteroides* and *Bifidobacterium* species that are

216 specifically associated with  $\beta$ -glucan utilization, showing the importance of these bacteria on this  
217 polysaccharide degradation.

218 **Figure 2** The CAZymes detected after community growth on selected substrates. Enzymes grouped  
219 by CAZyme families are shown as intensity of the protein level. For each protein the respective  
220 bacterial genus is displayed colour coded on the left side. Three independent replicates are shown.  
221 For accession numbers and full data see Supplementary Table S2. PCM – porcine colonic mucin, B-  
222 gluc –  $\beta$ -glucan, PecA – apple pectin, Xyl – xylan.

223

224 On pectin, we mostly detected CAZymes of various *Bacteroides* (*B. ovatus*, *B. thetaiotaomicron*, *B.*  
225 *vulgatus* and *Phocaecicola sartorii*) (Fig. 2, Supplementary Table S2). Pectin is composed of three  
226 main polysaccharides: homogalacturonan and rhamnogalacturonan (RG) I and II. The metaproteome  
227 analysis of microbiota grown on pectin revealed multiple CAZymes associated specifically with the  
228 degradation of these glycans, such as  $\beta$ -galactosidases (GH2), polygalacturonases (GH28),  
229 arabinofuranosidases (GH51 and GH43), unsaturated rhamnogalacturonyl hydrolases (GH105),  
230 rhamnosidases (GH106) and lyases of families 1, 9, 10 and 11 (Fig. 2, Supplementary Table S2). RG II,  
231 the most complex polysaccharide in nature, required additional enzymes for full degradation, such  
232 as sialidases (GH33), aceric acid hydrolases (GH127), rhamnosidases (GH78) and  $\alpha$ -galactosidases  
233 (GH95) (Fig. 2). We detected a PL1 enzyme that was previously described as critical in RG II  
234 degradation by *B. thetaiotaomicron*<sup>27</sup>. An enzyme from PL27, a family populated with L-rhamnose- $\alpha$ -  
235 1,4-D-glucuronate lyase active on arabinogalactan, was also associated with pectin degradation<sup>28</sup>.  
236 Surprisingly, although *Olsenella scatoligenes* monocultures have been shown to grow on rhamnose  
237<sup>29</sup> and the species was abundant on pectin+PCM (Fig. S5a), its CAZymes were not detected  
238 (Supplementary Table S2). Additionally, only a few CAZymes from *F. prausnitzii*, one of the most  
239 abundant species on pectin+PCM, were detected (Fig. 2) (Fig. 1e). These results suggest that both  
240 bacteria rely on cross-feeding in faecal cultures. The degradation of xylan (Fig. 2e) was mainly carried  
241 out by  $\beta$ -xylanases,  $\beta$ -glucuronidases, arabinofuranosidases and  $\beta$ -xylosidases belonging to families  
242 GH10, GH30, GH43, GH51, GH67, GH98, GH115 and GH120 (Fig. 2, Supplementary Table S2).  
243 *Bacteroides* enzymes account for the majority of the GHs associated with xylan degradation.  
244 Interestingly, several of these enzymes are found in PULs similar to the previously characterised *B.*  
245 *ovatus* xylan PULs<sup>30</sup>. Similar to fermentation of pectin, the abundance and number of CAZymes of *B.*  
246 *vulgatus* was higher on xylan in the absence of mucin (Fig. 1e, Supplementary Table S2).

247 Only *A. muciniphila*'s CAZymes were detected on sole PCM, a result consistent with the high  
248 abundance of this bacterium detected by 16S rRNA sequencing (Fig. 1b, e). In case of fibre+PCM, we  
249 also detected CAZymes from *Bacteroides* species known to be able to utilise mucin, such as *B.*

250 *caccae*, *B. fragilis* and *B. thetaiotaomicron* (Supplementary Table S2). These CAZymes belong to  
251 families known to contain mucin glycan degrading enzymes, such as GH2, ( $\beta$ -galactosidases), GH20  
252 and GH84 ( $\beta$ -*N*-acetylglucosaminidases), GH29 and GH95 ( $\alpha$ -fucosidases), GH89 ( $\alpha$ -*N*-  
253 acetylglucosaminidases) and GH33 (sialidases) (Fig. 2 and Supplementary Table S2). Specifically, the  
254 enzymes Amuc 1835 (GH33), Amuc 1120 (GH95), Amuc 0290 (GH2) and Amuc 1220 (GH89),  
255 detected on PCM, have been shown to be critical for the growth of *A. muciniphila* on PGM<sup>31</sup>  
256 (Supplementary Table S2). Interestingly, the GH16 endo-active *O*-glycanases<sup>12</sup> were only detected in  
257 mucin samples in the absence of dietary fibres. We detected multiple sulfatases from *A. muciniphila*,  
258 *B. fragilis* and *B. ovatus*, suggesting that these bacteria have a critical role on removing the capping  
259 sulfate groups from mucin *O*-glycans (Fig. 2, Supplementary Table S2). Surprisingly, the  $\alpha/\beta$ -*N*-  
260 acetylgalactosaminidases from mucin-specific family GH109 were detected in fibre samples in the  
261 absence of PCM. Interestingly, our data show the highest MUC2 consumption on xylan+PCM (Fig.  
262 S6). This culture was the only combination of fibre with mucin that led to an increased abundance of  
263 *A. muciniphila*. This suggests that although *A. muciniphila* has a key role in mucin degradation,  
264 additional bacteria present on xylan can efficiently degrade mucin glycans inaccessible to *A.*  
265 *muciniphila*.

266 **Supplementary Figure 6** Quantification of the MUC2 in the samples after fermentation of the chosen  
267 substrates. **a**, Intensity of porcine MUC2 measured by mass-spectrometry. **b**, Coverage of porcine  
268 MUC2 domains. Numbers indicate the end of a tryptic peptide in the porcine MUC2 amino acid  
269 sequence. Simplified MUC2 domain scheme has been adapted from UniProt database (protein  
270 sequence AOA5G2QSD1).

271

### 272 *Bacterial metabolites reflect different substrates and affect goblet cell mucin production*

273 Extracellular bacterial metabolites from the end of growth were measured to determine the impact  
274 of the different fibres and mucin on the community metabolism. Additionally, the bacterial  
275 metabolism was evaluated via metaproteome analysis. The highest concentration of acetate and the  
276 highest number of enzymes related to acetate synthesis were measured from pectin fermentation  
277 (Fig. 3a, Fig. S7a), likely due to its methylated and acetylated backbone (Fig. S3c) which is easily  
278 converted into acetate. Xylan promoted mixed acids fermentation, especially propionate, while  $\beta$ -  
279 glucan enhanced butyrate production (Fig. 3a, Fig. S7a-b). The complex fibres pectin and xylan  
280 promoted biogenic amine production, especially cadaverine and putrescine (Fig. 3a). Interestingly,  
281 PCM was critical for tyramine synthesis (Fig. 3a).

282 **Figure 3** Metabolites profile of fermentation of selected substrates. **a**, Boxplots representing the  
283 concentrations of measured metabolites (mmol/gDW) and pH. Colours indicate the choice of  
284 substrate, empty boxes represent samples from cultivation of fibre, filled boxes represent samples

285 from cultivation of fibre+PCM or sole PCM. All replicates shown (two-tailed paired t-test, \*p < 0.05).  
286 **b**, Average ( $\pm$ SEM) enzyme counts for reactions related to specific metabolite synthesis. n=3. **c**, The  
287 effect of microbial metabolites on murine colonic spheroids and mCherry-tagged MUC2 production.  
288 Counts and signal intensity of mCherry-positive goblet cells as a result of treating the spheroids with  
289 metabolites from fermentation of the selected substrates, measured by flow cytometry and  
290 normalized against medium control. n=3-4. B-gluc –  $\beta$ -glucan, InuHP – high-performance inulin,  
291 PecA – apple pectin, Xyl – xylan, PCM – porcine colonic mucin.

292

293 Sole PCM cultures had the highest concentrations of propionate and the highest number of  
294 propionate synthesis enzymes detected by metaproteomics (Fig. 3a-b). These enzymes were mostly  
295 from *A. muciniphila*, consistent with the high abundance of this taxon (Fig. 1e, 3c). Moreover, the  
296 fermentation of sole PCM supported the most effective conversion of succinate into CO<sub>2</sub> and  
297 propionate (Fig. 3a). Additionally, *A. muciniphila* produced acetyl-CoA via pyruvate:ferredoxin  
298 oxidoreductase, releasing NADH, which is needed for propionate synthesis (Fig. S7d). *A. muciniphila*  
299 is known to produce succinate via the reductive TCA cycle<sup>32</sup>. However, succinate can also be  
300 produced from  $\gamma$ -aminobutyric acid (GABA), an intermediate metabolite of the colonic microbiota.  
301 GABA is formed via the decarboxylation of glutamate (Glu), catalysed by Glu decarboxylase, which  
302 was detected in significant amount from *A. muciniphila* on sole PCM (Fig. 3b-d, Supplementary Table  
303 4). Although no GABA was detected in the spent medium, the decreased levels of Glu, associated  
304 with the detection of *A. muciniphila* Glu decarboxylase suggests that GABA was fully converted into  
305 succinate, leading to the elevated levels of propionate and CO<sub>2</sub> detected on PCM (Fig. 3b-c, S7c and  
306 Supplementary Table 4). Since the growth medium was supplemented with only minor amounts of  
307 Glu, it is likely that the additional Glu was produced from proline (Pro) from MUC2 (Fig. 3d). Indeed,  
308 Pro dehydrogenase was detected from *A. muciniphila* on PCM (Fig. 3b-c, Supplementary Table 4).  
309 Furthermore, the elevated numbers of threonine (Thr) dehydratase on sole PCM indicates that Thr  
310 could have been used for propionate production (Fig. 3b-c). As the backbone of MUC2 is made of  
311 repeating Pro-Thr-Ser units, these data suggest that the bacteria, especially *A. muciniphila*, were  
312 able to metabolise the protein backbone of MUC2. Additionally, the conversion of glycans into acids  
313 results in lowered pH, observed with all the substrates, except for sole PCM where the pH remained  
314 neutral (Fig. 3a). If *A. muciniphila* was able to utilise the MUC2 protein, free peptides were released  
315 in addition to ammonia from amino sugar metabolism<sup>32</sup>, acting as a buffer neutralising the pH, as  
316 was seen on sole PCM. Together, these results further support the hypothesis of MUC2 backbone  
317 being degraded by *A. muciniphila*.

318 **Supplementary Figure 7** Metabolites profile of fermentation of selected substrates. **a**, Boxplots  
319 representing the concentrations of measured metabolites (mmol/gDW). Colours indicate the choice  
320 of substrate, empty boxes represent samples from cultivation of fibre, filled boxes represent

321 samples from cultivation of fibre+PCM or sole PCM. All replicates shown. **b**, Boxplots representing  
322 Glu consumption ( $\Delta$ mmol/gDW). Colours indicate the choice of substrate, empty boxes represent  
323 samples from cultivation of fibre, filled boxes represent samples from cultivation of fibre+PCM or  
324 sole PCM. All replicates shown. **c**, Average ( $\pm$ SEM) enzyme counts for reactions related to specific  
325 metabolite synthesis. Colours indicate the choice of substrate, empty bars represent samples from  
326 cultivation of fibre, filled bars represent samples from cultivation of fibre+PCM or sole PCM. n=3. **d**,  
327 Average ( $\pm$ SEM) protein counts for two pyruvate synthesis enzymes on sole PCM fermentation by  
328 the 8 bacterial groups. B-gluc –  $\beta$ -glucan, InuHP – high-performance inulin, PecA – apple pectin, Xyl –  
329 xylan, PCM – porcine colonic mucin, Glu – glutamate, Bu – butyric group, A – akkermansia group, Bi –  
330 bifidoabacteria group, Ba – bacteroides group, E – enterobacteria group, L – lachnoclostridia group,  
331 As – asaccharolytic group, S – succinivorans group.

332

333 The bacterial metabolites, especially the SCFAs, are considered to have an important role in  
334 regulating the intestinal homeostasis, although the exact mechanisms remain unknown. Intestinal  
335 organoid models have been used to study the microbial metabolites' effect on cellular proliferation  
336 <sup>3,33,34</sup>. We used the spent medium from the fermentation of dietary fibre and/or colonic mucin on  
337 murine primary cell culture to test if the bacterial metabolites influenced MUC2 production and  
338 secretion (Fig. 3e, S8a). Briefly, spheroids were established from the colon of the transgenic mice  
339 carrying mCherry-tagged MUC2, treated with the spent medium, and monitored for 48 hours. The  
340 mCherry-tagged MUC2 signal was measured with flow cytometry to evaluate the synthesis and  
341 secretion of MUC2. The elevated numbers of mCherry-positive cells and their increased intensity  
342 suggest metabolites from fermentation of complex fibres pectin and xylan can lead to enhanced  
343 MUC2 levels (Fig. 3e, S8a).

344 **Supplementary Figure 8** The effect of microbial metabolites on murine colonic spheroids and  
345 mCherry-tagged MUC2 production. **a**, Average counts and intensity ( $\pm$ SEM) of mCherry-positive  
346 goblet cells as a result of treating the spheroids with metabolites from fermentation of the selected  
347 substrates, measured by flow cytometry and normalized against medium control. n=3-4. **b**, Example  
348 of the gating strategy used in flow cytometry experiments. B-gluc –  $\beta$ -glucan, InuHP – high-  
349 performance inulin, PecA – apple pectin, Xyl – xylan, PCM – porcine colonic mucin.

350

351

352 *Multiple bacterial groups are required for the metabolism of monosaccharides*

353 Pectin and xylan degradation resulted in the most diverse consortia producing potentially host-  
354 beneficial metabolite mixtures. Thereby, the metabolism of monosaccharides from these fibres and  
355 PCM was evaluated on metaproteome level. The central metabolism and crosstalk between the  
356 bacteria in consortia were elucidated with metaproteomic analysis, supported by calculations with a  
357 constructed Flux Balance Analysis (FBA) metabolic model. The bacteria were divided into eight  
358 metabolic groups to cover the total carbohydrate metabolism: 1) butyric – butyrate and 1,2-

359 propanediol producers, 2) akkermansia – derived from the main mucolytic species *A. muciniphila*, 3)  
360 bifido – lactate and acetate producers, 4) bacteroides – propionate/succinate and acetate  
361 producers, 5) enterobacteria – lactate, succinate and acetate producers, 6) lachnospiridia –  
362 mucolytic, formate and 1,2-propanediol consumers, 7) asaccharolytic – lactate and amino acid  
363 degraders, and 8) succinivorans – succinate consumers (Supplementary Table S5).

364 We studied the metabolism of all the monosaccharides found in PCM *O*-glycans: fucose (Fuc), sialic  
365 acid (Neu5Ac), *N*-acetyl-galactosamine (GalNAc), *N*-acetyl-glucosamine (GlcNAc) and galactose (Gal)  
366 (Fig. 2g). The metabolism of Fuc began with its conversion into (*S*)-lactaldehyde by the butyric,  
367 akkermansia, bacteroides, enterobacteria and lachnospiridia groups, followed by the synthesis of  
368 (*S*)-propane-1,2-diol (1,2-PD) by the butyric group (Fig. 4a). Neu5Ac, was converted into GlcNAc by  
369 the enterobacteria groups followed by conversion into *D*-fructose-6-phosphate by the butyric,  
370 akkermansia, bacteroides and enterobacteria groups and phosphorylation into fructose-1,6-  
371 bisphosphate (F1,6P) by the butyric, akkermansia and bacteroides groups (Fig. 4a). GalNAc, was first  
372 converted into galactose, followed by catabolism via the Leloir pathway by the akkermansia,  
373 bacteroides and enterobacteria groups (Fig. 4a). The bifido group metabolised *D*-fructose-6-P from  
374 GlcNAc and GalNAc via the Bifidobacterium shunt.

375 **Figure 4** Metabolic pathways of glycan degradation by faecal microbiota. **a**, The degradation of  
376 glycans from dietary fibres and mucin based on the metaproteomic analysis. The bacteria were  
377 divided into 8 groups based on their similar metabolism (see text). *n*=3. **b**, The degradation of  
378 glycans from dietary fibres and mucin and cross-feeding between bacterial groups based on Flux  
379 Balance Analysis. The bacteria were divided into 8 groups based on their similar metabolism (see  
380 text). *n*=3. PecA – apple pectin, Xyl – xylan, PCM – porcine colonic mucin.

381

382 Although glycolysis is the main energy production pathway for anaerobic C6 sugar metabolism, some  
383 of the carbon is required for the pentose phosphate pathway (PPP) for biomass production. The  
384 enterobacteria group accounts for the enzymes of the oxidative part of the PPP and the non-  
385 oxidative part of PPP was driven by the butyric, akkermansia, bacteroides, enterobacteria and  
386 asaccharolytic groups (Fig. 4a). The akkermansia, bacteroides and enterobacteria channelled some  
387 of the phosphoenolpyruvate from glycolysis into the reductive TCA cycle for succinyl-CoA and  
388 succinate synthesis. Propionate synthesis enzymes were identified from akkermansia and  
389 bacteroides (Fig. 4a). Acetyl-CoA was synthesized via the ferredoxin dependent pyruvate  
390 dehydrogenase (by the butyric, akkermansia, bifido, bacteroides, lachnospiridia and asaccharolytic  
391 groups) or via the pyruvate-formate lyase (by the butyric, akkermansia, bifido and enterobacteria  
392 groups). The acetyl-CoA was used for the synthesis of acetate or butyrate by the butyric,  
393 akkermansia, enterobacteria and asaccharolytic groups.

394

395 The pectin backbone is made of galacturonic acid (GalA) and rhamnose (Rha) decorated with  
396 arabinose (Ara) and Gal (Fig. S3c). GalA was metabolised via the Entner-Doudoroff pathway by the  
397 butyric, bifido, bacteroides and enterobacteria groups (Fig. 4a). Rha was used by the bacteroides  
398 group to produce glycerone phosphate and (S)-propane-1,2-diol (Fig. 4a). Ara was converted into D-  
399 xylulose-5-phosphate by the bifido, bacteroides and enterobacteria groups (Fig. 4a). Since Gal is also  
400 prevalent in PCM, it was impossible to distinguish the exact source or characterise the separate  
401 fluxes. The xylose from xylan was metabolised via the PPP by the bifido, bacteroides and  
402 enterobacteria groups (Fig. 4a). A small flow of it was used for the oxidative PPP by the bacteroides  
403 and enterobacteria, while most of it was either used for the reductive PPP or channelled into the  
404 glycolysis by the butyric, bacteroides and enterobacteria groups (Fig. 4a). The bifido group  
405 metabolised xylose via the Bifidobacterium shunt. The glucuronic acid (GlcA) from xylan was  
406 degraded into pyruvate by the butyric, bacteroides and enterobacteria groups.

407

408 The degradation of mucin components in the presence of pectin or xylan was similar to sole PCM  
409 fermentation, however, some critical differences were observed. In the presence of pectin *A.*  
410 *muciniphila* was not able to compete for the substrate, resulting in a change in mucin degraders  
411 (with higher activities of the butyric, bifido and bacteroides group). Interestingly, although *A.*  
412 *muciniphila* was highly abundant on xylan+PCM culture (Fig. 1b), this bacterium did not dominate  
413 the metabolism within this culture and some of the mucin degradation pathways were carried out  
414 by members of the butyric group, especially *E. tayi* and *F. prausnitzii* (Supplementary table S4).  
415 Additionally, the proportions of Gal degrading bacteria were altered with butyric and bifidobacterial  
416 groups being more active in the presence of fibre.

417

418 The calculations with the FBA model confirmed that the akkermansia group (consisting of *A.*  
419 *muciniphila*) was the most active taxon on sole PCM (Fig. 4b). The model predicted akkermansia to  
420 consume mainly GlcNAc, Fuc and Gal and to release acetate, propionate, CO<sub>2</sub> and H<sub>2</sub>S into the spent  
421 medium. On pectin+PCM, the model verified that the most active degraders were the butyric and  
422 bacteroides groups, especially *F. prausnitzii*, *B. ovatus*, *B. vulgatus*, *B. xylanisolvens* and *B. faecis* (Fig.  
423 4b, Supplementary Table S4). At last, the bacteroides group (*B. faecis*, *B. ovatus*, *B. vulgatus*, *B.*  
424 *xylanisolvens*) were confirmed to be the main xylose utiliser (Fig. 4b, Supplementary Table S4).  
425 Together, these data show that the dietary glycans are degraded by a complex community of  
426 bacteria and the presence of mucin can affect these metabolic pathways.

427



428

429

430 **DISCUSSION**

431 The microbiota colonises the mucus layer in the gut and is in contact with mucin glycans and dietary  
432 fibres. In this study, we utilised a human faecal microbiota to study the impact of mucin in the  
433 metabolism of 14 dietary fibres and oligosaccharides. We observed that the glycans with simple  
434 structures were degraded fast and supported the abundance of fast-growing taxa, such as  
435 *Bifidobacterium*. Complex host glycans such as mucin were only degraded by a subset of the host  
436 microbiota, while inulin and  $\beta$ -glucan were very easily degraded by multiple species. Additionally,  
437 the prolonged degradation of complex fibres enhanced the microbial diversity, especially the growth  
438 of various *Bacteroides* species. The number of detected CAZymes also reflected the complexity of  
439 the substrate, with pectin requiring more enzymes for its degradation. This observation agrees with  
440 previous studies showing that a single bacterium can encode 54 enzymes to degrade this complex  
441 plant cell wall polysaccharide<sup>26,27</sup>. These results are in line with previous studies demonstrating  
442 that the structure and accessibility of glycans is a key factor in modulating the microbial consortium  
443 <sup>17,35–38</sup>. Additionally, several studies with *Bacteroides* mono-cultures have shown this phylum to be  
444 particularly well adapted to utilising complex polysaccharides due to the high number of CAZymes  
445 encoded by these bacteria <sup>15,22,26,39,40</sup>.

446 Consistent with previous results <sup>10,11,41</sup>, the presence of mucin (and no fibre) led to an expansion of a  
447 microbial community adapted to degrade these host glycans. Importantly, the co-cultures with  
448 gastric and colonic mucin resulted in different microbiota communities. This is likely due to the  
449 differences in *O*-glycosylation in different mucins and highlights the need of using colonic mucins to  
450 study the metabolism of colonic microbiota. In contrast to the gastric mucin, the colonic mucin  
451 specifically supported the growth of propiogenic *Akkermansia muciniphila* and butyrogenic  
452 *Faecalibacterium prausnitzii*, both of which are prevalent gut commensals and potential next-  
453 generation probiotic species <sup>23,42–48</sup>. A recent study reported that in mono-culture *A. muciniphila*  
454 does not grow on colonic mucin *O*-glycans <sup>15</sup>. In our study we utilised a microbiota community and  
455 we speculate that the growth of *A. muciniphila* on PCM can be due to sharing mechanism between  
456 microbiota members or the presence of a key bacterium that encodes enzymes required to remove  
457 capping sugars, allowing *A. muciniphila* to access mucin glycans previously inaccessible. Indeed, in  
458 our study we detected multiple CAZymes expressed by *A. muciniphila* that can be implicated in  
459 mucin degradation, suggesting that this bacterium is able to utilise the *O*-glycans of colonic MUC2.  
460 Interestingly, we also observed that *A. muciniphila* degraded the mucin protein backbone as a  
461 carbon source. It was previously shown that *A. muciniphila* encodes proteases active on MUC2 in  
462 colonic cancer cells and is able to hydrolyse the peptide bond *N*-terminal to *O*-glycosylated serine  
463 and threonine residues <sup>49,50</sup>. Although we did not detect such proteases in our dataset, the high

464 abundance of *A. muciniphila*, the elevated concentration of propionate and CO<sub>2</sub> and the highly active  
465 GABA shunt on sole PCM suggest that this bacterium is able to degrade colonic mucin. Therefore,  
466 this unique ability to utilise mucin protein backbone is likely to contribute to the expansion of *A.*  
467 *muciniphila* in mucin cultures in the absence of dietary fibre.

468 Among the tested dietary fibres, the enrichment of *A. muciniphila* was observed only on xylan. This  
469 culture also showed one of the highest propionate and lowest formate concentrations, which is  
470 characteristic for *A. muciniphila* metabolism<sup>51</sup>. The propiogenic effect of xylan has been  
471 demonstrated previously<sup>17,52</sup>. When acetyl-CoA is synthesized using pyruvate-formate lyase,  
472 formate is released and no NADH is produced which is needed for propionate synthesis.  
473 Interestingly, to overcome this limitation, *A. muciniphila* primarily relied on pyruvate:ferredoxin  
474 oxidoreductase for acetyl-CoA production (Fig. S7d). In addition, xylan supported the most diverse  
475 consortium with one of the promoted species being *Eisenbergiella tayi*, a butyric acid producing  
476 bacterium. Our metaproteome analysis showed *E. tayi* to be active on various metabolic pathways.  
477 Little is known of this species<sup>53</sup>, however, its concomitant growth with *A. muciniphila* warrants a  
478 further investigation. The xylan+PCM culture achieved the highest mucin degradation, even though  
479 *A. muciniphila* did not dominate in the consortium. This suggests cross-feeding mechanisms between  
480 mucin-degrading taxa that were specifically promoted by xylan. Indeed, a recent study highlighted  
481 that the degradation of complex glycans might rely on a community, rather than on a single species  
482<sup>54</sup>.

483 Xylan and pectin fermentations resulted in mixtures of SCFAs and biogenic amines, especially  
484 cadaverine and putrescine. The potential effect of amines on the epithelial cells is varying, with  
485 tyramine shown to exert toxicity<sup>55</sup>, whereas putrescine and cadaverine have been shown to support  
486 cell proliferation and gut barrier function<sup>4,56</sup>. Indeed, the metabolites from xylan and pectin  
487 fermentation were shown to have a positive effect on the MUC2 levels in goblet cells. This result is in  
488 line with previous studies showing that mixed metabolites from a diverse consortium can have a  
489 direct impact on the gut epithelium, promoting proliferation and turnover, whereas only a single  
490 SCFA can exert inhibitory properties on cell proliferation<sup>3,33,34,57</sup>. Our data suggests that xylan and  
491 pectin could have potential host-beneficial effects, due to supporting diverse consortia and  
492 metabolites that promote MUC2 production. However, these are preliminary results and further  
493 studies are needed to address the molecular mechanisms behind this potential beneficial effect.

494 In conclusion, we showed detailed shifts in bacterial communities and metabolic activities on  
495 different glycans, supporting the idea that gut microbiota can be specifically manipulated by dietary  
496 fibres. Moreover, we revealed how dietary fibre degradation is affected by co-metabolism of host

497 glycans. For the first time in the literature, we demonstrated that differences between gastric and  
498 colonic mucins impact the microbiota community and metabolism. A result that highlights the need  
499 of using colonic mucins in future studies addressing the metabolism of colonic bacteria. Overall, by  
500 revealing the functional activities of the bacteria in consortia, this study contributes to a better  
501 understanding of the complex metabolic pathways within the human microbiota that can be  
502 manipulated to maximise beneficial microbiota-host interactions.

503

#### 504 **ACKNOWLEDGMENTS**

505 This project was supported by the National Institute of Health grant (R01 DK125445), The Knut and  
506 Alice Wallenberg Foundation grant (2017.0028) and Bill and Melinda Gates Foundation grant  
507 (OPP1202459) awarded to G. C. H.. The project was supported by Wilhelm and Martina Lundgren's  
508 Foundation. The work was supported by the Swedish Research council grants (2017-00958 and  
509 2021-01409) awarded to G. C. H. and A. S. L.. This project received funding from Swedish Society for  
510 Medical Research (Svenska Sällskapet för Medicinsk Forskning, grant S21-0026) and Sahlgrenska  
511 Academy International Starting Grant (GU2021/1070) awarded to A. S. L.. The work was supported  
512 by Ministry of Education and Research base funding for Tallinn University of Technology and  
513 European Regional Development Fund project EU48667 for Center of Food and Fermentation  
514 Technologies. The project was supported by European Regional Development Fund Education and  
515 Youth Board (5.10-6.1/20/20-2) and Archimedes Foundation (16-3.5/2011).

516 We thank Jekaterina Kazantseva, Johana Koppel, Kristel Tanilas and Marina Junusova for their help  
517 with the analytics.

518

#### 519 **AUTHOR CONTRIBUTIONS**

520 G. R, K. A. and L. A. conceived and designed the experiments. G. R., A. S. L., and L. A. wrote the draft  
521 manuscript. G. R., S. A. and K. A. performed the cultivations by isothermal microcalorimetry and  
522 analysed the gas composition and bacterial metabolites. G. R. performed the porcine colonic mucin  
523 extraction. C. J. performed the glycome analysis of mucins. G. R. and L. A. performed the  
524 metaproteomic analysis. G. R. and A. S. L. analysed the polysaccharide degradation data. I. M.  
525 constructed the flux balance analysis model and performed the bacterial metabolism calculations. G.  
526 R. and H. S. performed the cell culture experiments. G. R, I. M. and K. A. analysed the 16S rRNA  
527 sequencing and metabolomics data. G. C. H., A. S. L., K. A. and L. A. supervised and provided funding  
528 for the project. All authors read and approved the manuscript.

529

530 **COMPETING INTERESTS**

531 The authors declare no competing financial interests.

532

533 **ADDITIONAL INFORMATION**

534 (None)

535 **MATERIALS AND METHODS**

536 *Faecal samples*

537 The faecal samples were donated by seven healthy volunteers (19-37 years old, Caucasian) with  
538 exclusion criteria being the use of prebiotics, probiotics, laxatives and antibiotics four weeks prior to  
539 the donation. Faecal samples were collected freshly into faeces collection tubes (Sarstedt), the  
540 tubes inserted into previously frozen cryoblock and kept at -20 °C until transport to the lab, but no  
541 longer than two days. After arrival to the lab, the samples were stored at -80 °C.

542 The faecal slurries were prepared in an anaerobic chamber (Concept, Baker Ruskinn) flushed with  
543 95% N<sub>2</sub>. The faecal samples were homogenized in four volumes of sterile PBS (phosphate buffer  
544 saline) containing 5% (vol/vol) DMSO (dimethyl sulfoxide) and freshly autoclaved reducing agent  
545 sodium thioglycolate (final concentration 50 mg/ml). Equal volumes of the faecal slurries from  
546 different donors were pooled and stored as 0.5 ml aliquots at -80 °C until the cultivation  
547 experiments.

548 Collecting and handling the faecal samples was approved by the Tallinn Medical Research Ethics  
549 Committee, Estonia (protocol No. 554).

550

551 *Porcine colonic mucin extraction and purification*

552 Mucins were extracted from flushed porcine colonic tissues, that were acquired from a local butcher  
553 (Saaremaa Meat Factory, Estonia) and stored at -20 °C until extraction. The mucus layer was gently  
554 scraped from the thawed colon epithelium and collected on ice. A total of 138 g of mucosal  
555 scrapings were collected and mixed in 1:2 ratio with cold extraction buffer (6 M GuHCl, 5 mM EDTA,  
556 0.01 M NaH<sub>2</sub>PO<sub>4</sub>, pH 6.5) and centrifuged 30 min at 18,000 rpm, 10 °C. Floating fat and supernatant  
557 were aspirated and mucus pellet was solubilized in 1:1 ratio with cold extraction buffer. The mixture  
558 was gently stirred for 3 hours at 4 °C, after which centrifugation for 30 min at 18,000 rpm and 10 °C  
559 was repeated. Supernatant was aspirated and the mucus pellet was solubilized in 2:1 ratio with cold  
560 extraction buffer. The mixture was stirred gently overnight at 4 °C.

561 The mucus mixture extraction and centrifugation steps were repeated on two consecutive days,  
562 after which the mixture was left stirring for 48 hours at 4 °C. A final centrifugation for 30 min at  
563 18,000 rpm and 10 °C was carried out, resulting in 60 g mucus pellet. Freshly prepared reduction  
564 buffer (6 M GuHCl, 0.1 M Tris, 5 mM EDTA, 10 mM DTT) was added to the pellet and stirred gently at  
565 37 °C for 5 hours. Alkylation was carried out by adding 25 mM IAA (iodoacetamide) to the mixture

566 and stirred gently in the dark for overnight at room temperature. The mucins were dialysed with  
567 12.4 kDa pore size tubes (Sigma-Aldrich, D0530) against deionized water at 4 °C for 24 hours,  
568 changing the water every 4 hours.

569

#### 570 *Isothermal microcalorimetry (IMC)*

571 The batch cultivations were carried out in a 48-channel isothermal microcalorimeter (TAM IV, TA  
572 Instruments). A defined basal medium was used: 0.05 M potassium phosphate buffer was made  
573 from 1 M stock solutions (ml/l): K<sub>2</sub>HPO<sub>4</sub> (28.9) and KH<sub>2</sub>PO<sub>4</sub> (21.1); mineral salts (mg/l): MgSO<sub>4</sub>\*7H<sub>2</sub>O  
574 (36), FeSO<sub>4</sub>\*7H<sub>2</sub>O (0.1), CaCl<sub>2</sub> (9), MnSO<sub>4</sub>\*H<sub>2</sub>O (3), ZnSO<sub>4</sub>\*7H<sub>2</sub>O (1), CoSO<sub>4</sub>\*7H<sub>2</sub>O (1), CuSO<sub>4</sub>\*5H<sub>2</sub>O (1),  
575 (NH<sub>4</sub>)<sub>6</sub>Mo<sub>7</sub>O<sub>24</sub>\*4H<sub>2</sub>O (1), NaCl (527); L-amino acids (g/l): Ala (0.044), Arg (0.023), Asn (0.038), Asp  
576 (0.038), Glu (0.036), Gln (0.018), Gly (0.032), His (0.027), Ile (0.060), Leu (0.120), Lys-HCl (0.080), Met  
577 (0.023), Phe (0.050), Pro (0.041), Ser (0.095), Thr (0.041), Trp (0.009), Val (0.060), Tyr (0.015);  
578 vitamins (mg/l): biotin (0.25), Ca-pantothenate (0.25), folic acid (0.25), nicotinamide (0.25),  
579 pyridoxine-HCl (0.50), riboflavin (0.25), thiamine-HCl (0.25), cyanocobalamine (0.25) and other  
580 components (g/l): bile salts (0.5), NaHCO<sub>3</sub> (2.0), Tween-80 (0.5), Na-thioglycolate (0.5), Cys-HCl (0.5),  
581 hemin (5 mg/l), vitamin K1 (0.5 mg/l).

582 The substrate screening panel consisted of 14 dietary fibres in combination with commercially  
583 available porcine gastric mucin (Supplementary Table 1). Each polysaccharide and mucin were added  
584 at 2.5 g/l final concentration. Follow-up experiments with in-house extracted porcine colonic mucin  
585 were done similarly. Culture medium without any added carbohydrates or mucin was used as a  
586 negative control. The growth medium was pre-reduced in an anaerobic jar (Anaero-Gen™, Oxoid  
587 Inc.).

588 The growth experiments were carried out in sterile hermetically sealed 3 ml ampoules (2 ml working  
589 volume, 1 ml headspace). The ampoules were inoculated with 120x dilution of the pooled faecal  
590 slurry in an anaerobic chamber (Concept, Baker Ruskinn) and incubated for 64 hours at 37 °C in  
591 isothermal microcalorimeter. Heat flow (P, μW) and total accumulated heat (Q, J) were registered  
592 throughout the whole experiment, at 5 min intervals.

593 The ampoules were removed from the calorimeter and the composition of the gas in the headspace  
594 was analysed with gas chromatography. The ampoules were weighed, and the content divided into  
595 0.5 ml aliquots which were centrifuged for 10 min at 10,000 g. The pH of supernatants was  
596 measured with pH-meter (InLab® Solids, Mettler Toledo). Supernatants were stored at -20 °C and  
597 pellets at -80 °C until further analyses.

598

599 *DNA extraction and sequencing, bioinformatics*

600 DNA was extracted from the cell pellets using PureLink Microbiome DNA extraction kit (Thermo  
601 Fisher Scientific). PCR amplification of the V4 hypervariable regions of the 16S rRNA genes was  
602 carried out with universal primers F515 5'-GTGCCAGCMGCCGCGTAA-3' and R806 5'-  
603 GGACTACHVGGGTWTCTAAT-3. Sequencing libraries were prepared with Nextera XT Index Kit  
604 (Illumina). Prepared libraries were quantified with Qubit™ dsDNA HS Assay Kit (quantitation range  
605 0.2-100 ng; Thermo Fisher Scientific) or Qubit™ dsDNA BR Assay Kit (quantitation range 2-1000 ng;  
606 Thermo Fisher Scientific). Pooled libraries were sequenced using Illumina iSeq 100 platform and i1  
607 reagent kit. All reagent kits were handled in accordance with manufacturer's instructions. The  
608 amplified region was 291 bp long and in average 53,616 reads per sample were obtained.

609 The DNA sequence data was analysed using BION-meta ([www.box.com/bion](http://www.box.com/bion)). Sequences were first  
610 cleaned at both ends using a 99.5% minimum quality threshold for at least 18 of 20 bases for 5'-end  
611 and 28 of 30 bases for 3'-end. Obtained sequences were then joined and contigs shorter than 150 bp  
612 were removed. The sequences were then cleaned of chimeras and clustered by 95% oligonucleotide  
613 similarity (k-mer length of 8 bp, step size 2 bp). Consensus reads were aligned to the SILVA reference  
614 16S rRNA database (v138) using a word length of 8 and similarity cut-off of 90%.

615

616 *Metaproteomics*

617 The microbial cell pellets were dissolved in 60 µl of lysis buffer (4% SDS (sodium dodecyl sulfate), 100  
618 mM Tris-HCl (pH 7.5), 100 mM DTT (dithiothreitol)) and heated at 95 °C for 5 minutes, followed by 2-  
619 3 short pulses of ultrasonication (15 µm amplitude). Heating and sonication steps were repeated  
620 twice followed by centrifugation for 5 min at 14,000 g to pellet any debris. Cell lysates (30 µl) were  
621 digested with LysC and trypsin on 30 kDa cut-off filters (NanoSep, Pall Life Sciences) according to  
622 Filter Aided Sample Preparation (FASP) protocol<sup>58</sup>. Peptide yield was measured with a microvolume  
623 spectrophotometer (Nano Drop 2000; Thermo Fisher Scientific) at 280 nm wavelength. The samples  
624 were acidified with TFA (trifluoroacetic acid) to final concentration of 0.5% and 15 µg of peptides  
625 were cleaned and stored in C18-StageTip filters<sup>59</sup> at -20 °C.

626 Samples were analysed in triplicates with an EASY-nLC 1000 system (Thermo Fisher Scientific)  
627 connected to a Q-Exactive mass-spectrometer (Thermo Fisher Scientific) through a nanoelectrospray  
628 ion source. Peptides were separated with an in-house packed column [150 mm × 0.075 mm inner  
629 diameter (New Objective, Woburn), Reprosil-Pur C18-AQ 3 µm particles (Dr. Maisch)] using a



630 gradient: 3-25% B over 175 min, 25-45% B over 30 min, 45-100% B over 5 minutes and held for  
631 additional 20 min on 100% of B, at flow rate of 250 nl/min (A: 0.1% FA, B: 80% ACN , 0.1% FA). The  
632 Q-Exactive HF hybrid quadrupole-Orbitrap mass spectrometer (Thermo Fisher Scientific) was  
633 operated at 250 °C capillary temperature and 2.0 kV spray voltage. Full mass spectra were acquired  
634 in the Orbitrap mass analyser over a mass range from m/z 400 to 1600 with resolution of 60 000  
635 (m/z 200) after accumulation of ions to a 3e6 target value based on predictive AGC from the  
636 previous full scan. Twelve most intense peaks with a charge state  $\geq 2$  were fragmented in the HCD  
637 collision cell with normalized collision energy of 27%, and tandem mass spectrum was acquired in  
638 the Orbitrap mass analyser with resolution of 15 000, AGC target value 1e5. Dynamic exclusion was  
639 set to 30 s. The maximum allowed ion accumulation times were 20 ms for full MS scans and 50 ms  
640 for tandem mass spectrum.

641 A custom database was constructed for the metaproteomics searches. First, *de novo* peptide  
642 identification was done for the raw MS spectra, using PEAKS Studio software (version 8.5,  
643 Bioinformatics Solutions Inc) <sup>60</sup>. Average local confidence (ALC) was set to be  $\geq 80\%$ . The acquired list  
644 of peptides was analysed with ProteoClade <sup>61</sup> in order to annotate the *de novo* identified peptides to  
645 all potential organisms in the sample using the entire UniProt repository <sup>62</sup>. The list of taxa from  
646 ProteoClade was further optimized by i) including only taxa from kingdoms of bacteria, archaea and  
647 viruses, ii) removing taxa which were identified in < 3 samples per substrate group, iii) adding  
648 missing taxa from 16S rRNA gene sequencing analysis results. Protein sequences for each taxon were  
649 downloaded from UniProt database (2021.01.14, uniprot.org), reference proteomes preferred  
650 where possible. The final custom database contained 291 bacterial as well as pig and human  
651 proteomes and was used for the final analysis of MS/MS spectra with MaxQuant (version 1.4) <sup>63</sup>.  
652 Searches were performed using trypsin as an enzyme, maximum 1 missed cleavage, precursor  
653 tolerance of 20 ppm in the first search used for recalibration, followed by 7 ppm for the main search  
654 and 0.5 Da for fragment ions. Carbamidomethylation of cysteine was set as a fixed modification and  
655 methionine oxidation and protein N-terminal acetylation were set as variable modifications. The  
656 required false discovery rate (FDR) was set to 1% both for peptide and protein levels and the  
657 minimum required peptide length was set to seven amino acids. More than 21,000 protein groups  
658 were identified.

659 The mass spectrometry proteomics data have been deposited to the ProteomeXchange Consortium  
660 (<http://proteomecentral.proteomexchange.org>) via the PRIDE partner repository <sup>64</sup> with the dataset  
661 identifier PXD0XXXXX.

662

663 *Carbohydrate metabolism analysis*

664 All identified proteins were annotated for CAZymes using dbCAN  
665 (<http://bcb.unl.edu/dbCAN2/blast.php>). Three tools were used for automatic CAZyme annotation: a)  
666 HMMER to search against the dbCAN HMM (Hidden Markov Model) database; b) DIAMOND to  
667 search against the CAZy pre-annotated CAZyme sequence database; and c) Hotpep to search against  
668 the conserved CAZyme PPR (peptide pattern recognition) short peptide library. To improve  
669 annotation accuracy, a filtering step was used to retain only hits to CAZy families found by at least  
670 two tools <sup>65</sup>.

671

672 *Porcine mucin analysis*

673 The protein composition of porcine gastric and colonic mucins was analysed with mass-spectrometry  
674 system as described for metaproteomics analysis. Briefly, protein samples were digested with  
675 trypsin overnight according to FASP protocol <sup>58</sup>. Peptides were cleaned with C18-StageTip filters <sup>59</sup>  
676 and separated with a 45 min gradient of 5–60% B (A: 0.1% FA, B: 80% ACN , 0.1% FA). The raw  
677 MS/MS spectra were searched with MaxQuant (version 1.6.11.0) <sup>63</sup> against pig database downloaded  
678 from UniProt (2020.09.12) The mass spectrometry proteomics data have been deposited to the  
679 ProteomeXchange Consortium (<http://proteomecentral.proteomexchange.org>) via the PRIDE  
680 partner repository <sup>64</sup> with the dataset identifier PXDXXXXX.

681 Composite agarose-polyacrylamide (AgPAGE) gel was prepared according to the protocol of Schulz  
682 and co-workers <sup>66</sup>. Porcine gastric and colonic mucins were solubilized by the addition of 2-times  
683 reducing gel-loading buffer (62.5 mM TrisHCl pH 6.8, 2% SDS, 50 mM DTT 20% (v/v) glycerol) and  
684 heated for 5 min at 95 °C before separation via AgPAGE for 3.5 h at 30 mA and 6 °C and stained with  
685 Alcian blue. For controls HiMark™ Pre-stained Protein Standard (ThermoFisher Scientific, LC5699)  
686 and MUC2 purified from LS174T cells (LS material) as described previously <sup>67</sup> were used.

687

688 *Mucin glycan analysis*

689 O-glycans were released by reductive beta-elimination at a concentration of 10 mg/ml  $\beta$ -elimination  
690 solution (0.5 M NaBH<sub>4</sub> and 50 mM NaOH). Samples were covered tightly and incubated overnight  
691 (ca. 18 h) at 50 °C. The samples were acidified with glacial acetic acid (5%, v/v) and desalted using  
692 cation exchange resin packed in a C18 ZipTip <sup>66</sup>.

693 Released glycans were resuspended in water and analysed by liquid chromatograph-electrospray  
694 ionization tandem mass spectrometry (LC-ESI/MS). The oligosaccharides were separated on a  
695 column (10 cm × 250 μm) packed in-house with 5 μm porous graphite particles (Hypercarb, Thermo-  
696 Hypersil). The oligosaccharides were injected on to the column and eluted with an acetonitrile  
697 gradient (Buffer A, 10 mM ammonium bicarbonate; Buffer B, 10 mM ammonium bicarbonate in 80%  
698 acetonitrile). The gradient (0-45% Buffer B) was eluted for 46 min, followed by a wash step with  
699 100% Buffer B, and equilibrated with Buffer A in next 24 min. A 40 cm × 50 μm i.d. fused silica  
700 capillary was used as transfer line to the ion source.

701 The samples were analysed in negative ion mode on a LTQ linear ion trap mass spectrometer  
702 (Thermo Electron), with an IonMax standard ESI source equipped with a stainless-steel needle kept  
703 at -3.5 kV. Compressed air was used as nebulizer gas. The heated capillary was kept at 270 °C, and  
704 the capillary voltage was -50 kV. Full scan ( $m/z$  380-2000, two microscan, maximum 100 ms, target  
705 value of 30,000) was performed, followed by data dependent  $MS^2$  scans (two microscans, maximum  
706 100 ms, target value of 10,000) with normalized collision energy of 35%, isolation window of 2.5  
707 units, activation  $q=0.25$  and activation time 30 ms. The threshold for  $MS^2$  was set to 300 counts.  
708 Data acquisition and processing were conducted with Xcalibur software (Version 2.0.7). The LC-  
709 MS/MS data was processed using Progenesis Q1 (Nonlinear Dynamics, Waters).

710 The glycomic MS raw files have been deposited in the GlycoPOST database under the ID of XXXX  
711 (<https://glycopost.glycosmos.org/preview/174480073162c4138e3c5e5>, (code: 8410)).

712

713

#### 714 *Gas analysis*

715 The microcalorimeter ampoule headspace gas composition was analysed with a gas chromatograph  
716 (Agilent 490 Micro GC Biogas Analyzer, Agilent Technologies Ltd.) using CP-Molsieve 5A and CP-  
717 PoraPLOT U columns and a thermal conductivity detector. Soluble gas concentration ( $c$ ) was  
718 calculated using Henry law:  $c = H^{cp*} \cdot p$ , where  $p$  is the partial pressure of given gas in the gas phase  
719 and  $H^{cp*}$  (M/atm) the effective Henry constant of the given gas dependent on pH<sup>68</sup>.

720

#### 721 *Analysis of organic acids, free amino acids and amines*

722 The supernatant samples were filtered using centrifugal devices with a 3 kDa cut-off filter (Amicon®  
723 Ultra-0.5, Merck). The concentrations of organic acids were measured with high-performance liquid

724 chromatography (HPLC) system (Alliance 2795 system; Waters) equipped with BioRad HPX 87H  
725 column (Hercules) with isocratic elution of 0.005 M H<sub>2</sub>SO<sub>4</sub>, flow rate 0.5 ml/min, 35 °C. RI (model  
726 2414; Waters) and UV (210 nm; model 2487; Waters) detectors were used for quantification with  
727 external standards. The data were processed with Empower software (Waters).

728 The concentrations of free amino acids and amines were determined by the UPLC-UV methodology  
729 (Acquity; AccQ-Tag™ Ultra Derivatization Kit; Waters) developed by Waters with modifications. The  
730 standards and samples were derivatised with 6-aminoquinolyl-N-hydroxysuccinimidyl carbamate  
731 and then loaded on an AccQ-Tag Ultra RP column (130 Å, 1.7 µm, 2.1x100 mm; Waters). Amino acids  
732 and amines were separated using a gradient of eluent A (AccQ-Tag Ultra eluent A) and eluent B (1%  
733 formic acid in acetonitrile) as follows: 0-0.54 min 99.9% A and 0.1% B. A flow rate of 0.7 ml/min, an  
734 autosampler temperature of 8 °C, a column temperature of 55 °C and injection volume of 1 µl were  
735 used. Amino acids and amines were detected with a photodiode array detector (260 nm), and data  
736 were processed with Empower 2 software (Waters). The detection limit was 0.001 mM. All standard  
737 substrates were of analytical grade.

738

#### 739 *Spheroid culture*

740 Spheroid cultures were generated from distal colon crypts isolated from transgenic mice carrying  
741 mCherry-tagged human MUC2 (RedMUC2<sup>98trTg</sup>)<sup>69</sup>. The cultures were maintained as spheroids in  
742 Matrigel® Basement Membrane Matrix (Corning), using 50% conditioned medium (CM)  
743 supplemented with 10 µM ROCK-inhibitor (Y-27632 dihydrochloride, Tocris) and 10 µM transforming  
744 growth factor-β (TGF-β) type I receptor inhibitor (SB 431542, Tocris) as described by Miyoshi and  
745 Stappenbeck<sup>70</sup>. Spheroids were incubated at 37 °C, 5% CO<sub>2</sub> and used at passage numbers 11-16 for  
746 all assays. A wild-type (C57BL/6N; Taconic) mouse distal colon spheroid line was maintained  
747 simultaneously and used at passage number 15-20 as a negative control in all assays.

748 All animal work was approved by the Swedish Laboratory Animal Ethic Committee in Gothenburg,  
749 Sweden (ethical permits 2285-19, 3006-20) and conducted following the guidelines of Swedish  
750 animal welfare legislation which meets the European Convention for the Protection of Vertebrate  
751 Animals used for Experimental and other Scientific Purposes (Council of Europe No. 123, Strasbourg  
752 1985) and the European Union Directive 2010/63/EU on the protection of animals used for scientific  
753 purposes.

754

#### 755 *Flow cytometry*

756 The effects of microbial metabolites on MUC2 in spheroids were studied using flow cytometry (FC).  
757 Trypsinised cells were seeded on 24-well plates (Sarstedt) and maintained in 50% CM with 10  $\mu$ M Y-  
758 27632 dihydrochloride and 10  $\mu$ M SB 431542. The RedMUC2<sup>98trTg</sup> cells were seeded in density ca  
759 14,000 cells/well and the wild-type cells in density ca 3000 cells/well. To study the effect of bacterial  
760 metabolites on the early growth of intestinal cells, 10% dilutions of bacterial culture supernatants  
761 were prepared in 50% CM and added. After 24 hours, medium was replaced by 5% CM (1 volume of  
762 50% CM in 9 volumes of primary culture medium: advanced DMEM/F12 (Invitrogen, 12634-010),  
763 20% vol/vol FCS, 100 U/ml penicillin, 100  $\mu$ g/ml streptomycin, 2 mM Glutamax™) with 10  $\mu$ M Y-  
764 27632 and fresh 10% dilutions of bacterial culture supernatants. Cells in plain 5% CM and 50% CM  
765 were seeded simultaneously with the test samples and used as growth medium controls. Cells  
766 treated with DAPT and trypsin were used as positive controls. Wild-type mouse spheroids were used  
767 as negative control.

768 After 24 hours cells were harvested for FC. Spheroids were trypsinised for 3 min at 37 °C to obtain  
769 single cell suspensions and washed in 1xPBS by centrifugation. Samples were incubated on ice for 10  
770 min in YOYO™-1 nucleic acid stain (1:10,000; Thermo Fisher Scientific), washed by centrifugation at  
771 200 g and 4 °C for 5 min and resuspended in cold FC buffer (2% w/v BSA in 1xPBS). Samples were  
772 analysed using CytoFLEX flow cytometer (Beckman Coulter Life Sciences). The data were analysed  
773 with CytExpert software (version 2.4, Beckman Coulter Life Sciences). An example of the applied  
774 gating rules is in supplementary data (Fig S8). Gating strategies and thresholds were kept the same  
775 for all samples to obtain comparable results.

776

#### 777 *Construction of metabolic networks*

778 The 100 most abundant taxa from cultivations were grouped into 8 metabolic groups based on  
779 information acquired from phylogenetic data in NCBI database and genome annotation. Combined  
780 metabolic networks for each group were built using information from public databases MetaCyc<sup>71</sup>  
781 and KEGG<sup>72</sup> (reactions in pathways and their reversibility). The following networks were  
782 constructed:

- 783 1. Butyric group – butyrate producers with 1,2-propanediol production capacity, combines 12  
784 different species, 570 reactions, 429 metabolites
- 785 2. Akkermansia group – derived from the main mucin degrader *A. muciniphila* that has a  
786 unique metabolism, 1 species, 544 reactions, 424 metabolites

- 787 3. Bifidobacteria group – lactate and acetate producers, combines 5 different species, 453  
788 reactions, 355 metabolites
- 789 4. Bacteroides group – propionate/succinate and acetate producers, combines 8 different  
790 species, 609 reactions, 466 metabolites
- 791 5. Enterobacteria group – lactate, succinate and acetate producers, combines 3 different  
792 species, 607 reactions, 465 metabolites
- 793 6. Lachnospiridia group – mucin degrading and formate or 1,2-propanediol consumers,  
794 combines 6 different species, 511 reactions, 395 metabolites
- 795 7. Asaccharolytic group – lactate and amino acid degraders, combines 4 different species, 430  
796 reactions, 335 metabolites
- 797 8. Succinivorans group – succinate consumers (named after *Negativicoccus succinivorans*),  
798 combines 2 different species, 394 reactions, 309 metabolites

799 Individual metabolic networks representing respective metabolic groups (Supplementary Table S6)  
800 were combined to a Consortia type metabolic network by assigning common metabolite pool  
801 outside of intracellular space and removing duplicate exchange fluxes. The relative amounts of  
802 different species in consortia manifest through modified stoichiometric coefficients of transport  
803 reactions of respective bacteria that exchange matter between intracellular space and common  
804 metabolite pool. The final metabolic network of bacterial consortia consisted of 2774 metabolites  
805 and 3752 reactions.

806

### 807 *Biomass*

808 Biomass synthesis in model was described with separate consumption fluxes (sinks) for major  
809 biomass monomers and included 20 proteogenic amino acids, 8 (deoxy-)ribonucleotides, cell  
810 membrane lipids and peptidoglycan. The potential existence of glycogen, lipo- and  
811 exopolysaccharides in biomass was ignored as a simplification.

812 Biomass protein and RNA content were set to 50% and 12%, respectively and were assumed to be  
813 uniform in all species<sup>73</sup>. DNA content was determined assuming 1 chromosome per cell. The AA  
814 distribution in biomass was calculated from measured metaproteome data and was also assumed to  
815 be uniform in all species as simplification. Acquired values were inserted into model inputs  
816 (Supplementary Table 7). The cell mass was set to  $10^{-12}$  g and the shape was set to cylindrical with  
817 spherical caps with a height to radius ratio of 2 for all Gr+ groups (butyric, bifido, lachnospiridium,  
818 asaccharolytic and succinivorans) as well as Gr- groups (akkermansia, bacteroides and

819 enterobacteria). The amount of lipids and peptidoglycan needed per gram biomass was calculated  
820 from size and geometry of cells (Supplementary Table S8).

821

#### 822 *Flux Balance Analysis*

823 The flux balance analysis<sup>74</sup> model was generated in Wolfram Mathematica format using in-house  
824 software built in MatLab. Calculations were performed using Wolfram Mathematica 8.01 on a laptop  
825 computer with six-core Intel i7-8750H processor and 24GB RAM.

826 FBA input data (exchange fluxes, biomass sinks, Supplementary Table S7) were inserted into the  
827 model and calculations were performed with an increasing automatic error step of  $\pm 1\%$  to input  
828 fluxes until a feasible solution was found. Carbon mass balance analysis was performed to assess the  
829 physiological relevance of measured metabolome in respect of metabolic background of given  
830 organisms.

831

#### 832 *Sequence-based metabolism mapping from metaproteomics*

833 The metabolism of faecal cultures was mapped using an in-house database of bacterial metabolism.  
834 The DNA sequences for enzymes for key metabolic reactions were selected from the database and  
835 BLASTed using a local NCBI blastx function. The resulting amino acid sequences were then mapped  
836 to the peptides from the metaproteomic analysis. The sum of matching peptides per taxon was  
837 considered as protein copy number. The taxa were then divided into similar metabolic groups as in  
838 the Flux Balance Analysis (see “Construction of metabolic networks” under Materials and Methods).  
839 In total, 31 enzymes of central metabolism, 47 enzymes of glycan degradation and 26 enzymes of  
840 secondary metabolites synthesis were searched from 41 more abundant taxa.

841

#### 842 *Statistics*

843 Statistical analysis for fibre vs fibre+PCM comparisons was done with two-tailed paired t-test and  
844 corrected with Benjamini-Hochberg method. Multiple comparisons for all conditions were done  
845 with Dunn’s Kruskal-Wallis multiple comparisons and Benjamini-Hochberg correction. The  
846 statistical details of the experiments can be found in the figure legends, including the specific  
847 statistical tests used and the exact number of n. Differences were considered significant when  $p <$   
848 0.05.

849 Statistics were calculated with R version R-3-6-1.



850 **FIGURE LEGENDS**

851 **Figure 1** Fermentation of 14 dietary fibres and oligosaccharides by faecal microbiota using  
852 isothermal microcalorimetry. **a**, Heat evolution of substrate fermentation. Solid line represents  
853 average microbial growth curve on the selected poly- or oligosaccharide  $\pm$  95% CI, dotted line  
854 represents average microbial growth curve on the selected poly- or oligosaccharide + mucin  $\pm$  95%  
855 CI. n=2-7. **b**, Community composition on the selected substrates based on 16S rRNA sequencing.  
856 Average relative abundances of the top 17 genera. n=2-7. **c**, The number of different glycans  
857 identified from porcine gastric mucin (PGM) and porcine colonic mucin (PCM). **d**, Ordination plot of  
858 Bray-Curtis distances between microbial communities from cultivations on the selected substrates.  
859 Colours indicate the choice of dietary fibre, empty round dots represent samples from cultivation of  
860 fibre, filled round dots represent samples from cultivation of fibre+PCM or sole PCM. **e**, Boxplots  
861 showing changes in microbial numbers (mg/l) grown on the selected substrates. Colours indicate the  
862 choice of substrate, empty boxes represent samples from cultivation of fibre, filled boxes represent  
863 samples from cultivation of fibre+PCM or sole PCM. All replicates shown (two-tailed paired t-test, \*p  
864 < 0.05). GOS – galactooligosaccharides, Fur – furcellaran, InuHP – high-performance inulin, B-gluc –  
865  $\beta$ -glucan, PecA – apple pectin, Xyl – xylan, PGM – porcine gastric mucin, PCM – porcine colonic  
866 mucin, Med – growth medium control.

867

868 **Figure 2** The CAZymes detected after community growth on selected substrates. Enzymes grouped  
869 by CAZyme families are shown as intensity of the protein level. For each protein the respective  
870 bacterial genus is displayed colour coded on the left side. Three independent replicates are shown.  
871 For accession numbers and full data see Supplementary Table S2. PCM – porcine colonic mucin, B-  
872 gluc –  $\beta$ -glucan, PecA – apple pectin, Xyl – xylan.

873

874 **Figure 3** Metabolites profile of fermentation of selected substrates. **a**, Boxplots representing the  
875 concentrations of measured metabolites (mmol/gDW) and pH. Colours indicate the choice of  
876 substrate, empty boxes represent samples from cultivation of fibre, filled boxes represent samples  
877 from cultivation of fibre+PCM or sole PCM. All replicates shown (two-tailed paired t-test, \*p < 0.05).  
878 **b**, Average ( $\pm$ SEM) enzyme counts for reactions related to specific metabolite synthesis. n=3. **c**, The  
879 effect of microbial metabolites on murine colonic spheroids and mCherry-tagged MUC2 production.  
880 Counts and signal intensity of mCherry-positive goblet cells as a result of treating the spheroids with  
881 metabolites from fermentation of the selected substrates, measured by flow cytometry and  
882 normalized against medium control. n=3-4. B-gluc –  $\beta$ -glucan, InuHP – high-performance inulin,  
883 PecA – apple pectin, Xyl – xylan, PCM – porcine colonic mucin.

884

885 **Figure 4** Metabolic pathways of glycan degradation by faecal microbiota. **a**, The degradation of  
886 glycans from dietary fibres and mucin based on the metaproteomic analysis. The bacteria were  
887 divided into 8 groups based on their similar metabolism (see text). n=3. **b**, The degradation of  
888 glycans from dietary fibres and mucin and cross-feeding between bacterial groups based on Flux  
889 Balance Analysis. The bacteria were divided into 8 groups based on their similar metabolism (see  
890 text). n=3. PecA – apple pectin, Xyl – xylan, PCM – porcine colonic mucin.

891

892 **Supplementary Figure 1** Heat evolution of substrate fermentation. Solid line represents average  
893 microbial growth curve on the selected poly- or oligosaccharide  $\pm$  95% CI, dotted line represents  
894 average microbial growth curve on the selected poly- or oligosaccharide + mucin  $\pm$  95% CI. n=2-7. AP  
895 – amylopectin, InuHSI – high-soluble inulin, XOS – xylooligosaccharides, Car –  $\kappa$ -carrageenan, InuD –  
896 dahlia inulin, AG – arabinogalactan, PecC – citrus pectin, Psy – psyllium, PGM – porcine gastric  
897 mucin, PCM – porcine colonic mucin, Med – growth medium control.

898

899 **Supplementary Figure 2** Consortia composition assessed by 16S rRNA sequencing. **a**, Simpson alpha  
900 diversity indices for the panel of tested substrates. All replicates shown. **b**, The microbial  
901 composition of the inoculum. Pooled faecal samples from seven healthy donors. Average relative  
902 abundances of the top 21 genera. n=2 (separate aliquots of the pooled inoculum). **c**, Community  
903 composition on the selected substrates. Average relative abundances of the top 17 genera. n=2-7.  
904 Med – growth medium control, Inoc – inoculum control, AP – amylopectin, GOS –  
905 galactooligosaccharides, InuHSI – high-soluble inulin, XOS - xylooligosaccharides, Car –  $\kappa$ -  
906 carrageenan, Fur – furcellaran, InuD – dahlia inulin, InuHP – high-performance inulin, AG –  
907 arabinogalactan, B-gluc –  $\beta$ -glucan, PecA – apple pectin, PecC – citrus pectin, Psy – psyllium, Xyl –  
908 xylan, PGM – porcine gastric mucin, PCM – porcine colonic mucin.

909

910 **Supplementary Figure 3** Schematic representation of the polysaccharides and different putative  
911 CAZyme families targeting the respective linkages for **a**,  $\beta$ -glucan. **b**, inulin. **c**, pectin. **d**, xylan. **e**,  
912 mucin O- and N-glycans. Monosaccharide symbols are shown according to the Symbol Nomenclature  
913 for Glycan system <sup>75</sup>. GH – glycoside hydrolase, PL – polysaccharide lyase, CE – carbohydrate  
914 esterase.

915

916 **Supplementary Figure 4** Analysis of porcine gastric mucin (PGM) and colonic mucin (PCM)  
917 composition. **a**, Gel-forming mucins detected in different mucin samples by mass-spectrometry.  
918 Most abundant uncharacterised proteins in each sample were annotated with BLAST as: MUC2 –  
919 UniProt A0A4X1UH57; MUC5AC – UniProt A0A4X1UGK3; MUC6 – UniProt A0A4X1VZC0. **b**, Different  
920 glycan modifications detected in PGM and PCM. **c**, Mucin samples separated on a composite gel.  
921 MUC2 – Mucin-2, MUC5AC – Mucin-5AC, MUC6 – Mucin-6, PCM – porcine colonic mucin, PGM –  
922 porcine gastric mucin.

923

924 **Supplementary Figure 5** Boxplots showing changes in microbial numbers (mg/l) grown on the  
925 selected substrates. Colours indicate the choice of substrate, empty boxes represent samples from  
926 cultivation of fibre, filled boxes represent samples from cultivation of fibre+PCM or sole PCM. All  
927 replicates shown (two-tailed paired t-test, \*p < 0.05). **a**, Taxa affected by mucin addition. **b**, The  
928 most abundant taxa growing on InuHP. **c**, The most abundant taxa growing on B-gluc. B-gluc –  $\beta$ -  
929 glucan, InuHP – high-performance inulin, PecA – apple pectin, Xyl – xylan, PCM – porcine colonic  
930 mucin.

931

932 **Supplementary Figure 6** Quantification of the MUC2 in the samples after fermentation of the chosen  
933 substrates. **a**, Intensity of porcine MUC2 measured by mass-spectrometry. **b**, Coverage of porcine  
934 MUC2 domains. Numbers indicate the end of a tryptic peptide in the porcine MUC2 amino acid

935 sequence. Simplified MUC2 domain scheme has been adapted from UniProt database (protein  
936 sequence A0A5G2QSD1).

937

938 **Supplementary Figure 7** Metabolites profile of fermentation of selected substrates. **a**, Boxplots  
939 representing the concentrations of measured metabolites (mmol/gDW). Colours indicate the choice  
940 of substrate, empty boxes represent samples from cultivation of fibre, filled boxes represent  
941 samples from cultivation of fibre+PCM or sole PCM. All replicates shown. **b**, Boxplots representing  
942 Glu consumption ( $\Delta$ mmol/gDW). Colours indicate the choice of substrate, empty boxes represent  
943 samples from cultivation of fibre, filled boxes represent samples from cultivation of fibre+PCM or  
944 sole PCM. All replicates shown. **c**, Average ( $\pm$ SEM) enzyme counts for reactions related to specific  
945 metabolite synthesis. Colours indicate the choice of substrate, empty bars represent samples from  
946 cultivation of fibre, filled bars represent samples from cultivation of fibre+PCM or sole PCM. n=3. **d**,  
947 Average ( $\pm$ SEM) protein counts for two pyruvate synthesis enzymes on sole PCM fermentation by  
948 the 8 bacterial groups. B-gluc –  $\beta$ -glucan, InuHP – high-performance inulin, PecA – apple pectin, Xyl –  
949 xylan, PCM – porcine colonic mucin, Glu – glutamate, Bu – butyric group, A – akkermansia group, Bi –  
950 bifidoabacteria group, Ba – bacteroides group, E – enterobacteria group, L – lachnoclostridia group,  
951 As – asaccharolytic group, S – succinivorans group.

952

953 **Supplementary Figure 8** The effect of microbial metabolites on murine colonic spheroids and  
954 mCherry-tagged MUC2 production. **a**, Average counts and intensity ( $\pm$ SEM) of mCherry-positive  
955 goblet cells as a result of treating the spheroids with metabolites from fermentation of the selected  
956 substrates, measured by flow cytometry and normalized against medium control. n=3-4. **b**, Example  
957 of the gating strategy used in flow cytometry experiments. B-gluc –  $\beta$ -glucan, InuHP – high-  
958 performance inulin, PecA – apple pectin, Xyl – xylan, PCM – porcine colonic mucin.

959

960

961 **References**

- 962 1. Drula, E. *et al.* The carbohydrate-active enzyme database: Functions and literature. *Nucleic*  
963 *Acids Res.* **50**, D571–D577 (2022).
- 964 2. Barbeyron, T. *et al.* Matching the diversity of sulfated biomolecules: Creation of a  
965 classification database for sulfatases reflecting their substrate specificity. *PLoS One* **11**, 1–33  
966 (2016).
- 967 3. Park, J. H. *et al.* Promotion of intestinal epithelial cell turnover by commensal bacteria: Role  
968 of short-chain fatty acids. *PLoS One* **11**, 1–22 (2016).
- 969 4. Nakamura, A. *et al.* Symbiotic polyamine metabolism regulates epithelial proliferation and  
970 macrophage differentiation in the colon. *Nat. Commun.* **12**, 1–14 (2021).
- 971 5. Sabater-Molina, M. *et al.* Effects of dietary polyamines at physiologic doses in early-weaned  
972 piglets. *Nutrition* **25**, 940–946 (2009).
- 973 6. Hansson, G. C. Mucins and the Microbiome. *Annu. Rev. Biochem.* **89**, 769–793 (2020).
- 974 7. Arike, L. *et al.* Protein Turnover in Epithelial Cells and Mucus along the Gastrointestinal Tract  
975 Is Coordinated by the Spatial Location and Microbiota. *Cell Rep.* **30**, 1077-1087.e3 (2020).
- 976 8. Johansson, M. E. V. *et al.* Normalization of host intestinal mucus layers requires long-term  
977 microbial colonization. *Cell Host Microbe* **18**, 582–592 (2015).
- 978 9. Jakobsson, H. E. *et al.* The composition of the gut microbiota shapes the colon mucus barrier.  
979 *EMBO Rep.* **16**, 164–177 (2015).
- 980 10. Desai, M. S. *et al.* A Dietary Fiber-Deprived Gut Microbiota Degrades the Colonic Mucus  
981 Barrier and Enhances Pathogen Susceptibility. *Cell* **167**, 1339-1353.e21 (2016).
- 982 11. Schroeder, B. O. *et al.* Bifidobacteria or fiber protect against diet-induced microbiota-  
983 mediated colonic mucus deterioration. *Cell Host Microbe* **23**, 27–40 (2018).

- 984 12. Crouch, L. I. *et al.* Prominent members of the human gut microbiota express endo-acting O-  
985 glycanases to initiate mucin breakdown. *Nat. Commun.* **11**, (2020).
- 986 13. Taleb, V. *et al.* Structural and mechanistic insights into the cleavage of clustered O -glycan  
987 patches- containing glycoproteins by mucinases of the human gut. *Nat. Commun.* 1–15  
988 (2022). doi:10.1038/s41467-022-32021-9
- 989 14. Kostopoulos, I. *et al.* Akkermansia muciniphila uses human milk oligosaccharides to thrive in  
990 the early life conditions in vitro. *Sci. Rep.* **10**, 1–17 (2020).
- 991 15. Luis, A. S. *et al.* A single sulfatase is required to access colonic mucin by a gut bacterium.  
992 *Nature* **598**, 332–337 (2021).
- 993 16. Tran, T. H. T. *et al.* Adding mucins to an in vitro batch fermentation model of the large  
994 intestine induces changes in microbial population isolated from porcine feces depending on  
995 the substrate. *FEMS Microbiol. Ecol.* **92**, 1–13 (2016).
- 996 17. Adamberg, K., Kolk, K., Jaagura, M., Vilu, R. & Adamberg, S. The composition and metabolism  
997 of faecal microbiota is specifically modulated by different dietary polysaccharides and mucin:  
998 An isothermal microcalorimetry study. *Benef. Microbes* **9**, 21–34 (2018).
- 999 18. Adamberg, K., Raba, G. & Adamberg, S. Use of Changestat for Growth Rate Studies of Gut  
1000 Microbiota. *Front. Bioeng. Biotechnol.* **8**, 1–12 (2020).
- 1001 19. Raba, G., Adamberg, S. & Adamberg, K. Acidic pH enhances butyrate production from pectin  
1002 by faecal microbiota. *FEMS Microbiol. Lett.* **368**, 1–8 (2021).
- 1003 20. Rodríguez-Piñeiro, A. M. *et al.* Studies of mucus in mouse stomach, small intestine, and colon.  
1004 II. Gastrointestinal mucus proteome reveals Muc2 and Muc5ac accompanied by a set of core  
1005 proteins. *Am. J. Physiol. - Gastrointest. Liver Physiol.* **305**, 348–356 (2013).
- 1006 21. Holmén Larsson, J. M., Thomsson, K. A., Rodríguez-Piñeiro, A. M., Karlsson, H. & Hansson, G.

- 1007 C. Studies of mucus in mouse stomach, small intestine, and colon. III. Gastrointestinal Muc5ac  
1008 and Muc2 mucin O-glycan patterns reveal a regiospecific distribution. *Am. J. Physiol.*  
1009 *Gastrointest. Liver Physiol.* **305**, G357-363 (2013).
- 1010 22. Kaoutari, A. El, Armougom, F., Gordon, J. I., Raoult, D. & Henrissat, B. The abundance and  
1011 variety of carbohydrate-active enzymes in the human gut microbiota. *Nat. Rev. Microbiol.* **11**,  
1012 497–504 (2013).
- 1013 23. Png, C. W. *et al.* Mucolytic bacteria with increased prevalence in IBD mucosa augment in vitro  
1014 utilization of mucin by other bacteria. *Am. J. Gastroenterol.* **105**, 2420–2428 (2010).
- 1015 24. Tailford, L. E., Crost, E. H., Kavanaugh, D. & Juge, N. Mucin glycan foraging in the human gut  
1016 microbiome. *Front. Genet.* **5**, (2015).
- 1017 25. Belzer, C. *et al.* Microbial metabolic networks at the mucus layer lead to diet-independent  
1018 butyrate and vitamin B12 production by intestinal symbionts. *MBio* **8**, (2017).
- 1019 26. Luis, A. S. *et al.* Dietary pectic glycans are degraded by coordinated enzyme pathways in  
1020 human colonic Bacteroides. *Nat. Microbiol.* **3**, 210–219 (2018).
- 1021 27. Ndeh, D. *et al.* Complex pectin metabolism by gut bacteria reveals novel catalytic functions.  
1022 *Nature* **544**, 65–70 (2017).
- 1023 28. Munoz-Munoz, J. *et al.* An evolutionarily distinct family of polysaccharide lyases removes  
1024 rhamnose capping of complex arabinogalactan proteins. *J. Biol. Chem.* **292**, 13271–13283  
1025 (2017).
- 1026 29. Li, X., Jensen, R. L., Højberg, O., Canibe, N. & Jensen, B. B. *Olsenella scatoligenes* sp. nov., a 3-  
1027 methylindole- (skatole) and 4-methylphenol- (p-cresol) producing bacterium isolated from pig  
1028 faeces. *Int. J. Syst. Evol. Microbiol.* **65**, 1227 (2015).
- 1029 30. Rogowski, A. *et al.* Glycan complexity dictates microbial resource allocation in the large

- 1030 intestine. *Nat. Commun.* **6**, (2015).
- 1031 31. Davey, L., Dolat, L., Holmes, Z., Ansaldo, E. & Berkeley, U. C. Mucin foraging enables  
1032 *Akkermansia muciniphila* to compete against other microbes in the gut and to modulate host  
1033 sterol biosynthesis. *Under Rev. Nat. Portf.* (2022).
- 1034 32. Ottman, N. *et al.* Genome-Scale Model and Omics Analysis of Metabolic Capacities of  
1035 *Akkermansia muciniphila* Reveal a Preferential Mucin-Degrading Lifestyle. *Appl. Environ.*  
1036 *Microbiol.* **83**, 1–15 (2017).
- 1037 33. Kaiko, G. E. *et al.* The Colonic Crypt Protects Stem Cells from Microbiota-Derived Metabolites.  
1038 *Cell* **165**, 1708–1720 (2016).
- 1039 34. Dougherty, M. W. *et al.* Gut microbiota maturation during early human life induces  
1040 enterocyte proliferation via microbial metabolites. *BMC Microbiol.* **20**, 1–14 (2020).
- 1041 35. Chung, W. S. F. *et al.* Modulation of the human gut microbiota by dietary fibres occurs at the  
1042 species level. *BMC Biol.* **14**, 1–13 (2016).
- 1043 36. Ndeh, D. & Gilbert, H. J. Biochemistry of complex glycan depolymerisation by the human gut  
1044 microbiota. *FEMS Microbiol. Rev.* **42**, 146–164 (2018).
- 1045 37. Cantu-Jungles, T. M. & Hamaker, B. R. New View on Dietary Fiber Selection for Predictable  
1046 Shifts in Gut Microbiota. *MBio* **11**, 1–8 (2020).
- 1047 38. Cantu-Jungles, T. M. *et al.* Dietary Fiber Hierarchical Specificity: the Missing Link for  
1048 Predictable and Strong Shifts in Gut Bacterial Communities. (2021).  
1049 doi:<https://doi.org/10.1128/mBio.01028-21>
- 1050 39. Martens, E. C. *et al.* Recognition and degradation of plant cell wall polysaccharides by two  
1051 human gut symbionts. *PLoS Biol.* **9**, (2011).
- 1052 40. Petkovic, M., Seddon, K. R., Rebelo, L. P. N. & Pereira, C. S. Ionic liquids: A pathway to

- 1053 environmental acceptability. *Chem. Soc. Rev.* **40**, 1383–1403 (2011).
- 1054 41. Kostopoulos, I. *et al.* A Continuous Battle for Host-Derived Glycans Between a Mucus  
1055 Specialist and a Glycan Generalist in vitro and in vivo. *Front. Microbiol.* **12**, 1–14 (2021).
- 1056 42. Dao, M. C. *et al.* Akkermansia muciniphila and improved metabolic health during a dietary  
1057 intervention in obesity: Relationship with gut microbiome richness and ecology. *Gut* **65**, 426–  
1058 436 (2016).
- 1059 43. Depommier, C. *et al.* Supplementation with Akkermansia muciniphila in overweight and  
1060 obese human volunteers: a proof-of-concept exploratory study. *Nat. Med.* **25**, 1096–1103  
1061 (2019).
- 1062 44. Bian, X. *et al.* Administration of Akkermansia muciniphila Ameliorates Dextran Sulfate  
1063 Sodium-Induced Ulcerative Colitis in Mice. *Front. Microbiol.* **10**, 1–18 (2019).
- 1064 45. Zhang, T. *et al.* Alterations of Akkermansia muciniphila in the inflammatory bowel disease  
1065 patients with washed microbiota transplantation. *Appl. Microbiol. Biotechnol.* **104**, 10203–  
1066 10215 (2020).
- 1067 46. Sokol, H. *et al.* Faecalibacterium prausnitzii is an anti-inflammatory commensal bacterium  
1068 identified by gut microbiota analysis of Crohn disease patients. *Proc. Natl. Acad. Sci. U. S. A.*  
1069 **105**, 16731–16736 (2008).
- 1070 47. Carlsson, A. H. *et al.* Faecalibacterium prausnitzii supernatant improves intestinal barrier  
1071 function in mice DSS colitis. *Scand. J. Gastroenterol.* **48**, 1136–1144 (2013).
- 1072 48. Martín, R. *et al.* Faecalibacterium prausnitzii prevents physiological damages in a chronic low-  
1073 grade inflammation murine model. *BMC Microbiol.* **15**, 1–12 (2015).
- 1074 49. Meng, X. *et al.* A Purified Aspartic Protease from Akkermansia Muciniphila Plays an Important  
1075 Role in Degrading Muc2. *Int. J. Mol. Sci.* **22**, 1–2 (2021).

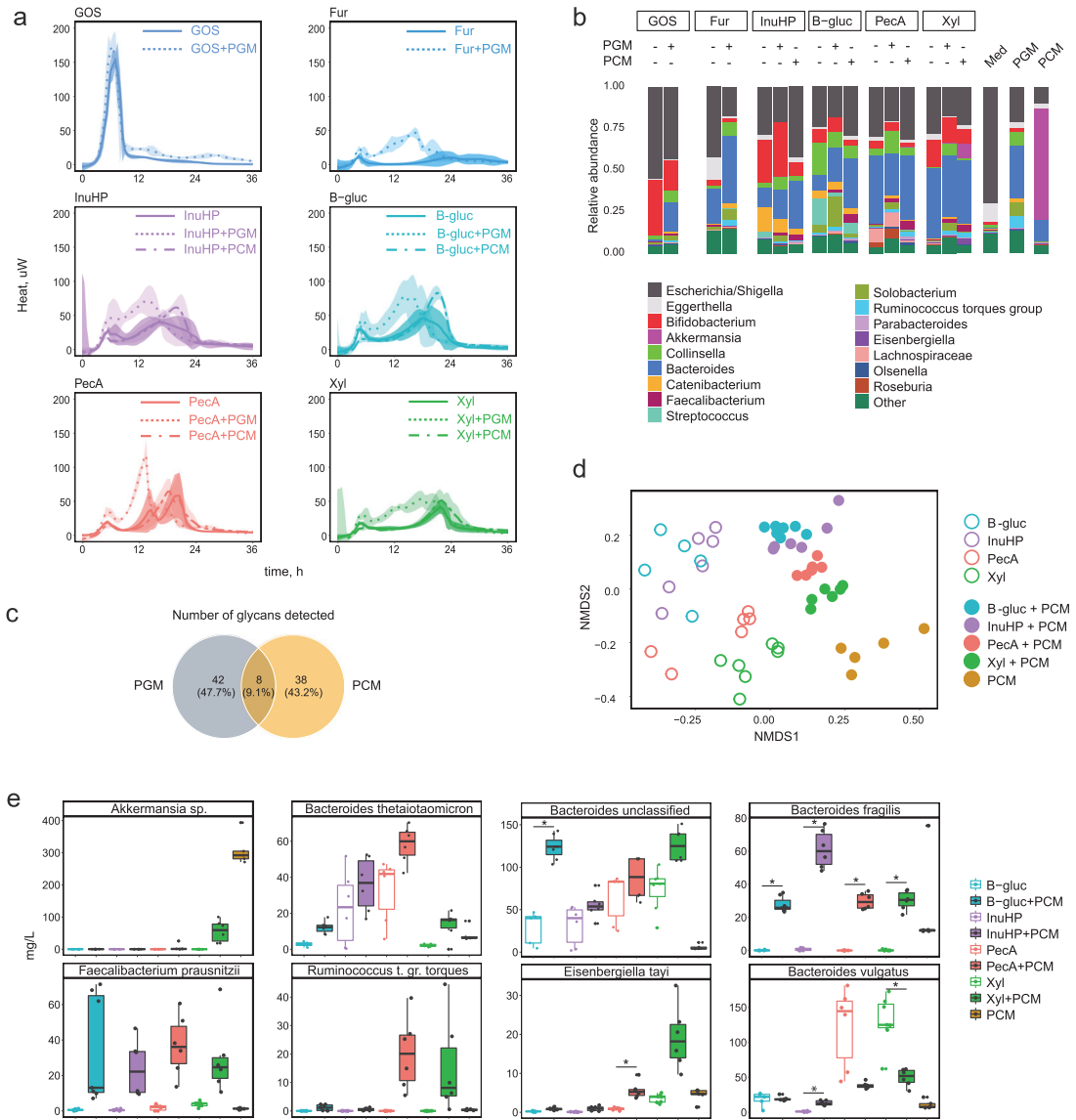


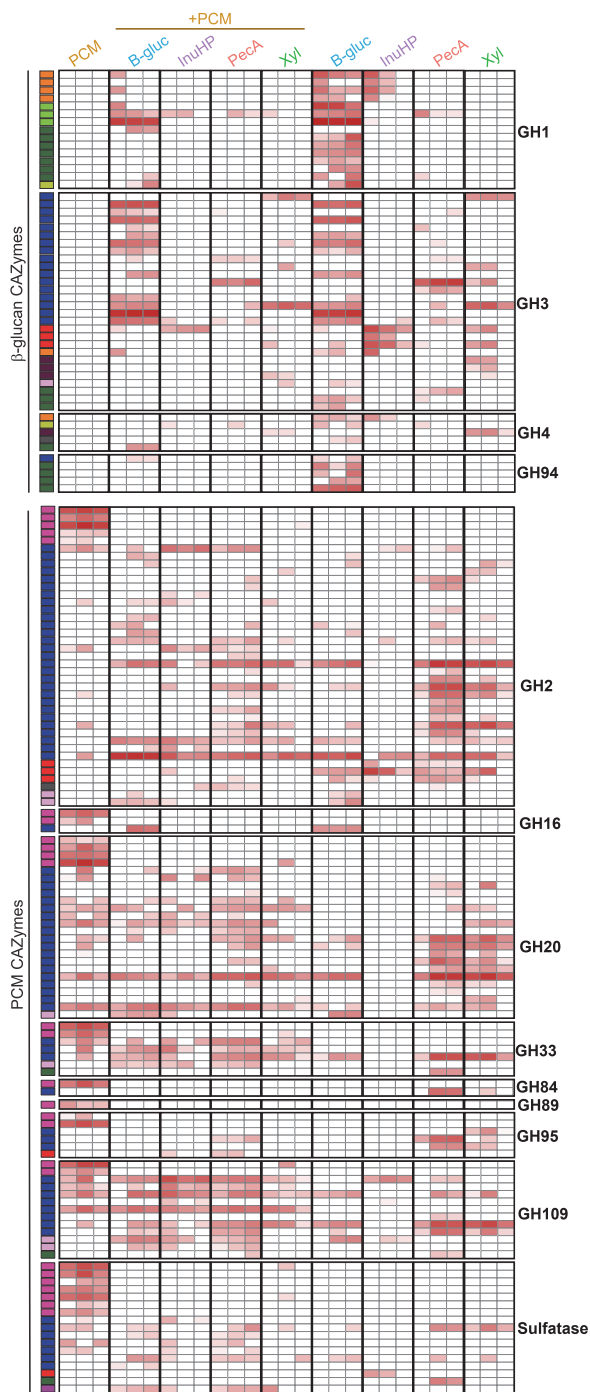
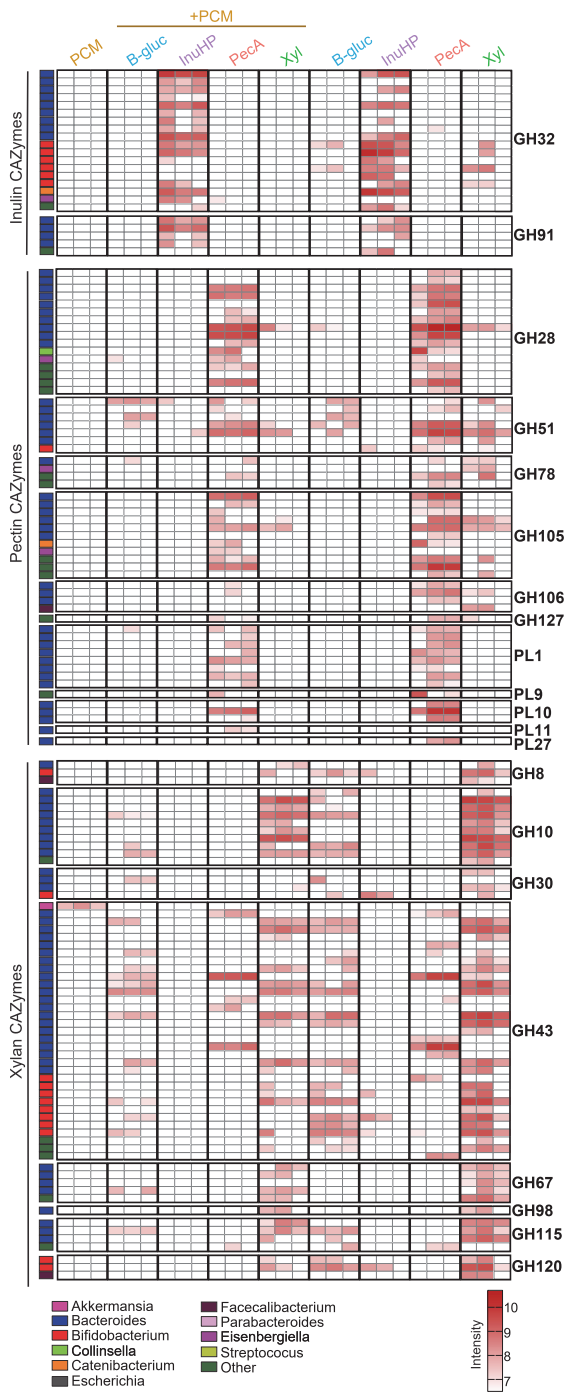
- 1076 50. Trastoy, B., Naegeli, A., Anso, I., Sjögren, J. & Guerin, M. E. Structural basis of mammalian  
1077 mucin processing by the human gut O-glycopeptidase OgpA from *Akkermansia muciniphila*.  
1078 *Nat. Commun.* **11**, 1–14 (2020).
- 1079 51. Derrien, M., Vaughan, E. E., Plugge, C. M. & de Vos, W. M. *Akkermansia muciniphila* gen. nov.,  
1080 sp. nov., a human intestinal mucin-degrading bacterium. *Int. J. Syst. Evol. Microbiol.* **54**,  
1081 1469–1476 (2004).
- 1082 52. La Rosa, S. L. *et al.* Wood-Derived Dietary Fibers Promote Beneficial Human Gut Microbiota.  
1083 *mSphere* **4**, 1–16 (2019).
- 1084 53. Bernard, K. *et al.* Characterization of isolates of *Eisenbergiella tayi*, a strictly anaerobic Gram-  
1085 stain variable bacillus recovered from human clinical materials in Canada. *Anaerobe* **44**, 128–  
1086 132 (2017).
- 1087 54. Ostrowski, M. P. *et al.* Mechanistic insights into consumption of the food additive xanthan  
1088 gum by the human gut microbiota. *Nat. Microbiol.* **7**, 556–569 (2022).
- 1089 55. del Rio, B. *et al.* An altered gene expression profile in tyramine-exposed intestinal cell  
1090 cultures supports the genotoxicity of this biogenic amine at dietary concentrations. *Sci. Rep.*  
1091 **8**, 1–8 (2018).
- 1092 56. Bekebrede, A. F., Keijzer, J., Gerrits, W. J. J. & de Boer, V. C. J. The molecular and physiological  
1093 effects of protein-derived polyamines in the intestine. *Nutrients* **12**, 1–18 (2020).
- 1094 57. Bilotta, A. J. *et al.* Propionate Enhances Cell Speed and Persistence to Promote Intestinal  
1095 Epithelial Turnover and Repair. *Cmgh* **11**, 1023–1044 (2021).
- 1096 58. Wiśniewski, J. R., Zougman, A., Nagaraj, N. & Mann, M. Universal sample preparation method  
1097 for proteome analysis. *Nat. Methods* **6**, 359–362 (2009).
- 1098 59. Rappsilber, J., Mann, M. & Ishihama, Y. Protocol for micro-purification, enrichment, pre-

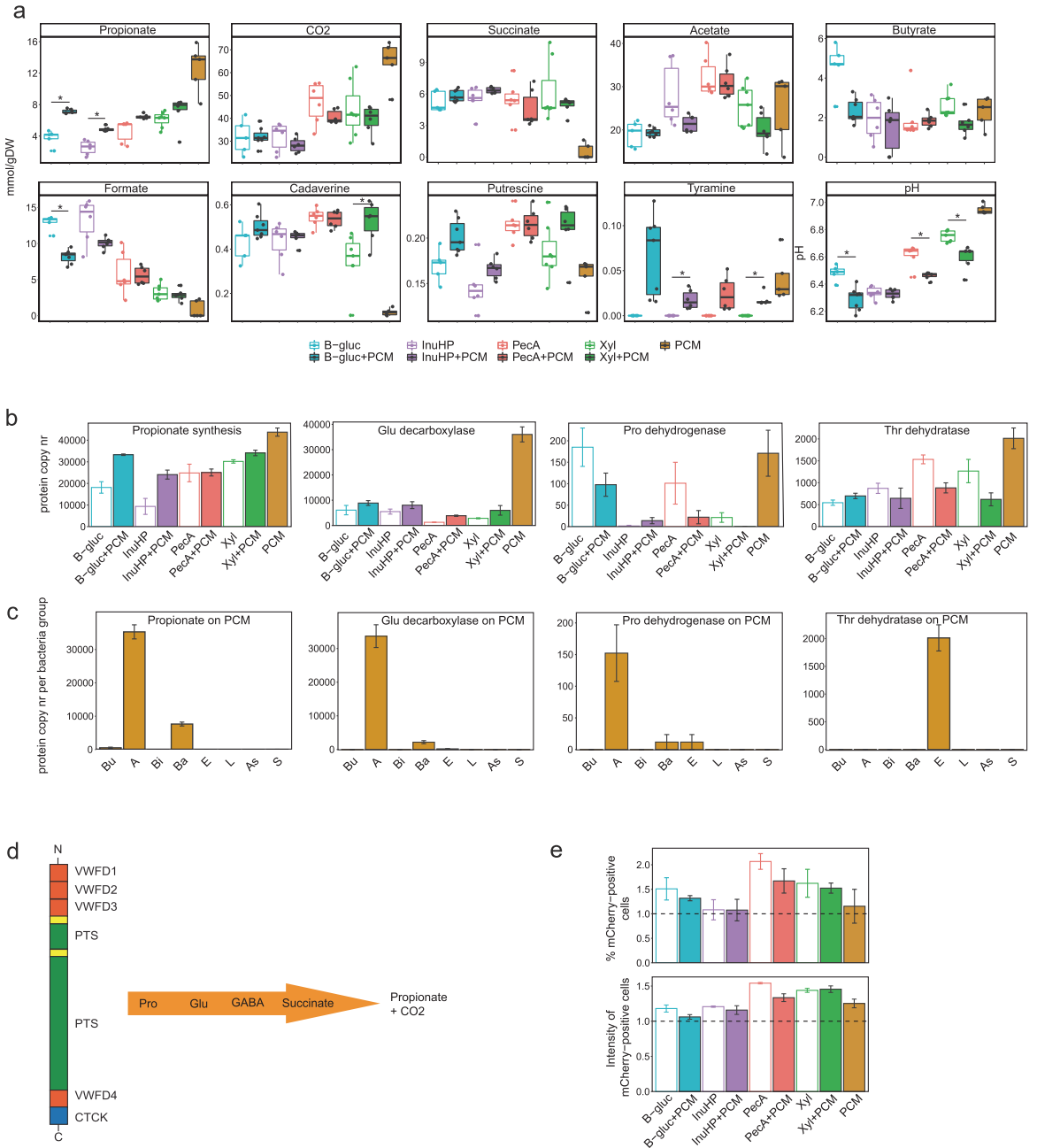
- 1099 fractionation and storage of peptides for proteomics using StageTips. *Nat. Protoc.* **2**, 1896–  
1100 1906 (2007).
- 1101 60. Ma, B. *et al.* PEAKS: Powerful software for peptide de novo sequencing by tandem mass  
1102 spectrometry. *Rapid Commun. Mass Spectrom.* **17**, 2337–2342 (2003).
- 1103 61. Mooradian, A. D., Van Der Post, S., Naegle, K. M. & Held, J. M. ProteoClade: A taxonomic  
1104 toolkit for multispecies and metaproteomic analysis. *PLoS Comput. Biol.* **16**, 1–12 (2020).
- 1105 62. Bateman, A. *et al.* UniProt: the universal protein knowledgebase in 2021. *Nucleic Acids Res.*  
1106 **49**, D480–D489 (2021).
- 1107 63. Cox, J. & Mann, M. MaxQuant enables high peptide identification rates, individualized p.p.b.-  
1108 range mass accuracies and proteome-wide protein quantification. *Nat. Biotechnol.* **26**, 1367–  
1109 1372 (2008).
- 1110 64. Vizcaíno, J. A. *et al.* The Proteomics Identifications (PRIDE) database and associated tools:  
1111 Status in 2013. *Nucleic Acids Res.* **41**, (2013).
- 1112 65. Ravi, A. Linking carbohydrate structure with function in the human gut microbiome using  
1113 hybrid metagenome assemblies. (2021).  
1114 doi:<https://whhttps://doi.org/10.1101/2021.05.11.441322>
- 1115 66. Schulz, B. L., Packer, N. H. & Karlsson, N. G. Small-scale analysis of O-linked oligosaccharides  
1116 from glycoproteins and mucins separated by gel electrophoresis. *Anal. Chem.* **74**, 6088–6097  
1117 (2002).
- 1118 67. Recktenwald, C. V. & Hansson, G. C. The reduction-insensitive bonds of the MUC2 mucin are  
1119 isopeptide bonds. *J. Biol. Chem.* **291**, 13580–13590 (2016).
- 1120 68. Sander, R. Compilation of Henry’s law constants (version 4.0) for water as solvent. *Atmos.*  
1121 *Chem. Phys.* **15**, 4399–4981 (2015).

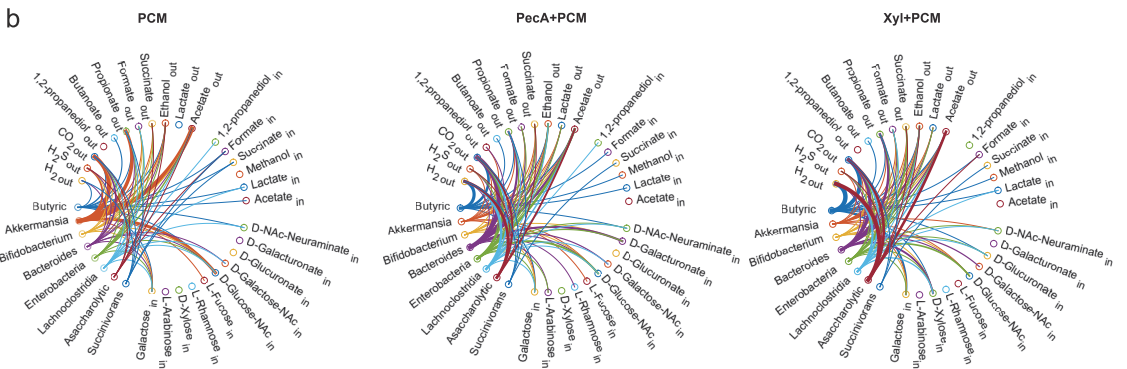
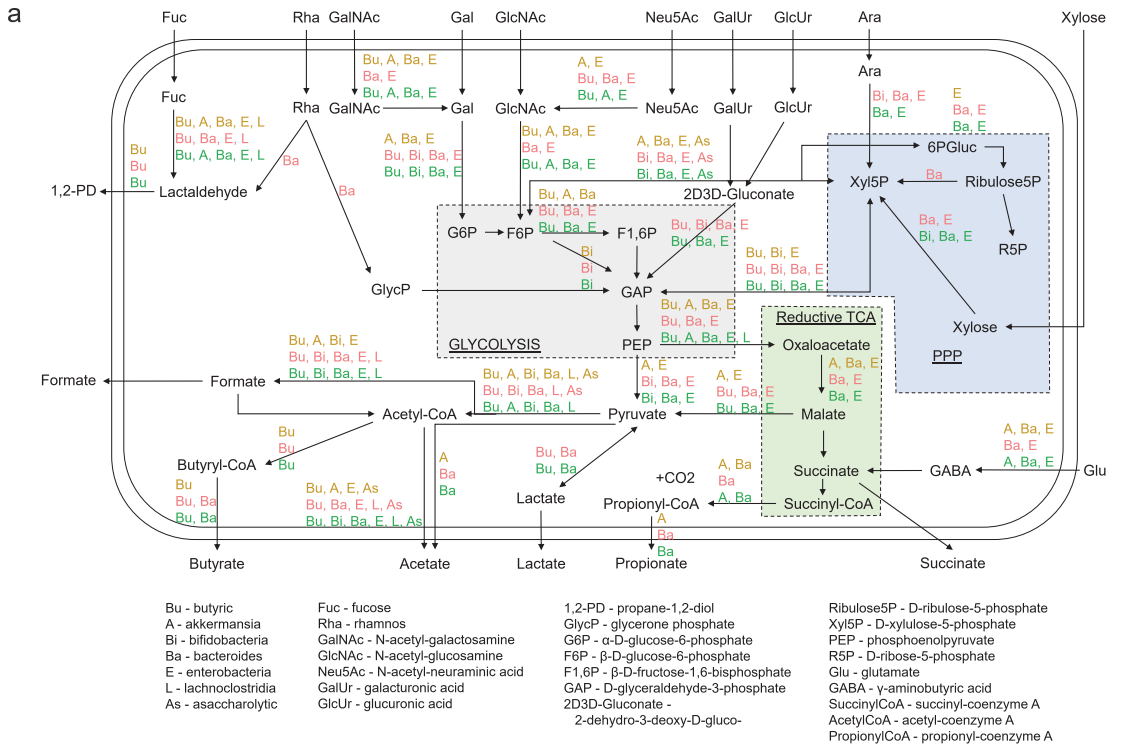
- 1122 69. Birchenough, G. M. H., Nystrom, E. E. L., Johansson, M. E. V. & Hansson, G. C. A sentinel  
1123 goblet cell guards the colonic crypt by triggering Nlrp6-dependent Muc2 secretion. *Science*  
1124 (80-. ). **352**, 1535–1542 (2016).
- 1125 70. Miyoshi, H. & Stappenbeck, T. S. In vitro expansion and genetic modification of  
1126 gastrointestinal stem cells in spheroid culture. *Nat. Protoc.* **8**, 2471–2482 (2013).
- 1127 71. Caspi, R. *et al.* The MetaCyc database of metabolic pathways and enzymes-a 2019 update.  
1128 *Nucleic Acids Res.* **48**, D455–D453 (2020).
- 1129 72. Kanehisa, M. & Goto, S. KEGG: Kyoto Encyclopedia of Genes and Genomes. *Nucleic Acids Res.*  
1130 **28**, 27–30 (2000).
- 1131 73. Hanegraaf, P. P. F. & Muller, E. B. The dynamics of the macromolecular composition of  
1132 biomass. *J. Theor. Biol.* **212**, 237–251 (2001).
- 1133 74. Orth, J. D., Thiele, I. & Palsson, B. O. What is flux balance analysis? *Nat. Biotechnol.* **28**, 245–  
1134 248 (2010).
- 1135 75. Varki, A. *et al.* Symbol nomenclature for graphical representations of glycans. *Glycobiology*  
1136 **25**, 1323–1324 (2015).
- 1137

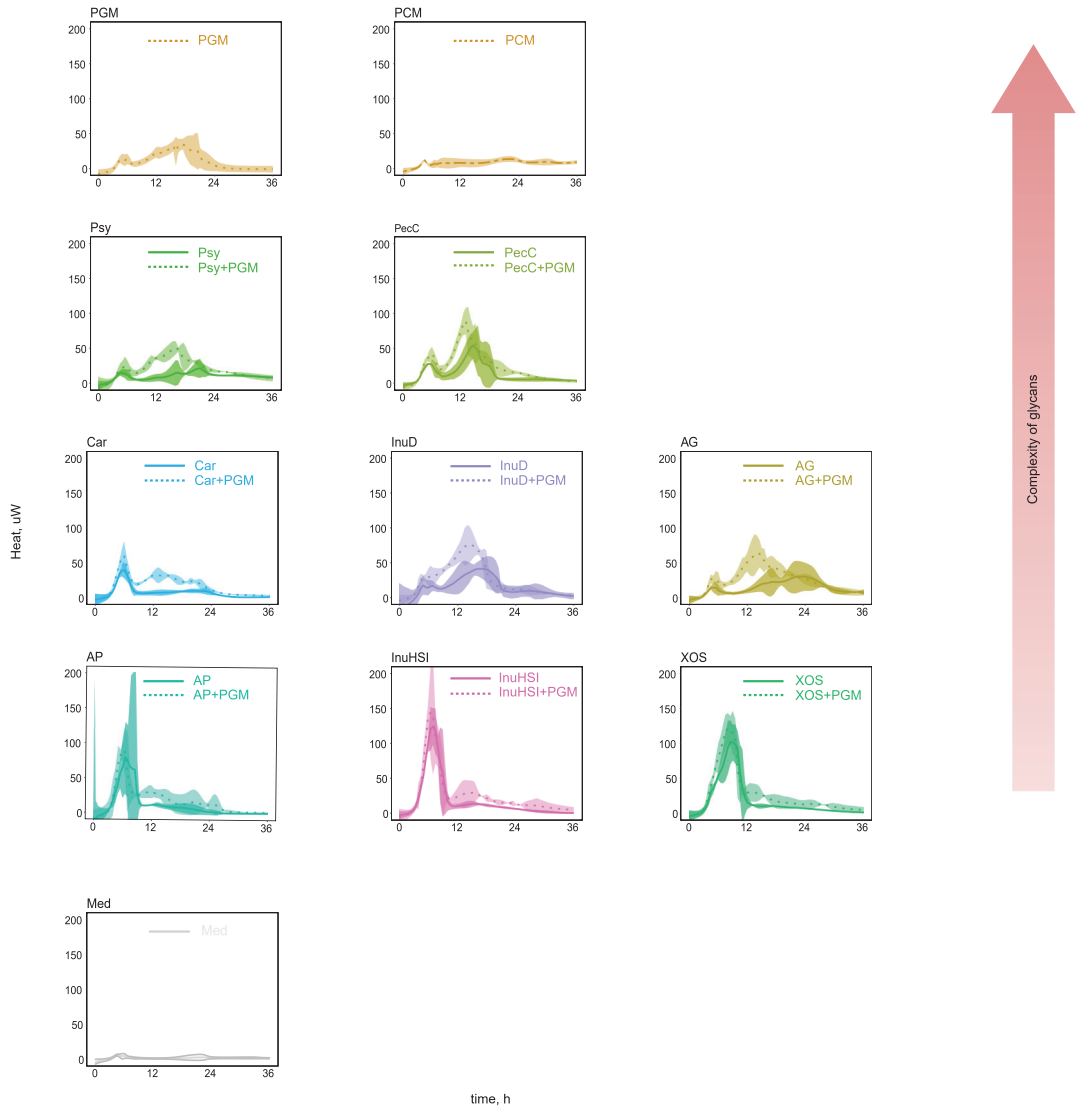
Figure 1





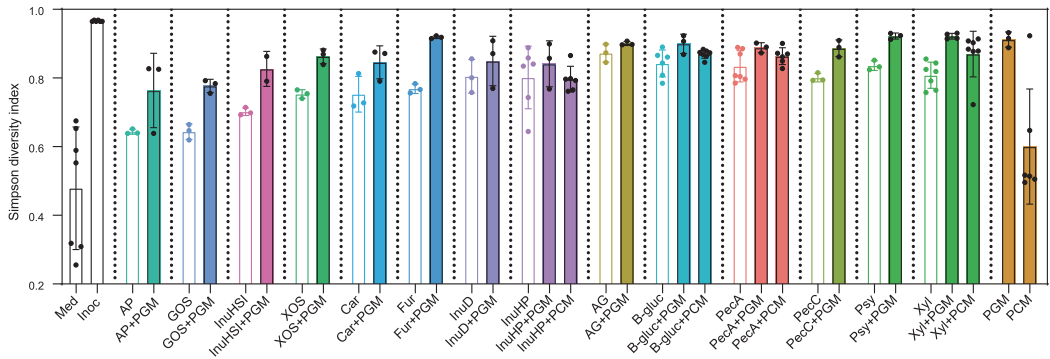




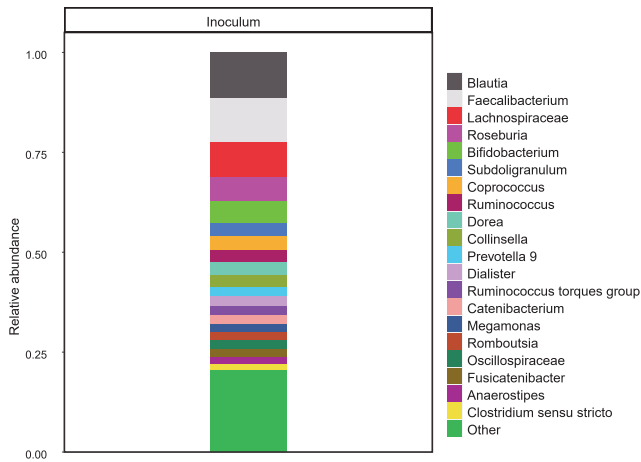




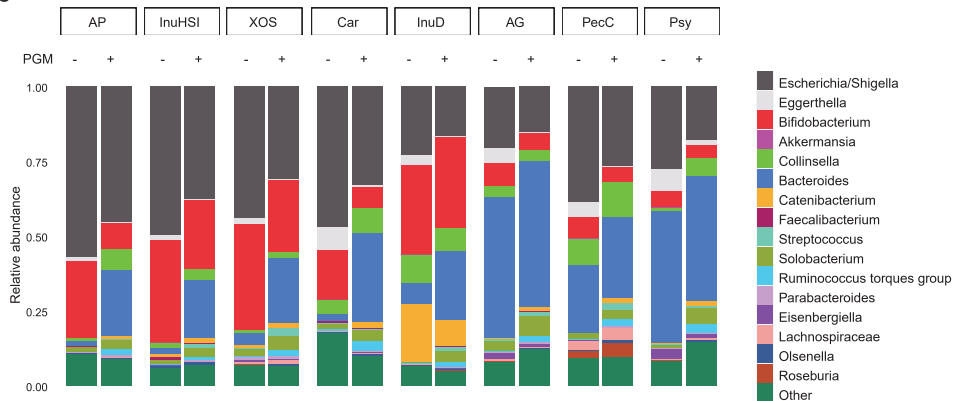
a



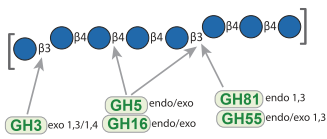
b



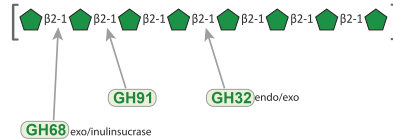
c



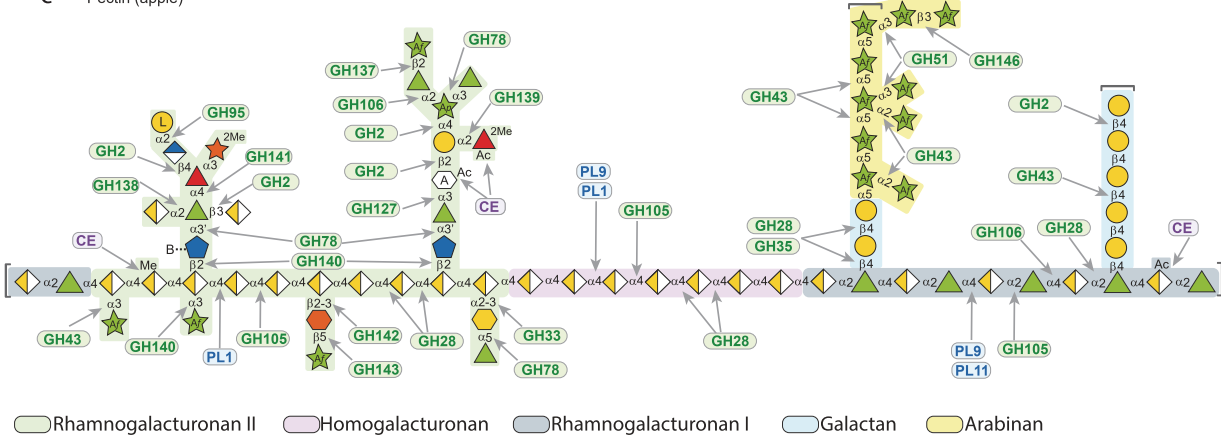
a  $\beta$ -glucan (oat)



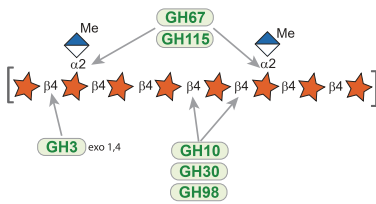
b Inulin



c Pectin (apple)

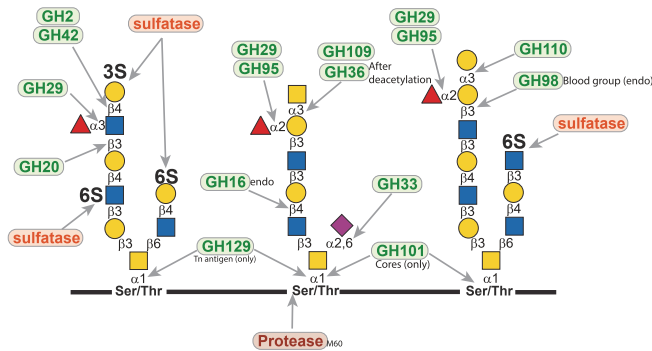


d Xylan (birchwood glucuronoxylan)

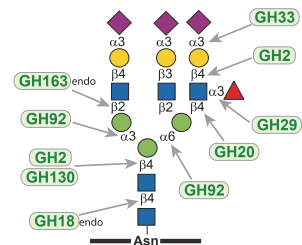


e Mucin (host) glycans

O-glycans

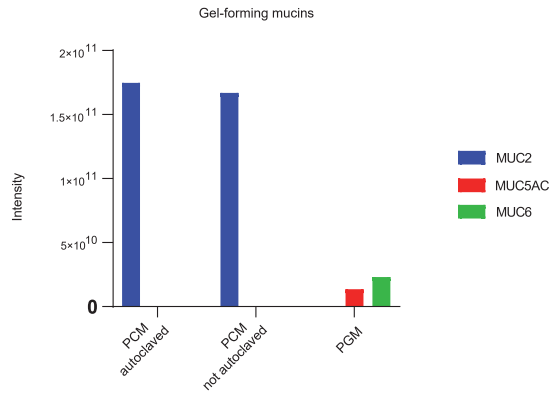


N-glycans

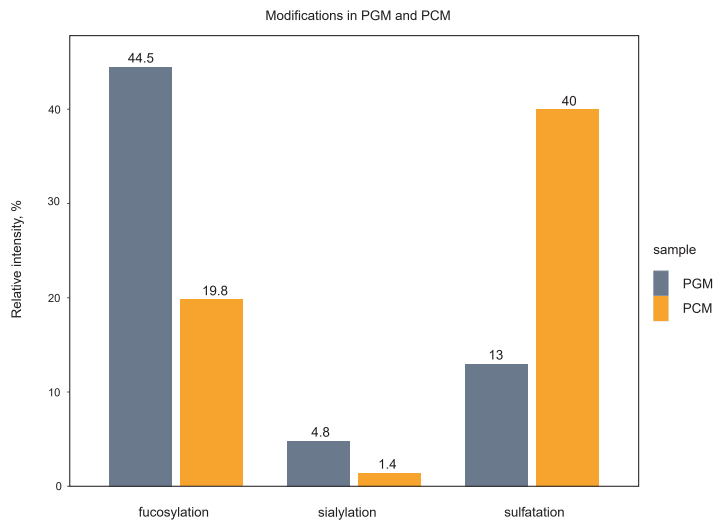


- |                     |                   |                             |                                  |
|---------------------|-------------------|-----------------------------|----------------------------------|
| D-Glucose           | D-Apiose          | L-Aceric acid               | N-Acetyl-D-galactosamine         |
| D-Fructose          | L-Fucose          | D-Dha                       | Mannose                          |
| D-Galacturonic acid | D-Glucuronic acid | D-Kdo                       | N-Acetyl-D-glucosamine           |
| L-Rhamnose          | D-Galactose       | <b>Me</b> Methyl ester      | N-Acetylneuraminic acid (Neu5Ac) |
| L-Arabinofuranose   | L-Galactose       | <b>2Me</b> 2-O-Methyl ester | <b>S</b> O-sulfate               |
| L-Arabinopyranose   | D-Xylose          | <b>Ac</b> Acetyl            |                                  |

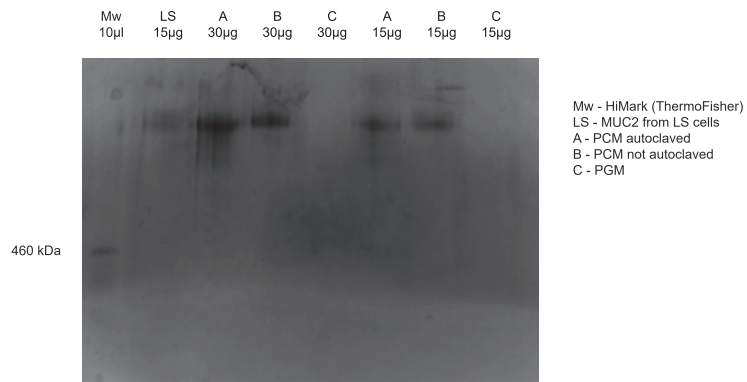
a



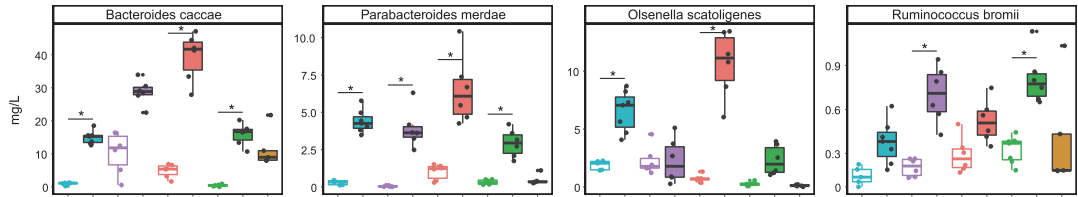
b



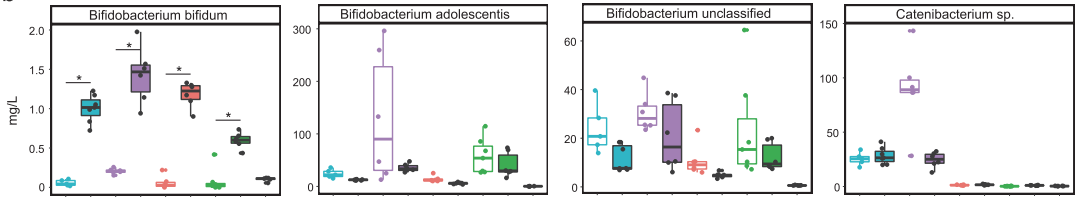
c



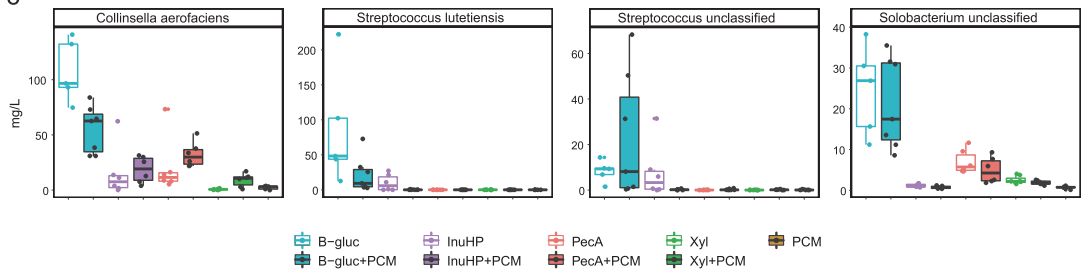
a

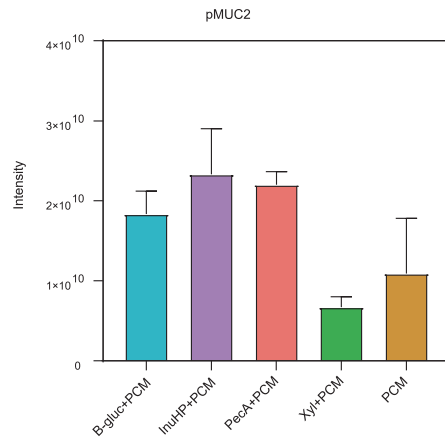


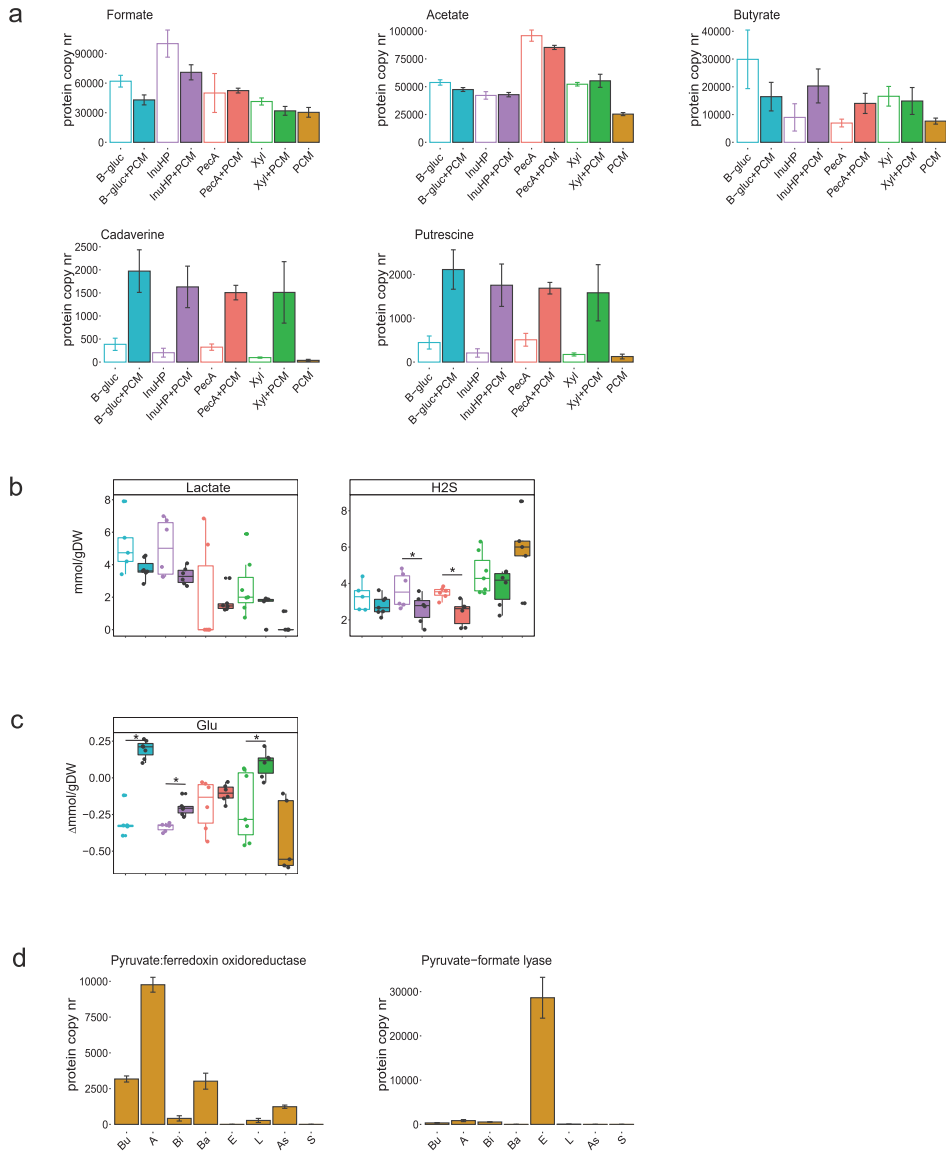
b



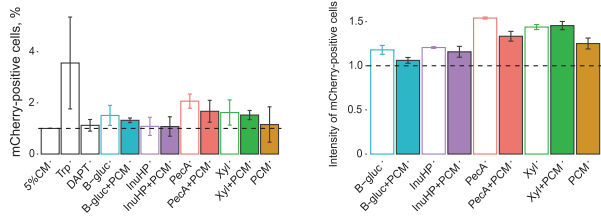
c



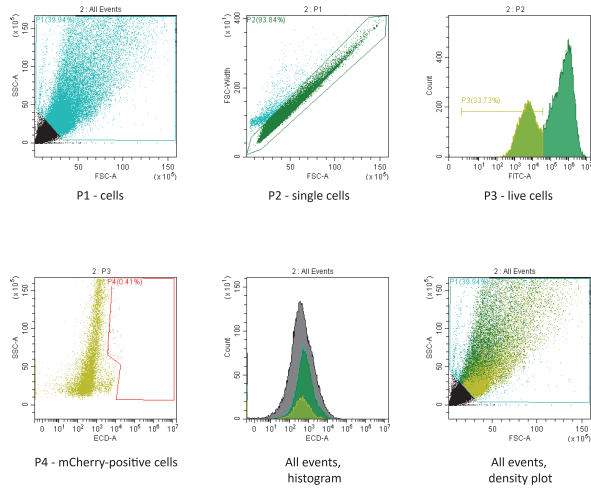




a



b



Tube Name: 2  
Sample ID:

Population	Events	% Total	% Parent	GeoMean ECD-A
● All Events	71105	100.00%	100.00%	358.4
● P1	28398	39.94%	39.94%	583.8
● P2	26649	37.48%	93.84%	594.3
● P3	8989	12.64%	33.73%	385.9
● P4	37	0.05%	0.41%	8299.5

# Curriculum vitae

## Personal data

Name: Grete Raba  
Date of birth: 02.10.1991  
Place of birth: Estonia  
Citizenship: Estonia

## Contact data

E-mail: greteraba@gmail.com

## Education

2016–2023 Tallinn University of Technology, PhD  
2014–2016 Tallinn University of Technology, MSc  
2011–2014 Tallinn University of Technology, BSc  
2008–2011 Viljandi Maagümnaasium, High school

## Language competence

Estonian Native  
English Fluent

## Professional employment

2022 Tallinn University of Technology, Junior Researcher (1.0)  
2017–2019 Tallinn University of Technology, Junior Researcher (0.9)  
2016 Tallinn University of Technology, Junior Researcher (0.75)  
2012–2013 Tallinn University of Technology, Other staff (0.5)

## Scholarships and awards

2021 FEMS Microbiology Letters Poster Prize on the occasion of 2<sup>nd</sup> International Conference on Microbial Food & Feed Ingredients  
2020 Dora Plus activity 1.2: PhD student mobility; Archimedes  
2019 Kristjan Jaak scholarship for study periods abroad; Archimedes  
2018 Erasmus+ learning mobility for students within Europe; Archimedes  
2018 Dora Plus activity 1.1: Short-term study mobility; Archimedes

## External studies

October–November 2020 University of Gothenburg; Gothenburg, Sweden  
March–May 2020 University of Gothenburg; Gothenburg, Sweden  
March–May 2019 University of Gothenburg; Gothenburg, Sweden



## Courses and conferences

November 2021	2 <sup>nd</sup> International Conference on Microbial Food & Feed Ingredients (MiFFI); Copenhagen, Denmark. Poster presentation
September 2019	Intensive course “Pro-, pre-, syn- and postbiotics: the effect on our microbiota and health”; Tartu, Estonia
July 2019	“Mucins in health and disease (15 <sup>th</sup> International Workshop on Carcinoma-associated Mucins)”; Cambridge, UK. Poster presentation
November 2018	University of Tartu Institute of Biomedicine and Translational Medicine workshop “Microbiome”; Tartu, Estonia
September 2018	8 <sup>th</sup> IUPAC International Conference on Green Chemistry; Bangkok, Thailand. Poster presentation
August 2018	Copenhagen Plant Science Centre PhD Summer School “Synthetic Biology: From Pro- to Eukaryotic Systems (SynBioSys)”; Copenhagen, Denmark
July 2018	International Conference on Organic Synthesis BOS 2018; Tallinn, Estonia. Poster presentation
September 2017	S3C Summer School on Sustainable Chemistry for Sustainable Development; Lüneburg, Germany
February 2017	Solvay Institute Workshop on Ionic Liquids: from fundamentals to applications; Brussels, Belgium. Poster presentation

## Supervised theses

2021	Julika Leppik “Relationships between microbiota, pH and organic acids”
------	------------------------------------------------------------------------

## Publications

**Raba, G.**, Luis, A. S. Mucin utilization by gut microbiota – recent advances on characterization of key enzymes. *Essays in Biochemistry*. 2023 Jan 25:EBC20220121. Doi: 10.1042/EBC20220121.

Kapitanov, I. V, **Raba, G.**, Špulák, M., Vilu, R., Karpichev, Y., Gathergood, N. Design of sustainable ionic liquids based on l-phenylalanine and L-alanine dipeptides: Synthesis, toxicity and biodegradation studies. *Journal of Molecular Liquids*. 2023, 374, 121285. Doi: 10.1016/j.molliq.2023.121285.

**Raba, G.**, Adamberg, S., Adamberg, K. Acidic pH enhances butyrate production from pectin by faecal microbiota. *FEMS Microbiology Letters*. 2021, 368, 7. Doi: 10.1093/femsle/fnab042. PMID: 33864456.

Adamberg, K., **Raba, G.**, Adamberg, S. Use of changestat for growth rate studies of gut microbiota. *Frontiers in Bioengineering and Biotechnology*. 2020, 8, 24. Doi: 10.3389/fbioe.2020.00024. PMID: 32117913.

## Elulookirjeldus

### Isikuandmed

Nimi: Grete Raba  
Sünniaeg: 02.10.1991  
Sünnikoht: Eesti  
Kodakondsus: Eesti

### Kontaktandmed

E-post: greteraba@gmail.com

### Hariduskäik

2016–2023 Tallinna Tehnikaülikool, PhD  
2014–2016 Tallinna Tehnikaülikool, MSc  
2011–2014 Tallinna Tehnikaülikool, BSc  
2008–2011 Viljandi Maagümnaasium, Keskkharidus

### Keelteoskus

Eesti keel Emakeel  
Inglise keel Kõrgtase

### Teenistuskäik

2022 Tallinna Tehnikaülikool, doktorant-nooremteadur (1.0)  
2017–2019 Tallinna Tehnikaülikool, nooremteadur (0.9)  
2016 Tallinna Tehnikaülikool, nooremteadur (0.75)  
2012–2013 Tallinna Tehnikaülikool, insener (0.5)

### Stipendiumid ja tunnustused

2021 FEMS Microbiology Letters postriauehind konverentsilt 2<sup>nd</sup> International Conference on Microbial Food & Feed Ingredients  
2020 Dora Pluss tegevus 1.2: doktorantide õpirände stipendium; Archimedes  
2019 Kristjan Jaagu välisõpingute stipendium; Archimedes  
2018 Erasmus+ Euroopa-sisese õpirände stipendium; Archimedes  
2018 Dora Pluss tegevus 1.1: lühiajalise õpirände stipendium; Archimedes

### Kursused ja konverentsid

November 2021 2<sup>nd</sup> International Conference on Microbial Food & Feed Ingredients (MiFFI); Kopenhaagen, Taani. Posterettekanne  
September 2019 Intensiivkursus "Pro-, pre-, syn- ja postbiootikumid: mõju meie mikrobiootale ja tervisele"; Tartu, Eesti  
Juuli 2019 "Mucins in health and disease (15<sup>th</sup> International Workshop on Carcinoma-associated Mucins)"; Cambridge, UK. Posterettekanne  
November 2018 Tartu Ülikooli bio- ja siirdemeditsiini instituudi koolitus "Mikrobiom"; Tartu, Eesti

September 2018	8 <sup>th</sup> IUPAC International Conference on Green Chemistry; Bangkok, Tai. Posterettekanne
August 2018	Copenhagen Plant Science Centre PhD suvekool "Synthetic Biology: From Pro- to Eukaryotic Systems (SynBioSys)"; Kopenhaagen, Taani
Juuli 2018	International Conference on Organic Synthesis BOS 2018; Tallinn, Eesti. Posterettekanne
September 2017	S3C suvekool Sustainable Chemistry for Sustainable Development; Lüneburg, Saksamaa
Veebruar 2017	Solvay Institute Workshop on Ionic Liquids: from fundamentals to applications; Brüssel, Belgia. Posterettekanne

### Juhendatud lõputööd

2021	Julika Leppik "Mikrobiota, pH ja orgaaniliste hapete vahelised seosed"
------	------------------------------------------------------------------------

### Publikatsioonid

**Raba, G.**, Luis, A. S. Mucin utilization by gut microbiota – recent advances on characterization of key enzymes. *Essays in Biochemistry*. 2023 Jan 25:EBC20220121. doi: 10.1042/EBC20220121.

Kapitanov, I. V, **Raba, G.**, Špulák, M., Vilu, R., Karpichev, Y., Gathergood, N. Design of sustainable ionic liquids based on l-phenylalanine and L-alanine dipeptides: Synthesis, toxicity and biodegradation studies. *Journal of Molecular Liquids*. 2023, 374, 121285. doi: 10.1016/j.molliq.2023.121285.

**Raba, G.**, Adamberg, S., Adamberg, K. Acidic pH enhances butyrate production from pectin by faecal microbiota. *FEMS Microbiology Letters*. 2021, 368, 7. doi: 10.1093/femsle/fnab042. PMID: 33864456.

Adamberg, K., **Raba, G.**, Adamberg, S. Use of changestat for growth rate studies of gut microbiota. *Frontiers in Bioengineering and Biotechnology*. 2020, 8, 24. doi: 10.3389/fbioe.2020.00024. PMID: 32117913.

ISSN 2585-6901 (PDF)  
ISBN 978-9949-83-963-6 (PDF)